Étude de l'impact de l'expression de variants d'épissage sur les fonctions biologiques de P2RX7 : rôle dans l'adénocarcinome broncho-pulmonaire humain

Jonathan Benzaquen

UNIVERSITÉ CÔTE D'AZUR

ÉCOLE DOCTORALE
SCIENCES DE LA VIE ET DE LA SANTÉ

THÈSE DE DOCTORAT

Etude de l'impact de l'expression de variants d'épissage sur les fonctions biologiques de P2RX7: Rôle dans l'adénocarcinome broncho-pulmonaire humain

Jonathan BENZAQUEN

Institut de Recherche sur le Cancer et le Vieillissement, Nice (IRCAN)

Présentée en vue de l'obtention du grade de docteur en Sciences de la Vie et de la Santé d'Université Côte d'Azur

Dirigée par : Valérie Vouret-Craviari, DR2/HDR
Soutenue le : 18/12/2020

Devant le jury, composé de :
Frédérique Végran, CR1/HDR, Université de Dijon
Benjamin Besse, PU-PH/HDR, Institut Gustave Roussy, Université Paris Saclay
Sébastien Roger, MCU/HDR, Université de Tours
Laetitia Seguin, CR1, Université Côte d'Azur
Valérie Vouret-Craviari, DR2/HDR, Université Côte d'Azur
Paul Hofman, PU-PH/HDR, Université Côte d'Azur
Charles-Hugo Marquette, PU-PH/HDR, Université Côte d'Azur

Etude de l'impact de l'expression de variants d'épissage sur les fonctions biologiques de P2RX7: Rôle dans l'adénocarcinome broncho-pulmonaire humain

Président du jury :

Paul Hofman, PU-PH/HDR, Université Côte d'Azur

Directrice de thèse :

Valérie Vouret-Craviari, DR2/HDR, Université Côte d'Azur

Rapporteurs :

Frédérique Végran, CR1/HDR, Université de Dijon

Benjamin Besse, PU-PH/HDR, Institut Gustave Roussy, Université Paris Saclay

Examinateurs :

Laetitia Seguin, CR1, Université Côte d'Azur

Sébastien Roger, MCU/HDR, Université de Tours

Membre invité :

Charles-Hugo Marquette, PU-PH/HDR, Université Côte d'Azur

Titre :

Etude de l'impact de l'expression de variants d'épissage sur les fonctions biologiques de P2RX7: Rôle dans l'adénocarcinome broncho-pulmonaire humain

Résumé :

Le cancer du poumon, découvert classiquement à un stade avancé et non opérable, est la première cause de décès par cancer. Les avancées en immunothérapie anti tumorale ont changé le pronostic de cette pathologie en positionnant cette approche comme un élément principal de la prise en charge à ce jour. Néanmoins la survie à cinq ans du cancer du poumon, tous stades confondus, reste inférieure à 20% et il est donc nécessaire de mieux comprendre sa physiopathologie afin d'identifier de nouvelles approches thérapeutiques.

Mon laboratoire d'accueil a récemment montré que le récepteur purinergique P2RX7 restreint le développement de tumeurs dans un modèle murin en orchestrant une réponse immunitaire anti tumorale. L'expression de P2RX7 a été montrée dans l'adénocarcinome bronchique humain (LUAD) mais sa fonction n'a jamais été étudiée. Les objectifs de mon projet de recherche étaient de comprendre pourquoi les cellules tumorales du LUAD expriment P2RX7 dont l'une des fonctions est de déclencher leur propre mort. Nous avons émis l'hypothèse que l'expression de variants d'épissage pourrait impacter les fonctions biologiques de P2RX7.

J'ai montré que l'isoforme *P2RX7A* pleine taille et trois variants d'épissage alternatif *P2RX7B*, *H*, *J* sont exprimés dans les tissus LUAD et qu'il y a globalement moins de messagers dans les tissus tumoraux que dans les tissus sains adjacents. Après avoir développé un essai pour mesurer l'activité biologique de P2RX7, nous avons démontré que seul P2RX7 exprimé dans les cellules immunitaires pulmonaires est fonctionnel, et qu'il existe une altération de ses fonctions biologiques uniquement dans le compartiment tumoral. J'ai ensuite caractérisé le mécanisme moléculaire qui conduit à l'expression d'un récepteur dont la fonction biologique est altérée. Ce mécanisme repose sur l'expression différentielle du variant d'épissage *P2RX7B* et à la capacité de l'isoforme P2RX7B d'hétéro-oligomériser avec P2RX7A pour former un récepteur moins fonctionnel. Enfin, j'ai observé que les tumeurs des patients LUAD qui présentent un niveau d'expression élevé de *P2RX7B* sont très faiblement infiltrées en cellules immunitaires.

L'ensemble de mes résultats positionnent P2RX7B comme un biomarqueur péjoratif pour les patients souffrant de LUAD, et comme un outil théranostique prometteur dans une perspective curative.

Mots clefs : P2RX7/P2X7 purinorécepteurs, ATPe, épissage alternatif, cancer, immunomodulation

Title :

Assessing the impact of the expression of splice variants on the biological functions of P2RX7: Role in human bronchopulmonary adenocarcinoma

Abstract :

Lung cancer, classically discovered at an advanced and non-operable stage, is the leading cause of cancer death. Advances in anti-tumor immunotherapy have changed the prognosis of this pathology by positioning this approach as a central element of therapy. Nevertheless, the five-year survival, all stages confused, remains less than 20% and it is therefore necessary to better understand the pathophysiology of this disease in order to identify new therapeutic approaches.

My PhD host laboratory has recently shown that the purinergic receptor P2RX7 restricts tumor development in a murine model by orchestrating an anti-tumor immune response. The expression of P2RX7 has been shown in lung adenocarcinoma (LUAD) but its function has never been studied. The aims of my research project were to understand why LUAD tumor cells express P2RX7, one of the functions of which is to trigger their own death. We hypothesized that the expression of splice variants could impact the biological functions of P2RX7.

I showed that the full size P2RX7A isoform and three alternative splice variants P2RX7B, H, J are expressed in LUAD tissues and that there are globally less messenger's RNA in tumor tissues than in adjacent healthy tissues. After developing an assay to measure the biological activity of P2RX7, we demonstrated that only P2RX7 expressed in lung immune cells is functional, and that there is an alteration of its biological activities only into tumor compartment. I then characterized the molecular mechanism that leads to the expression of a receptor whose biological function is altered. This mechanism is relying on the differential expression of the P2RX7B splice variant and the ability of the P2RX7B isoform to hetero-oligomerize with P2RX7A to form a less functional receptor. Finally, I observed that tumors of LUAD patients having a high level of P2RX7B expression are very poorly infiltrated with immune cells.

All these results position P2RX7B as a pejorative biomarker for LUAD patients and as a promising theranostic tool in a curative perspective.

Keywords : P2RX7/P2X7, purinoceptor, eATP, alternative splicing, cancer, immunomodulation

I. Abréviations

CNPC……cancer du poumon non à petites cellules

CPC……cancer du poumon à petites cellules

LUAD…….. adénocarcinome bronchique

SSP……. survie sans progression

SG……. survie globale

PD-1…… programmed cell death protein 1

PD-L1……. programmed cell death protein ligand 1

ICI…….. inhibiteurs des checkpoint de l'immunité

MET…….. microenvironnement tumoral

ATP…… adénosine tri-phosphate

ATPe…… ATP extracellulaire

NAD…… nicotinamide adénine dinucléotide

GTP…….. guanosine triphosphate

AMP…… adénosine monophosphate

CMH1…… complexe majeur d'histocompatibilité de classe 1

FAC…….. fibroblastes associés au cancer

HIF…….. Hypoxia Inducible Factor

TNF…… facteur de nécrose tumorale

IL-12…… interleukine-12

IL-10…… interleukine-10

Th…… lymphocytes T auxiliaires

MDSC…… myeloïd derived suppressor cell

NK…… natural killer

VEGF…….. vascular endothelial growth factor

P1R…….. purinocepteur P1

P2RX…… purinocepteur P2X

P2RY…… purinocepteur P2Y

NICD……. NAD induced cell death

LPS…… lipopolysaccharide

MAP……. modulateurs allostériques positifs

MAN…….. modulateurs allostériques négatifs

GFP…….. green fluorescent protein

DAMPS……dommages associés aux motifs moléculaires associés aux dégâts

PPR……..récepteurs de reconnaissance de patterns

IHC……. immunohistochimie

ARNm…… acide ribonucléique messager

MiR……. micro-ARN

SNP…….. polymorphisme nucléotidique simple

II. Figures

III. Introduction

A. Le cancer du poumon avancé

a. Faits et chiffres épidémiologiques

Le cancer du poumon, le plus souvent découvert à un stade avancé non opérable, est la première cause de décès par cancer. Il est responsable de plus de 33 000 décès par an en France et 1,8 millions de décès par an dans le monde. Les dernières données d'épidémiologie estiment son incidence à plus de 46 000 nouveaux cas par an en France et environ 2,1 millions de nouveaux cas par an dans le monde. Il constitue le 3ème cancer incident chez la femme et le 2ème cancer incident chez l'homme [1].

Les deux dernières décennies ont été marquées par la compréhension de mécanismes moléculaires clés de la cancérogenèse pulmonaire ; ces derniers ont permis de développer des thérapies ciblées efficaces, alors que les cinq dernières années ont vu l'application clinique du décryptage de l'immunité anti tumorale. Ces avancées ont considérablement enrichi la prise en charge du cancer du poumon mais cette pathologie demeure sévère, d'où l'importance d'améliorer la connaissance des mécanismes de la carcinogenèse.

b. Historique de la prise en charge

i. Prise en charge thérapeutique du cancer du poumon avancé

Le cancer du poumon est classé selon son type histologique. Il est historiquement divisé en cancer du poumon non à petites cellules (CNPC), le plus fréquent puisqu'il représente neuf cas sur dix, et en cancer du poumon à petites cellules (CPC), plus rare, rapidement évolutif et relevant toujours d'un traitement systémique. Il existe trois principaux types de cancer du poumon non à petites cellules. L'adénocarcinome bronchique (LUAD) est le plus fréquent et représente environ 40 % des cas. Il se situe le plus souvent en périphérie du poumon et se développe aux dépens des cellules glandulaires. Le carcinome épidermoïde a une localisation plus proximale, se développe aux dépens des cellules malpighiennes et représente environ 30% des cas, et le carcinome indifférencié à grandes cellules lui représente 10 à 15% des cas. (Figure 1)

Si le CNPC de stade précoce relève d'un traitement local, chirurgical et dans certains cas par radiothérapie, son traitement au stade tardif (stades IIIB-IV) repose sur l'administration de

traitements systémiques, la chirurgie ne pouvant plus offrir une approche curative à ce stade de la pathologie.

À ce jour, le traitement du CNPC au stade tardif peut être appréhendé en approche chimiothérapeutique, en thérapie ciblée et en immunothérapie seule ou en combinaison avec la chimiothérapie. Les schémas de chimiothérapie pour le traitement du CNPC reposent historiquement sur les sels de platine, qui demeurent le trépied de la chimiothérapie en oncologie thoracique. Les taxanes font également partie de cet arsenal thérapeutique et sont particulièrement indiqués dans le CNPC d'histologie épidermoïde. Le pemetrexed qui est un anti-folate [2], et les anti-VEGF (vascular endothelial growth factor) qui sont utilisés pour s'opposer à la néo-angiogénèse tumorale [3], sont deux agents utilisés dans les CNPC d'histologie non épidermoïde. En 2004, la découverte de certaines mutations tumorales à l'origine de la tumorogenèse qui sont directement ciblables, a révolutionné le traitement du cancer du poumon. Aujourd'hui, des traitements ciblés sont approuvés chez les patients atteints de cancer du poumon porteurs de mutations *EGFR* et *BRAF*, de réarrangements *ALK* et *ROS1*, de fusions de *NTRK* [4].

Alors que les traitements mentionnés ci-dessus ciblent directement les cellules cancéreuses, l'immunothérapie par inhibiteurs des points de contrôle (checkpoint) de l'immunité (ICI) utilisée en oncologie thoracique, a révolutionné la prise en charge thérapeutique du cancer en ciblant l'hôte et non plus la cellule tumorale elle-même. L'objectif ici est de restaurer une immunothérapie anti tumorale, en utilisant un anticorps ciblant la synapse immunologique comme un anti-PD-1 (program-death 1), un anti-PD-L1 (program-death-ligand-1), un anti-CTLA-4 (cytotoxic T-lymphocyte associated protein 4). Les premiers ICI testés dans le cadre du CNPC étaient les anticorps anti-PD-1, qui ont montré une amélioration de la survie globale dans les cas de CNPC avancés progressant après une chimiothérapie antérieure et ont donc été approuvés en 2015, comme option de deuxième ligne dans le CNPC. Par la suite, d'autres études ont permis de valider en première ligne cette modalité thérapeutique, et plus récemment l'association de la chimiothérapie et de l'immunothérapie en première ligne. L'arbre décisionnel repose non seulement sur l'état général du patient et le type histologique tumoral, mais aussi sur l'expression du PD-L1 en immunohistochimie, le seul marqueur théranostique validé à ce jour.

Nous assistons donc à un changement de paradigme puisque le CNPC avancé sans addiction oncogénique, bénéficie aujourd'hui de l'immunothérapie en première ligne qui, seule ou en association à la chimiothérapie, devient la pierre angulaire du traitement chez une majorité de patients.

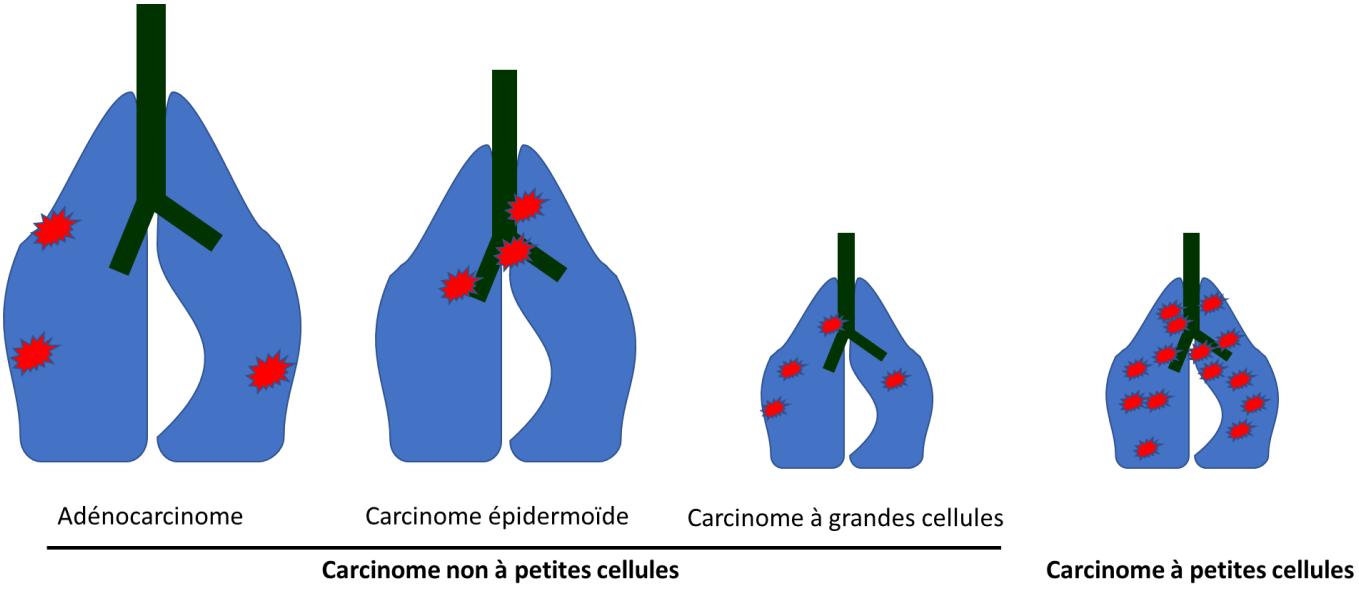

FIGURE 1 : Les différents types histologiques du cancer broncho-pulmonaire

ii. Limites et défis

Si les ICI ont amélioré drastiquement la prise en charge du CNPC avancé, seule une proportion limitée de patients obtient un bénéfice clinique durable. Certains patients ne répondent absolument pas au traitement voire se révèlent en hyper progression tumorale sous immunothérapie. A ce jour, l'expression du PD-L1 tumoral évaluée par immunohistochimie (IHC), permet de sélectionner les patients éligibles à l'immunothérapie en première ligne mais ne permet pas de prédire une réponse durable chez les patients traités par ICI ni de prédire les situations d'hyperprogression tumorale. C'est pourquoi de nombreux autres biomarqueurs, en citant par exemple l'expression de PD-L1 par les cellules immunitaires infiltrant la tumeur, l'infiltration tumorale en lymphocytes $CD8^+$, la charge mutationnelle intra tumorale, ou encore le volume tumoral global évalué par imagerie métabolique, ont été étudiés [5]. Il reste que, en pratique à ce jour les biomarqueurs de réponse ou de non-réponse à l'immunothérapie demeurent imparfaits. Ainsi se pose le défi de mieux comprendre la physiopathologie du cancer du poumon et des acteurs impliqués dans l'immunomodulation

positive ou négative de l'environnement tumoral, afin d'identifier non seulement de nouveaux biomarqueurs mais aussi pour étudier de nouvelles approches thérapeutiques. *In fine*, toutes ces connaissances pourront être étendues au bénéfice d'autres types de cancers.

B. Signalisation purinergique et cancer

a. Purines, ATP extracellulaire

La tumeur est une lésion résultant de la multiplication anarchique de cellules anormales ; ces cellules sont en communication permanente avec le microenvironnement tumoral (MET). Le MET comprend les cellules tumorales et les cellules de l'hôte : stromales et immunitaires (Figure 2). Il contient de nombreux acteurs impliqués dans la modulation des réponses immunitaires anti tumorales. L'environnement inflammatoire tumoral est en permanence exposé à des éléments qu'il va attribuer comme appartenant à l'hôte ou non. Sa composition conditionne d'une part le métabolisme et l'invasivité des cellules tumorales, et d'autre part les réponses immunitaires anti tumorales [6]. La compréhension du MET est cruciale pour identifier les facteurs impliqués dans le contrôle du développement tumoral [7].

Les purines sont une famille de composés organiques présentant un cycle imidazole, un des cycles azotés les plus courants. Les produits de dégradation des purines constituent des biomolécules cellulaires impliquées non seulement dans la signalisation mais aussi le métabolisme cellulaire, telles que l'adénosine tri-phosphate (ATP), le nicotinamide adénine dinucléotide (NAD), le guanosine triphosphate (GTP), l'adénosine monophosphate (AMP) cyclique, le coenzyme A [8].

L'ATP appartient à la famille des nucléotides, et a longtemps été considéré comme seulement confiné aux compartiments intracellulaires. Il est le principal substrat énergétique de la machinerie intracellulaire et est essentiellement produit lors de la respiration mitochondriale aérobie. Son rôle en tant que messager extracellulaire a été longtemps controversé. En effet, dès 1929, Szent-Györgyi et Drury ont mis en évidence les effets des purines sur le myocarde. Il a fallu néanmoins attendre les travaux de Burnstock en 1964 pour que soit posée l'hypothèse que des fonctions extracellulaires seraient attribuables à l'ATP. Ce n'est qu'à partir de 1972, après la confirmation de son hypothèse, que l'on assiste à un intérêt croissant pour le déchiffrage de la signalisation purinergique.

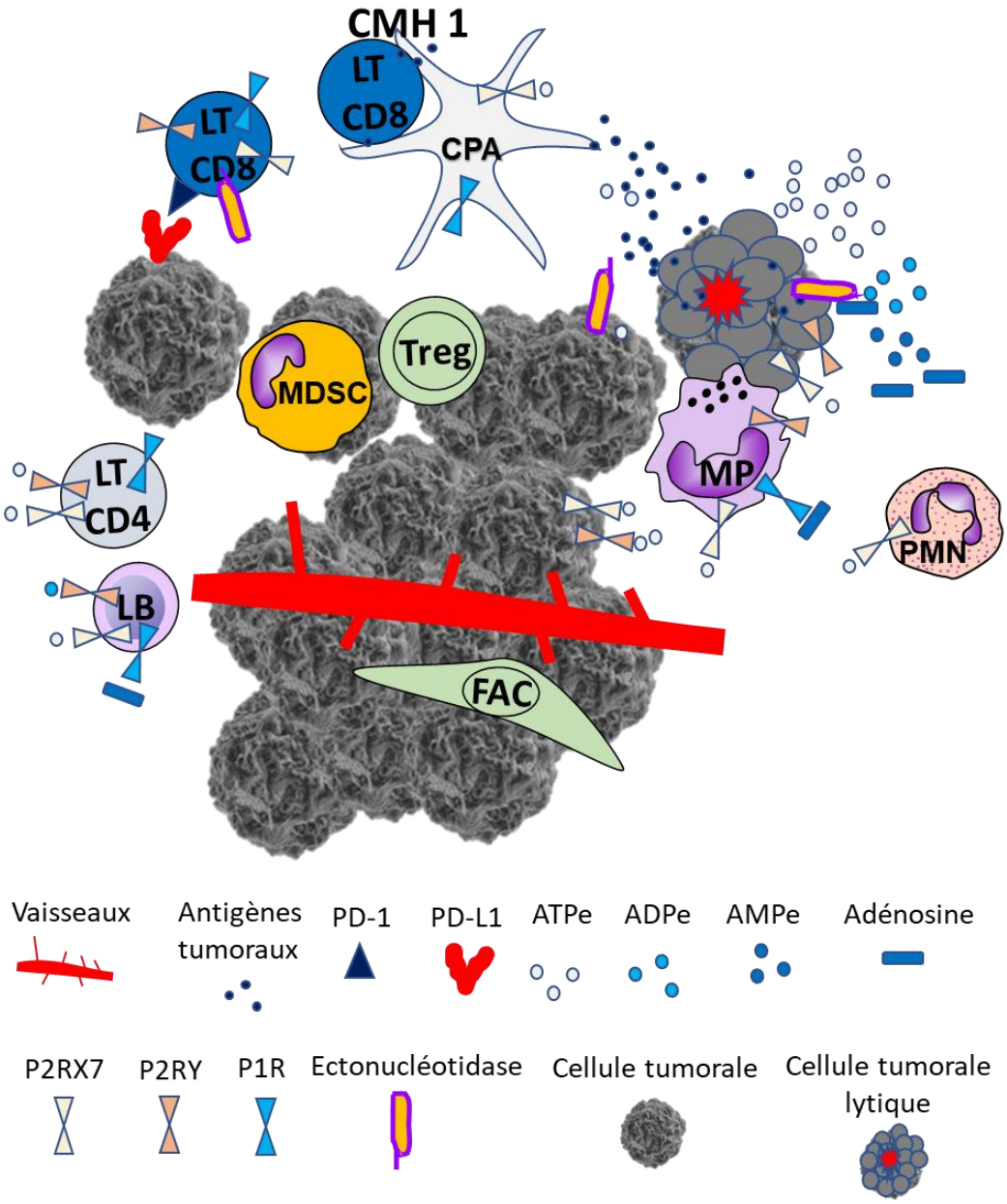

FIGURE 2 : Microenvironnement tumoral et signalisation purinergique

Adapté de Di Virgilio et al., Nat Rev Cancer 2018 [9]

Le microenvironnement tumoral est un ensemble complexe qui comprend les cellules tumorales mais aussi de l'hôte, immunitaires ou non comme les fibroblastes associés au cancer (FAC). Les cellules de l'immunité innée conduisent à la lyse de cellules tumorales. Les néoantigènes tumoraux libérés, sont capturés par les cellules présentatrices d'antigènes qui vont les présenter par le biais du complexe majeur d'histocompatibilité de classe 1 (CMH 1) aux lymphocytes T naïfs qui matureront en lymphocytes T cytotoxiques. La cytolyse tumorale entraine une libération d'ATP extracellulaire (ATPe) du compartiment intracellulaire vers le compartiment extracellulaire, qui peut se lier à P2RX7 pour activer ses fonctions canal et assemblage de l'inflammasome NLRP3 et de la cascade cytokinique pro-inflammatoire d'aval (fonctions non représentées sur ce schéma). Des ectonucléotidases membranaires catabolisent l'ATPe en ADP pouvant lier les récepteurs P2YR, en AMP puis enfin en adénosine capable d'activer les récepteurs P1R qui exercent un rétrocontrôle anti-inflammatoire et pro-tumoral.

b. Signalisation purinergique et cancer

La signalisation purinergique attire un intérêt croissant dans le domaine de l'immunomodulation du MET. L'ATPe ainsi que d'autres nucléotides, en particulier l'adénosine di-phosphate (ADP) obtenue par l'action d'ectonucléotidases membranaires, agissent comme des molécules de signalisation dans les tissus. Ces nucléotides sont les ligands extracellulaires de récepteurs purinergiques qui peuvent être de la famille des récepteurs ionotropiques P2RX, ou métabotropiques P1RX et P2RY (Figure 3), et sont détaillés dans la section III.C.

L'activité anti-néoplasique de l'ATP a été démontrée en 1983 par Rapaport qui a montré que l'ajout d'ATP exogène aux cellules de cancer du pancréas et du côlon inhibait la croissance cellulaire en provoquant un arrêt du cycle cellulaire en phase S [10]. L'ATPe, lorsqu'il transite dans le compartiment extracellulaire, est considéré comme un signal de danger pour l'hôte. Il est le témoin de la lyse cellulaire. En effet, il est libéré dans l'espace extracellulaire dans une situation d'altération ou de souffrance cellulaire, et en particulier dans les milieux inflammatoires et tumoraux où de telles conditions sont réunies [11,12]. Ce nucléotide, un des ligands essentiels de la signalisation purinergique, joue un rôle régulateur des réponses immunitaires [13] et est considéré comme un marqueur biochimique du cancer [14,15].

La libération d'ATPe n'est pas l'apanage des cellules tumorales, puisque toutes les cellules sont capables d'en libérer et c'est pourquoi l'ensemble des cellules du MET contribuent à la présence d'ATPe dans le tissu tumoral. Sa libération a été montrée pour les neutrophiles et a été associée à leur mobilisation vers le site inflammatoire [16], ainsi que pour une lignée de macrophage en présence de LPS [17]. La libération d'ATPe a également été montrée pour les cellules tumorales dans plusieurs lignées notamment dans des modèles de phéochromocytome [18], de cancer du poumon [19], de carcinome ovarien [20], de cancer testiculaire [21], de carcinome indifférencié d'Ehrlich [22]. En 2008, il a été montré, grâce à un essai utilisant une sonde couplée à la luciférase, que les concentrations d'ATPe sont mesurées à des taux drastiquement plus élevés dans les tissus tumoraux (100 à 500 µM) par rapport aux tissus sains (10 à 100 nM) [23]. Cet essai a été appliqué dans de nombreux types tumoraux, en particulier dans des modèles humains de carcinome ovarien et de mélanome, de leucémie et de carcinome colique murins, et dans un modèle métastatique de carcinome colique humain chez la souris, confirmant des niveaux élevés de concentration en ATPe au sein des tissus tumoraux [24–26]. L'accumulation de ce nucléotide, produit de l'activité métabolique

de la tumeur et de la cellule hôte, et de ses produits de dégradation dont l'adénosine, reflète aussi un processus actif de signalisation ayant des implications sur la carcinogénèse [26].

La dégradation de l'ATPe est orchestrée par les ectonucléotidases CD39 et CD73 [27] dans les tissus tumoraux [28] et conduit à l'accumulation de son produit de dégradation, l'adénosine. Cette adénosine agit comme un médiateur immunosuppresseur [29] et il a été montré que son accumulation favorise la croissance des tumeurs [30]. En effet il a été observé que des niveaux élevés d'ADPe élevés dans des microdyalisats issus de tissus tumoraux impactent l'infiltration lymphocytaire T intratumorale [31]. De plus certaines conditions tumorales comme l'existence d'un gradient d'oxygène entre le centre de la zone tumorale et la périphérie, favorisent l'expression du facteur HIF-1α (Hypoxia Inducible Factors-1α) et de son couplage à son partenaire HIF-1β, rendant le facteur HIF actif et apte à favoriser l'expression des ectonucléotidases CD39 et CD73 [32]. La signalisation purinergique fait ainsi intervenir un équilibre dynamique entre l'ATPe et l'adénosine qui représentent un point de contrôle immunitaire du cancer (Figure 3).

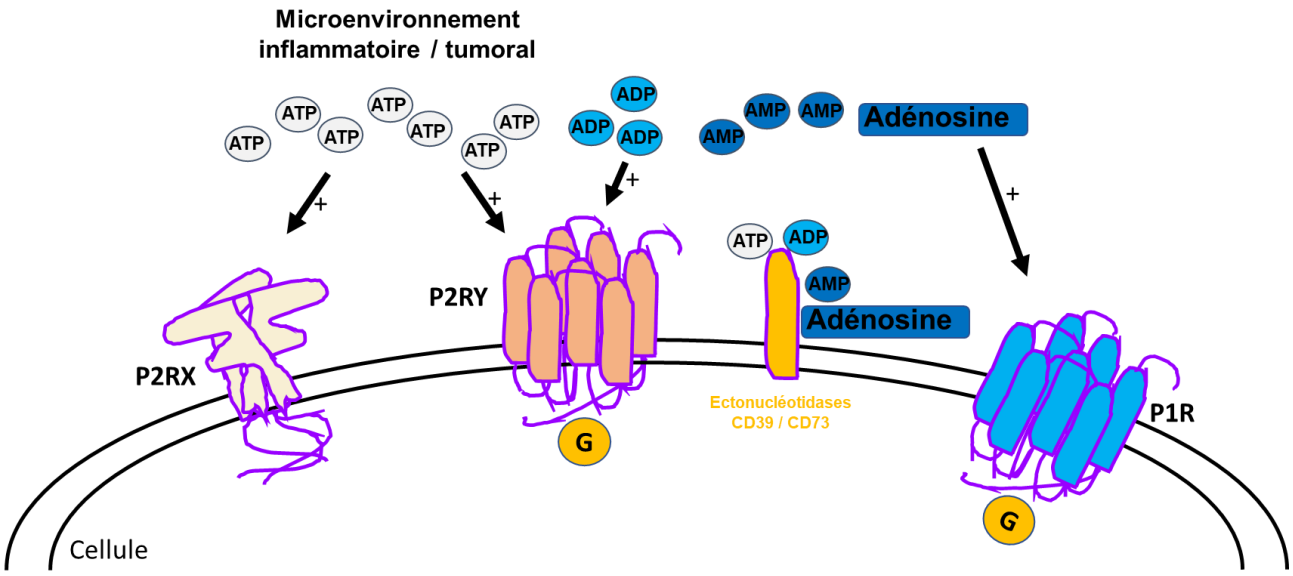

FIGURE 3 : Signalisation purinergique et ligands endogènes

Les récepteurs purinergiques P2RX ont pour ligand l'ATPe qui est retrouvé à de fortes concentrations dans les tissus inflammatoires et tumoraux. L'ATPe est hydrolysé en ADP, AMP et adénosine par les ectnucléotidases membranaires CD39 et CD73. L'ATPe et l'ADPe sont tous deux en mesure d'activer les récepteurs métabotropiques P2RY couplés aux protéines G, alors que l'adénosine représente le ligand essentiel des récepteurs métabotropiques P1R couplés aux protéines G.

C. P2RX7 : un immunomodulateur impliqué dans le contrôle tumoral

a. Les récepteurs purinergiques : définition, familles de récepteurs

Les récepteurs purinergiques, également appelés purinocepteurs, sont une famille de récepteurs membranaires activés par les purines. Il sont impliqués dans de nombreuses fonctions physiologiques comme l'apprentissage, la mémoire, les comportements [33], mais aussi de nombreuses fonctions cellulaires comme la prolifération et le migration cellulaire, la mort cellulaire, la sécrétion de cytokines [34].

L'existence d'une signalisation purinergique a été proposée en 1972 par Burnstock [35] bien avant le premier clonage des récepteurs purinergiques P2Y1 et P2Y2 en 1993 [36,37]. Quatre types de récepteurs P1, dont le ligand est l'adénosine (A1, A2A, A2B, A3), sept types de récepteurs P2X (P2RX1 à P2RX7) et huit types de récepteurs couplés à la protéine G (P2RY1, P2RY2, P2RY4, P2RY6, P2RY11, P2RY12, P2RY13 et P2RY14) ont été identifiés [38,39] (Figure 4).

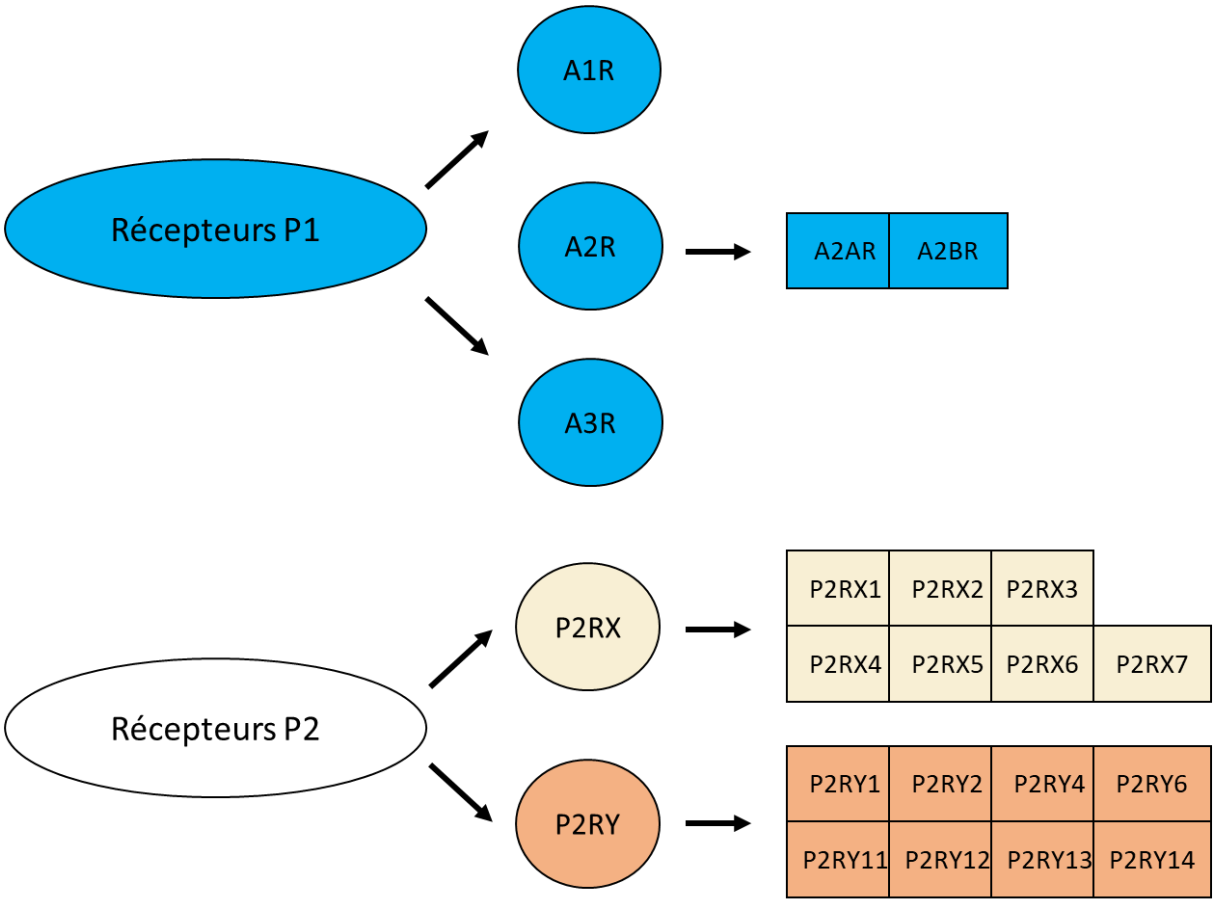

FIGURE 4 : La famille des récepteurs purinergiques

b. Rôle des P1R

Les récepteurs P1R ont pour ligand l'adénosine, et sont une famille constituée des récepteurs A1, A2 et A3. Ces derniers font parties de la famille des récepteurs à sept domaines transmembranaires couplés aux protéines G. Les récepteurs A2, par leur liaison à l'adénosine qui représente le produit de dégradation de l'ATPe présent dans les tissus inflammatoires, sont ainsi aptes à détecter les réponses inflammatoires et exercent un rétrocontrôle sur les cellules de l'immunité [40]. En particulier, le sous-type A2A a une haute affinité pour l'adénosine alors le récepteur A2B une faible affinité, conférant la capacité au récepteur de type A2 d'exercer une modulation des rétrocontrôles exercés en fonction de l'expression relative de ces deux sous-types. Ceci permet de moduler les réponses immunitaires grâce à l'action rapide des ectonucléotidases en prévenant notamment des réponses exagérées sur des zones tissulaires endommagées, riches en ATPe. Il faut noter que la signalisation de l'adénosine par les récepteurs A2A et A2B couplés à la protéine Gs (stimulatrice) peut être contrecarrée par les récepteurs A1 et A3 couplés à la protéine Gi (inhibitrice). De plus, il semble que, outre l'inhibition des processus inflammatoires, les récepteurs A2 ont également la capacité de rediriger la classe d'effecteurs de la réponse immunitaire et de modifier les schémas de sécrétion des cytokines et des chimiokines par les cellules immunitaires activées [41]. En activant les récepteurs A2, l'adénosine peut inhiber la production du facteur de nécrose tumorale alpha (TNFα), de l'interleukine-12 (IL-12) et de la chimiokine motif-C-X-C-ligand-10 (CXCL10), augmenter la sécrétion de l'interleukine-10 (IL-10) et augmenter la libération de la chimiokine motif-C-C-ligand-17 (CCL17). Ainsi, l'activation des récepteurs de l'adénosine A2 peut diminuer la capacité des cellules dendritiques présentatrices d'antigènes de conduire les réponses immunitaires des lymphocytes T auxiliaires de type 1 (Th1) et donc modifier l'équilibre entre les lymphocytes Th1 et les lymphocytes Th2 [42] (Figure 5).

Il a été montré dans le LUAD qu'il existe une surexpression de CD73 et des récepteurs A2A, et que l'expression à un niveau élevé du CD73 corrélait avec un moins bon pronostic des patients sur la survie globale (SG) et la survie sans récidive (SSR). A contrario, un haut niveau d'expression des récepteurs A2A corrélait avec une meilleure SG et SSR, indiquant que CD73 et les récepteurs A2A peuvent partager des effets pronostiques opposés, soulignant la modulation fine de l'immunomodulation P1R-dépendante [43].

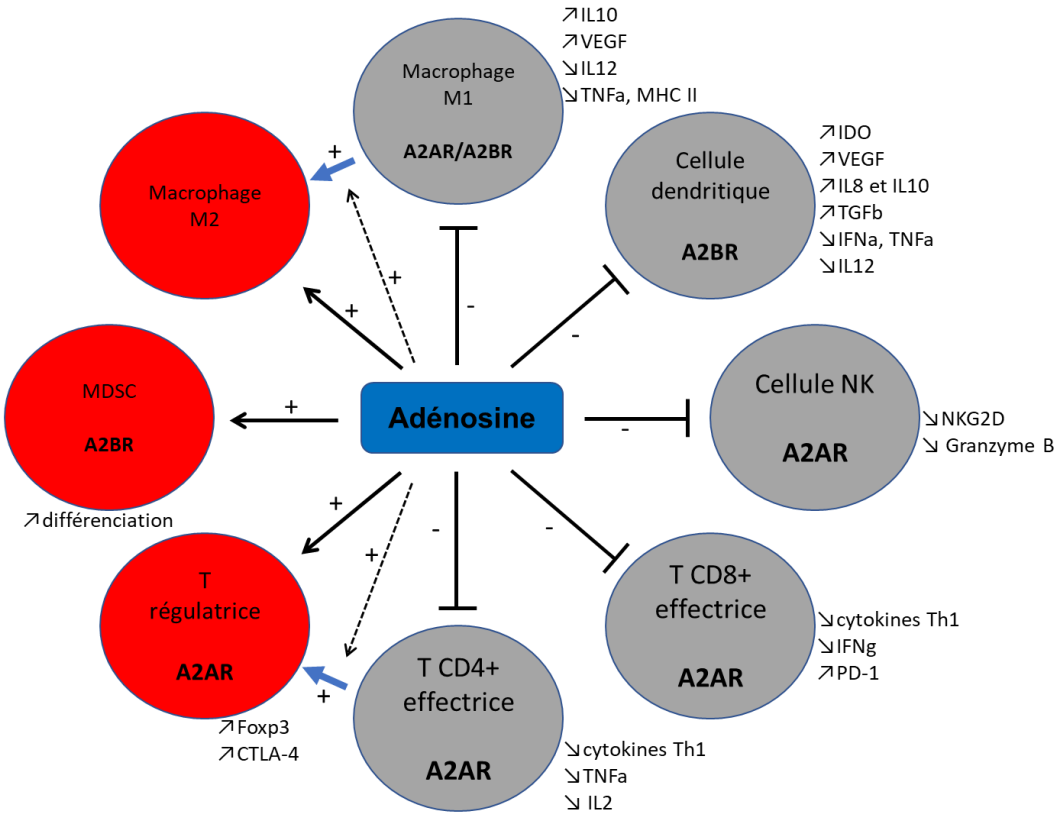

FIGURE 5 : Fonctions biologiques de l'adénosine

L'adénosine favorise l'immunosuppression selon un mécanisme multi-niveaux. Elle favorise la différenciation des lymphocytes T CD4 effecteurs en lymphocytes T régulateurs et augmente l'expression du marqueur Foxp3 et du CTLA-4 lymphocytaire qui exerce un frein sur les réponses immunitaires antitumorales. Elle favorise le recrutement et la différentiation des M-MDSC (cellules dérivées myéloïdes immunosuppressives), et promeut le changement de phénotype des macrophages M1 en macrophages M2 immunosuppresseurs et protumoraux. Elle exerce un frein sur les cellules cytotoxiques T CD4 effectrice et T CD8 par une moindre sécrétion de cytokines et une augmentation d'expression du PD-1 immunitaire. Elle diminue la fabrication des granzyme B par les cellules NK, et diminue l'expression du marqueur NKG2D. Elle augmente la sécrétion de facteur de croissance de l'endothélium vasculaire (VEGF) par les cellules dendritiques, qui favorise la néoangiogénèse tumorale, et s'oppose à la sécrétion de cytokines pro-inflammatoires.

c. Rôle des P2RY

Les récepteurs P2RY sont des récepteurs-canaux métabotropiques couplés à la protéine G. Ils sont impliqués dans la régulation de fonctions cellulaires et communiquent avec de nombreuses protéines comme les intégrines, des protéines du cytosquelette, des protéines de la jonction intercellulaire, et des protéine G intracytoplasmiques. Ils s'activent après liaison

à l'ATPe, mais aussi l'ADPe, l'uracile triphosphate (UTP) et l'uracile diphosphate (UDP) ainsi que l'UDP-glucose. Ils sont capables de s'oligomériser avec de nombreuses autres protéines c'est pourquoi le répertoire fonctionnel est vaste est incomplètement élucidé. Leur structure générale comprend une extrémité N terminale qui à la différence des P2RX, est extracellulaire, 7 domaines transmembranaires, et une extrémité C terminale intracytoplasmique. L'implication des récepteurs P2RY a été soulignée dans de nombreux processus physiopathologiques comme l'épilepsie, la douleur aigue et chronique, le syndrome dépressif, les processus neurodégénératifs en particulier la maladie d'Alzheimer et la maladie de Parkinson, mais aussi dans certains cancers neurologiques comme le gliome et le neuroblastome [44]. Cette famille de récepteurs serait également impliquée dans la mise en place de réponses immunitaires en synergie avec les récepteurs P2RX, comme détaillé dans la revue [45].

d. Rôle des P2RX

i. P2RX

Les purinorécepteurs P2X (P2XR ou P2RX) sont une famille de récepteurs-canaux essentiels à la physiologie humaine. Ces récepteurs ionotropiques, au nombre de sept, sont activés par l'ATPe. Ils présentent une structure oligomérique comportant trois monomères qui forment alors un canal ionique pouvant passer d'un état fermé à un état ouvert selon que l'ATP est lié au récepteur ou non. Après activation, ce canal permet un influx de sodium et de calcium et un efflux de potassium.

Ces récepteurs comprennent entre 379 à 595 acides aminés et sont constitués d'une extrémité N-terminale, de deux domaines transmembranaires formés chacun de six hélices α, d'une boucle extracellulaire comprenant des sites de glycosylation, de domaines de liaison de l'ATPe, et d'une extrémité C-terminale. La boucle extracellulaire et l'extrémité N-terminale sont particulièrement conservées entre les différents membres de la famille des P2RX. L'unité fonctionnelle du récepteur est oligomérique ; en particulier il a été démontré par cristallographie que P2RX4 de poisson zèbre [46] et P2RX7 de panda [47] sont assemblés sous forme d'un trimère. À ce jour, 27 structures de P2RX ont été définies avec une haute résolution de modélisation graphique, à partir de formes tronquées à l'exception du P2RX7 de rat qui a pu être étudié sous sa forme pleine taille [48]. L'ensemble de ces études montre que les récepteurs de la famille P2RX partagent une structure tertiaire et quaternaire semblable [49].

Les récepteurs P2RX sont subdivisés en deux sous-groupes, soient les récepteurs qui se désensibilisent très rapidement (de l'ordre de la centaine de millisecondes) après l'ajout du ligand, comme P2RX1 et P2RX3, et les autres qui se désensibilisent plus lentement, jusqu'à 1000 fois moins rapidement. P2RX7 constitue une exception puisqu'il ne se désensibilise pas ou très peu [50].

Le répertoire fonctionnel de chacun des récepteurs P2RX est varié et exhaustivement détaillé par Illes et al. [49]. Brièvement, P2RX1, est impliqué dans la motricité des canaux des voies excrétrices génitales, dans le chémotactisme des polynucléaires neutrophiles [51,52], et dans l'agrégation plaquettaire [53]. Les récepteurs P2RX2, P2RX3 sont notamment impliqués dans la perception douloureuse [54], dans les fonctions sensorielles gustatives et dans la douleur inflammatoire et neuropathique [55–58], le récepteur P2X4 est également impliqué dans la douleur neuropathique et la mémoire hippocampique [59,60], alors que le récepteur P2RX7, objet de notre étude, sera décrit plus en détail ci-après.

ii. Le récepteur P2RX7

1. Particularités de P2RX7

P2RX7 a initialement été mis en évidence dans les mastocytes de rats [61], alors nommé récepteur P2Z. Ce récepteur se distingue des autres P2RX par son affinité particulièrement faible pour l'ATPe, par la présence d'une longue extrémité C-terminale impliquée dans sa capacité unique à former un large pore membranaire, et par un répertoire fonctionnel étendu. Ce récepteur est dit ubiquitaire, puisque virtuellement exprimé dans toutes les cellules mammifères. Il est particulièrement exprimé par les cellules du système immunitaire [62,63], et est impliqué dans la régulation des réponses immunitaires innées et adaptatives.

Au cours de l'inflammation, l'expression de P2RX7 est régulée à la hausse sur les cellules immunitaires (neutrophiles, monocytes, éosinophiles, mastocytes, macrophages et lymphocytes) [64], et son activation par l'ATPe entraine la libération de cytokines pro-inflammatoires [64,65]. Ainsi, P2RX7 est qualifié de récepteur immunomodulateur et attire beaucoup d'intérêt en pathologie humaine. Ses fonctions biologiques ont été étudiées exhaustivement dans les monocytes, les macrophages et la microglie, où il est exprimé à un niveau élevé [66–68].

2. Structure du récepteur

a. 2D : domaines fonctionnels de l'isoforme pleine taille

P2RX7 code pour une protéine comprenant au total 595 acides aminés pour la forme pleine taille désignée P2RX7A. L'extrémité N-terminale est courte et comporte 26 acides aminés, la boucle extracellulaire est constituée de 282 acides aminés dont dix cystéines susceptibles de former des ponts disulfures, les deux domaines transmembranaires sont composés d'environ 24 acides aminés chacun. L'extrémité C-terminale comprend 239 acides aminés. Ce domaine est une particularité fondamentale de P2RX7 qui lui confère ses propriétés spécifiques. Des expériences de mutagénèse dirigée ont permis de montrer que cette région avait un rôle dans l'adressage membranaire de P2RX7 [69] et la formation de larges pores membranaires [70]. De multiples motifs de liaison aux lipides et aux protéines ont été identifiés dans ce domaine, dont une région de liaison aux lipopolysaccharides circulants endotoxiniques. De plus, des régions d'homologies de séquences avec celles de protéines impliquées dans l'assemblage du cytosquelette (acides aminés 389 à 405 et acides aminés 494 à 508), ou encore d' une partie du récepteur 1 du facteur de nécrose tumorale (TNFR1, acides aminés 436 à 531) ont été décrites [71]. L'ensemble de ces propriétés fait de P2RX7 un récepteur particulièrement intéressant sur un plan physiopathologique.

b. 3D : structure trimérique

L'association de trois monomères de P2RX7 forme l'unité fonctionnelle de ce récepteur canal. L'élucidation de la structure tridimensionnelle homotrimérique a été rendue possible par analyses cristallographiques, initialement conduites sur le récepteur P2RX4 de poisson zèbre [46] et sur le P2RX3 humain [72]. Dans tous les cas, c'est une forme tronquée pour la queue C-terminale qui a été étudiée. Ces analyses ont permis de montrer que les récepteurs P2RX présentent un site de liaison pour l'ATPe et que les monomères du récepteur prennent individuellement une forme décrite comme ressemblant à un « dauphin » [47,72]. L'association en trimère permet de former une tourelle dont la conformation est modulée par la fixation du ligand endogène, autorisant l'ouverture du récepteur canal [73]. Plus récemment, le P2RX7 de panda [47] et de poulet [74] tronqués pour l'extrémité C-terminale ont pu être cristallographiés. Ces résultats ont permis de de préciser l'emplacement d'un site

allostérique présent à l'interface interne entre deux sous unités successives, mais aussi des sites de liaison à l'ATPe qui se situent à la jonction entre chaque sous-unité successive constituant la tourelle du récepteur. Les auteurs ont modélisé le changement de conformation de la tourelle conduisant à l'ouverture du canal du P2RX7 de panda et l'ont illustré par une séquence vidéo [75] (Figure 6).

C'est par analogie avec ces données qu'a pu être modélisé en trois dimensions le récepteur P2RX7 humain [73], puisque jusqu'à 85% d'homologie existe entre les récepteurs P2RX7 de panda et de poulet avec celui de l'humain P2RX7A pleine taille [47]. Il faut noter que les formes de poulet et de panda cristallisées étaient dépourvues de l'extrémité C-terminale, mais les auteurs ont tiré un avantage de cette limite en démontrant que la fonction d'ouverture du large pore n'est pas exclusivement dépendante de l'extrémité C-terminale mais aussi de la composition lipidique membranaire. En effet cette fonction restait présente pour le P2RX7 tronqué C-terminal exprimé à la surface des liposomes, le taux élevé de cholestérol membranaire présent dans ce système d'étude étant corrélé avec une réduction de fluidité membranaire et une ouverture du large pore après stimulation du récepteur [75].

Plus récemment, la structure pleine taille du P2RX7 de rat [48] a pu être analysée par cryo-microscopie électronique et a révélé la présence de zones riches en cystéines au sein de l'extrémité C-terminale et palmitoylées, s'opposant à la désensibilisation du récepteur, ainsi qu'un complexe d'ions zinc et un site de fixation de la guanosine, dont les fonctions sont à ce jour inconnues.

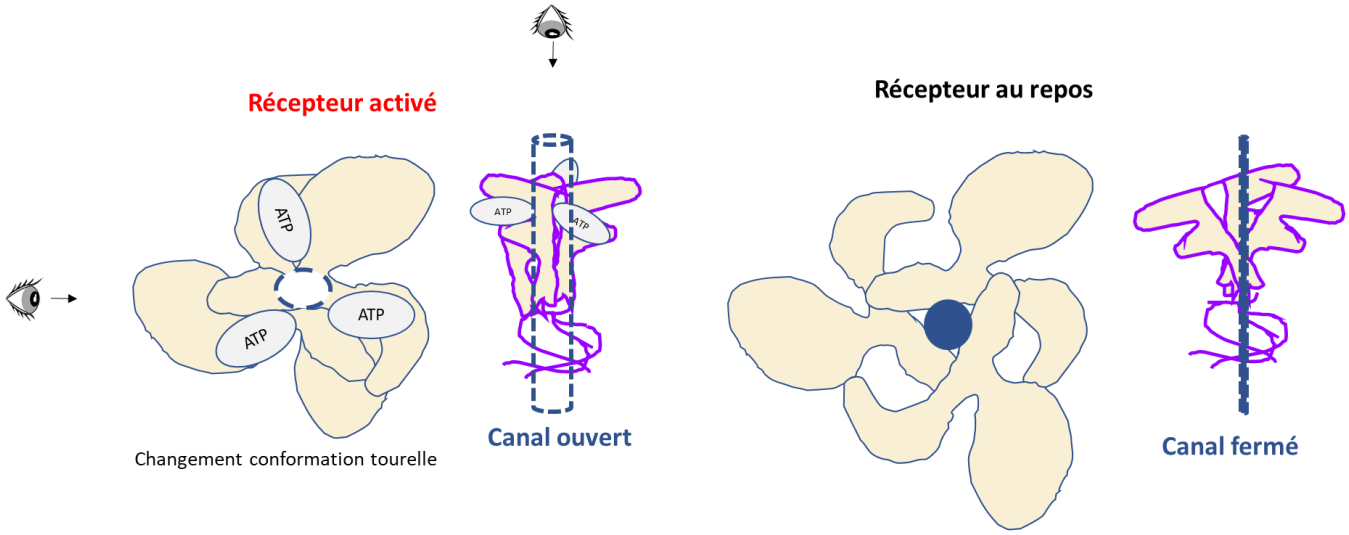

FIGURE 6 : Modélisation en trois dimensions de l'activation de la fonction canal de P2RX7

Jusqu'à trois molécules d'ATPe se fixent sur les sites de liaison du récepteur situés à l'interface entre deux sous-unités successives de la tourelle du récepteur. Un changement de conformation se produit alors et le canal de P2RX7 s'ouvre.

3. Ligands

a. Ligands nucléotidiques

L'ATPe est l'agoniste naturel de P2RX7. L'affinité de P2RX7 pour l'ATP est faible (de l'ordre de la centaine de micromolaires) en comparaison aux autres récepteurs P2RX (de l'ordre du nanomolaire). Les concentrations d'ATPe requises pour activer P2RX7 peuvent être observées dans les milieux tumoraux [76], mais aussi inflammatoires. En effet, l'analyse de lavages broncho alvéolaires a montré que les concentrations d'ATPe sont plus élevées chez des patients souffrant de fibrose pulmonaire idiopathique que chez les contrôles sains [77].

Chez la souris, un second mode d'activation a été décrit. Il repose sur le nicotinamide adénine dinucléotide (NAD) et l'enzyme mono-ADP-ribosyl-transférase (ART) 2, une enzyme présente au niveau de la surface membranaire cellulaire de lymphocytes T murins [78]. Le NAD est présent à de fortes concentrations dans les tissus inflammatoires [79] mais P2RX7 est insensible à la fixation directe du NAD. Néanmoins, ce dernier provoque l'activation du récepteur par un mécanisme indirect d'ADP-ribosylation des protéines membranaires, et ce à des concentrations de NAD cent fois plus faibles que celles nécessaires pour induire

l'activation de P2RX7 par l'ATPe. Cette activation est durable, elle se manifeste par un influx calcique, la formation d'un large pore membranaire et le clivage de CD62L. Elle induit également un mécanisme de mort cellulaire dépendant spécifiquement du NAD, appelé « NAD induced cell death » (NICD) [50,78–80]. Ce mécanisme n'est pas complètement élucidé, le NAD^+ se comportant soit comme un véritable agoniste du P2RX7, soit comme un agent potentialisateur qui abaisse le seuil d'activation par l'ATPe.

b. Ligands non nucléotidiques et modulateurs allostériques

L'activation de P2RX7 par l'ATPe, bien qu'étant le mode d'activation le plus classique, n'est pas exclusif. En effet il a été montré que l'activation par des agonistes non nucléotidiques était possible [81]. Dans les cellules microgliales de souris, les fonctions d'influx calcium, de modification de la structure cellulaire, de libération d'IL-1β caractéristique de l'activation de P2RX7, d'ouverture du large pore et de l'augmentation de cytotoxicité, pouvaient être observées en réponse à la présence de peptides amyloïdogènes β [82]. Le mécanisme d'activation direct par ligation, ou indirect par stimulation de la sécrétion d'ATP par P2RX7, reste discuté et non élucidé à ce jour [83].

Un autre agoniste non nucléotidique, le sérum amyloïde A (SAA) a également été étudié et montre une stimulation directe de la sécrétion d'IL-1β par P2RX7 [84], avec ici encore une question non résolue concernant le mode d'action engagé puisque, un pré-traitement par l'apyrase - une ATP-diphosphohydrolase dont la conséquence attendue est la réduction de la concentration en ATPe - potentialise l'activation de P2RX7 par le SAA, ce qui s'avère contre-intuitif. Néanmoins cela confirme que le SAA n'induit pas de libération d'ATP par P2RX7 mais semble interagir avec P2RX7 en le potentialisant, avec un mode d'action incompris, potentiellement compétitif avec celui de l'ATPe.

Certains antibiotiques naturels se comportent comme des agonistes de P2RX7. Les cathélicidines sont des peptides antimicrobiens endogènes exprimés chez les mammifères soit de manière constitutive, soit après une lésion tissulaire [85,86]. La cathélicidine LL-37, présente chez l'homme, est emmagasinée dans les cellules de l'immunité (granulocytes, lymphocytes, macrophages) et les cellules épithéliales. Ce peptide induit l'influx calcique,

l'ouverture du large pore et la libération IL-1β ainsi que la libération d'ATP par la cellule [87,88]. Il favorise la prolifération cellulaire via P2RX7 [89]. Ce peptide a aussi été décrit pour permettre la restauration d'une activité d'ouverture du large pore de P2RX7 sur un système d'expression hétérologue (cellules HEK293) qui exprime un variant de P2RX7 murin tronqué pour la queue C-terminale, un domaine historiquement décrit comme nécessaire à la formation du large pore [38].

Le lipopolysaccharide (LPS), endotoxine bactérienne classiquement présente lors d'une décharge bactériémique toxinique, a été montré comme un agoniste de P2RX7 par un mécanisme au moins indirect lié à la stimulation de la sécrétion d'ATP cellulaire [90] couplé à l'abaissement du seuil d'activation de P2RX7 [91].

La fonction de P2RX7 peut être modulée par des modulateurs allostériques positifs (MAP) ou négatifs (MAN) [92]. Certains ions, en particulier Mg^{2+}, Ca^{2+}, Zn^{2+}, des stéroïdes et des lipides dont les polyphosphates de phosphatidylinositol (PIP) [93] se comportent comme des MAN de P2RX4 et par extension pour P2RX7. Un antibiotique d'origine bactérienne, la polymyxine B, agit comme un MAP de P2RX7 en potentialisant l'influx calcique, l'ouverture du large pore et la cytotoxicité liée à P2RX7, chez des lignées murines et chez des macrophages humains [94,95]. L'ivermectine, utilisée comme agent antiparasitaire, interagit avec certains canaux ioniques [96,97] et agit comme un MAP de P2RX7 chez l'homme [98]. Sur la base de molécules antagonistes de P2RX7 dont la structure a été modifiée, des MAP ont été développés comme le dérivé anthraquinonique Cibacron Blue [99] et module positivement et de façon non sélective les récepteurs P2RX. Plus récemment, des ginsénosides structurellement apparentés aux stéroïdes et étant particulièrement présents dans le ginseng - une plante utilisée en phytothérapie - ont montré une activité de MAP pour P2RX4 et P2RX7 [100,101]. Ainsi, l'utilisation de MAP ou de MAN pourrait représenter une approche prometteuse pour cibler P2RX7.

c. Site catalytique (ATP)

P2RX7 est constitué de trois sous unités du récepteur formant un récepteur trimérique, et la poche de fixation de l'ATPe est située à l'interface entre deux sous unités successives [47] ce qui représente donc au total trois sites de liaison de l'ATPe pour un récepteur. Ces sites de

liaisons sont particulièrement peu accessibles sur un plan structurel et stéréochimique par rapport aux autres P2RX, ce qui explique la faible affinité de P2RX7 pour son ligand endogène. Une particularité pour P2RX7 réside dans la bordure de la poche de liaison qui comporte des acides aminés chargés positivement, au nombre de sept, et deux acides aminés hydrophobes [102,103], ainsi que quatre résidus lysines qui participent de la sensibilité particulièrement importante de ce récepteur à l'inhibition par de l'ATP oxydé [104]. De plus, l'absence du résidu isoleucine en 217 expliquerait également la moindre sensibilité de P2RX7 à l'ATPe et la nécessité de fortes concentrations de ce ligand pour entrainer une activation du récepteur [83].

d. Site allostérique

P2RX7 possède comme d'autres P2RX, en plus de son site catalytique de liaison à l'ATPe, un site allostérique constitué d'une poche qui est située à l'interface entre deux sous-unités adjacentes, à proximité et en dedans du site de liaison à l'ATPe. Cette poche allostérique est particulièrement étudiée pour le développement pharmacologique de MAN ou MAP, qui constituent des candidats thérapeutiques potentiels pour traiter des maladies inflammatoires ou cancéreuses. L'analyse cristallographique de P2RX7 lié à des MAN a montré que lorsque ces derniers sont positionnés dans le site allostérique, ils empêchent la rotation de la tourelle de P2RX7 et de ce fait empêchent l'ouverture du canal cationique [47] (Figure 7).

La connaissance de la structure et de l'emplacement des sites allostériques par rapport aux sites catalytiques est fondamentale et pose certaines questions. En effet, d'après les modélisations tridimensionnelles, le site allostérique se rétrécirait lors de la fixation de l'ATPe, le rendant moins accessible une fois le récepteur en conformation activée, suggérant que l'utilisation de modulateurs allostériques thérapeutiques positifs ou négatifs ciblant cette poche allostérique, soient d'utilisation peu aisée en termes de pharmacocinétique et de pharmacodynamique. Ainsi, un milieu tissulaire riche en ATPe pourrait rendre P2RX7 insensible à l'usage de ce type d'agent pharmacologique, et pourrait nécessiter plutôt l'utilisation d'agent (agonistes ou antagonistes) compétitifs de très haute affinité ciblant le site catalytique pour moduler P2RX7 [83]. Néanmoins, sachant que l'affinité de ce récepteur pour l'ATPe est particulièrement faible [38], nous pouvons présumer que des modulateurs de haute

affinité pourront toujours accéder au site de fixation allostérique quelle que soit la concentration d'ATPe dans le MET.

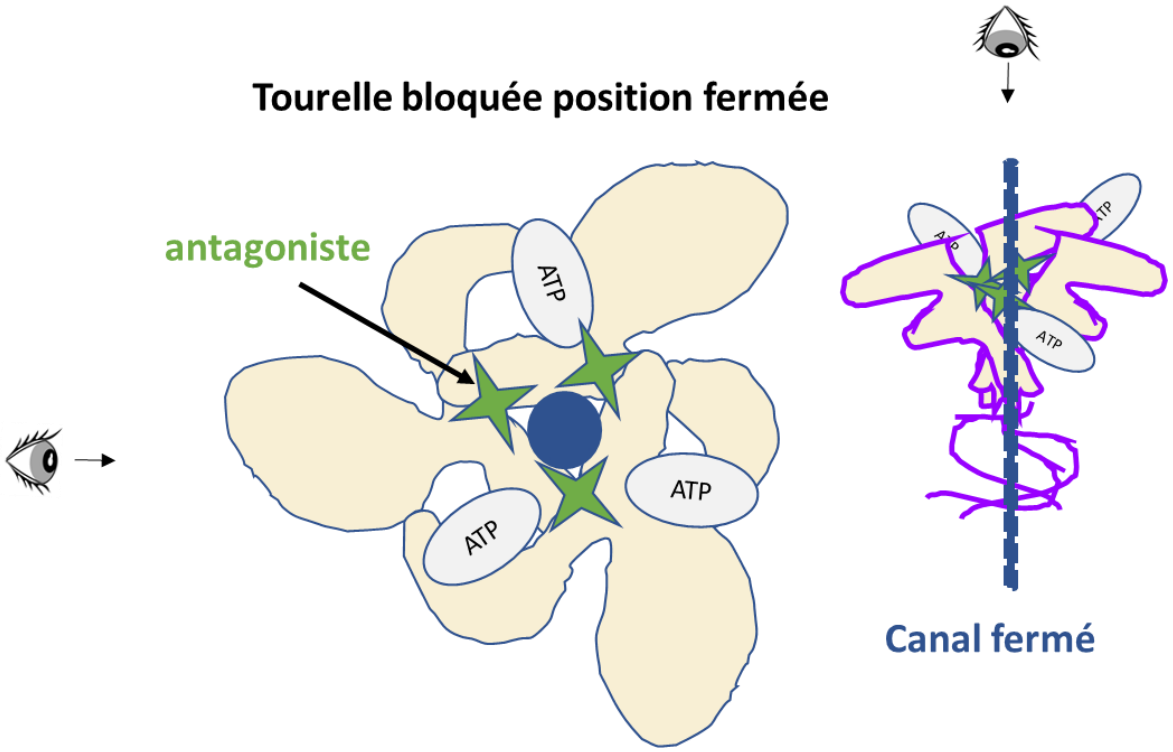

FIGURE 7 : Modélisation en trois dimensions de l'antagonisation du site allostérique de P2RX7

L'utilisation d'antagoniste de P2RX7 n'est pas seulement possible par antagonisme compétitif du site catalytique mais aussi par l'utilisation de molécules spécifiques du site allostérique. L'occupation du site allostérique par de tels composés bloque la conformation de la tourelle du récepteur qui ne peut plus se mouvoir ni induire de rotation, ce qui verrouille le canal en position fermé, malgré la présence de son ligand endogène au niveau des sites de liaison.

4. Eléments influençant la localisation du récepteur

a. Extrémité C-terminale

Pour être fonctionnel, le récepteur doit être correctement inséré dans la membrane, et certains domaines constitutifs ou éléments associés à P2RX7 sont en mesure de contrôler cette localisation.

L'extrémité C-terminale constitue près de 40% de la protéine P2RX7. Elle est localisée en intracellulaire mais contient un segment lipophile de 21 amino-acides qui forme une boucle de réentrée intramembranaire. La présence de cette extrémité C-terminale est importante pour la formation du large pore membranaire [38,105] et la pleine fonction d'influx calcique

[105,106], et participe de façon non exclusive à l'adressage de P2RX7 à la surface cellulaire [105]. Des expériences de criblage par mutagénèse dirigée [69] ont permis de montrer que 95% de l'extrémité C-terminale, étaient nécessaires à la fonction d'ouverture du large pore et que certains domaines (résidus 551-581 ainsi que certaines mutations ponctuelles notamment C572G, R574G, ou F581G) étaient indispensables à la localisation membranaire du récepteur [107]. Ceci souligne l'importance fondamentale portée par l'extrémité C-terminale de P2RX7. En plus des fonctions sus-citées, l'extrémité C-terminale est impliquée dans la liaison au LPS [91,108] et à la calmoduline, un modulateur de l'influx calcique et un carrefour enzymatique et ionotropique essentiel [109,110]. Par ailleurs, certaines régions présentent une homologie avec les sites de liaison pour les protéines cytosquelettiques (discuté dans la section III.C.ii.2.a) et ont été identifiées comme permettant la liaison aux filaments d'actine [108,111], alors que d'autres (en amont des acides aminés 354 à 364 et en aval des acides aminés 378-387) présentent des motifs de reconnaissance du cholestérol [112] pouvant modifier l'angle d'inclinaison de TM2 ou agir comme un ancrage membranaire et ainsi faciliter les mouvements nécessaires à l'ouverture du canal et/ou des pores [75,107,113] (Figure 8).

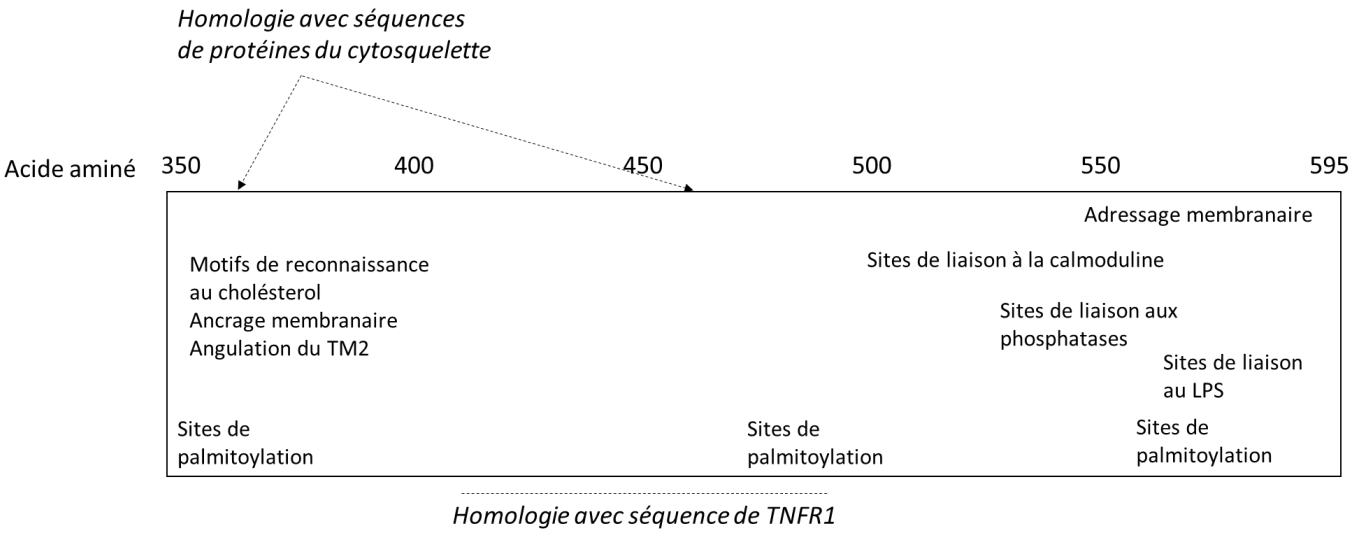

FIGURE 8 : Sites de liaison et séquences homologues de l'extrémité C terminale de P2RX7

L'extrémité C-terminale est symbolisée par l'encadrement rectangulaire, la position des sites de liaison est indiquée en regard du niveau de la séquence d'amino-acides. Les régions dont la séquence est homologue à la séquence codante pour d'autres protéines notables, sont indiquées en italique.

b. Extrémité N-terminale, influence des étiquettes peptidiques

L'influence de l'extrémité N-terminale sur la fonction du récepteur est un élément qui a été très étudié et discuté. Ce domaine contient un site consensus de phosphorylation de la protéine kinase C conservé dans tous les sous-types P2X [65] (Figure 9). L'importance d'un domaine N-terminal intègre est souligné par une étude réalisée en 2018 qui a montré qu'une étiquette peptidique de petite taille, l'hémagglutinine (HA), impacte les fonctions d'ouverture du large pore de P2RX7 humain sans influencer les fonctions d'influx calcique, alors qu'une étiquette de plus grande taille, la protéine fluorescente verte (eGFP), impacte ces deux fonctions. En revanche, l'étiquette eGFP en C-terminal n'impacte aucune des fonctions biologiques de P2RX7. Ces données sont en contradiction avec des études réalisées sur p*2rx7* de rongeurs, dont le transcrit pleine taille partage 80% d'homologie avec celui du *P2RX7* humain [114]. En effet, si une étiquette en N-terminal impacte les fonctions de P2RX7 humain, il a été constaté que cette même étiquette sur le récepteur P2RX7 de rat, n'avait aucune conséquence sur la localisation (étude en microscopie confocale) et les fonctions d'influx calcique et d'ouverture du large pore [115,116]. Ces données corroborent une étude indépendante réalisée en 2002 par Smart et coll. qui a comparé l'étiquetage N-terminal à l'étiquetage C-terminal sur la localisation et les fonctions biologiques de P2RX7 de rat exprimé dans des ovocytes de Xénope ainsi que dans la lignée HEK293, et qui concluait à une absence d'impact de l'étiquette en N-terminal alors que celle en C-terminal impactait les fonctions d'influx calcique, bien que l'insertion à la membrane était conservée [117]. Collectivement, ces résultats soulignent l'importance d'une extrémité C-terminale intègre pour assurer la fonction canal de P2RX7, et posent la question de l'impact des étiquettes peptidiques utilisées dans les études fonctionnelles de P2RX7 humain et murin.

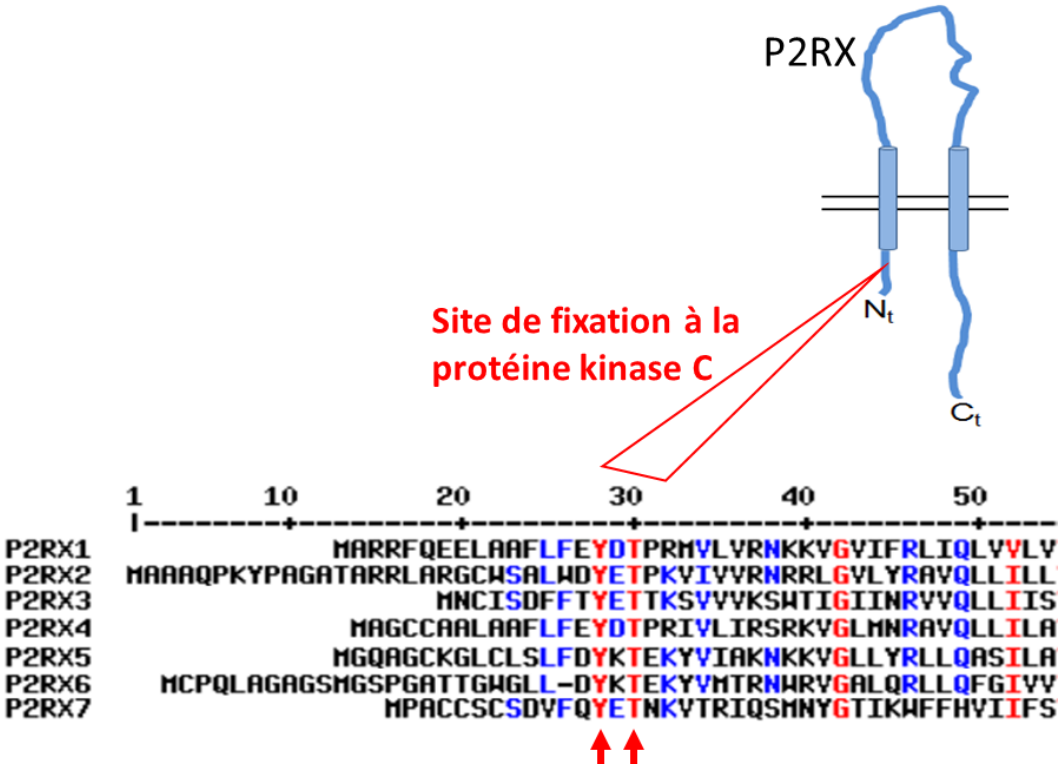

FIGURE 9 : Conservation au sein des récepteurs P2RX d'un site consensus de liaison à la protéine kinase C

Le site de fixation à la protéine kinase C (tyrosine en position 28 et thréonine en position 30, indiquées par les flèches rouges) est consensuel à tous les récepteurs P2RX après alignement de séquences (Outil en ligne "Multiple sequence alignment with hierarchical clustering", F. Corpet, 1988, Nucl. Acids Res., 16 (22), 10881-10890).

c. Palmitoylation, glycosylation

Alors que l'organisation spatiale de P2RX7 est fortement dépendante de son intégrité structurale (extrémité N-terminale, domaines transmembranaires, boucle extracellulaire, longue extrémité C-terminale), il a été suggéré que les phospholipides membranaires soient capables de moduler la localisation du récepteur. Cette régulation s'effectuerait par le biais d'interactions de ces phospholipides avec l'extrémité C-terminale, contrôlant le trafic membranaire de P2RX7 [108]. Une telle association entre P2RX7 et les radeaux lipidiques a été observée dans les cellules T [118], dans les cellules épithéliales alvéolaires de poumon de souris [119], et dans les cellules de la glande sous-mandibulaire de rat [120]. La régulation fonctionnelle de P2RX7 par le phosphatidylinositol 4,5-bisphosphate (PIP2) a également été démontrée dans des expériences de patch-clamp avec des ovocytes de *Xenopus laevis*, où certains acides aminés de P2RX7 humain se sont avérés importants pour l'interaction avec le

PIP2 [121]. De plus, comme vu précédemment, la composition lipidique membranaire conditionne les propriétés de la membrane cellulaire et l'opportunité de la formation du large pore membranaire, qui n'est donc pas exclusivement dépendant de la présence de l'extrémité C-terminale, bien que sa présence soit cruciale [83].

Par ailleurs, le degré de palmitoylation est aussi nécessaire pour le bon adressage membranaire de P2RX7. La palmitoylation est une modification post-traductionnelle réversible qui est susceptible d'affecter la stabilité et le trafic des protéines entre les différents compartiments de la machinerie cellulaire [122]. Il existe 16 sites potentiels de palmitoylation de P2RX7 et cette palmitoylation du récepteur est fondamentale pour l'association de P2RX7 à la surface membranaire et son maintien à la membrane en allongeant la demi-vie du récepteur [123]. Les mécanismes qui régulent la palmitoylation de P2RX7 ne sont pas décrits à ce jour ; néanmoins, il a été montré qu'ils ne sont pas influencés par la présence ou non d'ATPe.

L'adressage membranaire de P2RX7 repose aussi sur son état de glycosylation. Le P2RX7 humain est glycosylé sur cinq acides aminés (187, 202, 213, 241 et 284). Une mutation au niveau de l'acide aminé 187 impacte la localisation membranaire de P2RX7 et les événements de signalisation induits par les ligands nucléotidiques du récepteur. La région extracellulaire de P2RX7 entourant le site de glycosylation du résidu 187 est donc essentielle pour assurer l'adressage membranaire et la fonction de P2RX7 [124].

5. Fonctions biologiques du récepteur

a. Fonction canal-macropore

P2RX7 est un récepteur canal capable d'induire un influx calcique et influx de sodium, et un efflux de potassium, lorsqu'il est stimulé par son ligand. Cette fonction est partagée par l'ensemble des récepteurs P2RX, et est intimement liée à certains acides aminés présents dans le deuxième domaine transmembranaire [125]. La fonction d'influx calcique attire particulièrement l'attention dans la compréhension de phénomènes physiopathologiques, ce cation représentant un second messager essentiel dans les fonctions de signalisation cellulaire et en particulier dans la fonction immunitaire. En effet, le calcium, stocké dans le cytoplasme est impliqué dans la régulation de nombreux facteurs de transcription. Il est capable

d'interagir avec la calmoduline et de moduler sa conformation, permettant, via la fixation à la calcineurine, d'entrainer la localisation nucléaire des facteurs de transcription NFAT (facteur nucléaire des lymphocytes T activés) et NF-κB (facteur nucléaire kappa-B) qui régulent l'expression de gènes contrôlant des fonctions de réponses immunitaires lymphocytaires [126]. De plus, le calcium est impliqué dans la dégranulation mastocytaire, l'activation des macrophages, des cellules natural Killer (NK) et des cellules dendritiques [127]. Alors qu'une courte activation du récepteur P2RX7 est susceptible d'induire un influx calcique prolongé, il existe un fort potentiel pathogène théorique d'une stimulation au long cours de P2RX7 dans les tissus. Ce potentiel pathogène a été étudié notamment dans des états inflammatoires tissulaires chroniques comme l'ostéoporose, les pathologies inflammatoires chroniques (maladie inflammatoire chronique intestinale, broncho-pneumopathie chronique obstructive, fibrose pulmonaire idiopathique), les pathologies auto-immunes, les rejets de greffe, le cancer [127–130].

Une des spécificités de P2RX7 au sein de la famille des récepteurs P2RX, est sa fonction d'ouverture d'un large pore membranaire autorisant le passage de molécules dont la taille peut aller jusqu'à 900 Da [131]. Cette caractéristique positionne l'intérêt de P2RX7 en pathologie humaine inflammatoire et cancéreuse. En effet une stimulation soutenue et prolongée dans le temps, peut conduire à la lyse cellulaire par perméabilisation membranaire [132]. La faible affinité de P2RX7 pour l'ATPe s'oppose à une sur-stimulation et une mort cellulaire exagérée médiée par ce récepteur, qui pourrait entrainer un cercle vicieux avec libération d'ATP intra-cellulaire dans le milieu extracellulaire, et de dommages associés aux motifs moléculaires associés aux dégâts (DAMPS) [133].

Deux mécanismes de formation du large pore ont été proposés, avec en premier lieu une hypothèse de dilatation du canal de P2RX7 qui passerait d'un état de canal sélectif aux cations à un état de pore non sélectif qui autorise le passage de larges molécules. Une autre hypothèse, faisant intervenir d'autres protéines pourvoyeuses de pores membranaires notamment la Pannexine 1, a été soulevée [134]. Finalement, des études plus récentes ont permis, par analyses électrophysiologiques et photochimiques, de montrer que l'hypothèse de dilatation d'un seul et même pore intrinsèque à la structure de P2RX7, serait à privilégier et constituerait la voie de passage de larges molécules comme le N-méthyl-D-glucamine ou la

spermidine [83], et que la perméabilisation aux cations serait quasiment simultanée à la perméabilisation aux larges molécules [75,135–138].

b. Activation de l'inflammasome

Le système immunitaire inné est la première ligne de défense de l'hôte et c'est par les récepteurs de reconnaissance de motifs ou « patterns » (PPR) reconnaissant les DAMPS, dont l'ATPe, ou les PAMP (motifs moléculaires associés aux agents pathogènes), que les voies inflammatoires vont s'activer [139]. Les inflammasomes sont définis comme des complexes protéiques de détection (PPR) qui, en réponse aux DAMPs ou PAMP, s'oligomérisent pour former une plate-forme d'activation de la pro-caspase-1 en caspase-1 qui est une voie inflammatoire majeure. L'inflammasome NLRP3 (NOD-like receptor family, pyrin domain containing 3) est un complexe protéique constitué d'un domaine pyrine amino-terminal (PYD), un domaine central de liaison aux nucléotides et d'oligomérisation (NOD ; aussi appelé NACHT), et un domaine répété riche en leucine (LRR) [140]. Le domaine pyrine du NLRP3 interagit avec le domaine pyrine du domaine de recrutement de la caspase (ASC) pour initier l'assemblage de l'inflammasome [141]. Le domaine NOD a une activité ATPase qui est nécessaire pour l'oligomérisation de NLRP3 après son activation [142]. La voie ATP/P2RX7/NLRP3 est étroitement liée à la production des cytokines pro inflammatoires IL-1β et IL-18. [90,143,144]. L'évènement initial est la stimulation de P2RX7 par l'ATPe et l'ouverture des larges pores membranaires qui permettent l'entrée de DAMPs dans la cellule, et ces DAMPs induisent l'assemblage de l'inflammasome NLRP3 [145,146]. Ce complexe va recruter la protéine accessoire ASC, qui elle-même recrute la pro-caspase-1 inactive, entrainant un clivage en caspase-1 active à capacité protéolytique, et cette dernière clive les formes immatures pro-IL-1β et pro-IL-18 en formes matures IL-1β et IL-18 [147,148]. Ces données sont soutenues par les études qui montrent que les macrophages isolés de souris dépourvues d'ASC ou de NLRP3 sont incapables de sécréter de l'IL-1β en réponse à l'ATPe [148–151].

La production des cytokines pro-inflammatoires IL-1β et IL-18 par les cellules dendritiques et les macrophages, qui sont des cellules présentatrices d'antigènes, est requise pour activer et différencier les lymphocytes T naïfs en lymphocytes T effecteurs afin d'induire une réponse

immunitaire [152]. Ainsi, sous la dépendance d'une forte stimulation par l'ATPe, l'ouverture du large pore et l'activation de l'inflammasome par P2RX7 conditionnent une fonction de modulation positive de l'immunité [152].

En contraste, une libération prolongée d'ATPe, comme nous pouvons l'observer dans les inflammations tissulaires chroniques, qu'elles soient d'origine infectieuses, inflammatoires ou cancéreuses, a pour conséquence un effet anti-inflammatoire et une condition d'immuno dépression localisée [153,154]. Cette condition est potentialisée par l'action des ectonucléotidases impliquant l'hydrolyse de l'ATPe en ADPe [40] qui active les récepteurs P1R. En conséquence de cette activation, la sécrétion de l'interleukine IL-12 et des cytokines pro-inflammatoires est inhibée, tandis que celle des cytokines anti-inflammatoires IL-4 et IL-10 est potentialisée [155].

e. P2RX7 et contrôle du développement tumoral

i. Rôle pro tumoral

De nombreux auteurs ont étayé un rôle pro-tumoral à P2RX7 après avoir observé sa surexpression dans plusieurs cancers comme le sein [156], la prostate [157], le colon [158], la thyroïde [159], le pancréas [160], le cholangiocarcinome. Cette action pro tumorale passerait par l'activation des voies de signalisation intracellulaires (AKT, MAPK) par les cellules tumorales, qui promeuvent croissance, prolifération, migration et invasion cellulaire [161–164]. Cette hypothèse est soutenue par l'observation que des niveaux élevés d'ATPe sont observés dans les tissus tumoraux [23] et ceci se vérifie dans le cancer du sein, où l'activation de P2RX7 augmente l'influx de calcium et la croissance et migration des cellules tumorales [165]. Dans le cancer du sein mais aussi de la prostate, l'expression à un niveau élevé du récepteur P2RX7 activerait les voies de signalisation PI3K/AKT/mTOR et ERK1/2, et augmenterait le niveau d'expression de l'IL-8 et de la métalloprotéase 3 et favoriserait la transition épithélio-mésenchymateuse [166,167] et une prolifération tumorale. Un rôle pro-tumoral a aussi été décrit dans le cancer du côlon, par activation de la voie de signalisation AKT/mTOR [168] par les cellules tumorales et dans le cancer du pancréas par activation de la protéine kinase C, de ERK1/2 et de la kinase c-Jun N-terminale par les cellules tumorales [169]. Des études sur le craniopharyngiome et les carcinomes épidermoïdes ORL ont montré que

l'expression de P2RX7 à un niveau élevé, corrélait avec l'accumulation de corpuscules de l'inflammasome NLRP3, entrainant une prolifération tumorale [170,171]. De plus, des études de survie *in silico* montrent que la surexpression de *P2RX7* serait corrélée avec une moindre survie globale dans le cancer du côlon [171,172]. Néanmoins, comme discuté en III.C.e, une surexpression *in silico* ne veut pas dire que la protéine est fonctionnelle et capable d'induire la lyse cellulaire.

ii. Rôle anti tumoral

Bien que de nombreuses études aient soulevé l'hypothèse d'un rôle pro-tumoral de P2RX7 notamment en démontrant l'intérêt d'antagoniser P2RX7 dans des modèles de lignées tumorales comme vu en section III.C.f, la croissance tumorale est significativement plus importante chez les souris *p2rx7* KO. En effet, une étude de carcinogénèse *in situ* colique induite par le dioctyl sodium sulfosuccinate (DSS), réalisée par l'équipe de mon laboratoire de thèse, a montré que l'inactivation génétique et pharmacologique de P2RX7 atténue l'inflammation colique induite par le DSS [173]. Cette même étude a également montré que la progression tumorale de souris ayant subi une injection sous-cutanée de la lignée de cellules de cancer du poumon Lewis Lung Carcinoma (LLC), était plus importante pour les souris excisées pour *p2rx7* que pour les souris sauvages [173]. Des résultats similaires ont été obtenus dans deux autres modèles tumoraux, de mélanome (B16) et de cancer colorectal (CT26) par une équipe indépendante [174]. Cette dernière étude a montré qu'il existe une moindre infiltration en cellules immunitaires intratumorales chez les souris *p2rx7* KO que chez les souris contrôles [174]. Ces résultats démontrent l'importance de P2RX7 dans le recrutement de cellules immunitaires intratumorales. L'équipe de De Marchi a ensuite démontré que l'infiltrat immunitaire intra-tumoral de souris *p2rx7* KO était appauvri en lymphocytes $CD8^+$ et plus riche en lymphocytes T régulateurs surexprimant OX40, PD-1, et CD73, à la faveur d'un MET peu favorable à une réponse immunitaire anti tumorale et d'un infiltrat tumoral plus agressif [161]. Ces études mettent en exergue le rôle immunomodulateur positif de P2RX7.

Ces différents résultats soulignent la controverse qui existe quant au rôle de P2RX7 dans la carcinogenèse. Son expression non seulement par les cellules tumorales pour lesquelles le maintien d'une fonction d'ouverture du large pore et de perméabilisation cellulaire contrôlerait le développement tumoral, doit être mis en balance avec les fonctions pro-

prolifératives du récepteur, ainsi qu'avec l'état d'immunomodulation qu'il exerce sur les cellules de l'hôte. Il est vraisemblable que le récepteur ne présente pas un rôle statique, mais que son rôle pro ou antitumoral dépend des concentrations de ligand (ATPe) présentes dans le milieu, de la structure conformationnelle du récepteur, de sa topographie spatiale d'expression cellulaire et tissulaire, du cancer étudié, et de l'ensemble de ces éléments combinés.

f. Expression de P2RX7 dans les tumeurs humaines solides

L'expression de P2RX7 a été largement étudiée dans les tumeurs solides, et il a été historiquement affirmé que le récepteur y était surexprimé. Le MET étant un milieu riche en ATPe, et P2RX7 étant impliqué dans la perméabilisation et la lyse cellulaire sous la dépendance de ce ligand, objectiver l'expression et la fonction de P2RX7 par les cellules tumorales est d'une importance cruciale [175]. En pratique, la plupart des études ayant étudié l'expression de P2RX7 dans les tumeurs, ont utilisé des outils d'immunohistochimie qui ciblaient soit un épitope en C-terminal, soit en N-terminal, soit au niveau de la boucle extracellulaire, ou des outils de qPCR, qui ne permettent pas d'objectiver les fonctions biologiques du récepteur. Un anticorps ciblant spécifiquement les formes non fonctionnelles, nommé nfP2RX7, est utilisé dans certaines études.

L'expression de P2RX7 dans le cancer de prostate a été montrée en immunohistochimie (IHC) [176]. Une étude mettant en œuvre l'usage de l'anti-nfP2RX7, a mis en évidence un lien entre cette expression du nfP2RX7 et un moins bon pronostic des patients souffrant de cancer de prostate [177].

Le carcinome rénal à cellules claires a été étudié par IHC (anti-N-terminal), dans lequel l'expression de P2RX7 est plus faible en zone tumorale qu'en zone non tumorale, avec un impact sur la survie lorsque P2RX7 était surexprimé en zone tumorale [178].

Le récepteur a été identifié dans le cancer colorectal par IHC (anti-C-terminal) [179], et une corrélation entre la surexpression du récepteur tumoral et un plus gros volume tumoral avec moindre survie a été retenue [172], avec des disparités de niveau d'expression entre les patients, et une présence du nfP2RX7 [177,180]. L'expression de P2RX7 a aussi été montrée

dans le cancer gastrique, avec une corrélation entre le niveau d'expression élevé et la moindre survie des patients [181], ainsi que dans le carcinome épidermoïde œsophagien [182].

L'étude de P2RX7 dans le cancer du sein en IHC a été réalisée et a montré que les carcinome lobulaire et canalaires exprimaient des niveaux élevés de nfP2RX7 [183] alors que le sein non tumoral ne l'exprimait pas. Une diminution de l'expression de P2RX7 en zone tumorale versus non tumorale a été montrée en IHC (anti-C-ter) [179,184].

Les carcinomes basocellulaires étudiés en IHC (anti-C-ter), expriment P2RX7 à un niveau élevé [185], et nfP2RX7 a été montré comme étant surexprimé dans ce cancer [186].

P2RX7, étudié en IHC (anti-C-ter), est surexprimé par le mélanome [187], et le nfP2RX7 a été également détecté dans cette tumeur alors qu'il n'est pas présent en peau saine.

Le neuroblastome exprime P2X7 à un niveau élevé en IHC, quel que soit le grade de la tumeur [188], et une corrélation entre surexpression de l'ARNm et moindre survie a été établie dans une étude indépendante [189].

L'expression de P2X7 a été analysée par IHC (anticorps et épitope inconnus) dans le carcinome ovarien et comparée à l'épithélium ovarien sain [20], l'expression était présente à un niveau équivalent entre les deux zones, et nfP2X7 était exprimé dans le carcinome ovarien [180,190].

P2RX7 est exprimé en IHC (anti-C-ter) dans le cancer de l'endomètre, mais à un niveau moins élevé en zone tumorale par rapport à la zone non tumorale du cancer de l'endomètre [179]. Par ailleurs, les cellules dysplasiques du col de l'utérus expriment nfP2X7 par rapport au tissu sain adjacent [190].

Le cancer de vessie exprime P2RX7 en analyse en IHC (anti-C-ter), et une étude distincte a confirmé l'expression de nfP2X7 dans le tissu tumoral vésical [180,190].

Le cancer papillaire de la thyroïde exprime P2RX7 en analyse en IHC (anti-C-ter) et en analyse de l'ARNm, avec une expression à un niveau plus élevé dans la zone tumorale par rapport à la zone saine adjacente [191]. Cette observation est aussi vraie pour le cancer du pancréas qui montre une hyperexpression en zone tumorale par rapport à la zone saine, en IHC (anti-C-ter) et en ARNm [192], par ailleurs nfP2R7 est exprimé dans le tissus cancéreux pancréatique [180,190]. Cette hyperexpression en zone tumorale par rapport à la zone saine, est une particularité propre au cancer papillaire thyroïdien et au cancer du pancréas [179].

L'expression de P2RX7 dans le cancer du poumon a été observée en IHC (anti-N-ter) dans le LUAD et le carcinome épidermoïde bronchique [193], et également en PCR temps réel (qPCR) qui objective une surexpression du messager de *P2RX7* dans les cellules du lavage broncho-alvéolaire de tumeurs métastatiques [194].

Bien que la mise en évidence du nfP2RX7, qui dépend d'un anticorps non commercialisé, puisse objectiver la présence un récepteur non fonctionnel sur tissu tumoral fixé, l'expression en IHC et de l'ARNm ne permet pas de préjuger factuellement de la fonction de P2RX7, et peu d'études ont analysé la fonction de P2RX7 exprimé par les cellules tumorales issues de cancers solides *ex vivo* chez l'homme.

Les cellules tumorales humaines *ex vivo* prouvées fonctionnelles pour P2RX7 sont, à notre connaissance, le carcinome ovarien où la stimulation de P2RX7 conduit à l'activation des voies AKT/mTOR et ERK [20] ; le carcinome papillaire thyroïdien où l'activation de P2RX7 conduit à la sécrétion d'IL6, un effet reversé par un antagoniste de P2RX7 [191] ; le mélanome où l'activation de P2RX7 conduit à l'ouverture de son large pore [187] ; les cellules de carcinome épidermoïde œsophagien cultivées en culture primaire pour lesquelles la stimulation de P2RX7 conduit à un effet antiprolifératif, effet reversé par l'utilisation d'un antagoniste spécifique et d'un ARN interférant [182].

P2RX7 est exprimé dans le CNPC, mais ses fonctions biologiques n'ont pas été caractérisées. Le fait que des cellules tumorales humaines de CNPC expriment P2RX7 qui est impliqué dans la lyse cellulaire, pose la question de la fonction de ce récepteur dans ces cellules. En effet, les niveaux d'ATPe dans le tissu tumoral sont compatibles avec l'activation de P2RX7 et nous avons émis l'hypothèse que P2RX7 exprimé dans le CNPC devait être peu ou non fonctionnel.

g. *P2RX7* : Génétique descriptive

i. Le gène *P2RX7*

P2RX7 est un gène qui s'étend sur 53 Kilobases et comprend 13 exons. Il est situé à la position chromosomique 12q24 (Figure 10). L'organisation de ce gène a été décrite pour la première

fois chez l'humain par Buell et al. [195]. Il possède une région 3' non traduite (UTR) qui contient des cibles accessibles à des micro-ARN (miR) régulateurs, notamment les miR-150 et miR-186. Ces derniers ont été décrits pour réprimer la traduction de *P2RX7* [196], mais ces miRs n'ont pas montré de conséquence physiopathologique dans le CNPC à ce jour.

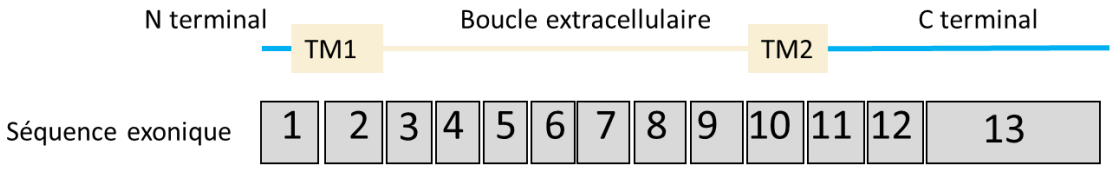

FIGURE 10 : Le gène *P2RX7*

Les domaines transmembranaires et la boucle extracellulaire sont représentés en beige, les extrémités intracytoplasmiques N terminale et C terminale sont représentées en bleu. Les exons sont positionnés en regard des domaines pour lesquels ils codent.

ii. Polymorphismes nucléotidiques simples

Le gène *P2RX7* est hautement polymorphe et contient de nombreux polymorphismes de nucléotides simples (SNPs) dont de nombreux sont synonymes ou présents en région intronique et peu étudiés. Certains SNPs non synonymes de *P2RX7* ont été étudiés plus particulièrement comme détaillés par Sluyter [197] et ont été associés à un impact fonctionnel de P2RX7 dans la physiopathologie de certaines affections chroniques infectieuses comme la tuberculose [198], inflammatoires comme la polyarthrite rhumatoïde [199], mais aussi cancéreuses comme la leucémie lymphoïde chronique [200] ou le cancer du sein [152]. Cependant, aucun de ces SNP n'est à ce jour utilisé en pratique clinique.

iii. Epissage alternatif

1. Description générale

L'épissage est un mécanisme de régulation de l'expression des gènes omniprésents qui permet la génération de plus d'une espèce d'ARN messagers (ARNm) à partir d'un seul gène. La majorité des gènes sont épissés, et ce mécanisme est impliqué dans la différenciation cellulaire en lignée et dans l'acquisition d'une différenciation tissulaire et le maintien structurel des organes [201]. Il s'agit non seulement d'un mécanisme physiologique de

modulation du protéome [202], mais aussi d'un mécanisme de pathogénie impliqué dans des affections variées [203]. L'épissage alternatif peut générer des ARNm qui diffèrent dans leurs régions non traduites (UTR) ou dans leurs régions codantes par de multiples mécanismes.

Le saut d'exon correspond à la suppression d'exons, soit par exons mutuellement exclusifs, soit par la sélection de sites d'épissage alternatif donneurs 5' ou accepteurs 3', soit par rétention d'introns, soit par un promoteur alternatif, soit par un site alternatif de polyadénylation (Figure 11). Par ailleurs, la modification du cadre de lecture peut aussi conduire à un épissage alternatif, entraînant la génération de différentes isoformes de protéines aux fonctions diverses. Des études génomiques ont permis de montrer que jusqu'à 95 % des pré-ARNm humains subissent un épissage alternatif [202,204] et plus d'un tiers d'entre eux génère de multiples isoformes protéiques [205], augmentant la diversité protéique. Ces protéines ne sont néanmoins pas toutes fonctionnelles. En effet, un transcrit d'ARNm peut être non codant et donc ne pas être traduit en une protéine.

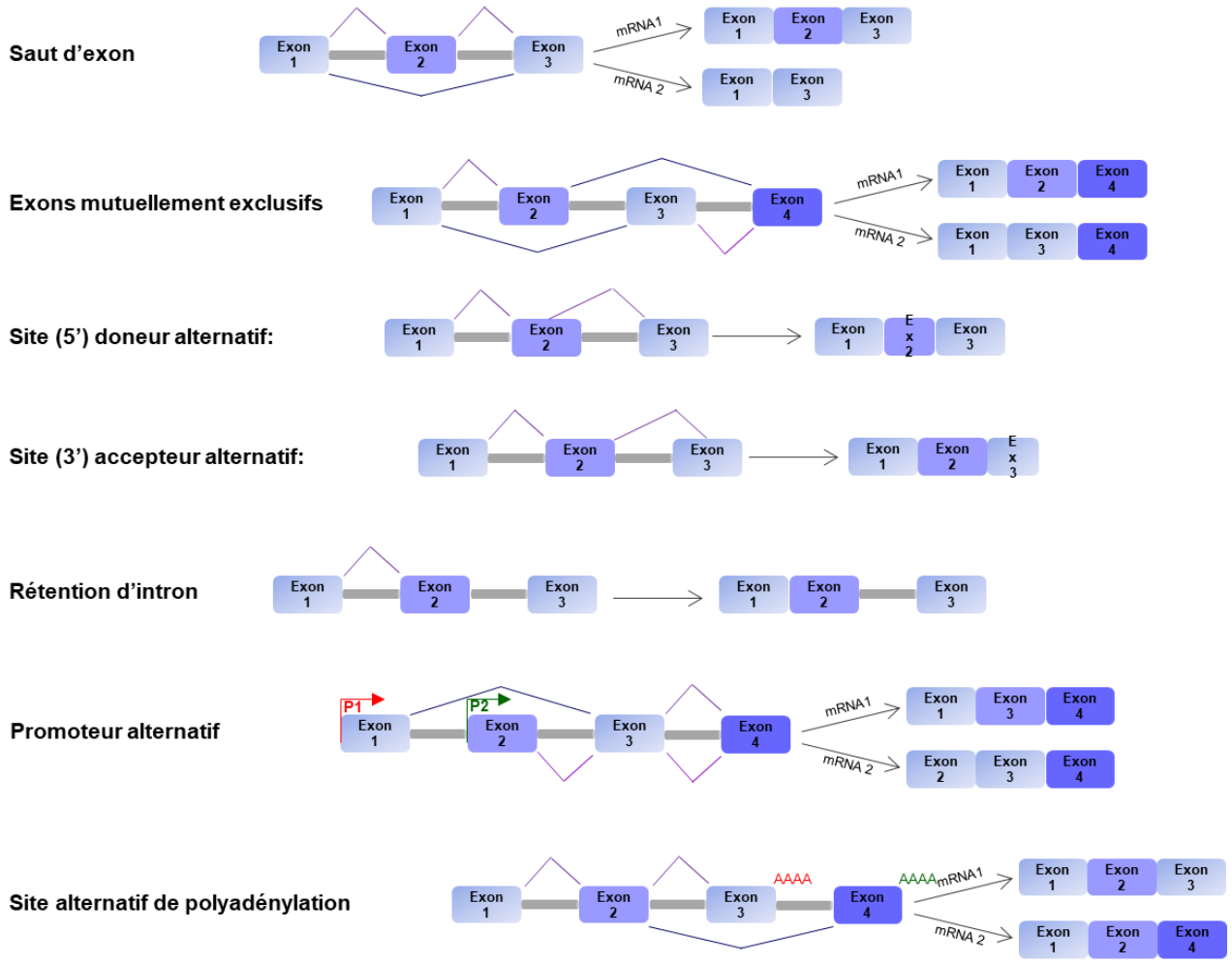

FIGURE 11 : Les mécanismes de l'épissage alternatif

2. Implications fonctionnelles

a. Sur les fonctions des protéines

Plusieurs modèles d'épissage alternatif plus ou moins complexes existent et participent à la diversité protéique de l'organisme. Ces combinaisons peuvent être spécifiques d'un organe, d'un tissu ou d'un type de cellule [203,206], les événements d'épissage alternatif conférant un gain biologique de fonctions étant étroitement liés au phénomène d'évolution de l'espèce. Pour mettre en évidence les épissages alternatifs conservés au cours de l'évolution d'un organisme, une approche utilisant des analyses de séquençage du transcriptome (ARN Seq) sur neuf tissus de cinq vertébrés [207] a permis de conclure que 500 exons avec des épissages alternatifs sont très bien conservés chez les mammifères. Ces exons codent pour des sites de phosphorylation, et leur épissage spécifique aux tissus peut avoir un effet important sur les voies de signalisation cellulaire. Il existe de fortes variations de ces épissages alternatifs inter-espèces, à un niveau qui dépasse les différences d'épissage alternatif entre les tissus au sein d'une même espèce [207]. Ainsi l'épissage alternatif ne dépend pas exclusivement d'une régulation locale inhérente à un organe ou un tissu, mais également de caractéristiques propres à une espèce et à son adaptation à son environnement, comme nous le détaillons dans la revue [63].

L'épissage et la régulation de la transcription permettent de contrôler la physiologie cellulaire, mais peuvent volontiers être impliqués dans diverses maladies humaines en modifiant ou même en supprimant certaines régions fonctionnelles de protéines essentielles. Les facteurs permettant la régulation précise de l'épissage alternatif sont eux-mêmes soumis à des régulations, qui peuvent à leur tour moduler tous les processus biologiques. En particulier, la phosphorylation des facteurs d'épissage est impliquée dans la régulation de l'épissage alternatif de gènes suppresseurs de tumeurs et de gènes régulateurs de la signalisation cellulaire et de l'apoptose, et joue un rôle dans le contrôle du développement tumoral [208]. La relation entre ce type de mutations et l'évolution vers un état pathologique a été étudiée par des approches informatiques [209] et des modèles animaux [210].

L'épissage alternatif est ainsi non seulement impliqué dans la diversité du protéome physiologique, mais aussi dans des pathologies aussi diverses que le diabète, les maladies neurologiques, les maladies cardiovasculaires, les maladies immunologiques et infectieuses ainsi que le cancer.

b. Sur la carcinogénèse chez l'homme

De nombreux exemples de pathologies cancéreuses ont été rattachées à un épissage alternatif pathogène. Cependant, dans quelques cas seulement, une relation de cause à effet a été démontrée. Parmi ces exemples, nous pouvons citer certains gènes notables, connus pour être impliqués en carcinogénèse [211].

LKB1 est un gène suppresseur de tumeur qui code pour une protéine kinase sérine/thréonine impliquée dans le contrôle de plusieurs processus cellulaires, notamment l'arrêt du cycle cellulaire, l'apoptose médiée par p53, la transformation induite par RAS, la polarité des cellules. L'épissage alternatif affectant l'intron 2 de *LKB1* conduit à une protéine tronquée par codon stop prématuré, que l'on observe chez des patients atteints du syndrome de Peutz-Jeghers, un trouble autosomique dominant associé à une polypose gastro-intestinale et à un surrisque de cancer [212].

Un autre exemple concerne le proto-oncogène *cKIT*, qui code pour une tyrosine kinase dont l'activation promeut la croissance de tumeurs stromales gastro-intestinales. L'épissage alternatif de l'exon 11 a été retrouvé chez des patients qui voient l'activité kinase décuplée avec perte du rétro-contrôle négatif [213].

Le gène *KLF6* est également cité, il s'agit d'un facteur de transcription considéré comme un suppresseur de tumeur, qui est impliqué dans le cancer de la prostate [214] et qui présente un site de régulation de l'épissage intronique qui peut entrainer un épissage alternatif de l'exon 2 et conduire à une protéine tronquée pour certains domaines fonctionnels. Cette protéine perd alors sa fonction suppresseur de tumeur, et se comporte comme un dominant négatif [214].

Le gène *CDH17* (Cadhérine 17) exprimé dans les carcinomes hépatocellulaires, conduit à un mauvais pronostic et à un surrisque de récidive tumorale [215] lorsque se produit un épissage alternatif de son exon 7.

Enfin, le gène *BRCA1*, gène classiquement recherché dans les cancers du sein et de l'ovaire familiaux, peut être affecté par une mutation ponctuelle héréditaire dans l'exon 18 en provoquant un saut d'exon [216].

Ainsi, l'épissage alternatif est en mesure de moduler la fonction de protéines impliquées dans la carcinogénèse, et nous avons émis l'hypothèse que les fonctions de P2RX7 dans le CNPC pourraient être impactées par l'expression de variants d'épissage.

3. Epissage alternatif de *P2RX7* chez l'homme

L'épissage constitutif de *P2RX7* conduit à l'ARNm commun *P2RX7A* pleine taille, mais 12 transcrits supplémentaires ont été décrits issus d'épissages alternatifs (Figure 12) [217]. Parmi ces variants d'épissage, dix ont été étudiés plus en détail. Quatre d'entre eux, les variants *P2RX7C, P2RX7E, P2RX7F* et *P2RX7G*, codent pour des protéines très tronquées qui ne sont pas en mesure d'être associées à un quelconque adressage membranaire ni fonctionnalité. Les variants d'épissage *P2RX7B* et *P2RX7J* ont été décrits comme potentiellement exprimés chez l'homme, et pouvant impacter les fonctions biologiques de P2RX7 [217].

Le variant *P2RX7B* en particulier, dont l'ARNm est présent dans presque toutes les cellules eucaryotes, est caractérisé par l'excision de ses 249 derniers acides aminés situés au niveau de l'extrémité C-terminale, et ces résidus sont remplacés par 18 acides aminés alternatifs [217]. P2RX7, pour être fonctionnel, doit s'associer sous forme d'un trimère membranaire, l'homotrimère décrit comme conservant une activité de canal ionique et d'ouverture du large pore étant celui de P2RX7A. Des homotrimères de P2RX7B ont été retrouvés dans les cellules. Ces homotrimères ont été décrits comme incapables d'ouvrir le large pore. Néanmoins, l'hétérotrimère P2RX7A/P2RX7B, qui existe dans des modèles d'expression hétérologue, a été décrit comme ayant une fonction d'ouverture du large pore incrémentée, et comme favorisant la croissance cellulaire [105].

L'épissage alternatif de l'exon 8, qui conduit à une mutation par modification du cadre de lecture avec apparition d'un codon stop prématuré, produit le variant *P2RX7J* [217]. La protéine résultante est composée de l'extrémité N-terminale, du premier domaine transmembranaire et des 2/3 de la boucle extracellulaire. Le récepteur P2RX7J est inactif seul, mais lorsqu'il est co-exprimé avec P2RX7A, il hétéro-oligomérise et confère un effet dominant négatif, ce qui peut protéger certains types de cellules de la mort cellulaire induite par l'ATPe [70].

P2RX7H, *P2RX7D* et *P2RX7F* résultent d'un épissage alternatif conduisant à l'insertion d'un exon supplémentaire et à la délétion des exons 5 et 8, respectivement [217]. Les protéines correspondantes sont dénuées d'extrémité N-terminale, du premier domaine transmembranaire et d'une partie de la boucle cytoplasmique. Ces isoformes ne sont donc pas correctement insérées dans la membrane cellulaire et conduisent à des formes non fonctionnelles, mais pourraient théoriquement être localisées dans le cytoplasme ou dans des vésicules intracellulaires.

L'épissage alternatif résultant d'un exon N3 additionnel, dont la structure est celle de *P2RX7H* mais que les auteurs nomment *P2RX7-V3* non codant, a été décrit comme exprimé à des niveaux élevés dans des lignées cellulaires issues de mélanome uvéal [218]. Il se comporterait comme un long ARN non codant oncogène et les auteurs le positionnent comme un biomarqueur intéressant dans cette pathologie.

Plus récemment, l'épissage alternatif *P2RX7L* a été décrit, résultat d'un saut d'exons 7 et 8 conduisant à une perte des sites de liaison de l'ATPe, et pouvant être induit par l'expression du SNP rs208307 capable de réguler cet épissage alternatif [219]. Les auteurs montrent que P2RX7L est capable d'hétéro-oligomériser avec P2RX7A et d'impacter la fonction d'ouverture du large pore du récepteur.

La formation d'hétéro-oligomères de P2RX7 associant P2RX7A et P2RX7B a été documentée dans la littérature, et serait en mesure d'augmenter les fonctions d'ouverture du large pore de P2RX7 [105]. Néanmoins, le delta d'augmentation d'EC50 de l'ouverture du large pore, de quelques micromolaires entre P2RX7A monotransfecté *versus* la transfection de l'hétéro-oligomère P2RX7AB, associé à l'absence de documentation des niveaux précis d'expression relative de l'isoforme P2RX7A et P2RX7B, devrait conduire à interpréter ces données prudemment. En effet, l'expression relative non pas de la protéine mais des ARNm de *P2RX7A* et *P2RX7B* seulement, était analysée en guise de contrôle. Certains auteurs ont en outre démontré dans un modèle d'ostéosarcome que les cellules exprimant les deux isoformes étaient plus prolifératives et plus enclines à induire une minéralisation [220].

Les variants d'épissage de P2RX7 sont en mesure d'affecter ses fonctions biologiques. Nous avons émis l'hypothèse que de tels variants d'épissage pourraient être exprimés dans le CNPC. Ainsi, l'objectif de mon travail de thèse a été de caractériser les fonctions biologiques de

P2RX7 dans le CNPC et d'étudier l'impact de l'expression de variants d'épissages de *P2RX7* sur les fonctions biologiques du récepteur.

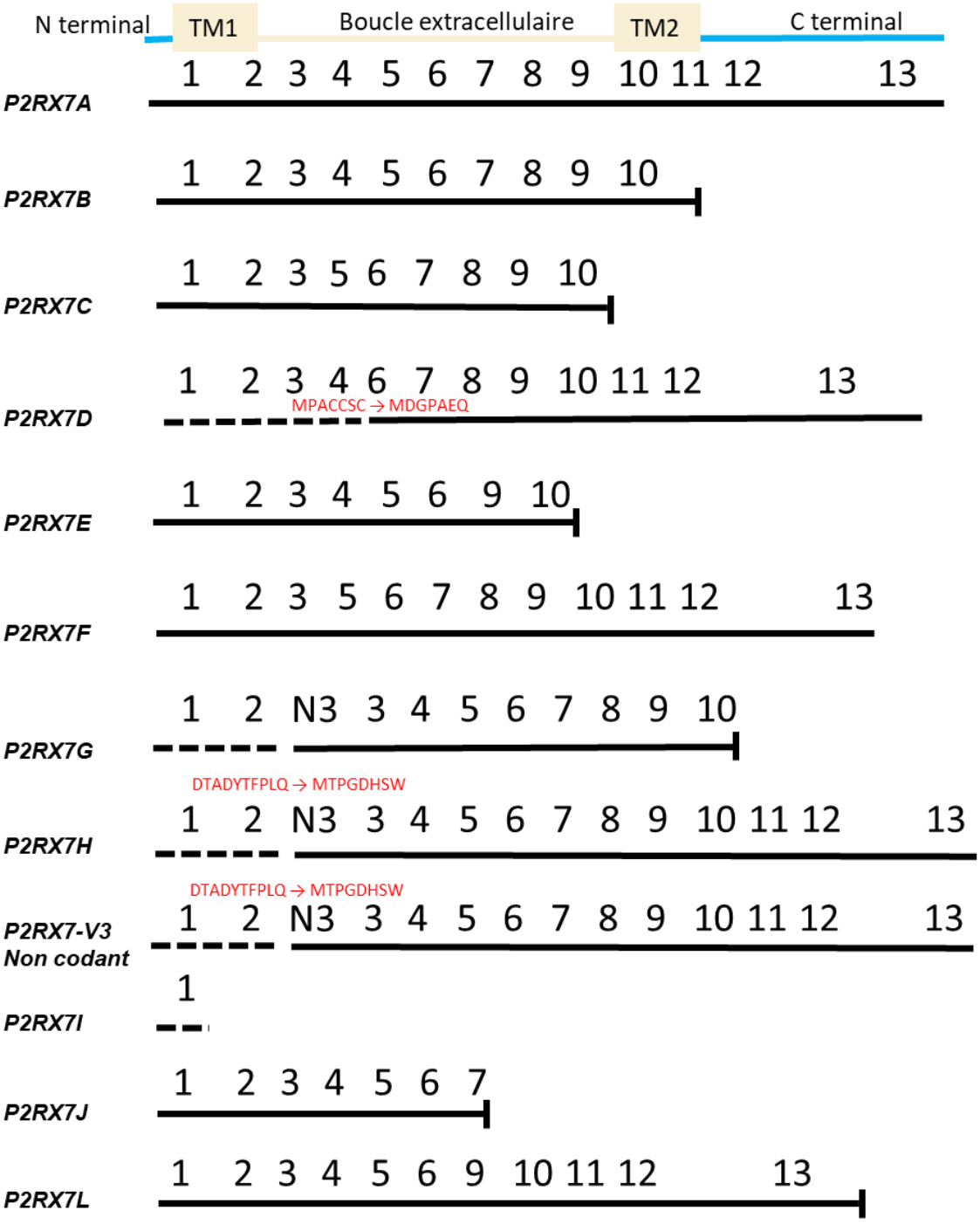

FIGURE 12 : Variants d'épissage de *P2RX7*

D. Revue de la littérature. Etat des lieux de l'épissage alternatif de *P2RX7*, conséquences physiopathologiques

Article publié (Biomedical Journal 2019, 42(3):141-154. doi: 10.1016/j.bj.2019.05.007)

Dans cette revue, nous présentons l'épissage alternatif de *P2RX7*, ses conséquences fonctionnelles et son retentissement en pathologie humaine.

Nous proposons une description générale de l'épissage alternatif des ARNm et des mécanismes impliqués, puis introduisons le récepteur P2RX7. Nous présentons les études qui documentent l'expression d'un récepteur fonctionnel dans les cellules humaines *ex vivo* non tumorales et tumorales, puis décrivons les épissages alternatifs connus pour *P2RX7* et leurs implications fonctionnelles. Nous analysons ensuite si des SNPs sont en mesure de réguler ces épissages alternatifs et présentons leur distribution chez l'homme. Nous concluons que les SNPs situés dans les zones de régulation de l'épissage de *P2RX7* sont faiblement distribués chez l'homme, ce qui rend improbable leur implication dans la promotion d'un épissage alternatif particulier. Il est à noter que ces données sont antérieures à la récente description du variant d'épissage *P2RX7L* dont la régulation dépend d'un SNP [221].

L'analyse des variants d'épissage de *P2RX7* utilise classiquement des outils de PCR qualitative et quantitative dont la stratégie est celle d'utiliser des amorces qui superposent les zones d'épissage alternatif comme illustré en Figure 13. Ceci pose une certaine limite quant à l'amplification du variant pleine taille *P2RX7A,* qu'il n'est à notre connaissance pas possible d'amplifier de façon spécifique.

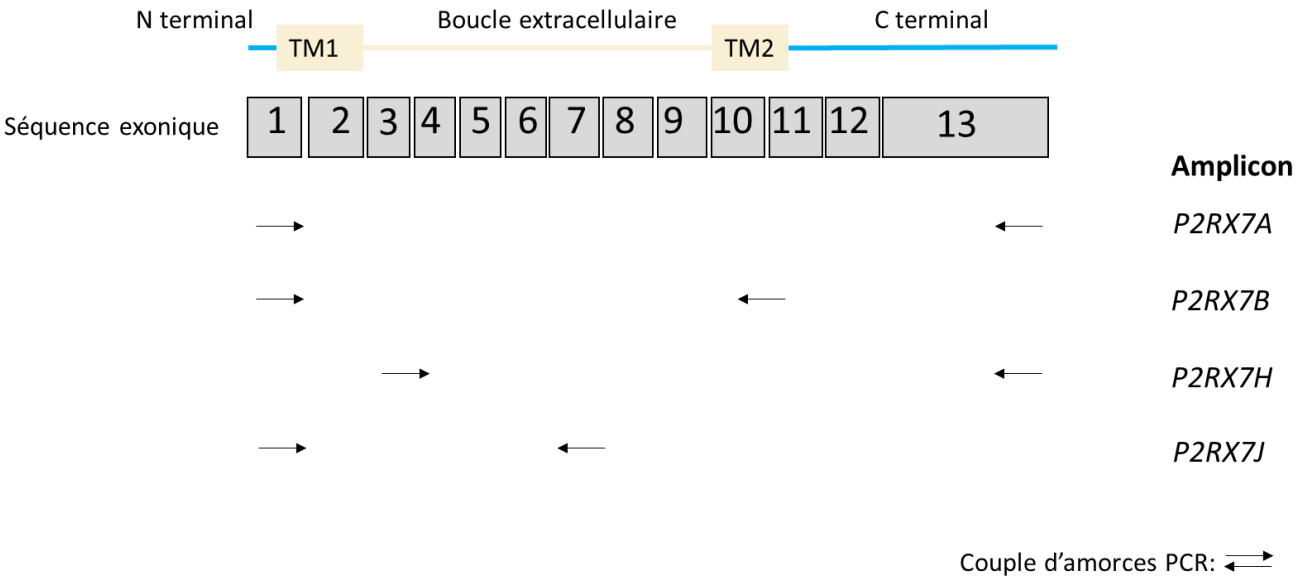

FIGURE 13 : Exemple de stratégie d'amplification de variants d'épissage de *P2RX7*

Available online at www.sciencedirect.com

ScienceDirect

Biomedical Journal

journal homepage: www.elsevier.com/locate/bj

Review Article

Alternative splicing of *P2RX7* pre-messenger RNA in health and diseases: Myth or reality?

Jonathan Benzaquen [a,d], *Simon Heeke* [a,b,d], *Séréna Janho dit Hreich* [a], *Laetitia Douguet* [a], *Charles Hugo Marquette* [a,d,e], *Paul Hofman* [a,b,c,d], *Valérie Vouret-Craviari* [a,d,*]

[a] *University of Cote d'Azur, CNRS, INSERM, IRCAN, Nice, France*
[b] *Laboratory of Clinical and Experimental Pathology and Biobank, Pasteur Hospital, Nice, France*
[c] *Hospital-Related Biobank (BB-0033-00025), Pasteur Hospital, Nice, France*
[d] *FHU OncoAge, Nice, France*
[e] *University of Cote d'Azur, CHU de Nice, Department of Pulmonary Medicine, FHU OncoAge, Nice, France*

Dr. Valerie Vouret-Craviari

ARTICLE INFO

Article history:
Received 2 April 2019
Accepted 24 May 2019
Available online 15 July 2019

Keywords:
Purinergic signaling
P2X7
ATP
Onco-immunology

ABSTRACT

Alternative splicing (AS) tremendously increases the use of genetic information by generating protein isoforms that differ in protein–protein interactions, catalytic activity and/or subcellular localization. This review is not dedicated to AS in general, but rather we focus our attention on AS of P2RX7 pre-mRNA. Whereas P2RX7 mRNA is expressed by virtually all eukaryotic mammalian cells, the expression of this channel receptor is restrained to certain cells. When expressed at the cell membrane, P2RX7 controls downstream events including release of inflammatory molecules, phagocytosis, cell proliferation and death and metabolic events. Therefore, P2RX7 is an important actor of health and diseases. In this review, we summarize the general mechanisms leading to AS. Further, we recapitulate our current knowledge concerning the functional regions in P2RX7, identified at the genetic or exonic levels, and how AS may affect the expression of these regions. Finally, the potential of P2RX7 splice variants to control the fate of cancer cells is discussed.

Splicing and alternative splicing

The first description of alternative splicing (AS) was reported by Chow and colleagues in 1977 who described a new mechanism for the biosynthesis of mRNA in mammalian cells [1]. For this discovery, Richard Roberts and Philips Sharp were awarded the Nobel Prize in 1993. Since then, more than 32,000 articles can be found on Pubmed using "alternative splicing" as key word. Of importance, AS is linked to diseases and cancer, with 6269 and 7553 publications found at the beginning of 2019.

General mechanisms leading to splicing

The regulation of splicing is a complex mechanism that requires several factors involved in the precise selection of splicing sites and subsequent splicing processes [2]. As illustrated in [Fig. 1A], the splicing consists of six sequential steps

* *Corresponding author*. University of Cote d'Azur, CNRS, INSERM, IRCAN, 33 avenue de Valombrose, 06108 Nice, France.
E-mail address: vouret@univ-cotedazur.fr (V. Vouret-Craviari).
Peer review under responsibility of Chang Gung University.
https://doi.org/10.1016/j.bj.2019.05.007

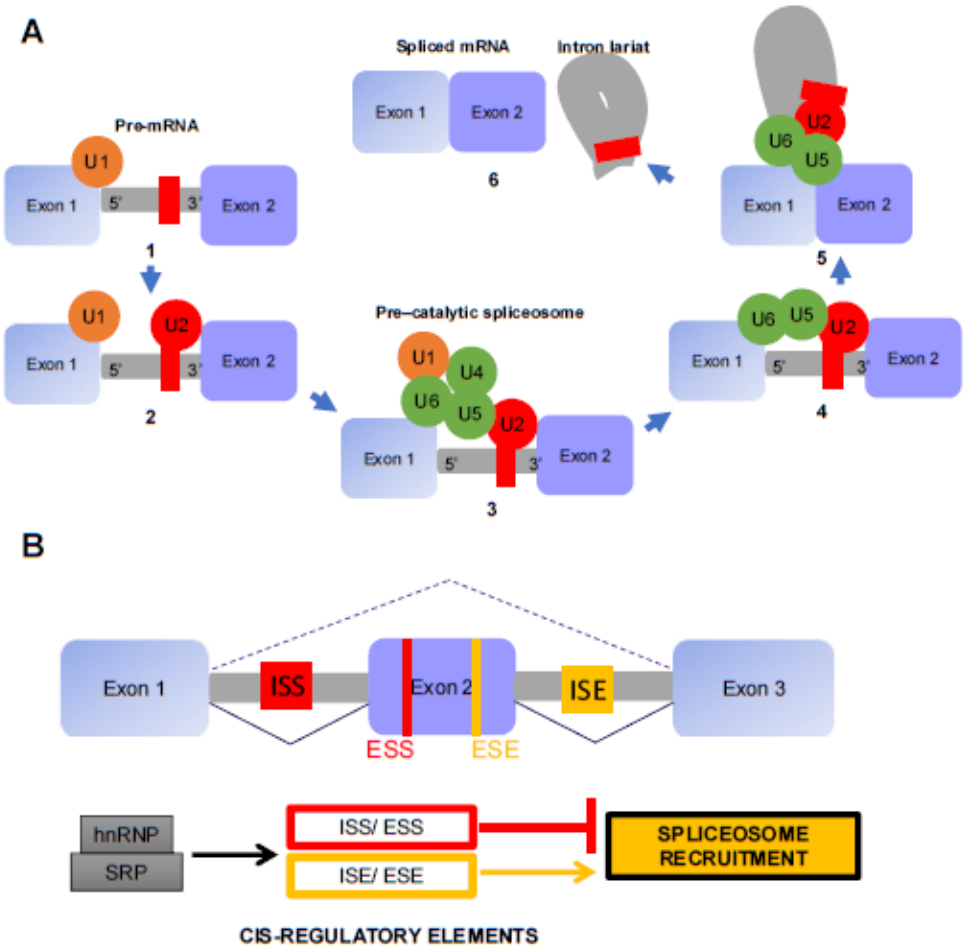

Fig. 1 Alternative Splicing requires two levels of regulation. (A) *Pre-mRNA splicing* require 6 sequential steps: 1: Pre-mRNA splicing starts with U1 snRNP (yellow circle) binding to the 5′-splice site; 2: U2 snRNP binds to the branch point (red rectangle) of the intronic sequence (gray bar); 3: Pre-assembled U4/U5/U6 snRNP (green circles) bind to U1 and U2 forming the pre-catalytic complex, and U1 snRNA 5′ site is transferred to U6; 4: Spliceosome activation starts with U1 and U4 snRNP exclusion; 5: Intramolecular stem-loop between U2 and U6 allows transesterifications steps which lead to exons linking and 6: Spliced mRNA is released as a ribonucleoproteic particle; intronic sequence is released as a « lariat » (gray loop). Note: The protein composition of each spliceosomal complex is not shown in this figure for the purpose of simplification. (B) *pre-mRNA splicing regulation.* Cis-regulatory elements are sequences localized in exonic or intronic pre-mRNA which regulate alterative splicing and spliceosome recruitment. ESS (in red letters) and ISS (highlighted in red), exonic splicing silencer and intronic splicing silencer inhibit the splicing of pre-mRNA. ESE (in yellow letters) and ISE (highlighted in yellow), exonic splicing enhancer and intronic splicing enhancer are sequences which promote the splicing of pre-mRNA and will conduct in the present illustration to Exon 2 skipping (broken line). This splicing mechanism involves the recruitment of regulation proteins such as hnRNPs (Heterogeneous nuclear ribonucleoproteins), and SRP (Serine-Arginine rich proteins), which can bind on cis-regulatory elements and regulate splicing.

leading to the removal of specific sequences in a vast genomic sequence background. This "scissor mechanism" relies on five small nuclear ribonucleoproteins (snRNP U1, U2, U4, U5 and U6) which together form the core of the spliceosome. In brief, pre-mRNAs splicing is initiated by the binding of U1 on the 5′-splice site (step 1) and U2 on the branch point (step 2). Then, U4, U5 and U6 associate with U1 and U2 to form the pre-catalytic spliceosome complex (step 3). Further, U1 5′ snRNA site is transferred to U6, leading to the activation of the spliceosome and to the removal of U1 and U4 from the complex (step 4). Consequently, U6 replaces U1 location and the interaction between U6 and U2 gathers the 5′-splice site and the branch point allowing the 5th transesterification step. The two exons are then brought to close proximity by U5 and finally joint ending the splicing procedure (step 6). The splicing regulation does not only depend on the composition of splice sites, indeed, ribonuclear–protein complexes, referred as RNPs in [Fig. 1B], associate with pre-mRNA to facilitate exon recognition [3]. These regulatory proteins are classified in two major classes: heterogeneous nuclear ribonucleoproteins (hnRNPs) which bind to RNA, and SR proteins which contain serine and arginine rich protein regions involved in protein recognition. Both families regulate splicing via binding of intronic or exonic splicing silencers or enhancers as illustrated in [Fig. 1B] [2,4–6]. Finally, additional levels of regulation are sustained by the secondary structure

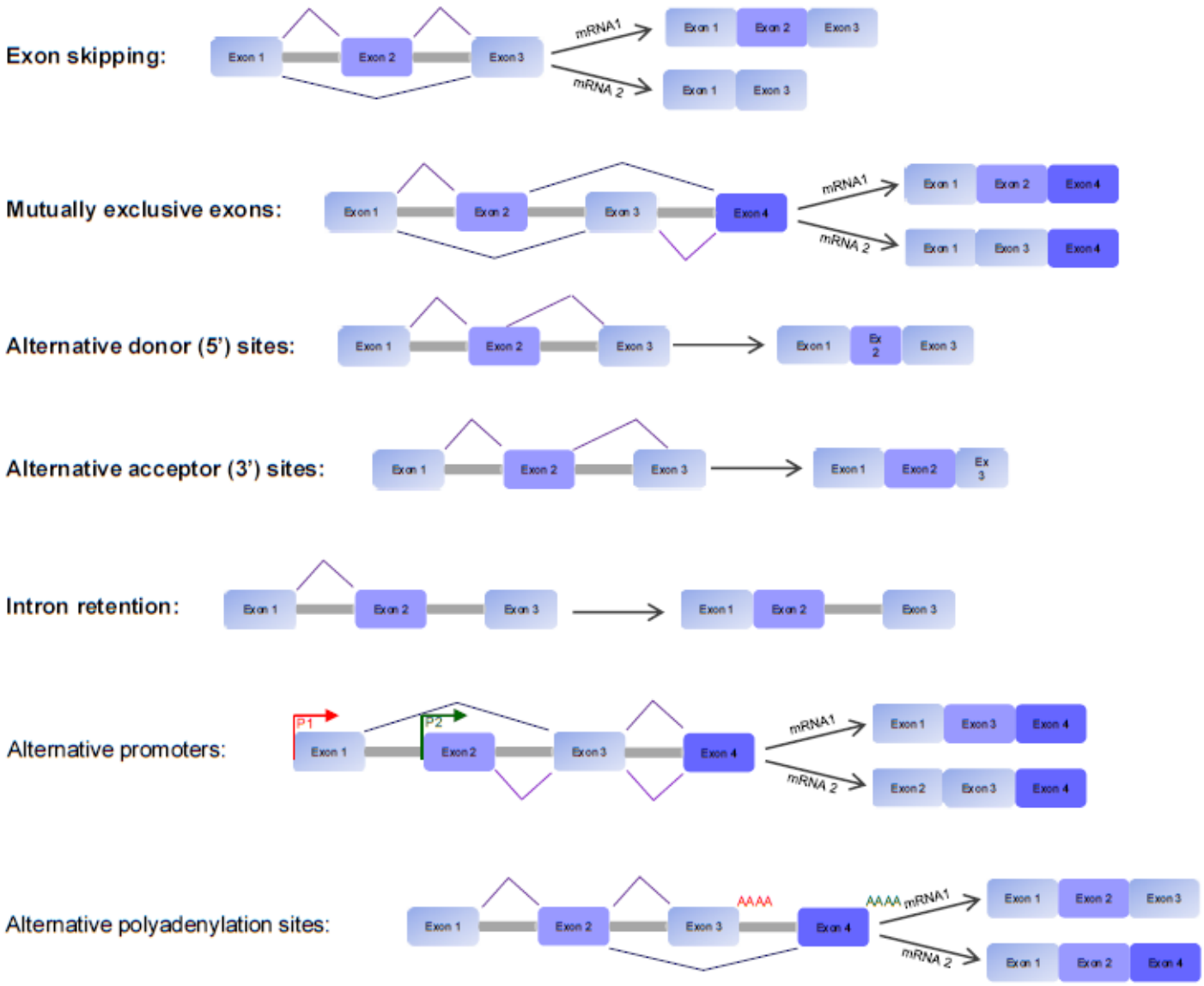

Fig. 2 From one pre-mRNA to various mRNAs. The seven described modes of alternative splicing increase the mRNA diversity. Bold characters are for the most common AS modes. Exon skipping, also named cassette exons, allows the exclusion of a full exon. Mutually exclusive exons lead to the egress of one exon out of two. Alternative donor 5′ site uses an alternative 5′ splice donor site to generate mRNA. Alternative acceptor 3′ site uses an alternative 3′ splice acceptor site. Intron retention corresponds to the addition of an intronic sequence within mRNA. Alternative promoter mode describes the use of different promoters resulting in a different start site of the mRNA transcript. An alternative promoter can be located at the 5′ exon location or within an exon. Alternative polyadenylation sites refer to a splicing based on the presence and recognition of different polyadenylation sites.

of the pre-mRNA that can influence the recognition of splice sites [6], but also by cellular signal transduction pathways inducing phosphorylation events as reviewed by Stamm [7].

Alternative splicing

Most of protein-encoding genes have multiple exons that are alternatively combined to form distinct mRNAs [8,9]. As illustrated in [Fig. 2], several patterns of alternative splicing (AS) with varying complexity exist and participate in the expansion of genetic diversity. These alternative combinations can be organ-specific, tissue-specific or cell-type specific [2,10].

It is usually accepted that events conferring biological gain of functions are conserved throughout evolution. To address whether specific AS are conserved within evolution, Merkin and collaborators performed a transcriptome sequencing (RNA Seq) analysis using paired-end short or long read sequencing of poly-A-selected RNA on nine tissues from five vertebrates [11]. Doing so, they identified almost 500 exons with conserved AS that are highly conserved in mammals. Interestingly, these exons often encode phosphorylation sites, and their tissue specific splicing may have important effect on signaling pathways. Unexpectedly, the authors described an extensive variation in the splicing of these exons between species, at a level that even exceeds intraspecies differences

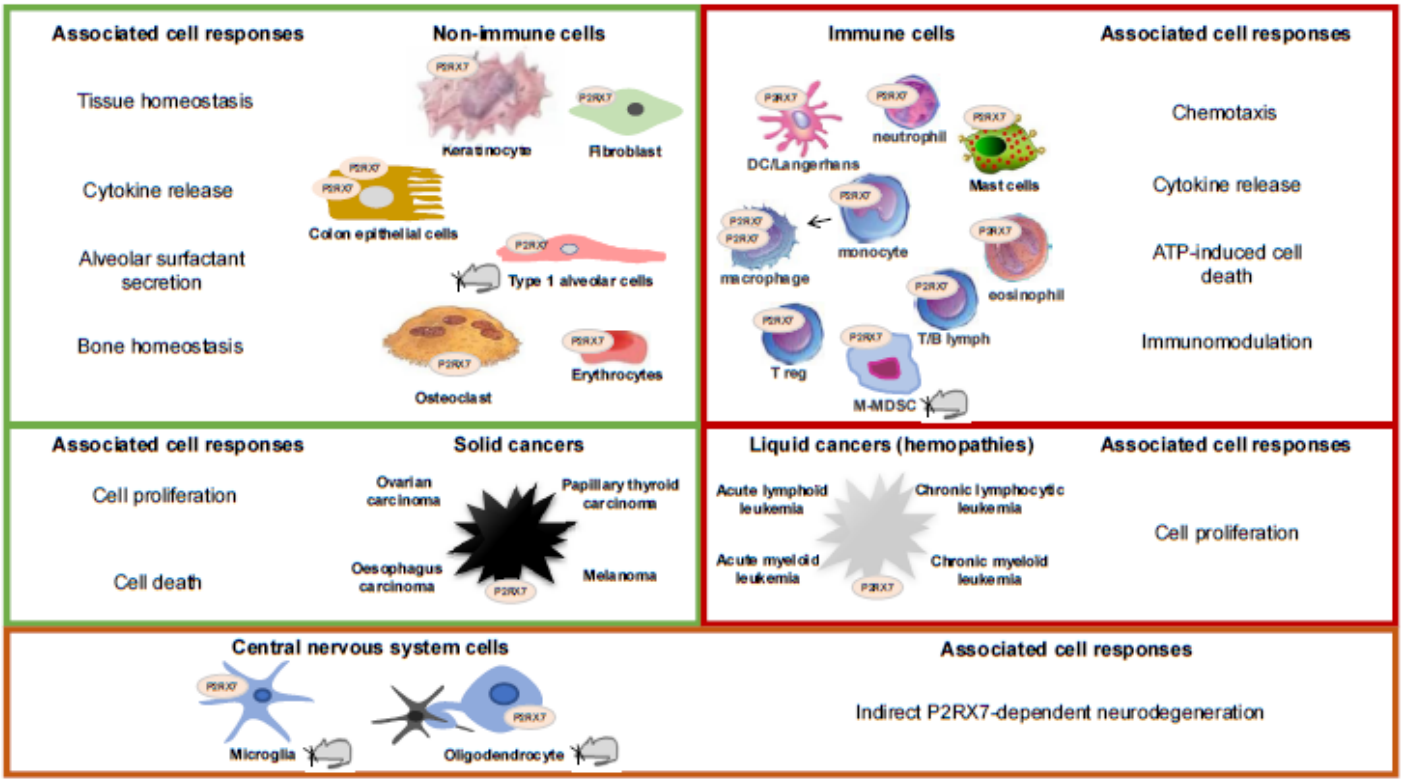

Fig. 3 P2RX7 expression in eukaryotic cells. The best way to sense cell stress is to express a receptor that is activated by molecules, like nucleotides, that are normally sequestered in the cells. Release of nucleotides, in response to mechanical injury, necrosis, apoptosis or inflammatory cell activation, depends on several molecular pathways, such as vesicular ADP release from platelets, pannexin-mediated ATP release during apoptosis, connexin- or pannexin-mediated ATP and autophagy. By sensing extracellular ATP, P2RX7 which is expressed by a large variety of cells plays such a role. In non-immune cells, functional P2RX7, (i.e. characterized by its expression at cell membrane, channel activity and/or macropore opening) has been found in colon [12] and lung epithelial cells [13], keratinocytes [14], osteoclasts [15], fibroblasts [16], and erythrocytes [17], where its activation has been shown to support tissue homeostasis, proliferation, survival and metabolism. In immune cells, expression of P2RX7 was documented in dendritic cells [18–20], neutrophils [21], mast cells [22], monocytes/macrophages [23,24], lymphocytes [25], eosinophils [26] and M-MDSC [27]. In these cells, P2RX7 expression is involved in chemotaxis, cytokine release, ATP-induced cell death and immunomodulation. In addition, P2RX7 expression was found in both solid [28–32] and liquid cancers [33–35], where it was described to sustain cell proliferation or cell death. Other publications claimed that P2RX7 was overexpressed in cancer from various origins [35,36]. Yet, these conclusions were obtained from immunohistochemistry analyses, where the identification of P2RX7 expressing cells is somehow difficult to characterize. Finally, P2RX7 was described to be expressed in microglia and oligodendrocytes [37]. Note: Here we showed P2RX7 expression reported to be functional in human cells, or in mouse cells when no data were available for human (a mouse drawing is then symbolized in this case).

between tissues [11]. In a complementary study, Barbosa-Morais and collaborators showed that in the mammalian lineage, organs of primate species have higher AS frequencies than organs of other vertebrates. They concluded that organs' AS profiles are more closely correlated to the identity of a species than to the organ, in contrast to the well conserved organ-dependent differences in mRNA expression during vertebrate evolution [38]. Together, these studies reveal that AS and transcription regulation are not subjected to the same evolutionary constraints; apparition of new mRNA variants is dominated by species-specific differences that accumulate more rapidly than transcriptional regulation even during a short period of evolution.

Whereas transcriptional regulation and constitutive splicing maintain normal cell physiology, AS can result in various human diseases by modifying, or even abrogating, some functional regions of proteins that are involved in cell homeostasis [39]. In fact, the hundreds of factors allowing the precise regulation of AS are themselves subjected to modifications, which in turn can cause deregulation of each of the signaling pathways across virtually all biological processes. For instance and as recently reviewed by Czubay and Piekiello-Witkowska, phosphorylation of splicing factors results in changed AS of tumor suppressors, regulators of cell signaling or apoptosis resulting in an impact on cancer development and progression [40]. Modification of AS is also the result of sequence variation. Indeed, it was reported that 22% of missense disease alleles alter splicing and it was predicted that one third of all mutations affect splicing [41]. To fully appreciate the relationship between missense mutation,

AS and diseases, computational approaches [42] and animal models [43] have been developed.

Altogether, deregulation of AS has been described to play a role in diseases as diverse as diabetes, neurological diseases, cardiovascular diseases, immunological and infectious diseases as well as cancer. As this topic is far beyond the scoop of this review, we invite interested readers to refer to an excellent review published by Kim and collaborators [10].

Alternative splicing of P2RX7

The purinergic P2RX7 receptor

Half a century was necessary to link purine nucleotides and nucleosides as extracellular ligands [44] to the existence of two families of purinergic receptors [45]. It is now well described that the P1 [46] and the P2 receptors comprise numerous members and that the P2 family is divided in two subgroups P2Y and P2X receptors [47]. The purinergic P2X receptors are activated by extracellular adenosine 5′-triphosphate (eATP) [47,48]. This family includes seven members which all share a common structure based on two transmembrane spanning regions, a large extracellular loop and intracellular N- and C-termini [48]. Within this family, sequence identity from the N terminus to the second transmembrane domain is relatively high. By contrast, their C-termini are specific to the individual P2X receptors and contain consensus binding motifs for protein kinases and other regions that may be involved in cell-signaling. This is particularly true for the seventh member of the P2X family, previously described as P2Z receptor [49], which is characterized by the presence of a long intracytoplasmic C-terminal sequence [48] and now referenced as P2RX7.

In the presence of eATP, P2RX7 trimeric receptors form a poorly-selective channel leading to membrane depolarization, potassium efflux and calcium and sodium influx [48]. Whereas *P2RX7* mRNA is expressed by virtually all mammalian cells, the expression of the protein was described in immune but also in non-immune cells [Fig. 3]. In cells expressing P2RX7 at the membrane, its expression was thought to induce various downstream events including cell proliferation and cell death, metabolic events, phagocytosis and release of inflammatory molecules [50–53]. As discussed later in this manuscript, P2RX7 could be expressed but maintained within the cytoplasm. In this condition protein expression is dissociated from protein activation. In addition, it was shown in mouse CD8 T cells that the sensitivity to eATP depends more on the stage of cell differentiation than on the level of P2RX7 expression [54]. Within the P2RX family, P2RX7 is unique. First, it is activated by relatively unusual high concentration of eATP (1 mM under physiological concentration), second it allows the permeation of large molecules up to 900 Da and third it is responsible for eATP-dependent cell lysis, a response that depends on the presence of the C-terminal sequence [49]. The recently described crystal structure of mammalian P2RX7 (from panda) gave new insights on the architecture of this receptor [55]. Importantly, the trimeric association of P2RX7 was confirmed by this study; the same conclusion was drawn by Kasuya and collaborators studying the crystal structure of the chicken P2RX7 [56]. As previously described for P2RX4 and P2RX3, the single subunit of a C-terminal truncated P2RX7 resembles a "dolphin-like" shape [57–59]. In the absence of eATP, the transmembrane helices constrict the channel gate at residues G338, S339 and S342. Hence, this conformation may represent the closed state. Unfortunately, the crystal structure in the presence of eATP was not sufficiently stable to be studied and the proposed mechanism is yet to be confirmed. By contrast, the crystal structure of P2RX7 in the presence of five different antagonists highlighted the existence of a drug binding pocket in the upper body domain which is close to the eATP binding pocket. Therefore, available antagonists act as non-competitive inhibitors. Combining different analyses, the following mechanism for P2RX7 activation and inhibition was proposed: In the presence of eATP, both the drug binding pocket and the inter-subunit cavity in the upper body domain (also called turret) of P2RX7 undergo conformational rearrangements. This leads to the narrowing of these domains, which consequently allows the enlargement of the lower body domain resulting in the opening of the channel. When allosteric antagonists are bound to P2RX7, turret closure is restrained and the channel remains closed [55]. This mechanism implies that when eATP is within its binding pocket, the drug binding pockets are inaccessible, preventing the binding of allosteric inhibitors.

Noteworthy, the crystal structure has been obtained using a C-terminally truncated version of P2RX7 which may represent a caveat in the understanding of P2RX7 biology. Indeed, the long C-terminal tail of P2RX7 has been described to be essential to sustain permeation of large molecules and cytolysis [49]. Here again, the group of Kawate improved understanding on the role of the C-termini of P2RX7 by investigating the effect of the membrane's lipid composition on P2RX7 functionality [60]. Using purified panda P2RX7 reconstituted into liposomes, it was elegantly demonstrated that the dye-permeant pore opens independently of the long C-terminal tail. Further, the authors highlighted the capacity of phosphatidylglycerol and sphingomyelin to facilitate channel activity by modifying the lipid composition of the liposomes, whereas cholesterol drastically attenuated dye-uptake by directly acting on P2RX7 transmembrane domains. So, if the dye-permeable pore of P2RX7 is independent of the N- and C-terminal extremity, do these intracytoplasmic sequences have a biological function? Part of the answer was brought by Robinson and collaborators who linked cholesterol sensitivity of P2RX7 channel activity to the presence of multiple cholesterol recognition amino acid consensus motifs within both N-terminal and proximal C-terminal regions of P2RX7 [61,62]. Additionally, it was shown that the juxta-transmembrane amino and carboxyl termini are involved in the regulation of P2RX7 gating [63]. And finally, it was demonstrated that the C-terminal Cysteine-rich region of P2RX7 counteracts the inhibitory effect of cholesterol [60]. All these evidences, combined with new technologies to analyze dilatation of P2RX7 eATP-induced pore opening [64,65], push aside the old dogma postulating that the formation of the large pore is a consequence of P2RX7 cation-selective channel dilatation and rather

highlight the importance of lipid composition to modulate the size of the pore. In agreement with this, it was shown that P2RX7 is associated with lipid rafts, which are dependent of palmitoylation of Cys residues located in the C-terminal region [61]. Yet, as nicely discussed by Di Virgilio and collaborators, we cannot exclude that consequently to P2RX7 stimulation, other permeability pathways are activated [66].

P2RX7: one gene, many proteins

P2RX7 gene was investigated in mammalian and non-mammalian species, the more studied species being human, rat and mouse, as detailed in the well documented review published elsewhere [53]. We will focus here on human and mouse, with an emphasis on *P2RX7* splice variants.

Human splice variants

The P2RX7 gene, which is localized on chromosome 12q24, consists of 13 exons. Constitutive splicing leads to the common *P2RX7-A* mRNA, but 12 additional transcripts have been described due to alternative splicing [67]. Among those splice variants, nine were studied in more detail [Fig. 4A]. Three of them, the variants -C, -E and -G, code for very short proteins and are assumed to be unable to form a channel receptor. By contrast, the variants *-B* and *-J* have been described to be expressed under normal and/or pathological conditions and to interfere with P2RX7-induced biological responses [67]. The *P2RX7-B* variant, which is expressed in almost all eukaryotic cells and appears to be regulated in immune cells, is characterized by the deletion of the last 249 amino acids from the C-terminal extremity that have been replaced by 18 different amino acids [67]. The homotrimer was described to retain ion–channel activity when expressed in a heterologous cell system. However, the EC50 for BzATP reaches 500 μM, which questions its ability to really channel Ca^{2+}. In addition, P2RX7-B homotrimers were described to be non-permeant to dyes, such as Yo-pro-1. On the contrary, the heterotrimer P2RX7-A/P2RX7-B was described to be more efficient than P2RX7-A, in particular by supporting cell growth [68]. With the C-terminal extremity of P2RX7 being involved in trafficking and cell surface expression, it could be that the increased efficiency of the heterotrimer is correlated with an improved expression at the plasma membrane [69–71]. Alternative splicing of exon 8 which is leading to a frameshift mutation with a new stop codon produces the *P2RX7-J* variant. The resulting protein is composed of the N-terminal extremity, the first transmembrane domain and 2/3 of the extracellular loop. The P2RX7-J receptor is inactive alone, but when co expressed with P2RX7-A, the association of -A and -J isoforms has a dominant negative effect over the P2RX7-A homotrimer which may protect certain cell types from eATP-induced cell death [72,73]. *P2RX7-H, -D and -F* result from alternative splicing leading to the insertion of an extra exon, or deletion of exons 5 and 8, respectively. The corresponding proteins are missing the N-terminal sequence, the first transmembrane domain and part of the cytoplasmic loop [Fig. 4B]. Given the fact that normal trafficking toward the cell surface requires the N-terminal sequence, it is likely that these isoforms are not correctly inserted in cell membrane. However, if expressed, these isoforms can be localized in the cytoplasm or in intracellular vesicles. Yet, only few *P2RX7-H* mRNA are expressed in tissues from different origins [67]. It is important to keep in mind that all these results were obtained after overexpression of splice variants in the HEK293 heterologous cell system. Undeniably, additional studies are required to examine the endogenous expression of P2RX7 isoforms, and their functional consequences, in human cells.

Mouse splice variants

The murine gene of *P2rx7*, which is located on chromosome 5, maintains the same genomic organization as human *P2RX7*. The common *P2rx7-a* mRNA is made of 13 exons. Four alternative splice variants have been described in mice so far, *P2rx7-b*, *-c*, *-d* and *-k* [Fig. 4A]. Two of them, *P2rx7-b*, *-c*, correspond to deletions within exon 13 and give rise to shorten proteins which are characterized by lower channel activity [53]. The P2RX7-d isoform corresponds to the shortest form of the protein with a large truncation in the extra-cytoplasmic loop, loss of both the second transmembrane domain and the intracytoplasmic C-terminal tail [74]. Interestingly, this largely truncated protein retains the ability to be correctly inserted within the membrane when co-transfected with P2RX7-a. It is likely that the heterotrimer is formed during vesicle trafficking towards the cell membrane, and once inserted in the membrane, P2RX7-d downregulates eATP-induced macropore formation. On the contrary, P2RX7-k protein, which results from an alternative splicing of exon 1, differs from P2RX7-a in the N-terminal cytoplasmic extremity and most of the first transmembrane domain [75]. *P2rx7-k* mRNA is expressed in all tissues but more expressed than *P2rx7-a* in spleen and liver. P2RX7-k homotrimer is more sensitive than P2RX7-a to ATP and is more potent to permeate ions and large cations. In addition, it was shown that P2RX7-k could be activated by ADP-ribosylation, which correspond to a second mode of activation [76]. P2RX7-k seems to be exclusively expressed by T cells and no co-expression of *P2rx7-k* and *P2rx7-a* was described. This mutually exclusive expression suggests a regulation at the level of the promoter. Whether this regulation is due to epigenetic modifications (such as methylation), specific expression of transcription enhancers/inhibitors or both remains to be determined. *P2rx7-k* mRNA escapes gene deletion in the Glaxo $P2rx7^{-/-}$ mice, where *LacZ* gene was inserted after ATG at the 5′ end [75]. The existence of these splice variants led to a careful re-evaluation of the expression of P2RX7 receptor isoforms in the Pfizer transgenic *P2rx7* KO mice, where region encoding Cys^{506} to Pro^{532} was replaced with the neomycin resistant gene [76,77]. While P2RX7-k protein is expressed in T cells from the "Glaxo mice", Pfizer KO mice express ΔC isoforms (namely P2RX7-b, -c, -d). However, these proteins were inefficiently trafficked to the cell surface and consequently not responsive to agonistic stimulation [78]. Together, these results indicate that the Pfizer model is the preferential one to evaluate the functional role of P2RX7 in homeostasis and pathological conditions. In the same line, the third *P2rx7* KO model, in which the beta galactosidase/Neomycin genes were inserted within the exon 2 [79], is expected to be a good model, with none of the variant being expressed. In addition, two additional knock-in

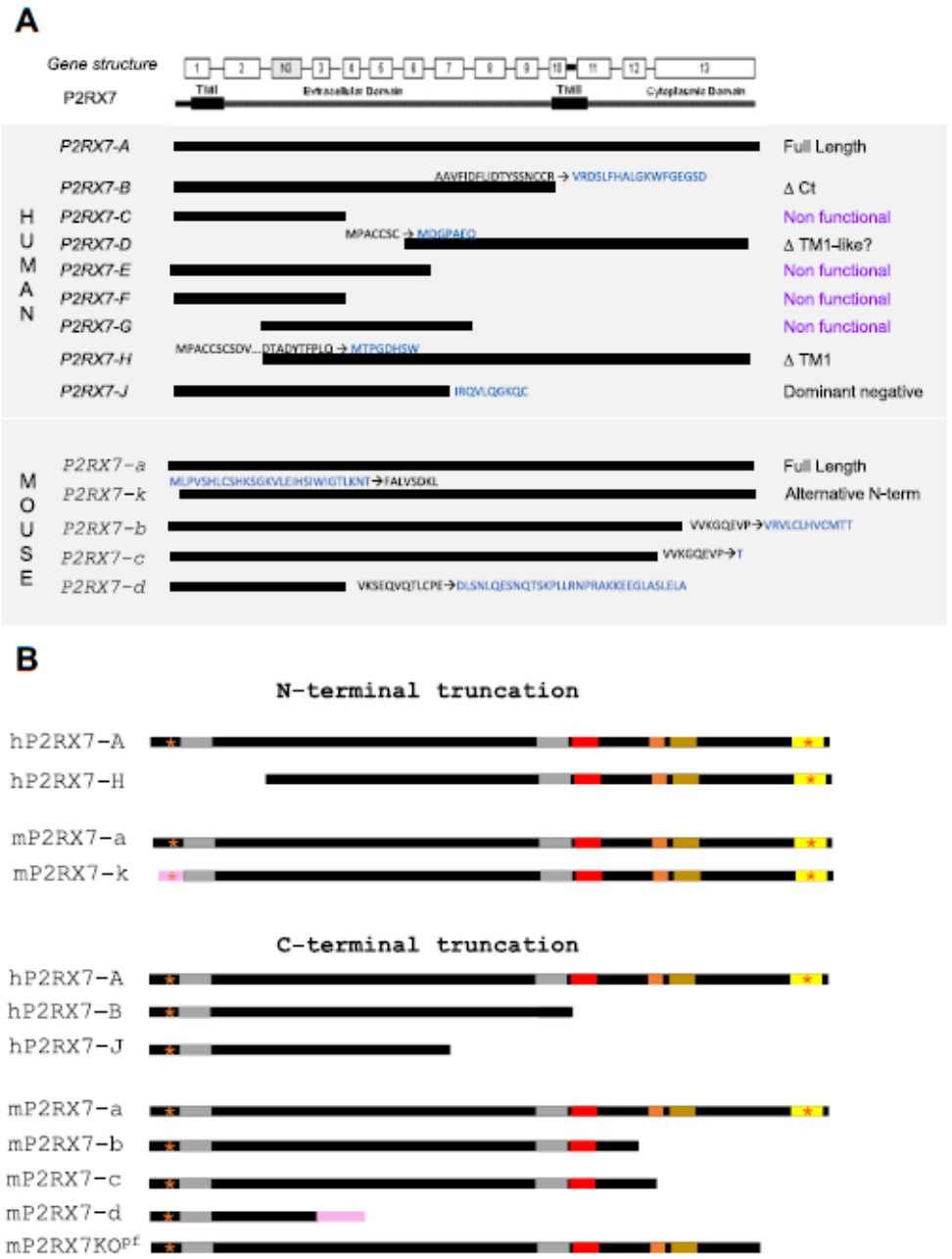

Fig. 4 Human and mouse *P2RX7* splice variants. (A) Genomic organization. New sequences resulting from AS are shown in blue. Protein isoforms corresponding to P2RX7-C, -E, -F and -G were described to be nonfunctional. Yet, P2RX7-E and -F isoforms are structurally closed to the mouse P2RX7-d protein, which has been described to down regulate P2RX7 activity when co-expressed with P2RX7-A [Table 2]. By the same way, P2RX7-D corresponds to a shorter version of P2RX7-H, which has been described to be a non-functional receptor. (B) Schematic illustration showing the overall organization and the functional regions in isoforms identified at the genetic or exonic levels. Grey box: transmembrane domain 1 and 2; red box: Cys rich regions (including C371,373, 374- C477, 479, 482-C498,499, 506 and C572, 573); orange box: A actinin binding sequences; brown box: SH3 binding domain and TNF death receptor; yellow box: LPS binding domain; orange star: cholesterol sensitizing; red star: amino acids involved in trafficking and cholesterol sensitizing. The pink boxes highlighted the presence of new sequences due to splicing.

transgenic mice were generated. The first one corresponds to humanized P2RX7 mice in which the mouse exon 2 was substituted by the human cDNA covering exons 2 to 13 [80]. The second one relies on the introduction of an EGFP sequence in the 5' of exon 13 [37]. Both models were useful to characterize the expression of P2RX7 in the central nervous system (see [Fig. 3]).

Expression of splice variants: a way to regulate P2RX7 activity? As a receptor, P2RX7 has to be correctly inserted into the cell membrane to be functional. Indeed, assembly and trafficking to the plasma membrane has been described as a regulatory mechanism, at least in some immune cells [23,81]. In addition to membrane receptor density, the concentration of extracellular ions was demonstrated to be crucial for the regulation of IL-1β

Table 1 Description of Single Nucleotide Polymorphisms of the Human P2RX7 gene that could affect alternative splicing of variant B, H and J.

dbSNP ID	Localization	"Affected" variant	Major allele	Minor allele Frequency
rs1397153443	−3, exon 11	Variant B	C	T = 0.0000
rs778937864	−4, exon 11	Variant B	C	T = 0.0000
rs756931719	−10, exon11	Variant B	T	G = 0.00001
rs190080059	−20/−40, exon 11	Variant B	G	A/T = 0.00002
rs373584182	−20/−40, exon 11	Variant B	G	T = 0.00004
rs1352183219	−20/−40, exon 11	Variant B	G	A = 0.0000
rs760740502	−20/−40, exon 11	Variant B	G	A = 0.00002
rs916695614	−20/−40, exon 11	Variant B	C	C *none*
rs201650139	−20/−40, exon 11	Variant B	A	G *none*
rs368885357	−20/−40, exon 11	Variant B	G	T = 0.0000
rs1376166550	+2, exon 2	Variant H	T	C *none*
rs754634787	+3, exon 2	Variant H	G	A/T = 0.0000
rs965276754	−10, exon 3	Variant H	T	A *none*
rs201960043	−20/−40, exon 3	Variant H	T	Inscc = 0.0537 (InsDel)
rs200429438	−20/−40, exon 3	Variant H	C	A *nd*
rs1373724698	−20/−40, exon 3	Variant H	T	G = 0.0001
rs186332279	−20/−40, exon 3	Variant H	G	C = 0.00002
rs757343268	−20/−40, exon 3	Variant H	TTCAAA	Del, 0.00001
rs1475267143	+2, exon 7	Variant J	T	C = 0.0000
rs764748109	−8, exon 8	Variant J	T	C = 0.00001
rs1239860541	−20/−40, exon 8	Variant J	A	G = 0.0000
rs28360455	−20/−40, exon 8	Variant J	T	C = 0.0021
rs774175036	−20/−40, exon 8	Variant J	C	G/T = 0.00002
rs771002311	−20/−40, exon 8	Variant J	A	G = 0.0000
rs1210563466	−20/−40, exon 8	Variant J	C	T = 0.0000
rs1488167709	−20/−40, exon 8	Variant J	C	T = 0.00001
rs1239860541	−20/−40, exon 8	Variant J	A	G = 0.0000

secretion [82]. As discussed above, a third mode of regulation could result from the expression of homotrimer isoforms but also from the formation and expression of heterotrimeric isoforms, where the full-length form is associated with truncated splice variants.

To evaluate the role of AS in P2RX7 regulation, we focused on human and mouse P2RX7 isoforms. As shown in [Fig. 4B], two groups can be distinguished. In the first one, splicing events modify the N-terminal part of the protein, a sequence that contains amino acids critical for the localization of P2RX7 at the cell membrane. Currently, there is no evidence for a functional role of the P2RX7H isoform, which is unlikely to be trafficked to the cell membrane and does not respond to Bz-ATP [67]. However, considering the trimeric organization of P2RX7, one may speculate that a chimeric P2RX7-A/-H receptor could be assembled during ER trafficking and once correctly inserted in cell membrane, tune the amplitude of eATP-induced cell responses. However, further in-depth characterization is needed to confirm this hypothesis. On the contrary, AS in the first exon of the mouse *P2rx7* pre-mRNA produces a highly sensitive P2RX7 isoform, which is involved in immune T cells homeostasis [83]. This variant has not been described in human, even though the sequence of human intron 1-2 predicted the existence of a possible alternative splice site in exon 1 [75]. In the second group, splicing events affect exons that are crucial in mediating large cation permeation. As mentioned above, heterologous expression of human and mouse homotrimer isoforms lead to the expression of receptors characterized by functional Ca^{2+} flux and blocked permeation of large cations. Expression of these new receptors could be considered as the first level of regulation. More interestingly, the co-expression of two isoforms bring additional levels of regulation. The heterotrimer -A/-J is dominant negative in human for instance, while in mouse the co-expression of -a/-b, -a/-c, and -a/-d downregulated, or even inhibited P2RX7 function. Strikingly, co-expression of P2RX7-A/-B in HEK293 cells seems to increase the overall activity of P2RX7 as discussed earlier [68,84]. This result was unexpected considering the contrary effect observed with the mouse heterotrimeric receptors. However, one could speculate that the overall effect on heterotrimer P2RX7 activity depends on the ratio of A versus B. For instance, 2A and 1B could be more active than 3A whereas 1A and 2B could be less active. Undoubtably, additional experiments are needed to fully document in which cells and at which levels P2RX7 isoforms are expressed and what the functional consequences of heterotrimeric P2RX7 expression are? Another important question that remains to be solved is whether the non-functional P2RX7, that is expressed on cancer cells [85], is a consequence of AS leading to the formation of heterotrimeric P2RX7 that would not be recognized by the conformational antibody generated by Buell and co-workers [86], and that would alter P2RX7 activity [85]. This may be particularly relevant considering that the C-terminal truncation of P2RX7 leads to the deletion of several binding motifs involved in P2RX7-induced cell signaling pathways [50,87].

Table 2 Biological activities of human and mouse P2RX7 isoforms.

P2RX7 isoforms	Cells	Localization at the membrane	Membrane depolarization	Ca2+ influx	Macropore formation	IL1B release	Refs
P2RX7-A	HEK293,	IF	++	++	++		[49,67,68,79]
P2RX7-B	HEK293	IF	+/−	Low & transient	no	Casp1	[67,68]
P2RX7-H	HEK293		no	no	no	No casp 1	[67]
P2RX-7-J	Cervical cancer cells, MDCK	IF		low	no		[72]
P2RX7-A/-B	HEK293	IF	>-A	>-A	>-A		[67,83]
P2RX7-A/-J	HEK293	wb		<-A	<-A		[72]
P2RX7-a	Macrophages				++	++	[75]
	Brain, spleen, salivary gland, HEK293	wb	++	++	++		[76,77]
	Astrocytes	wb			++		[73,77]
	Pancreatic stellate cells	wb		++			[77]
P2RX7-b	Brain, spleen, salivary gland, HEK293	wb, ↓↓ vs P2RX7-a	↓↓ vs P2RX7-a				[77,78]
	HEK293				no		[74]
P2RX7-d	HEK293				no		[74]
P2RX7-k	T Lymphocytes						[76]
	HEK293	wb	++ (sustained vs -a)		++		[75]
P2RX7-a/-b	HEK 293	wb, b = dominant negative	b = dominant negative		↓↓ vs P2RX7-a alone		[74,78]
	Astrocytes (overexpression)				↓↓ vs P2RX7-a alone		[74]
P2RX7-a/-d	HEK293, astrocytes (overexpression)				↓↓ vs P2RX7-a alone		[74]

P2RX7 splice variants and diseases

SNPs and splice variants

On the beginning of 2019, 13,252 single nucleotide polymorphism (SNP) have been described in the *P2RX7* gene (https://www.ncbi.nlm.nih.gov/snp). While non-synonymous SNPs have been linked to pathologies as diverse as infectious diseases, bone, psychiatric, inflammatory and cardiovascular disorders or cancers, as reviewed by Sluyter [88], SNPs located within intronic regions have been poorly studied. Splicing regulatory elements can be located within intronic sequences, therefore one could assume that intronic SNPs may affect splicing and in turn cause diseases [89]. Splicing regulatory sequences include the 5′ and 3′ splice sites defining the boundary of an intron with its upstream and downstream exon, but also the branch site upstream of the 3′ splice site. Examination of the human *P2RX7* sequence indicates that the major U2 class splice site consensus sequence, including GT at the 5′ end and AG at the 3′ end, is present on the boundary of each of the P2RX7's introns.

We speculated that SNPs might lead to alternative splicing of *P2RX7* pre-mRNA. To test this hypothesis, we first listed SNPs located at the introns' boundaries. As shown in [Table 1], only one SNP, rs1475267143, changes a T to C at +2 of the 7th intron. This change, that corresponds to the most common class of non-consensus splice sites [90], may affect the splicing of exon 7, even though this hypothesis has not been tested experimentally. However, the minor allele frequency is close to zero, and therefore it is not expected that such a frequency could significantly impact the expression of *P2RX7-J*. We further extended our analysis to minus 10 to cover branchpoints of each boundaries' intron. As shown in [Table 1], we found several SNPs that can affect the splicing of *P2RX7-B*, *-H* and *-J*. Once again, all these SNPs are too sparsely expressed to envisage that they could regulate splicing events and are involved in diseases. Finally, because branchpoints within U2-type constitutive introns were located in between the position −40 to −20 from the 3' splice site, we extended our analysis to −40 nucleotides [36]. Doing so, we identified two SNPs rs28360455 and rs201960043 that could contribute to the alternative splicing of *P2RX7-J* and *P2RX7-H*, respectively. Today, no studies demonstrated that these two SNPs are linked to the expression of spliced *P2RX7* mRNA but given their relative high frequency it is tempting to speculate on the existence of such a regulation. By contrast, we were unable to identify SNPs that could modulate splicing of *P2RX7-B*. Yet, we cannot exclude that such SNPs exist, but are located within an unstudied intronic region. Alternatively, one could hypothesize that P2RX7-B is indeed constitutively expressed in some tissues. This idea is sustained by studies showing that P2RX7-B is expressed in various organs and resting immune cells [67], and when co expressed with P2RX7-A, may affect the binding/gating properties of P2RX7 [84]. Undoubtedly, new progresses

will be made with the implementation of novel tools to specifically assess the level of expression but also the biological activity of P2RX7 splice variants.

P2RX7 splice variants and cancer

One of the most intriguing questions considering P2RX7 is to explain how a receptor that induces cell death in the presence of its endogenous ligand, namely eATP, could be overexpressed in some cancers [91]. Indeed, knowing that the tumor microenvironment, like the inflammatory tissue, contain hundreds of micromolar eATP [92], it is counterintuitive to imagine that a protein leading to cell death is overexpressed by cancer cells. The best way to harmonize these two observations is to hypothesize that the receptor expressed at the surface of cancer cells is unable to trigger cell death. This idea is sustained by several studies showing that P2RX7 expressed at the surface of diseased cells is a non-functional conformation [85]. The first description of the expression of a non-functional P2RX7 (nfP2RX7) was made in cancerous breast lesions where the group of Julian Barden used an antibody designed against an epitope located in the extracellular loop close to the eATP binding pocket and which is inaccessible in cells expressing normal functional P2RX7 [93,94]. Furthermore, the expression of non-functional P2RX7 on the surface of cancer cells was shown in organs as diverse as gut, ovary, cervix, lung, liver, and bladder [85]. Intriguingly, nfP2RX7 electrophoretic feature is indistinguishable from P2RX7 and today, the exact nature of this receptor channel remains a mystery. Gilbert and collaborators characterized the expression of nfP2RX7 from a panel of tumor cell lines using a new humanized antibody (BIL03) that is specific to the extracellular domain of nfP2RX7 [95]. As suggested by previous reports, they confirmed that nfP2RX7 is expressed in many cancer cell lines. They showed that nfP2RX7 is molecularly distinct from P2RX7 using specific antibodies and biological assays (EtBr uptake). Finally, the authors reported that nfP2RX7 is stored intracellularly and localized to the cell membrane upon eATP stimulation, an event that requires protein synthesis. Strikingly, it seems that expression of nfP2RX7 is mutually exclusive since its localization to the cell membrane correlates with the loss of P2RX7. As this non-functional receptor lacks apoptotic activity but retains residual non-selective cations channel, it was proposed that it promotes tumor growth. The mechanisms leading to the expression of nfP2RX7 is not fully understood nowadays, but at least two main hypotheses could be drawn. The first one, as discussed previously, relies on the formation of an heterotrimer, composed of P2RX7-A and P2RX7-B, which may lack the potential to induce cell death. In their study, Gilbert and collaborators did not check if expression of nfP2RX7 requires mRNA translation, however they hypothesized that intracellular nfP2RX7 may correspond to a misfolded protein and it is known that P2RX7-B lack C-terminal region that participates to the trafficking to the cell surface. The second one relies on the ability of cholesterol to control P2RX7-dependent large cation influx, as elegantly demonstrated by Karasawa and collaborators [60] and discussed earlier in this review. Considering that cancer cell membranes contain more saturated lipids, it is tempting to speculate that this change in lipid composition affects P2RX7 biology [96]. This hypothesis is supported by the discovery that, in a human prostate cancer cell line (LNCaP), oxidative stress-induced cell death is reversed when cells were pretreated with Soraphen A, an inhibitor of acetyl CoA carboxylase which modulates the synthesis of very long chain saturated, mono- and polyunsaturated fatty acids [97]. While this paper highlighted a direct relation between lipid composition and stress-induced cell death, no link was made with the eATP/P2RX7 signaling. By contrast, it is well established that P2RX7 activates phospholipid signaling pathways in epithelial cells through the modulation of phospholipases and sphingomyelinase [98]. Additionally, activation of P2RX7 drives the production of phosphatidic acid in RAW 264.7 macrophages which in turn delays eATP-induced pore opening and cytolysis. Therefore, a direct link between P2RX7 activation, membrane lipid composition and cell death was described at least in some immune cells [99,100]. Additional research is required to establish the relationship between eATP, expression of cell surface nfP2RX7, lipid metabolism and lack of pore opening-induced cell death. Undoubtedly, if this holds true it will reconciliate the fact that cancer cells are positively stained by antibodies directed against ubiquitously expressed P2RX7 epitopes.

Recently, a new P2RX7 splice variant was described, namely P2RX7-V3 which contains an extra exon N3 and corresponds to a long non-coding RNA [101]. Long non-coding RNAs do not code for proteins but have been involved in diverse cellular processes by interfering with chromatin-modifying complexes and transcription factors [102]. P2RX7-V3 is expressed at high levels in cell lines derived from uveal melanoma where it works as an oncogene. Even though the mode of action of this splice variant and its expression in other cancer tissues need to be investigated, the authors proposed that P2RX7-V3 may be an informative biomarker of cancer. Beyond, this report suggests that at least one P2RX7 splice variant might by itself, regulate cellular processes relevant for cancer, a field that has not yet been explored.

Conclusion

Here, we discussed the role of alternative splicing in the field of P2RX7 signaling. Our attempts were to discuss if expression of P2RX7A and its splice variants in a same cell could impact the functionality of P2RX7 and to bring new thoughts on the nature of nfP2RX7 that is expressed at the membrane of cancer cells. Despite the quantity of data published over the last two decades, there are still unresolved questions regarding the role of P2RX7 in health and diseases. Undoubtedly, development of new specific tools to unravel the expression of P2RX7 splice variants and the functionality of P2RX7 will bring new insights in biology and medicine. This is particularly relevant in the light of the recent discovery that

tumor-specific splicing produces numerous splicing associated potential neoantigens that may affect the immune response and could be exploited in the field of onco-immunology [103].

Conflicts of interest

The authors declare they have no conflicts of interest.

Acknowledgments

We also would like to thank Patrick Brest and Lionel Arnaud for stimulating discussions and Jean Kanellopoulos for critical reading of the manuscript. The funding sources for this work were Institut National du Cancer (INCa), Canceropole PACA, INSERM, CNRS, Bristol-Myers Squibb Foundation for Research in Immuno-Oncology, La Ligue contre le Cancer and the French Government (National Research Agency, ANR through the "Investments for the Future" LABEX SIGNALIFE: program reference #ANR-11-LABX-0028-01).

Appendix A. Supplementary data

Supplementary data to this article can be found online at https://doi.org/10.1016/j.bj.2019.05.007.

REFERENCES

[1] Chow LT, Gelinas RE, Broker TR, Roberts RJ. An amazing sequence arrangement at the 5′ ends of adenovirus 2 messenger RNA. Cell 1977;12:1–8.
[2] Tazi J, Bakkour N, Stamm S. Alternative splicing and disease. Biochim Biophys Acta – Mol Basis Dis 2009;1792:14–26.
[3] Bessonov S, Anokhina M, Krasauskas A, Golas MM, Sander B, Will CL, et al. Characterization of purified human Bact spliceosomal complexes reveals compositional and morphological changes during spliceosome activation and first step catalysis. RNA 2010;16:2384–403.
[4] Chabot B, Shkreta L. Defective control of pre-messenger RNA splicing in human disease. J Cell Biol 2016;212:13–27.
[5] Keren H, Lev-Maor G, Ast G. Alternative splicing and evolution: diversification, exon definition and function. Nat Rev Genet 2010;11:345–55.
[6] Buratti E, Baralle M, Baralle FE. Defective splicing, disease and therapy: searching for master checkpoints in exon definition. Nucleic Acids Res 2006;34:3494–510.
[7] Stamm S. Regulation of alternative splicing by reversible protein phosphorylation. J Biol Chem 2008;283:1223–7.
[8] Pan Q, Shai O, Lee LJ, Frey BJ, Blencowe BJ. Deep surveying of alternative splicing complexity in the human transcriptome by high-throughput sequencing. Nat Genet 2008;40:1413–5.
[9] Wang ET, Sandberg R, Luo S, Khrebtukova I, Zhang L, Mayr C, et al. Alternative isoform regulation in human tissue transcriptomes. Nature 2008;456:470–6.
[10] Kim HK, Pham MHC, Ko KS, Rhee BD, Han J. Alternative splicing isoforms in health and disease. Pflugers Arch Eur J Physiol 2018;470:995–1016.
[11] Merkin J, Russell C, Chen P, Burge CB. Evolutionary dynamics of gene and isoform regulation in mammalian tissues. Science (80) 2012;338:1593–9.
[12] Cesaro A, Brest P, Hofman V, Hébuterne X, Wildman S, Ferrua B, et al. Amplification loop of the inflammatory process is induced by P2X 7 R activation in intestinal epithelial cells in response to neutrophil transepithelial migration. Am J Physiol Cell Physiol 2010;299:32–42.
[13] Mishra A, Chintagari NR, Guo Y, Weng T, Su L, Liu L. Purinergic P2X 7 receptor regulates lung surfactant secretion in a paracrine manner. J Cell Sci 2011;124:657–68.
[14] Ruzsnavszky O, Telek A, Gönczi M, Balogh A, Remenyik É, Csernoch L. Journal of Photochemistry and Photobiology B : biology UV-B induced alteration in purinergic receptors and signaling on HaCaT keratinocytes. J Photochem Photobiol B Biol 2011;105:113–8.
[15] Jørgensen NR, Henriksen Z, Sørensen OH, Eriksen EF, Civitelli R, Steinberg TH. Intercellular calcium signaling occurs between human osteoblasts and osteoclasts and requires activation of osteoclast P2X7 receptors *. J Biol Chem 2002;277:7574–80.
[16] Solini A, Chiozzi P, Morelli A, Fellin R, Di Virgilio F. Human primary fibroblasts in vitro express a purinergic P2X 7 receptor coupled to ion fluxes, microvesicle formation and IL-6 release. J Cell Sci 1999;305:297–305.
[17] Sluyter R, Shemon AN, Barden JA, Wiley JS. Extracellular ATP increases cation fluxes in human erythrocytes by activation of the P2X 7 receptor *. J Biol Chem 2004;279:44749–55.
[18] Georgiou JG, Skarratt ÃKK, Fuller ÃSJ, Martin ÃCJ, Richard I, Wiley JS, et al. Human epidermal and monocyte-derived langerhans cells express functional P2X 7 receptors. J Investig Dermatol 2005;125:482–90.
[19] Baroni M, Pizzirani C, Pinotti M, Ferrari D, Adinolfi E, Calzavarini S, et al. Stimulation of P2 (P2X 7) receptors in human dendritic cells induces the release of tissue factor-bearing microparticles. FASEB J 2007;21:1926–33.
[20] Idzko M, Dichmann S, Ferrari D, Di Virgilio F, La Sala A, Girolomoni G, et al. Nucleotides induce chemotaxis and actin polymerization in immature but not mature human dendritic cells via activation of pertussis toxin-sensitive P2y receptors. Blood 2002;100:925–32.
[21] Christenson K, Bjo L, Ta C, Bylund J. Serum amyloid A inhibits apoptosis of human neutrophils via a P2X7-sensitive pathway independent of formyl peptide receptor like 1. J Leukoc Biol 2008;83:139–48.
[22] Wareham K, Vial C, Wykes RCE, Bradding P, Seward EP. Functional evidence for the expression of P2X1, P2X4 and P2X7 receptors in human lung mast cells abbreviations. Br J Pharmacol 2009;157:1215–24.
[23] Gu BJ, Zhang WY, Bendall LJ, Chessell IP, Buell GN, Wiley JS. Expression of P2X7 purinoceptors on human lymphocytes and monocytes: evidence for nonfunctional P2X7 receptors. Am J Physiol Cell Physiol 2000;279:1189–97.
[24] Chiozzi P, Sanz JM, Ferrari D, Falzoni S, Aleotti A, Buell GN, et al. Spontaneous cell fusion in macrophage cultures expressing high levels of the P2Z/P2X 7 receptor. J Cell Biol 1997;138:697–707.

[25] Borges H, Beura LK, Wang H, Hanse EA, Gore R, Scott MC, et al. Fitness of long-lived memory CD8 + T cells. Nature 2018;559:264.
[26] Idzko M, Dichmann S, Panther E, Ferrari D, Herouy Y, Virchow C, et al. Functional characterization of P2Y and P2X receptors in human eosinophils. J Cell Physiol 2001;188:329–36.
[27] Bianchi G, Vuerich M, Pellegatti P, Marimpietri D, Emionite L, Marigo I, et al. ATP/P2X7 axis modulates myeloid-derived suppressor cell functions in neuroblastoma microenvironment. Cell Death Dis 2014;5. e1135-12.
[28] Deli T, Varga N, Adam A, Kenessey I, Raso E, Puskas L, et al. Functional genomics of calcium channels in human melanoma cells. Int J Cancer 2007;121:55–65.
[29] Solini A, Cuccato S, Ferrari D, Santini E, Gulinelli S, Callegari MG, et al. Increased P2X 7 receptor expression and function in thyroid papillary cancer : a new potential marker of the disease? Endocrinology 2008;149:389–96.
[30] Vázquez-cuevas FG, Martínez-ramírez AS, Robles-martínez L, Garay E, García-carrancá A, Pérez-montiel D, et al. Paracrine stimulation of P2X7 receptor by ATP activates a proliferative pathway in ovarian carcinoma cells. J Cell Biochem 2014;1966:1955–66.
[31] Santos AAJ, Cappellari AR, De Marchi FO, Gehring MP, Zaparte A, Brandão CA, et al. Potential role of P2X7R in esophageal squamous cell carcinoma proliferation. Purine Pyrimidine Recept Pharmacol (Jacobson KA, Linden J, Eds) 2017;13:279–92.
[32] Li X, Qi X, Zhou L, Fu W, Gorodeski GI. P2X 7 receptor expression is decreased in epithelial cancer cells of ectodermal, uro-genital sinus, and distal paramesonephric duct origin. Purinergic Signal 2009;5:351–68.
[33] Adinolfi E, Melchiorri L, Falzoni S, Chiozzi P, Morelli A, Tieghi A, et al. Brief report P2X 7 receptor expression in evolutive and indolent forms of chronic B lymphocytic leukemia. Blood 2002;99:706–9.
[34] Zhang X, Zheng G, Ma X, Yang Y, Li G, Rao Q, et al. Expression of P2X7 in human hematopoietic cell lines and leukemia patients. Leuk Res 2004;28:1313–22.
[35] Chong J, Zheng G, Zhu X, Guo Y, Wang L, Ma C, et al. Abnormal expression of P2X family receptors in Chinese pediatric acute leukemias. Biochem Biophys Res Commun 2010;391:498–504.
[36] Pineda JMB, Bradley RK. Most human introns are recognized via multiple and tissue-specific branchpoints. Genes Dev 2018;32:577–91.
[37] Kaczmarek-Hajek K, Zhang J, Kopp R, Grosche A, Rissiek B, Saul A, et al. Re-evaluation of neuronal P2X7 expression using novel mouse models and a P2X7-specific nanobody. Elife 2018;7:1–29.
[38] Barbosa-Morais NL, Irimia M, Pan Q, Xiong HY, Gueroussov S, Lee LJ, et al. The evolutionary landscape of alternative splicing in vertebrate species. Science (80) 2012;338:1587–93.
[39] Graveley BR. Alternative splicing: increasing diversity in the proteomic world. Trends Genet 2001;17:100–7.
[40] Czubaty A, Piekiełko-Witkowska A. Protein kinases that phosphorylate splicing factors: roles in cancer development, progression and possible therapeutic options. Int J Biochem Cell Biol 2017;91:102–15.
[41] Lim KH, Ferraris L, Filloux ME, Raphael BJ, Fairbrother WG. Using positional distribution to identify splicing elements and predict pre-mRNA processing defects in human genes. Proc Natl Acad Sci Unit States Am 2011;108:11093–8.
[42] Carazo F, Romero JP, Rubio A. Upstream analysis of alternative splicing: a review of computational approaches to predict context-dependent splicing factors. Briefings Bioinf 2018:1–18.
[43] Montes M, Sanford BL, Comiskey DF, Chandler DS. RNA splicing and disease: animal models to therapies. Trends Genet 2019;35:68–87.
[44] Drury AN, Szent-Györgyi A. The physiological activity of adenine compounds with especial reference to their action upon the mammalian heart. J Physiol 1929;68:213–37.
[45] Burnstock G. Is there a basis for distinguishing two types of purinergic receptor. Gen Pharmacol 1985;16:141–54.
[46] Jacobson KA. Introduction to adenosine receptors as therapeutic targets. Handb Exp Pharmacol 2009;193:1–24.
[47] Burnstock G, Williams M. P2 purinergic receptors: modulation of cell function and therapeutic potential. J Pharmacol Exp Ther 2000;23:862–9.
[48] North RA. Molecular physiology of P2X receptors. Physiol Rev 2002;82:1013–67.
[49] Surprenant A, Rassendren F, Kawashima E, North RA, Buell G. The cytolytic P2Z receptor for extracellular ATP identified as a P2X receptor (P2X7). Science (80-) 1996;272:735–8.
[50] Denlinger LC, Fisette PL, Sommer JA, Watters JJ, Prabhu U, Dubyak GR, et al. Cutting edge: the nucleotide receptor P2X7 contains multiple protein- and lipid-interaction motifs including a potential binding site for bacterial lipopolysaccharide. J Immunol 2001;167:1871–6.
[51] Burnstock G, Kennedy C. P2X receptors in health and disease. In: Jacobson KA, Linden J, editors. Purine Pyrimidine Recept. Pharmacol, vol. 61; 2011. p. 333–72.
[52] Darmellah A, Rayah A, Auger R, Cuif MH, Prigent M, Arpin M, et al. Ezrin/radixin/moesin are required for the purinergic P2X7 receptor (P2X7R)-dependent processing of the amyloid precursor protein. J Biol Chem 2012;287:34583–95.
[53] Sluyter R. The P2X7 receptor. Adv Exp Med Biol 2017;1051:17–53.
[54] Mellouk A, Bobé P. CD8 + , but not CD4 + effector/memory T cells, express the CD44 high CD45RB high phenotype with aging, which displays reduced expression levels of P2X 7 receptor and ATP-induced cellular responses. FASEB J 2019;33:3225–36.
[55] Karasawa A, Kawate T. Structural basis for subtype-specific inhibition of the P2X7 receptor. Elife 2016;5:e22153.
[56] Kasuya G, Fujiwara Y, Tsukamoto H, Morinaga S, Ryu S, Touhara K, et al. Structural insights into the nucleotide base specificity of P2X receptors. Sci Rep 2017;7:45208.
[57] Kawate T, Michel JC, Birdsong WT, Gouaux E. Crystal structure of the ATP-gated P2X4ion channel in the closed state. Nature 2009;460:592–8.
[58] Hattori M, Hibbs RE, Gouaux E. A fluorescence-detection size-exclusion chromatography-based thermostability assay to identify membrane protein expression and crystallization conditions. Structure 2012;20:1293–9.
[59] Mansoor SE, Lü W, Oosterheert W, Shekhar M, Tajkhorshid E, Gouaux E. X-ray structures define human P2X 3 receptor gating cycle and antagonist action. Nature 2016;538:66–71.
[60] Karasawa A, Michalski K, Mikhelzon P, Kawate T. The P2X7 receptor forms a dye-permeable pore independent of its intracellular domain but dependent on membrane lipid composition. Elife 2017;6:e31186.
[61] Gonnord P, Delarasse C, Auger R, Benihoud K, Prigent M, Cuif MH, et al. Palmitoylation of the P2X7 receptor, an ATP-

[25] Borges H, Beura LK, Wang H, Hanse EA, Gore R, Scott MC, et al. Fitness of long-lived memory CD8 + T cells. Nature 2018;559:264.
[26] Idzko M, Dichmann S, Panther E, Ferrari D, Herouy Y, Virchow C, et al. Functional characterization of P2Y and P2X receptors in human eosinophils. J Cell Physiol 2001;188:329–36.
[27] Bianchi G, Vuerich M, Pellegatti P, Marimpietri D, Emionite L, Marigo I, et al. ATP/P2X7 axis modulates myeloid-derived suppressor cell functions in neuroblastoma microenvironment. Cell Death Dis 2014;5. e1135-12.
[28] Deli T, Varga N, Adam A, Kenessey I, Raso E, Puskas L, et al. Functional genomics of calcium channels in human melanoma cells. Int J Cancer 2007;121:55–65.
[29] Solini A, Cuccato S, Ferrari D, Santini E, Gulinelli S, Callegari MG, et al. Increased P2X 7 receptor expression and function in thyroid papillary cancer : a new potential marker of the disease? Endocrinology 2008;149:389–96.
[30] Vázquez-cuevas FG, Martínez-ramírez AS, Robles-martínez L, Garay E, García-carrancá A, Pérez-montiel D, et al. Paracrine stimulation of P2X7 receptor by ATP activates a proliferative pathway in ovarian carcinoma cells. J Cell Biochem 2014;1966:1955–66.
[31] Santos AAJ, Cappellari AR, De Marchi FO, Gehring MP, Zaparte A, Brandão CA, et al. Potential role of P2X7R in esophageal squamous cell carcinoma proliferation. Purine Pyrimidine Recept Pharmacol (Jacobson KA, Linden J, Eds) 2017;13:279–92.
[32] Li X, Qi X, Zhou L, Fu W, Gorodeski GI. P2X 7 receptor expression is decreased in epithelial cancer cells of ectodermal, uro-genital sinus, and distal paramesonephric duct origin. Purinergic Signal 2009;5:351–68.
[33] Adinolfi E, Melchiorri L, Falzoni S, Chiozzi P, Morelli A, Tieghi A, et al. Brief report P2X 7 receptor expression in evolutive and indolent forms of chronic B lymphocytic leukemia. Blood 2002;99:706–9.
[34] Zhang X, Zheng G, Ma X, Yang Y, Li G, Rao Q, et al. Expression of P2X7 in human hematopoietic cell lines and leukemia patients. Leuk Res 2004;28:1313–22.
[35] Chong J, Zheng G, Zhu X, Guo Y, Wang L, Ma C, et al. Abnormal expression of P2X family receptors in Chinese pediatric acute leukemias. Biochem Biophys Res Commun 2010;391:498–504.
[36] Pineda JMB, Bradley RK. Most human introns are recognized via multiple and tissue-specific branchpoints. Genes Dev 2018;32:577–91.
[37] Kaczmarek-Hajek K, Zhang J, Kopp R, Grosche A, Rissiek B, Saul A, et al. Re-evaluation of neuronal P2X7 expression using novel mouse models and a P2X7-specific nanobody. Elife 2018;7:1–29.
[38] Barbosa-Morais NL, Irimia M, Pan Q, Xiong HY, Gueroussov S, Lee LJ, et al. The evolutionary landscape of alternative splicing in vertebrate species. Science (80) 2012;338:1587–93.
[39] Graveley BR. Alternative splicing: increasing diversity in the proteomic world. Trends Genet 2001;17:100–7.
[40] Czubaty A, Piekiełko-Witkowska A. Protein kinases that phosphorylate splicing factors: roles in cancer development, progression and possible therapeutic options. Int J Biochem Cell Biol 2017;91:102–15.
[41] Lim KH, Ferraris L, Filloux ME, Raphael BJ, Fairbrother WG. Using positional distribution to identify splicing elements and predict pre-mRNA processing defects in human genes. Proc Natl Acad Sci Unit States Am 2011;108:11093–8.
[42] Carazo F, Romero JP, Rubio A. Upstream analysis of alternative splicing: a review of computational approaches to predict context-dependent splicing factors. Briefings Bioinf 2018:1–18.
[43] Montes M, Sanford BL, Comiskey DF, Chandler DS. RNA splicing and disease: animal models to therapies. Trends Genet 2019;35:68–87.
[44] Drury AN, Szent-Györgyi A. The physiological activity of adenine compounds with especial reference to their action upon the mammalian heart. J Physiol 1929;68:213–37.
[45] Burnstock G. Is there a basis for distinguishing two types of purinergic receptor. Gen Pharmacol 1985;16:141–54.
[46] Jacobson KA. Introduction to adenosine receptors as therapeutic targets. Handb Exp Pharmacol 2009;193:1–24.
[47] Burnstock G, Williams M. P2 purinergic receptors: modulation of cell function and therapeutic potential. J Pharmacol Exp Ther 2000;23:862–9.
[48] North RA. Molecular physiology of P2X receptors. Physiol Rev 2002;82:1013–67.
[49] Surprenant A, Rassendren F, Kawashima E, North RA, Buell G. The cytolytic P2Z receptor for extracellular ATP identified as a P2X receptor (P2X7). Science (80-) 1996;272:735–8.
[50] Denlinger LC, Fisette PL, Sommer JA, Watters JJ, Prabhu U, Dubyak GR, et al. Cutting edge: the nucleotide receptor P2X7 contains multiple protein- and lipid-interaction motifs including a potential binding site for bacterial lipopolysaccharide. J Immunol 2001;167:1871–6.
[51] Burnstock G, Kennedy C. P2X receptors in health and disease. In: Jacobson KA, Linden J, editors. Purine Pyrimidine Recept. Pharmacol, vol. 61; 2011. p. 333–72.
[52] Darmellah A, Rayah A, Auger R, Cuif MH, Prigent M, Arpin M, et al. Ezrin/radixin/moesin are required for the purinergic P2X7 receptor (P2X7R)-dependent processing of the amyloid precursor protein. J Biol Chem 2012;287:34583–95.
[53] Sluyter R. The P2X7 receptor. Adv Exp Med Biol 2017;1051:17–53.
[54] Mellouk A, Bobé P. CD8 + , but not CD4 + effector/memory T cells, express the CD44 high CD45RB high phenotype with aging, which displays reduced expression levels of P2X 7 receptor and ATP-induced cellular responses. FASEB J 2019;33:3225–36.
[55] Karasawa A, Kawate T. Structural basis for subtype-specific inhibition of the P2X7 receptor. Elife 2016;5:e22153.
[56] Kasuya G, Fujiwara Y, Tsukamoto H, Morinaga S, Ryu S, Touhara K, et al. Structural insights into the nucleotide base specificity of P2X receptors. Sci Rep 2017;7:45208.
[57] Kawate T, Michel JC, Birdsong WT, Gouaux E. Crystal structure of the ATP-gated P2X4ion channel in the closed state. Nature 2009;460:592–8.
[58] Hattori M, Hibbs RE, Gouaux E. A fluorescence-detection size-exclusion chromatography-based thermostability assay to identify membrane protein expression and crystallization conditions. Structure 2012;20:1293–9.
[59] Mansoor SE, Lü W, Oosterheert W, Shekhar M, Tajkhorshid E, Gouaux E. X-ray structures define human P2X 3 receptor gating cycle and antagonist action. Nature 2016;538:66–71.
[60] Karasawa A, Michalski K, Mikhelzon P, Kawate T. The P2X7 receptor forms a dye-permeable pore independent of its intracellular domain but dependent on membrane lipid composition. Elife 2017;6:e31186.
[61] Gonnord P, Delarasse C, Auger R, Benihoud K, Prigent M, Cuif MH, et al. Palmitoylation of the P2X7 receptor, an ATP-

gated channel, controls its expression and association with lipid rafts. FASEB J 2009;23:795–805.
[62] Robinson LE, Shridar M, Smith P, Murrell-Lagnado RD. Plasma membrane cholesterol as a regulator of human and rodent P2X7 receptor activation and sensitization. J Biol Chem 2014;289:31983–4.
[63] Allsopp RC, Evans RJ. Contribution of the juxtatransmembrane intracellular regions to the time course and permeation of ATP-gated P2X7 receptor ion channels. J Biol Chem 2015;290:14556–66.
[64] Pippel A, Stolz M, Woltersdorf R, Kless A, Schmalzing G, Markwardt F. Localization of the gate and selectivity filter of the full-length P2X7 receptor. Proc Natl Acad Sci USA 2017;114:2156–65.
[65] Harkat M, Peverini L, Cerdan AH, Dunning K, Beudez J, Martz A, et al. On the permeation of large organic cations through the pore of ATP-gated P2X receptors. Proc Natl Acad Sci USA 2017;114:3786–95.
[66] Di Virgilio F, Schmalzing G, Markwardt F. The elusive P2X7 macropore. Trends Cell Biol 2018;28:392–404.
[67] Cheewatrakoolpong B, Gilchrest H, Anthes JC, Greenfeder S. Identification and characterization of splice variants of the human P2X7ATP channel. Biochem Biophys Res Commun 2005;332:17–27.
[68] Adinolfi E, Cirillo M, Woltersdorf R, Falzoni S, Chiozzi P, Pellegatti P, et al. Trophic activity of a naturally occurring truncated isoform of the P2X7 receptor. FASEB J 2010;24:3393–404.
[69] Smart ML, Gu B, Panchal RG, Wiley J, Cromer B, Williams DA, et al. P2X7 receptor cell surface expression and cytolytic pore formation are regulated by a distal C-terminal region. J Biol Chem 2003;278:8853–60.
[70] Denlinger LC, Sommer JA, Parker K, Gudipaty L, Fisette PL, Watters JW, et al. Mutation of a dibasic amino acid motif within the C terminus of the P2X7 nucleotide receptor results in trafficking defects and impaired function. J Immunol 2003;171:1304–11.
[71] Murrell-Lagnado RD, Qureshi OS. Assembly and trafficking of P2X purinergic receptors (Review). Mol Membr Biol 2008;25:321–31.
[72] Feng YH, Li X, Wang L, Zhou L, Gorodeski GI. A truncated P2X7 receptor variant (P2X7-j) endogenously expressed in cervical cancer cells antagonizes the full-length P2X7 receptor through hetero-oligomerization. J Biol Chem 2006;281:17228–37.
[73] Guzman-Aranguez A, Pérez de Lara MJ, Pintor J. Hyperosmotic stress induces ATP release and changes in P2X7 receptor levels in human corneal and conjunctival epithelial cells. Purinergic Signal 2017;13:249–58.
[74] Kido Y, Kawahara C, Terai Y, Ohishi A, Kobayashi S, Hayakawa M, et al. Regulation of activity of P2X7 receptor by its splice variants in cultured mouse astrocytes. Glia 2014;62:440–51.
[75] Nicke A, Kuan YH, Masin M, Rettinger J, Marquez-Klaka B, Bender O, et al. A functional P2X7 splice variant with an alternative transmembrane domain 1 escapes gene inactivation in P2X7 knock-out mice. J Biol Chem 2009;284:25813–22.
[76] Schwarz N, Drouot L, Nicke A, Fliegert R, Boyer O, Guse AH, et al. Alternative splicing of the N-terminal cytosolic and transmembrane domains of P2X7 controls gating of the ion channel by ADP-ribosylation. PLoS One 2012;7:e41269.
[77] Haanes KA, Schwab A, Novak I. The P2X7 receptor supports both life and death in fibrogenic pancreatic stellate cells. PLoS One 2012;7:e51164.
[78] Masin M, Young C, Lim K, Barnes SJ, Xu XJ, Marschall V, et al. Expression, assembly and function of novel C-terminal truncated variants of the mouse P2X7 receptor: Re-evaluation of P2X7 knockouts. Br J Pharmacol 2012;165:978–93.
[79] Csóka B, Németh ZH, Töro G, Idzko M, Zech A, Koscsó B, et al. Extracellular ATP protects against sepsis through macrophage P2X7 purinergic receptors by enhancing intracellular bacterial killing. FASEB J 2015;29:3626–37.
[80] Metzger M, Walser S, Aprile-Garcia F, Dedic N, Chen A, Holsboer F, et al. Genetically dissecting P2rx7 expression within the central nervous system using conditional humanized mice 2016;13:153–70.
[81] Gudipaty L, Humphreys BD, Buell G, Dubyak GR. Regulation of P2X7 nucleotide receptor function in human monocytes by extracellular ions and receptor density. Am J Physiol Cell Physiol 2001;280:C943–53.
[82] Gudipaty L, Munetz J, Verhoef PA, Dubyak GR. Essential role for Ca^{2+} in regulation of IL-1β secretion by $P2X_7$ nucleotide receptor in monocytes, macrophages, and HEK-293 cells. Am J Physiol Physiol 2003;285:C286–99.
[83] Rissiek B, Haag F, Boyer O, Koch-Nolte F, Adriouch S. P2X7 on mouse T cells: one channel, many functions. Front Immunol 2015;6:1–9.
[84] Liang X, Samways DSK, Bowles EA, Richards JP, Wolf K, Egan TM, et al. Quantifying Ca 2+ current and permeability in ATP-gated P2X7 receptors. J Biol Chem 2015;290:7930–42.
[85] Barden JA. Non-functional P2X7: a novel and ubiquitous target in human cancer. J Clin Cell Immunol 2014;05:237–41.
[86] Buell G, Chessell IP, Michel a D, Collo G, Salazzo M, Herren S, et al. Blockade of human P2X7 receptor function with a monoclonal antibody. Blood 1998;92:3521–8.
[87] Kim M, Jiang LH, Wilson HL, North RA, Surprenant A. Proteomic and functional evidence for a P2X7 receptor signalling complex. EMBO J 2001;20:6347–58.
[88] Sluyter R, Stokes L. Significance of P2X7 receptor variants to human health and disease. Recent Pat DNA Gene Sequences 2011;5:41–54.
[89] Zhang J, Manley JL. Misregulation of pre-mRNA alternative splicing in cancer. Cancer Discov 2013;3:1228–37.
[90] Wu Q, Krainer AR. AT-AC pre-mRNA splicing mechanisms and conservation of minor introns in voltage-gated ion channel genes. Mol Cell Biol 2015;19:3225–36.
[91] Adinolfi E, Raffaghello L, Giuliani AL, Cavazzini L, Capece M, Chiozzi P, et al. Expression of P2X7 receptor increases in vivo tumor growth. Cancer Res 2012;72:2957–69.
[92] Pellegatti P, Raffaghello L, Bianchi G, Piccardi F, Pistoia V, Di Virgilio F. Increased level of extracellular ATP at tumor sites: in vivo imaging with plasma membrane luciferase. PLoS One 2008;3:1–9.
[93] Barden JA, Sluyter R, Gu BJ, Wiley JS. Specific detection of non-functional human P2X7 receptors in HEK293 cells and B-lymphocytes. FEBS Lett 2003;538:159–62.
[94] Slater M, Danieletto S, Pooley M, Gidley-Baird A, Cheng Teh L, Barden JA, et al. Differentiation between cancerous and normal hyperplastic lobules in breast lesions. Breast Cancer Res Treat 2004;83:1–10.
[95] Gilbert S, Oliphant C, Hassan S, Peille A, Bronsert P, Falzoni S, et al. ATP in the tumour microenvironment drives expression of nfP2X7, a key mediator of cancer cell survival. Oncogene 2018;38:194–208.
[96] Zaidi N, Lupien L, Kuemmerle NB, Kinlaw WB, Swinnen JV, Smans K. Lipogenesis and lipolysis: the pathways exploited by the cancer cells to acquire fatty acids. Prog Lipid Res 2013;52:585–9.
[97] Rysman E, Brusselmans K, Scheys K, Timmermans L, Derua R, Munck S, et al. De novo lipogenesis protects cancer cells from free radicals and chemotherapeutics by

promoting membrane lipid saturation. Cancer Res 2010;70:8117–26.
[98] Garcia-Marcos M, Pochet S, Marino A, Dehaye J. P2X7 and phospholipid signalling: the search of the "missing link" in epithelial cells. Cell Signal 2006;18:2098–104.
[99] Le Stunff H, Raymond MN. P2X7 receptor-mediated phosphatidic acid production delays ATP-induced pore opening and cytolysis of RAW 264.7 macrophages. Cell Signal 2007;19:1909–18.
[100] Costa-Junior HM, Marques-da-Silva C, Vieira FS, Vieira FS, Monção-Ribeiro LC, Coutinho-Silva R. Lipid metabolism modulation by the P2X7 receptor in the immune system and during the course of infection: new insights into the old view. Purinergic Signal 2011;7:381–92.
[101] Pan H, Ni H, Zhang LL, Xing Y, Fan J, Li P, et al. P2RX7-V3 is a novel oncogene that promotes tumorigenesis in uveal melanoma. Tumor Biol 2016;37:13533–43.
[102] Fernandes J, Acuna S, Floeter-Winter L, Muxel S. Long non-coding RNAs in the regulation of gene expression: physiology and disease. Non-Coding RNA 2019;5:E17.
[103] Kahles A, Lehmann K, Toussaint N, Huser M, Stark S, Sachsenberg T, et al. Comprehensive analysis of alternative splicing across tumor form 8705 patients. Cancer Cell 2019;34:211–24.

IV. Objectifs de la thèse

L'objectif principal de cette thèse était de définir si le récepteur P2RX7, impliqué dans la perméabilisation membranaire et la lyse cellulaire, est fonctionnellement exprimé par les cellules du LUAD. Je me suis donc attaché à caractériser l'expression et la fonction de P2RX7 dans le LUAD chez l'humain, et de tester l'hypothèse selon laquelle l'expression de variants d'épissage pourraient impacter les fonctions biologiques du récepteur dans cette pathologie.

La revue présentée en III.D fait un état de la littérature et a permis de guider la mise en œuvre des travaux de recherche afin de répondre à cet objectif. La publication scientifique présentée en V.A étaye les résultats obtenus pour cet objectif, ainsi que les outils spécifiquement élaborés à cette fin.

L'objectif complémentaire de cette thèse, était de participer à la caractérisation d'un nouveau modulateur chimique positif de P2RX7 dans le CNPC chez la souris.

Les outils de caractérisation de P2RX7 utilisés dans la publication présentée en V.A ont été utilisés pour cet objectif, dont les résultats sont présentés en V.B.

V. Résultats

A. Publication scientifique N°1. Les cellules immunitaires infiltrant la tumeur d'un adénocarcinome pulmonaire humain expriment un variant d'épissage tronqué de *P2RX7* ce qui entrave la localisation membranaire et l'activité macropore du récepteur.

Article publié (Theranostics 2020; 10(24):10849-10860. doi:10.7150/thno.48229)

Dans ce travail nous analysons l'expression chez l'homme de *P2RX7* et de ses variants d'épissage dans les cellules immunitaires et non immunitaires du LUAD et de la zone tissulaire non tumorale adjacente.

Nous montrons que *P2RX7* et ses variants d'épissage *P2RX7B, H, J* sont exprimés mais négativement régulés dans la zone tumorale de l'adénocarcinome pulmonaire. Nous montrons que les cellules immunitaires pulmonaires intra et extratumorales expriment un récepteur P2RX7 dont la fonction d'ouverture du large pore est conservée. Nous montrons que, bien que les cellules immunitaires infiltrant la tumeur conservent cette fonction d'ouverture du large pore, elle y est altérée, et ceci corrèle avec l'expression du variant d'épissage *P2RX7B*. Nous montrons que les patients dont l'expression de *P2RX7B* est la plus forte dans les cellules immunitaires infiltrant la tumeur, présentent des tumeurs très faiblement infiltrées en cellules immunitaires. Nous montrons enfin dans un modèle d'expression hétérologue que P2RX7B est capable d'hétéro-oligomériser avec la forme pleine taille P2RX7A, impactant la localisation membranaire du récepteur et sa fonction d'ouverture du large pore.

Ce travail montre que *P2RX7B* pourrait représenter un marqueur théranostique prometteur dans le LUAD dans une perspective translationnelle.

IVYSPRING INTERNATIONAL PUBLISHER

Theranostics

2020; 10(24): 10849-10860. doi: 10.7150/thno.48229

Research Paper

P2RX7B is a new theranostic marker for lung adenocarcinoma patients

Jonathan Benzaquen[1,4,5,6], Serena Janho Dit Hreich[1,5], Simon Heeke[1,2], Thierry Juhel[1,5], Salomé Lalvee[2,3], Serge Bauwens[1], Simona Saccani[1], Philippe Lenormand[1], Véronique Hofman[1,2,3,4], Mathilde Butori[1], Sylvie Leroy[4,6,7], Jean-Philippe Berthet[8], Charles-Hugo Marquette[1,4,6], Paul Hofman[1,2,3,4] and Valérie Vouret-Craviari[1,4,5]✉

1. Université Côte d'Azur, CNRS, INSERM, IRCAN UMR 7284, 06108 Nice, France.
2. Laboratory of Clinical and Experimental Pathology and Biobank, Pasteur Hospital, Nice, France.
3. Hospital-Related Biobank (BB-0033-00025), Pasteur Hospital, Nice, France.
4. FHU OncoAge, Nice, France.
5. Centre Antoine Lacassagne, 06107 Nice, France.
6. Department of Pulmonary Medicine and Oncology, Pasteur Hospital, Nice, France.
7. Université Côte d'Azur, CNRS UMR 7275 - IPMC, Sophia Antipolis, France.
8. Department of Thoracic surgery, Pasteur Hospital, Nice, France.

✉ Corresponding author: Valérie VOURET-CRAVIARI, IRCAN, 33 avenue de Valombrose, 06108 Nice, France. Telephone number: 00 33 492031223; E-mail: vouret@unice.fr.

Received: 2020.05.15; Accepted: 2020.06.21; Published: 2020.08.29

Abstract

Rationale: The characterization of new theranostic biomarkers is crucial to improving the clinical outcome of patients with advanced lung cancer. Here, we aimed at characterizing the P2RX7 receptor, a positive modulator of the anti-tumor immune response, in patients with lung adenocarcinoma.

Methods: The expression of *P2RX7* and its splice variants was analyzed by RT-qPCR using areas of tumor and non-tumor lung adenocarcinoma (LUAD) tissues on both immune and non-immune cells. The biological activity of P2RX7 was studied by flow cytometry using fluorescent dyes. Bi-molecular fluorescence complementation and confocal microscopy were used to assess the oligomerization of P2RX7. Tumor immune infiltrates were characterized by immunohistochemistry.

Results: Fifty-three patients with LUAD were evaluated. *P2RX7A*, and 3 alternative splice variants were expressed in LUAD tissues and expression was down regulated in tumor versus adjacent non-tumor tissues. The protein retained biological activity only in immune cells. The *P2RX7B* splice variant was differentially upregulated in immune cells ($P < 0.001$) of the tumor and strong evidence of oligomerization of P2RX7A and B was observed in the HEK expression model, which correlated with a default in the activity of P2RX7. Finally, LUAD patients with a high level of *P2RX7B* had non-inflamed tumors ($P = 0.001$).

Conclusion: Our findings identified P2RX7B as a new theranostic tool to restore functional P2RX7 activity and open alternative therapeutic opportunities to improve LUAD patient outcome.

Key words: lung cancer, P2X7R, purinergic signaling, ATP, splice variant

Introduction

Lung cancer is the leading cause of cancer-related deaths in the world. More than two thirds of lung cancers are diagnosed at an advanced stage [1] and need medical treatment including chemotherapy, targeted therapies and immunotherapies. Despite these new approaches, the 5-year survival rate of patients with any type of lung cancer remains at around 20%, all stages combined and ranges from 57% in localized lung cancers to 5% in metastatic lung cancers [1]. Therefore, deciphering new theranostic tools and understanding processes involved in the development of pro- or anti-tumor micro-

environments are of crucial importance to improve patient outcome.

Purinergic receptors for extracellular nucleotides (ATP, ADP, UTP, UDP) and the nucleoside adenosine have attracted growing interest since the discovery that inflammatory and cancer tissues contain high levels of extracellular ATP (eATP) [2] and adenosine (its degradation product), which has been described as an immunosuppressor [3]. The purinergic receptor family is divided into two major families, P2X and P2Y [4]. Depending on the receptor involved, extracellular purines orchestrate either immuno-stimulation or immunosuppression of host cells, as well as proliferation or cytotoxicity of tumor cells [5]. We focused on P2RX7, an ubiquitous receptor [6] described to be expressed at a particularly high level in white blood cells from the immune system, especially in monocytes/macrophages, lymphocytes and dendritic cells [7–10].

The full length P2RX7 receptor is an ATP-gated ion channel composed of three protein subunits encoded by *P2RX7A* mRNA. Activation of P2RX7 by high doses of eATP leads to Na^+ and Ca^{2+} influx and, after prolonged activation, to the opening of a larger conductance membrane pore, also defined as macropore activity or macropore opening [11]. One consequence of this macropore opening, a unique characteristic of P2RX7, is to induce cell death in eATP rich micro-environments. This feature is linked principally to the presence of a long C-terminal domain [12].

The use of transplantable murine tumor models has demonstrated that P2RX7 expressed by host immune cells coordinates anti-tumor immune responses [13,14]. The expression of a functional P2RX7 receptor on human white blood cells and in human hemopathies has been largely documented in the literature [15–17]. However, whereas numerous publications claimed that P2RX7 is over-expressed in solid tumors, on the basis of P2RX7 immunostaining using mostly antibodies directed against either the extracellular loop [18,19] or the C-terminal domain [20–26], only a little data are available regarding functional P2RX7 in *ex vivo* human solid cancer cells. This is of particular importance considering that P2RX7 functionality can be affected by single nucleotide polymorphisms (SNP). Over the 13252 SNPs described within *P2RX7* gene in 2020, the phenotype of 16 non-synonymous SNPs has been studied, some of which leading to numerous pathologies including infectious, bone, neuro-psychiatric, inflammatory, cardiovascular and cancerous diseases, but also poorer survival of cancer patients [27,28]. In addition, we found 27 SNPs located to the boundary of mRNA splicing sites within intronic regions which may affect splicing events. However, these SNPs are too sparsely expressed to envisage that they could be involved in diseases [29].

The function of P2RX7 can also be affected by alternative splicing. Nine alternative splice variants were identified [30,31]. The function of only three of them, P2RX7H with a deletion in the first transmembrane domain (ΔTM1) leading to a loss of ion channel function, P2RX7B with a deletion in the C-terminal domain (ΔCt) leading to a loss of large pore forming function, and P2RX7J with a deletion in the second transmembrane domain leading to a negative dominant isoform, have been studied in more detail [18,19,30–33].

P2RX7 protein expression in lung adeno-carcinoma (LUAD) was reported by Boldrini et al. [34], but it is currently unknown whether functional P2RX7 is expressed in LUAD. In this study we aimed at deciphering the expression of P2RX7 and its splice variants, and the implication of such variants on the biological function of the receptor and on inflammatory infiltration of tumors.

Materials and Methods

Patients

Twenty-four bronchopulmonary samples were obtained from the middle of the tumor and from non-tumor tissue for each patient operated on for early stage (I-IIIA) LUAD. The diagnosis and the margin of the samples were confirmed as tumoral by two lung cancer pathologists. The median age was 68 years-old and 79% of the patients were smokers or former smokers. In the retrospective study, twenty-nine LUAD samples were obtained from the biobank of the Nice University Hospital (Clinical and Experimental Pathology Laboratory) and were taken from patients operated on at the thoracic surgery department of the Nice University Hospital for early stage (I-IIIA) LUAD. The median age was 67 years-old and 100% of the patients were smokers or former smokers (see Table 1). Free and informed consent was obtained for each patient with the agreement of the South East CPP.

Tumor processing

After surgery, tumor tissues were kept in RPMI (Roswell Park Memorial Institute medium, Gibco®) at 4°C, for a maximum of 12 h. Sample preparation included scissor dissociation, incubation in Human Tumor Dissociation Kit (MACS®) buffer at 37°C for 40 min and washed by DPBS 10% FBS. Cells were counted and a trypan blue test was performed to ensure cell viability. Cells were magnetically sorted (mouse anti-CD45 MicroBeads, Miltenyi®) according

to the manufacturer's procedure. A sorting enrichment control experiment was performed using a humanized anti-CD45 AF488 coupled antibody (Miltenyi®) after Fc blocking (Figure S1A).

Table 1. Main epidemiological data of LUAD patients

Retrospective study (n=29)		
Age (years)	Mean (Range)	67 (41 – 85)
Sex	Female	6 (20.7%)
	Male	23 (79.3%)
Smoking history	Smokers or smoking history	29 (100%)
	Non smoker	0 (0%)
COPD #	Yes	18 (62%)
	No	11 (37.9%)
Stage at surgery	I	15 (51.7%)
	II	10 (34.4%)
	III	2 (6.9%)
	IV	0 (0%)
Adjuvant chemotherapy	Yes	3 (10.3%)
	No	26 (89.7%)
Relapse	Yes	7 (24.1%)
	No	19 (65.6%)
	Unknown	3 (10.3%)
Prospective study (n=24)		
Age (years)	Mean (Range)	68 (44 – 80)
Sex	Female	12 (50%)
	Male	12 (50%)
Smoking history	Smokers or smoking history	19 (79.2%)
	Non smoker	5 (20.8%)
COPD	Yes	6 (25%)
	No	17 (70.8%)
	Unknown	1 (4.2%)
Stage at surgery	I	12 (50%)
	II	4 (17%)
	III	8 (33%)
	IV	0 (0%)
Adjuvant chemotherapy	Yes	9 (37.5%)
	No	15 (62.5%)
Relapse	Yes	5 (20.8%)
	No	11 (45.8%)
	Unknown	8 (33.3%)

COPD: chronic obstructive pulmonary disease.

Immunofluorescence

After tumor processing as described in the dedicated section, the cell suspension was homogenized, 500 000 LUAD cells were plated on slide and fixed by drying at room temperature (RT) and stained. To ensure that cells came exclusively from the intratumor area of LUAD, the margins were checked on the corresponding tissue blocks and confirmed as adenocarcinomatous by two lung cancer pathologists. HEK293T cells were plated at 600 000 cells in a 6-wells culture plate containing coverslip poly-D-lysin (Gibco) coated and transfected as described below. Anti CD16/CD32 antibodies (Fc Block, BD Biosciences) were used (1 h, RT) to reduce the non-specific signal, and primary antibodies were added for 2 h at 4°C. After washing, secondary antibodies were added for an additional 1 h at RT. Anti-P2RX7 hybridoma (dil1/2) was used. This antibody is routinely used to detect the expression of functional P2RX7 [6]. Anti-CD45-FITC (dil1/50, recombinant human IgG1, REA747 clone, MACS®) and anti-goat Alexa fluor 594, (1/200, Thermofisher) antibodies were used. The nuclei were counterstained with 4'6-Diamidine-2-phenylindole dihydrochloride (DAPI) in the mounting medium (Invitrogen Life Technologies™).

P2RX7 functional assay

The overall cellular P2RX7 activity was evaluated by flow cytometry. This assay allows simultaneous study of live cells stimulated with BzATP (a stable analogue of ATP), for variations in calcium levels (FLUO-4-AM dye) and macropore opening (TO-PRO-3 dye) (Figure S3). In practice, cells were incubated in functional assay buffer (sucrose 300 mM, KCl 5 mM, $MgCl_2$ 1 mM $CaCl_2$ 1 mM, glucose 10 mM, HEPES pH 7.4 20 mM) and loaded with Fluo-4-AM (500 nM), for 30 min at RT. Propidium iodide was added for the last 5 min to stain both dying cells and P2RX7's independent permeabilization events, which will be excluded from the final analysis. FLUO-4-AM and propidium iodide were removed by 2 washes with DPBS containing FBS 5%, and 400 000 cells were incubated in the functional buffer and stimulated with BzATP in the presence of TO-PRO-3 (633 nM, Invitrogen) for the indicated time. The reaction was stopped with 2 mM $MgCl_2$ and washed with DPBS containing FBS 5%. Flow cytometry analysis was performed on a propidium negative population using a FACS Canto® II (BD Bioscience®) and data were analyzed using DIVA® or FlowJo® software. The normalization of fluorescence intensity was performed by retrieving at every time-point the fluorescence intensity (I) (FLUO-4-AM and TO-PRO-3) of the first time point (I_0). Normalized data were presented as violin plot.

RT-qPCR

Total RNA extraction from purified cell subpopulations or frozen tissues was performed using the AllPrep RNA Mini Qiagen® kit and reverse transcription of 37.2 ng total RNA was performed with the Applied Biosystems® kit. The cDNA was subjected to quantitative PCR using the Fast Sybr®Green Master Mix kit (Applied biosystems) and a StepOnePlusTM thermocycler. Relative expression was determined using the log2 fold change ($2^{-\Delta\Delta Ct}$) method with *RPLP0* as the housekeeping gene. The oligonucleotides, designed to overlap splicing sites, are presented in Figure S6A. QPCR amplicons were sequenced to confirm their specificity (data not shown) and used as matrices of standard amplification curves to validate the absolute

quantification rate and the amplification efficiency of each oligonucleotides couple (Figure S6B).

Cell cultures and transfection

HEK293T cell line, provided by ATCC, were cultured in DMEM medium supplemented with 10% FBS and 100 U/mL penicillin and 100 mg/mL streptomycin at 37°C in a humid atmosphere containing 5% CO_2. P2RX7A and P2RX7B splice variants were synthesized by Eurofins® and sequenced. HEK293T cells were transfected with pcDNA expression vector coding for the indicated cDNA using Lipofectamine® 3000 (Thermofisher) according to the manufacturer's instructions. "PcDNA3.1 venus 1" and "pcDNA3.1 venus 2" were provided by Dr Saccani's team. Transient expression analyses were processed 48-h post transfection. For the establishment of stable cell lines expressing the untagged P2RX7A, P2RX7B or P2RX7AB, blasticidin 1 µg/mL and puromycin 1 µg/mL were added to the growth media. After 3 weeks, clones were selected and tested for protein expression by Western blotting.

Western blotting

Western blot analysis was performed following the standard protocol. In brief, cells were lysed on-ice in TR3 buffer (SDS 3%, glycerol 10%, Na_2PO_4 10 mM + Complete™ Protease Inhibitor Cocktail, Roche), 20 to 50 µg of total proteins were subjected to 9% SDS-PAGE and transferred onto PVDF membranes (Immobilon Millipore®). Blots were than blocked for 20 minutes with 5% non-fat dried milk and incubated with primary antibodies (Rabbit anti-Human extracellular loop of P2RX7, APR-008, Alomone), overnight at 4°C, followed by three 5-min washes with Tris-Buffered Saline 0.1% Tween® 20 detergent, then incubated with species specific secondary IgG antibodies coupled to Horseradish peroxidase (HRP) (Goat anti-Rabbit, AP307P, Sigma, and Goat anti-Mouse, AP308P, Sigma) 1 h at RT, followed by 3 more washes as described before. The signal was revealed using PXi imaging (Syngene). In a second step, αTubulin (Mouse anti-tubulin, Sigma) level was monitored as a control for protein loading.

Immunohistochemistry

Immunohistochemical (IHC) staining for CD45, CD3, CD8, CD20 and CD33, was performed on tumor sections obtained from LUAD patients of the prospective cohort. In brief, formalin fixed paraffin embedded 4 µm thick tissue sections were stained with specific anti-human antibodies on an automated staining platform (Benchmark ULTRA; Ventana) using the appropriate concentration. An OptiView DAB IHC Detection Kit (Ventana) and an OptiView Amplification Kit (Ventana) were used according to the manufacturer's recommendations for the visualization of the bound antibodies; sections were counter-stained with hematoxylin. Blinded quantification of the brown staining was done as follows: 5 different zones of the scanned tumor section (NanoZoomer 2.0 HT from Hamamatsu) were selected at low magnification (1×) and images of the selected fields were analyzed at 40× magnification. Scoring of the staining was as follows: 1 = 0-10% positive cells, 2 = 10-50% positive cells and 3 = ≥ 50% positive cells.

Bioinformatic and statistical analysis

Quantitative data were described and presented graphically as medians and inter quartiles or means and standard deviations. The distribution normality was tested with the Shapiro's test and homoscedasticity with Bartlett's test. For two categories, statistical comparisons were performed using the Student's *t*-test or the Mann–Whitney test. Overall survival was defined as the interval between the date of diagnosis and the date of death from any cause. These data were estimated and presented graphically using the Kaplan–Meier method. The survival curves were compared using the log-rank test. All statistical analyses were performed using GraphPad Prism® v.8.0.2. Tests of significance were two-tailed and considered significant with an alpha level of $P < 0.05$. SnapGene 4.3.8 was used for plasmid construction. The results shown in Figure 4B and Supplementary Figure 7 are based on data generated by the TCGA project for which we are grateful.

Results

P2RX7 is expressed in LUAD

To analyze the expression levels of conformational P2RX7 in LUAD, tumor tissue was dissociated, and the cells stained with the anti-P2RX7 antibody directed against the external domain of the tertiary structure of P2RX7, which has been described to antagonize its activity [6]. Whereas most of the cells were labeled, a small fraction of cells with large nuclei, a characteristic of tumor cells, were negative (Figure 1A). Next, an anti-CD45 antibody was used to characterize the nature of P2RX7 expressing cells and we observed that only $CD45^+$ cells were stained with the anti-P2RX7 antibody. Since cells were permeabilized, the lack of staining in $CD45^-$ cells was not due to intracellular retention of P2RX7 (Figure S2). To extend this observation, immune ($CD45^+$) and non-immune ($CD45^-$) cells were isolated from three LUAD specimens and subjected to western blot analysis using a second antibody which recognizes the extracellular domain of P2RX7A and P2RX7B

monomers (Figure 1B). A protein of 70kDa corresponding to P2RX7A was found to be expressed by CD45⁺ immune cells in 2 of 3 LUAD patients. These patients only showed very limited (if any) expression of P2RX7 on tumor cells. By contrast, we observed P2RX7A expression on tumor cells of the third LUAD patient. We also noticed the presence of additional bands (from 80 to 56kDa). These bands are of undetermined nature, being not recognized by the antibody in the HEK cell expression system transfected with P2RX7A. In this patient, expression of P2RX7A was poorly detected on immune cells. Instead, a protein of 55kDa, which could correspond to P2RX7B, was observed.

Therefore, using two independent antibodies, our results showed that P2RX7A is preferentially expressed on immune cells of LUAD patients.

The macropore function of P2RX7 is impaired in immune cells of LUAD

Since P2RX7 expression could not predict P2RX7 activity, we investigated the macropore function of P2RX7 in both immune and non-immune cells of LUAD specimens and paired corresponding adjacent non-cancerous tissues (Figure 2 and Figure S4). BzATP increased the uptake of TO-PRO-3 in immune cells from both non-tumor and tumor areas (Figure 2A-B). This increase was prevented in cells pre-treated with the specific P2RX7 inhibitor, GSK1370319A [35], indicating that TO-PRO-3 uptake was dependent on the expression of P2RX7. In addition, the macropore activity was delayed in the tumor compartment. In fact, 15 min post stimulation, the normalized median percentage of TO-PRO-3⁺ cells

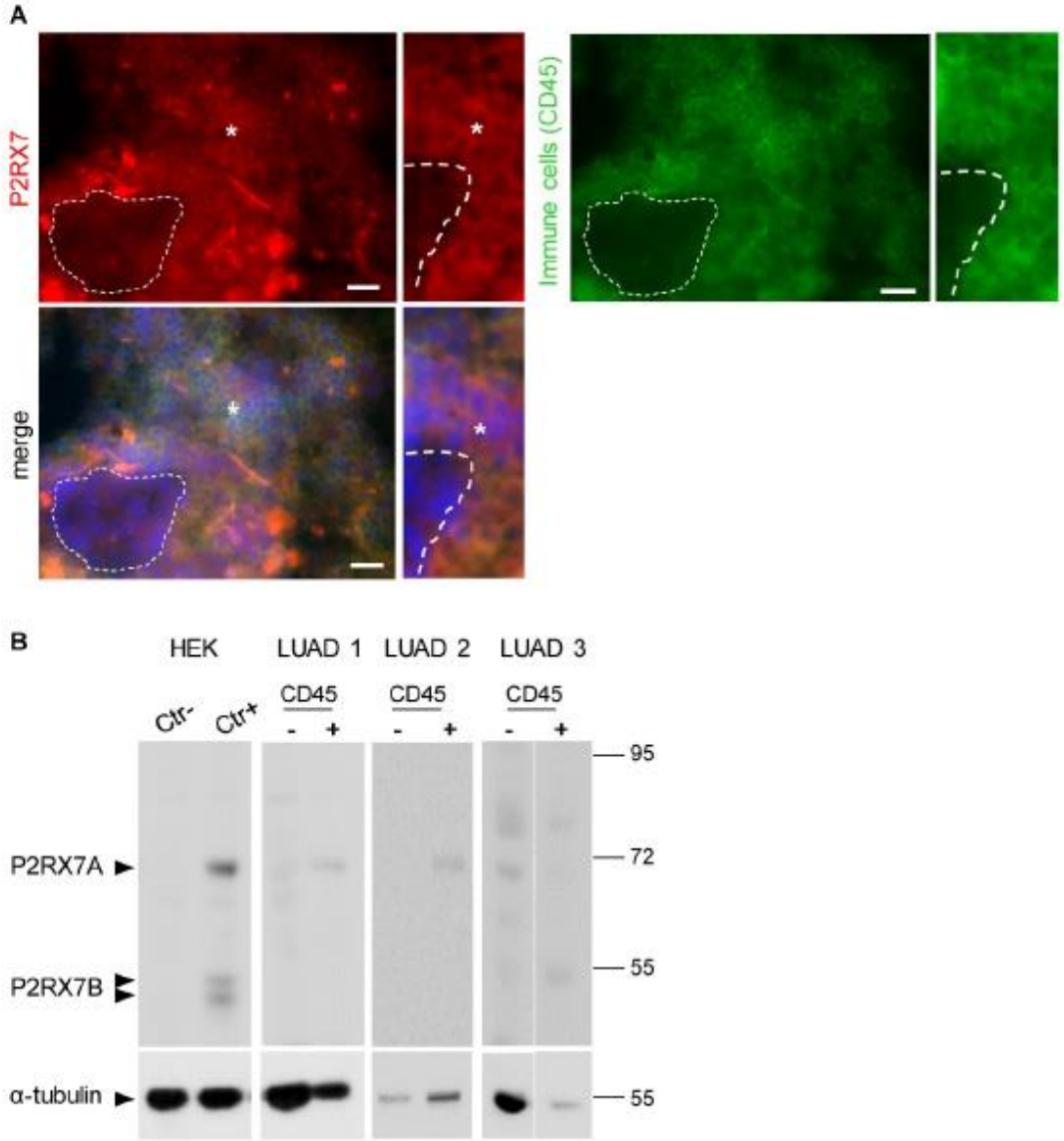

Figure 1. LUAD patients express P2RX7. **A.** Representative images of P2RX7 staining in LUAD tissue using the conformational anti-P2RX7 antibody, in red. CD45 staining highlighted immune cells, in green. * showed P2RX7 expressing cells. The hatched line shows CD45⁻ cells. DAPI staining shows nuclei. Magnification 20X, scale bar = 200 µm. **B.** Representative Western blot showing P2RX7 expression in HEK cells transfected with empty vector (Ctr⁻), cells transfected with both P2RX7A and P2RX7B expressing vectors and purified CD45⁺ and CD45⁻ cells isolated from tumor areas of LUAD patients using the anti P2RX7extracellular loop antibody (Alomone, APR-008, 1/1000). The total αTubulin level was monitored as a control for protein loading.

was 1.2% in the tumor infiltrate (Figure 2B), while it reached 5.7% in the non-tumor infiltrate (Figure 2A). This difference was still observed 30 min post stimulation. These results suggest that P2RX7 expressed by immune cells within the tumor area was less functional.

Considering the differential activation status of P2RX7 in immune cells compared to non-immune cells, we hypothesized that alternative splicing of *P2RX7* mRNA may generate hetero-P2RX7 trimers with altered receptor functions.

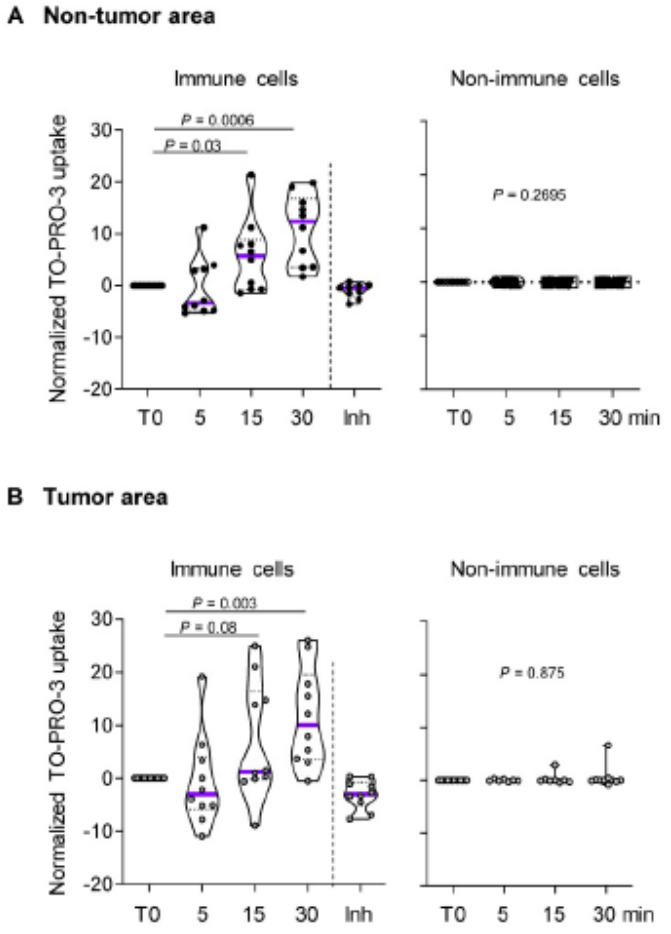

Figure 2. P2RX7 expressed by immune cells of LUAD patients is functional. **A.** Time course of macropore opening in purified immune and non-immune cells isolated from an adjacent non-tumor area of LUAD patients. When indicated we used a specific P2RX7 inhibitor (Inh) demonstrating that TO-PRO-3 uptake depends on P2RX7 activity. **B.** Time course of macropore opening in purified immune and non-immune cells isolated from the tumor area of LUAD tissue. The percentage of TO-PRO-3 positive cells in response to BzATP (250 µM) is shown (paired Student's *t* test). n=10 paired LUAD specimens and corresponding adjacent non-cancerous tissues from our prospective cohort. The median value is highlighted by the violet line.

P2RX7B is differentially upregulated in the LUAD immune infiltrate

We designed probes for the five variants described to be transcribed and translated, namely *P2RX7A, B, D, H* and *J* and analyzed their expression on human peripheral blood mononuclear cells by qualitative PCR analysis (Figure S5A). PBMCs expressed the *P2RX7A, B, H* and *J* variants (Figure S5B). Next, using qPCR probes (Figure S6), we quantified *P2RX7* expression on LUAD tissues using our two in-house cohorts (see Table 1). Using the probe which amplifies *P2RX7A, B* and *H* (further designed as *P2RX7*), we observed that *P2RX7* was 2.5-fold less expressed in tumor versus non-tumor areas of LUAD (Figure 3A). Likewise, the specific expression of the *P2RX7B, H* and *J* splice variants was decreased 3.2-, 3.6- and 5.6-fold, respectively. These results were confirmed with TCGA RNA-seq expression data from a larger cohort of 57 LUAD (Figure S7). Further, we analyzed the expression levels of all P2RX7 mRNA in both non-tumor and tumor areas and observed that while *P2RX7* was down-regulated in non-immune cells (Figure 3B), it was up-regulated in immune cells (Figure 3C). In the tumor area, *P2RX7* was 15-fold up-regulated in immune cells compared to non-immune cells and the alternative splice variants *P2RX7B, H* and *J* were 7-, 6- and 15-fold up-regulated, respectively. Next, we compared the expression levels of each *P2RX7* splice variant in immune cells purified from normal and tumor tissues and showed that the *P2RX7B* variants were differentially up-regulated in the immune infiltrates of LUAD patients (37% of the constitutive splicing), whereas the other variants were almost absent (Figure 3D). To evaluate whether up-regulation of *P2RX7* may impact the fate of LUAD patients, we analyzed overall survival (OS) of the LUAD TCGA cohort, separated into two groups, stage I and stage II. A Kaplan-Meier analysis of patients with LUAD and a high expression of *P2RX7* had a significantly poorer OS (38 months) than those with a low expression of P2RX7 (136 months). This tendency was present only in early-stage I LUAD and disappeared at stage II (Figure 4). At this point, no correlation with *P2RX7B* expression levels could be done, since neither the nature of *P2RX7* splice variants nor the nature of P2RX7 expressing cells were present in TCGA database.

Collectively, these results suggest that the more *P2RX7B* was expressed, the more the macropore function was dysfunctional in the immune infiltrate of LUAD.

P2RX7B expression negatively impacts the P2RX7 activity

It was previously reported that P2RX7B could heteromerized with P2RX7A [31]. Therefore, P2RX7B may be co-expressed with P2RX7A and form a chimeric receptor in the immune infiltrate of LUAD. To test this hypothesis and characterize the cellular localization of such a chimeric protein, we explored the expression and the function of P2RX7AB using a bi-molecular fluorescent complementation approach.

First, we controlled that cells transfected with individual hemi venus 1 (v1) or hemi venus 2 (v2) tagged-P2RX7 (P2RX7A and P2RX7B) did not emit a fluorescent GFP signal (Figure S8A). Thanks to the conformational anti-P2RX7 antibody, we demonstrated that individual v1- or v2-tagged P2RX7A formed homo trimers that are correctly localized at the cell membrane (Figure S8A). Next, we transiently co-transfected HEK cells with v1-P2RX7A and v2-P2RX7A. The interaction of the proteins brought the two hemi GFP within proximity, allowing GFP to reform its native structure and emit a fluorescence signal (Figure 5A). Confocal microscopy showed that v1+v2-P2RX7 was expressed at the cell surface. Furthermore, the tagged-P2RX7 adopted a normal conformation when stained with the conformational anti-P2RX7 antibody. Importantly, we verified that this antibody did not stain the P2RX7B protein (Figure S9A). We also noticed that some GFP^+ small dots remained within the cytoplasm. To study the impact of P2RX7B expression on P2RX7 function, HEK cells were transiently co-transfected with v1-P2RX7B and v2-P2RX7A (Figure 5A, lower panel). When expressed, the chimeric GFP^+ P2RX7AB receptor was found to be correctly inserted into the cell membrane (asterisk). The GFP chimeric proteins co-localized with P2RX7 stained with the conformational antibody (asterisk), suggesting that the chimeric receptor, like P2RX7, was inserted into the cell membrane. To confirm this finding, we quantified the percentage of tagged receptors that co-localized with P2RX7 at the membrane and observed that 35% of the chimeric protein co-localized with proteins stained with the conformational antibody (Figure 5B and S8B). We also observed the presence of numerous GFP^+ aggregates within the cytoplasm (arrowhead). We then tested whether the expression of P2RX7B modified the overall activity of P2RX7. To do so, transfected cells were stimulated with increasing doses of BzATP for 15 min, GFP^+ cells were sorted by FACS and the percentage of $TO\text{-}PRO\text{-}3^+$ cells within this fraction was analyzed (Figure 5C). BzATP dose dependency for TO-PRO-3 uptake was shifted to the right in HEK v2Av1B P2RX7 (P2RX7AB) cells compared to HEK v1Av2A P2RX7 (P2RX7A). We then calculated the EC_{50} for macropore formation in both chimeric tagged P2RX7AB or tagged P2RX7A and P2RX7B and observed an increase of 30% (20µM vs 14 µM) in cells co-transfected with both P2RX7A and P2RX7B (Figure 5C). By contrast, cells transfected with v1Bv2B P2RX7 (P2RX7B) did not show any TO-PRO-3 uptake, indicating that the homo trimer P2RX7B was unable to form a macropore, despite its expression at the cell membrane and its ability to induce Ca^{2+} influx (Figure S9B). To go further and given the impact of the tag on membrane localization, we decided to co-express non tagged P2RX7A and P2RX7B and reevaluate the overall activity of P2RX7. To allow a meaningful comparison, we selected clones expressing comparable protein levels of P2RX7A and P2RX7B, using an antibody specific for the extracellular loop and known to recognize both P2RX7A and P2RX7B (Figure 5D). We then assayed both the macropore and the Ca^{2+} channel activities. Whereas the overall macropore activity of the cells transfected with both P2RX7A and P2RX7B proteins was inhibited by 50% compared to control cells transfected with P2RX7A only (EC50 =6.3 µM vs 13.1 µM and maximum $TO\text{-}PRO\text{-}3^+$ cells = 58% vs 84%), we did not observe any significant effect on the intracellular Ca^{2+} concentration (Figure 5E). These results supported the notion that expression of the P2RX7B negatively impacted the overall macropore activity of P2RX7. At this point, we were unable to analyze the macropore activity of chimeric P2RX7AB itself. Indeed, we cannot exclude the hypothesis that the fraction of GFP^+ cells used to assay the macropore activity also expressed functional P2RX7A homo trimers allowing the influx of TO-PRO-3 in response to BzATP. However, based on the presence of large cytoplasmic aggregates in cells expressing both P2RX7A and P2RX7B, we can reasonably propose that P2RX7A is retained intracellularly. Such cell retention could impact the quantity of functional P2RX7 expressed at the cell membrane and consequently the macropore activity. In contrast, the absence of the effect on BzATP-induced increased Ca^{2+} concentration might not be surprising considering that Ca^{2+} is able to permeate more easily than a large dye, such as TO-PRO-3, across the pore formed by P2RX7.

Expression of *P2RX7B* correlates with decreased T cell infiltration in LUAD

We next wondered whether *P2RX7B* expression could impact the composition of the immune infiltrate in LUAD. Analysis of the ratio of *P2RX7B* versus *P2RX7A* mRNA expression allowed us to separate two populations within the prospective cohort (Figure 6A). We clustered patients expressing 1 *P2RX7B* for 2 to 4 *P2RX7A* (ratio comprised between 0.2 to 0.4), which corresponded to 60% of the specimens, from patients expressing 1 *P2RX7B* for 10 or more *P2RX7A* (ratio comprised between 0.1 to 0.0003). We then performed immunohistochemistry to qualify tumor infiltrating immune cells, focusing on leukocytes ($CD45^+$ cells) (Figure 6B), and T lymphocytes ($CD3^+$), $CD8^+$ T cells, B lymphocytes ($CD20^+$) and myeloid cells ($CD33^+$). Quantification of the staining of these cells showed that the less *P2RX7B*

is expressed the higher the number of leukocytes recruited into LUAD (Figure 6C). This was observed for the lymphoid lineage (T lymphocytes, CD8 T lymphocytes and B lymphocytes). However, we noticed an inverse correlation regarding the myeloid lineage (monocytes/macrophages, MDSC), characterized by cells expressing the transmembrane receptor CD33.

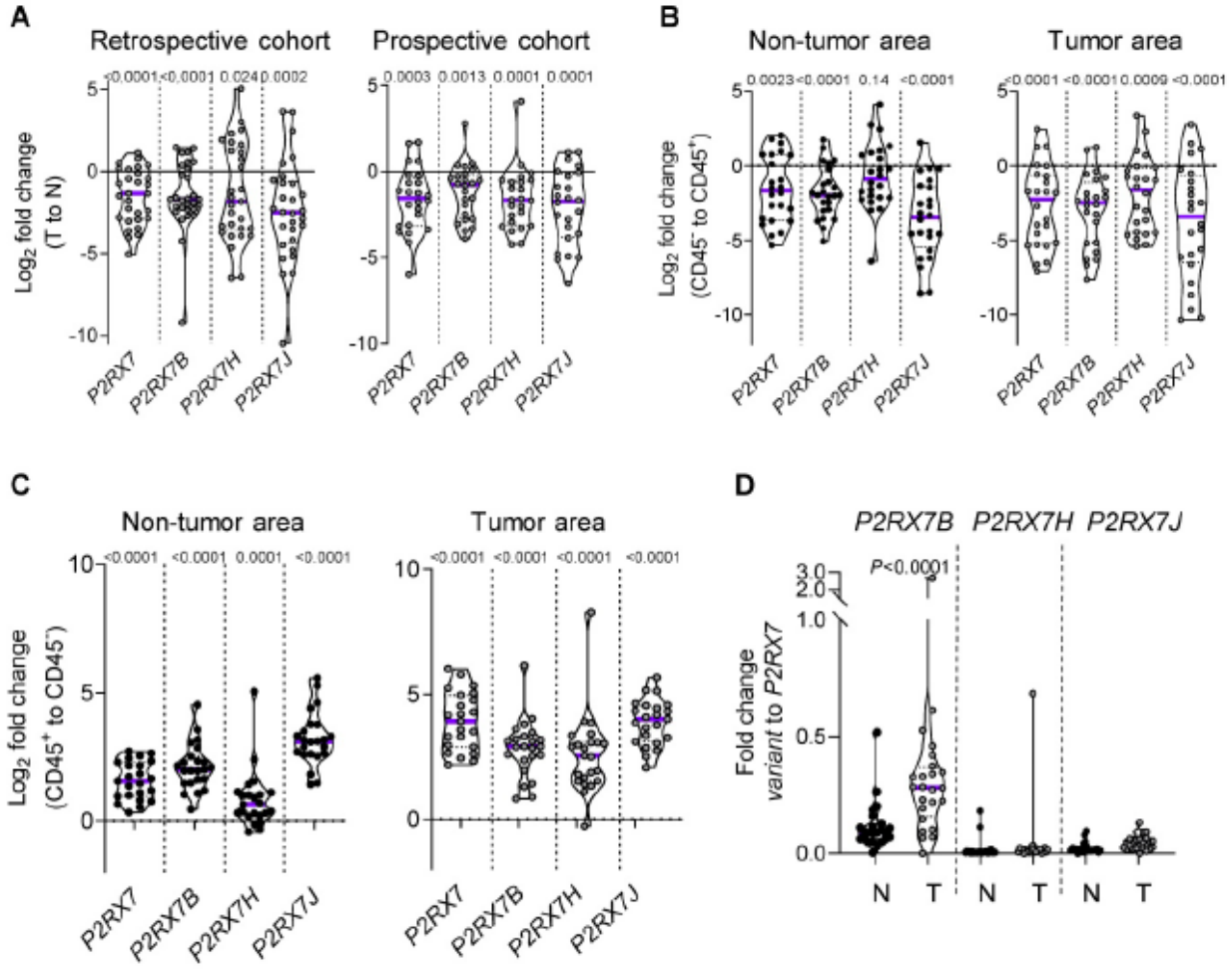

Figure 3. LUAD patients express *P2RX7A, B, H and J* mRNAs. **A.** *P2RX7* splice variant expression in the retrospective (n=29) and prospective cohorts (n=24) of tumor area of LUAD tissues (T) versus adjacent non-tumor lung tissues (N). **B.** *P2RX7* splice variant expression in CD45- cells isolated from adjacent non-tumor and tumor areas of LUAD patients (n=24). **C.** *P2RX7* splice variant expression in CD45+ cells isolated from adjacent non-tumor and tumor areas of LUAD patients (n=24). Results are expressed in Log_2 fold change (meaning Log_2 of 1 = 2-fold and Log2 of -1 = 0.5-fold). **D.** Differential up-regulation of *P2RX7B* in immune cells. n=24 (Mann-Whitney test).

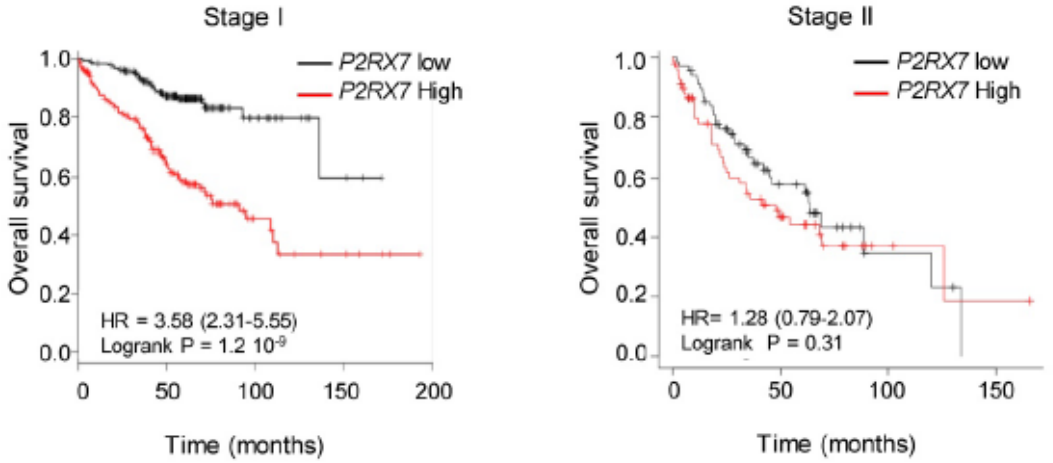

Figure 4. High expression of *P2RX7* is an indicator of poor survival in LUAD patients. Kaplan-Meier survival analysis (http://kmplot.com) [41] according to the *P2RX7* expression in patients with LUAD of indicated stage. High expression corresponds to value > *P2RX7* median expression, low expression corresponds to value < *P2RX7* median expression. Probability of survival of patients: Stage I: n=370 patients, low expression (n=187) median OS: 136 months; high expression (n=183) median OS: 38 months, HR: 3.58, 95% CI: 2.31-5.55, $p=1.2\ 10^{-9}$. Stage II: n=136 patients, low expression (n=68) median OS: 63 months; high expression (n=68) median OS=38 months, HR: 1.28, 95% CI: 0.79-2.07, $p=0.31$ (log-rank test). Vertical tick-marks represent censored data.

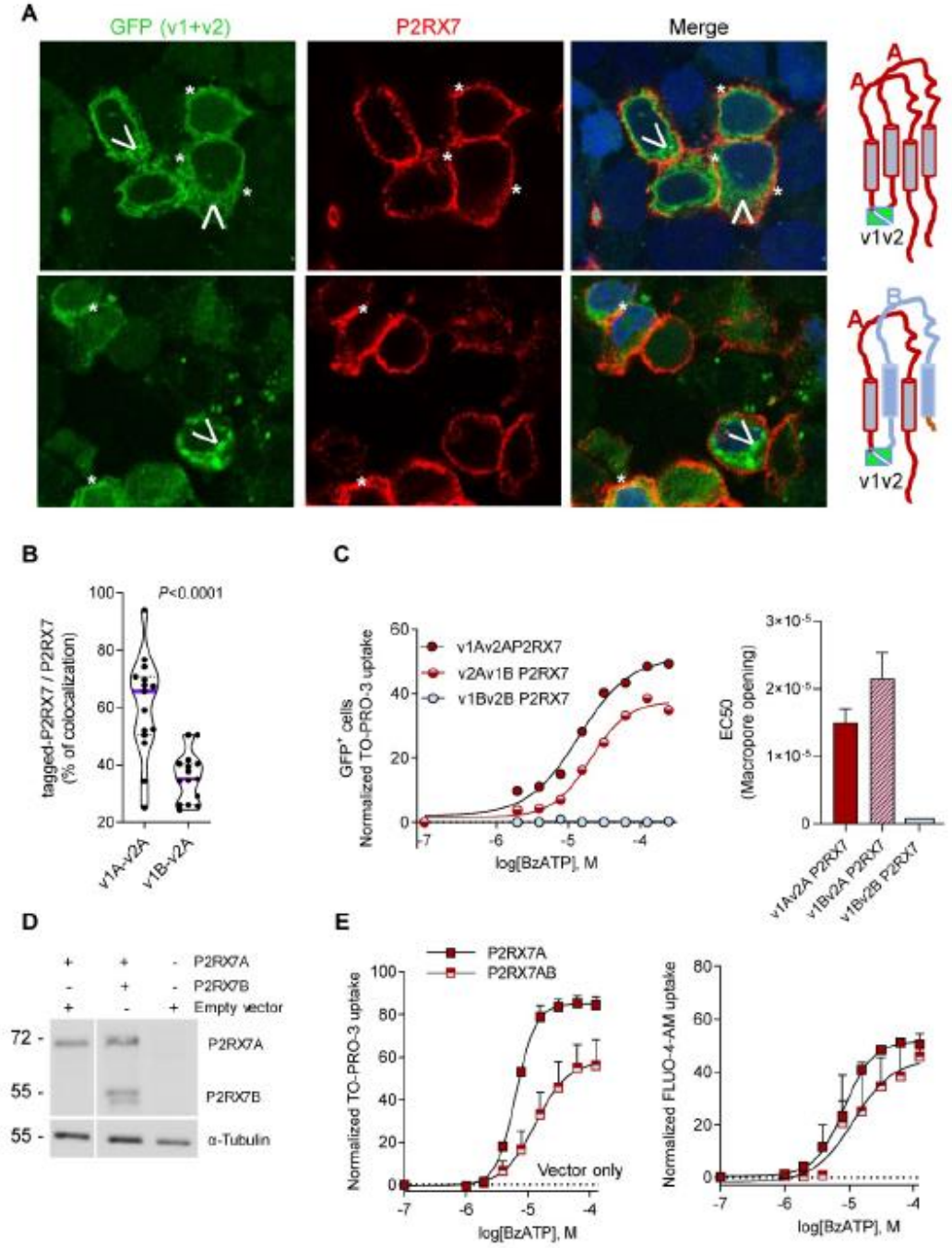

Figure 5. Expression of P2RX7B decreases the overall activity of P2RX7. A. Representative images of P2RX7 immunofluorescence in HEK cells transiently transfected with P2RX7A or with P2RX7 A + B pDNA. The tagged receptor (P2RX7A or P2RX7AB) is shown in green. The conformational receptor (P2RX7A) is shown in red. *: P2RX7 expressed at the membrane. Arrowhead: intracellular chimeric receptor. **B.** Quantification of data presented in A. n = 30 cells from 2 independent experiments. (unpaired Student's *t* test). **C.** Impact of P2RX7B expression on the P2RX7 macropore activity. HEK cells were transiently transfected with tagged-A, -B and -A+-B P2RX7 isoforms and the macropore activity was studied on GFP+ cells (right panel). The left panel shows the EC_{50} for macropore formation for 3 independent experiments. **D.** The expression of P2RX7A and P2RX7B was detected in stably transfected HEK clones by Western blotting using the P2RX7 anti-extracellular loop antibody. The total αTubulin level was monitored as a control for protein loading. **E.** P2RX7 activity in stably transfected HEK clones with untagged-A and -A+-B P2RX7 isoforms or vector alone (hatched line). Dose response of BzATP-induced macropore opening (left panel) and an intracellular Ca^{2+} variation (right panel).

Discussion

In this study we characterized the expression levels and the functionality of P2RX7 in LUAD patients and showed that whereas P2RX7 was found to be expressed in both tumor and immune cells, only immune cells expressed a functional receptor. Mechanistically, we observed differential expression of the *P2RX7B* splice variant in immune cells within tumor areas. Upregulation of P2RX7B was previously described in human osteosarcoma [32]. To document P2RX7B expression, the authors used a differential screening approach, based on two antibodies, the first one recognizes both P2RX7A and P2RX7B, whereas the second is specific to P2RX7A only. Thank to this approach, specimens positively labeled with the first antibody and negatively labeled with the second were described to be positive for P2RX7B. Considering that

there is no antibody specific to P2RX7B, this technic represents a smart way to document P2RX7B expression. However, each antibody has his own affinity for its specific epitope and from this affinity depends the strength of the signal. Therefore, a subtractive strategy to qualify the expression of P2RX7B is a tricky approach to handle. To overcome this limitation, the authors further transfected Te85 osteosarcoma cell line with either P2RX7A, P2RX7B or both. Doing so, they demonstrated that cells expressing both isoforms were more proliferative and more prone to induce mineralization. More recently, expression of P2RX7B has been described to be upregulated during the osteogenic process [18]. Evidence suggesting that P2RX7A and P2RX7B might heteromerized were obtained in the X. *laevis* oocyte expressing system after co-immunoprecipitation of tagged P2RX7A and P2RX7B [31]. In addition, transfection of HEK cells with both P2RX7A and P2RX7B suggested that P2RX7B disguises P2RX7A's cytotoxic activity. If true, expression of P2RX7B will give a growth advantage and explain how P2RX7 expression (likely A and B isoforms) could have been linked to tumor growth and invasiveness in several cancer types [36–39]. Indeed, considering that P2RX7 is a pro-apoptotic receptor, it is counterintuitive to imagine that tumor cells express a receptor capable of inducing their own death. It has been proposed that tumor cells express a non-conformal receptor (nfP2RX7), which is unable to induce cell death but retains calcium channel activity and therefore could promote tumor growth. Herein, we observed that P2RX7 expressed by tumor cells, but also normal epithelial cells, lacked the macropore function, whereas immune cells retained it. At this time, we still do not know whether the isoform of P2RX7 expressed by tumor cells corresponds to nfP2RX7, since the only way to characterize its expression relies on the use of an anti-nfP2RX7 antibody, which is not commercially available. We explored the hypothesis that the lack of macropore activity in tumor and non-tumor epithelial cells could be the consequence of expression of truncated P2RX7 isoforms, resulting from alternative splicing of P2RX7 mRNA rather than SNPs. Indeed, allele frequency of SNPs located to the boundary of mRNA splicing regulation sites within intronic regions is too low to envisage that these SNPs could explain the significant dysfunction in P2RX7 that we observed in 10 LUAD patients. Our study revealed for the first time that 3 alternative splice variants of *P2RX7* are expressed in LUAD patients, namely *P2RX7B, P2RX7H* and *P2RX7J*. We also observed that all *P2RX7* variants were down-regulated by at least 2.5-fold in tumor tissues versus adjacent non-tumor tissues. Since each *P2RX7* variant was down-regulated to the same extend in non-immune cells, we believe that the lack of P2RX7 function is a consequence of decreased protein expression rather than the formation of hetero trimers that may be stored in intracellular vesicles, as it was proposed for nfP2RX7 [40].

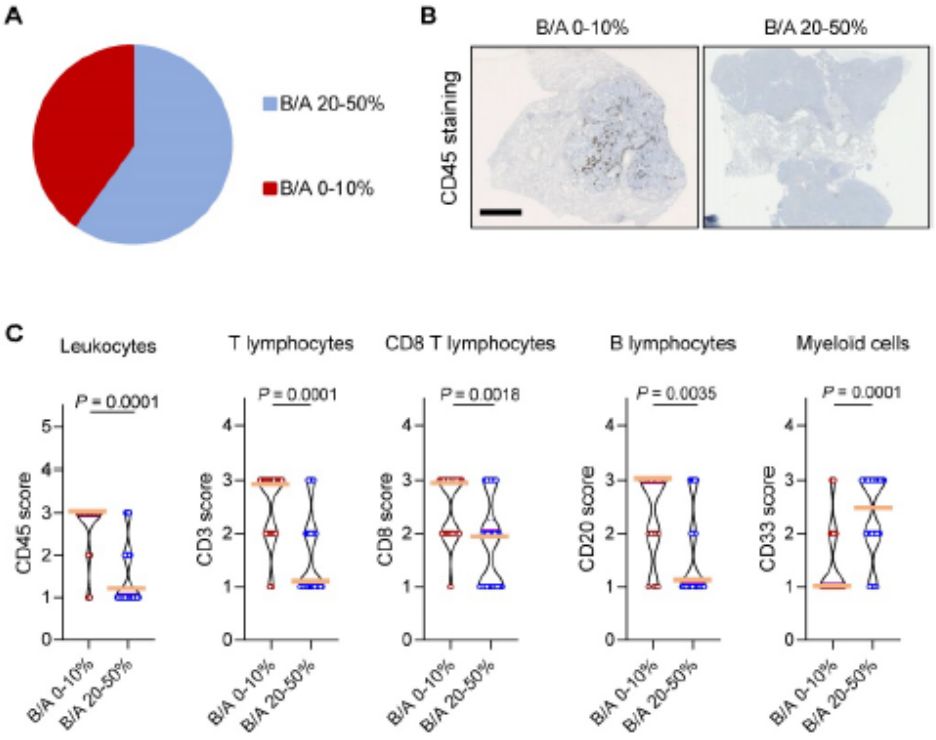

Figure 6. High expression of *P2RX7B* mRNA correlates with low leukocyte infiltration in LUAD patients. A. Clustering of LUAD patients expressing *P2RX7B* for the prospective cohort. **B.** Representative images of CD45+ IHC staining of samples from LUAD patients depending on the *P2RX7B* expression. Bar = 5mm. **C.** Quantification of CD45, CD3, CD8, CD20 and CD33 staining. B/A 20-50%, n=6; B/A 0-10%, n=4. (CD45, CD3 and CD8: Mann-Whitney test. CD20 and CD33: unpaired Student's *t* test).

Whereas each *P2RX7* variant was equally down-regulated in the epithelial compartment of tumor tissues versus adjacent non-tumor tissues, we observed differential up-regulation of P2RX7B in the tumor immune compartment. Over expression of *P2RX7B* has already been reported in *ex vivo* mitogenic-induced immune cells, in particular in lymph nodes and lymphocytes [31], and the authors proposed that expression of P2RX7B correlated with lymphocyte proliferation. Our results do not support this proposition since we showed that the more *P2RX7B* is expressed the less the tumors were infiltrated by T and B lymphocytes. Besides suggesting a physiological role for the truncated P2RX7B isoform, this result questions how P2RX7B expression can impact on the immune infiltrate composition. Using the bi-molecular fluorescent approach, we confirmed that a chimeric P2RX7AB receptor is formed, and we showed for the first time that a large fraction (63%) was retained intracellularly. To avoid potential bias linked to the presence of the N-terminal venus tag, we co-transfected HEK cells with untagged P2RX7A or P2RX7A+P2RX7B and we selected stable clones expressing comparable protein levels of both isoforms. Doing so, we were able to demonstrate that cells expressing both P2RX7A and P2RX7B isoforms were less prone than cells expressing only P2RX7A to form a macropore, whereas they retained the same ion channel capability. This result does not confirm what was previously published indicating that P2RX7B expression positively modulates P2RX7 function [31] but they confirm that P2RX7B expression could disguise P2RX7's macropore activity [19,33]. Whether this alteration in macropore function observed *ex vivo* is due to the coexistence of cells expressing only homo trimeric P2RX7B and only homo trimeric P2RX7A, or to the existence of cells expressing intracellular chimeric P2RX7AB, or both remains to be determined. However, our results showed that tumors of LUAD patients with a high *P2RX7B* expression were less infiltrated with B and T cells and more infiltrated with myeloid cells, suggesting that differential expression of *P2RX7B* critically regulated the quality of tumor immune cell infiltration. Whether differential expression of *P2RX7B* results from tumor conditioning of the lung tissue or specific expression in immune cells before tumor conditioning is still an open question. Nevertheless, considering that expression of *P2RX7B* in LUAD correlated with both an alteration in the P2RX7 function and the lesser infiltrated tumor phenotype (also called "cold" tumor), it is tempting to propose that P2RX7B participates in tumor development and may therefore represent an attractive theranostic tool.

Supplementary Material

Supplementary figures and tables.
http://www.thno.org/v10p10849s1.pdf

Acknowledgments

The authors wish to thank Dr Laetitia Douguet for her helpful advice on flow cytometry and Dr Dominic Van Essen for his advice on the bimolecular fluorescent approach. Drs Sahil Adriouch, Pascal Lopez and Patrick Brest are thanked for their helpful discussion. The authors greatly acknowledge the IRCAN's Flow Cytometry and PICMI facilities supported by FEDER, GIS IBISA, the Ministère de l'Enseignement Supérieur, Région Provence Alpes-Côte d'Azur, Conseil Départemental 06, ITMO Cancer Aviesan (plan cancer), Cancéropole PACA, CNRS and Inserm.

Funding

The funding sources for this work were Institut National du Cancer (INCa), Institut National de la Santé et Recherche Médicale (INSERM) Plan Cancer 2014-2019: Soutien pour la formation à la recherche fondamentale et translationnelle en cancérologie, RESPIR Foundation, the "Ligue National Contre le Cancer", the French Government (National Research Agency, ANR through the "Investments for the Future" LABEX SIGNALIFE: program reference #ANR-11-LABX-0028-01), the Centre National de la Recherche Scientifique (CNRS).

Competing Interests

The authors have declared that no competing interest exists.

References

1. Siegel RL, Miller KD, Jemal A. Cancer statistics, 2020. CA Cancer J Clin. 2020; 70: 7–30.
2. Pellegatti P, Raffaghello L, Bianchi G, Piccardi F, Pistoia V, Di Virgilio F. Increased level of extracellular ATP at tumor sites: *In vivo* imaging with plasma membrane luciferase. PLoS One. 2008; 3: e2599.
3. Allard B, Beavis PA, Darcy PK, Stagg J. Immunosuppressive activities of adenosine in cancer. Curr Opin Pharmacol. 2016; 29: 7–16.
4. Jacob F, Novo CP, Bachert C, Van Crombruggen K. Purinergic signaling in inflammatory cells: P2 receptor expression, functional effects, and modulation of inflammatory responses. Purinergic Signal. 2013; 9: 285–306.
5. White N, Burnstock G. P2 receptors and cancer. Trends Pharmacol Sci. 2006; 27: 211–7.
6. Buell G, Chessell IP, Michel AD, Collo G, Salazzo M, Herren S, et al. Blockade of human P2X7 receptor function with a monoclonal antibody. Blood. 1998; 92: 3521–8.
7. Chiozzi P, Sanz JM, Ferrari D, Falzoni S, Aleotti A, Buell GN, et al. Spontaneous cell fusion in macrophage cultures expressing high levels of the P2Z/P2X7 receptor. J Cell Biol. 1997; 138: 697–706.
8. Baroni M, Pizzirani C, Pinotti M, Ferrari D, Adinolfi E, Calzavarini S, et al. Stimulation of P2 (P2X7) receptors in human dendritic cells induces the release of tissue factor-bearing microparticles. FASEB J. 2007; 21: 1926–33.
9. Borges Da Silva H, Beura LK, Wang H, Hanse EA, Gore R, Scott MC, et al. The purinergic receptor P2RX7 directs metabolic fitness of long-lived memory CD8+ T cells. Nature. 2018; 559: 264–8.
10. Di Virgilio F, Sarti AC, Falzoni S, De Marchi E, Adinolfi E. Extracellular ATP and P2 purinergic signalling in the tumour microenvironment. Nat Rev Cancer. 2018; 18: 601–18.

11. Rassendren F, Buell GN, Virginio C, Collo G, North RA, Surprenant A. The permeabilizing ATP receptor, P2X7. Cloning and expression of a human cDNA. J Biol Chem. 1997; 272: 5482–6.
12. Smart ML, Gu B, Panchal RG, Wiley J, Cromer B, Williams DA, et al. P2X7 receptor cell surface expression and cytolytic pore formation are regulated by a distal C-terminal region. J Biol Chem. 2003; 278: 8853–60.
13. Hofman P, Cherfils-Vicini J, Bazin M, Ilie M, Juhel T, Hébuterne X, et al. Genetic and pharmacological inactivation of the purinergic P2RX7 receptor dampens inflammation but increases tumor incidence in a mouse model of colitis-associated cancer. Cancer Res. 2015; 75: 835–45.
14. Adinolfi E, Capece M, Franceschini A, Falzoni S, Giuliani AL, Rotondo A, et al. Accelerated tumor progression in mice lacking the ATP receptor P2X7. Cancer Res. 2015; 75: 635–44.
15. Chong J-H, Zheng G-G, Zhu X-F, Guo Y, Wang L, Ma C-H, et al. Abnormal expression of P2X family receptors in Chinese pediatric acute leukemias. Biochem Biophys Res Commun. 2010; 391: 498–504.
16. Zhang XJ, Zheng GG, Ma XT, Yang YH, Li G, Rao Q, et al. Expression of P2X7 in human hematopoietic cell lines and leukemia patients. Leuk Res. 2004; 28: 1313–22.
17. Adinolfi E, Melchiorri L, Falzoni S, Chiozzi P, Morelli A, Tieghi A, et al. P2X7 receptor expression in evolutive and indolent forms of chronic B lymphocytic leukemia. Blood. 2002; 99: 706–8.
18. Carluccio M, Zuccarini M, Ziberi S, Giuliani P, Morabito C, Mariggiò MA, et al. Involvement of P2X7 receptors in the osteogenic differentiation of mesenchymal stromal/stem cells derived from human subcutaneous adipose tissue. Stem Cell Rev Reports. 2019; 15: 574–89.
19. Ziberi S, Zuccarini M, Carluccio M, Giuliani P, Ricci-Vitiani L, Pallini R, et al. Upregulation of epithelial-to-mesenchymal transition markers and P2X7 receptors is associated to increased invasiveness caused by P2X7 receptor stimulation in human glioblastoma stem cells. Cells. 2019; 9: 85.
20. Greig AVH, Linge C, Healy V, Lim P, Clayton E, Rustin MHA, et al. Expression of purinergic receptors in non-melanoma skin cancers and their functional roles in A431 cells. J Invest Dermatol. 2003; 121: 315–27.
21. White N, Butler PEM, Burnstock G. Human melanomas express functional P2X7 receptors. Cell Tissue Res. 2005; 321: 411–8.
22. Raffaghello L, Chiozzi P, Falzoni S, Di Virgilio F, Pistoia V. The P2X7 receptor sustains the growth of human neuroblastoma cells through a substance P-dependent mechanism. Cancer Res. 2006; 66: 907–14.
23. Künzli BM, Berberat PO, Giese T, Csizmadia E, Kaczmarek E, Baker C, et al. Upregulation of CD39/NTPDases and P2 receptors in human pancreatic disease. Am J Physiol - Gastrointest Liver Physiol. 2007; 292: G223–30.
24. Solini A, Cuccato S, Ferrari D, Santini E, Gulinelli S, Callegari MG, et al. Increased P2X7 receptor expression and function in thyroid papillary cancer: A new potential marker of the disease? Endocrinology. 2008; 149: 389–96.
25. Li X, Qi X, Zhou L, Fu W, Abdul-Karim FW, MacLennan G, et al. P2X7 receptor expression is decreased in epithelial cancer cells of ectodermal, uro-genital sinus, and distal paramesonephric duct origin. Purinergic Signal. 2009; 5: 351–68.
26. Bae JY, Lee SW, Shin YH, Lee JH, Jahng JW, Park K. P2X7 receptor and NLRP3 inflammasome activation in head and neck cancer. Oncotarget. 2017; 8: 48972–82.
27. Ghiringhelli F, Apetoh L, Tesniere A, Aymeric L, Ma Y, Ortiz C, et al. Activation of the NLRP3 inflammasome in dendritic cells induces IL-1B-dependent adaptive immunity against tumors. Nat Med. 2009; 15: 1170–8.
28. Sluyter R, Stokes L. Significance of p2x7 receptor variants to human health and disease. Recent Patents DNA Gene Seq. 2011; 5: 41–54.
29. Benzaquen J, Heeke S, Janho dit Hreich S, Douguet L, Marquette CH, Hofman P, et al. Alternative splicing of P2RX7 pre-messenger RNA in health and diseases: Myth or reality? Biomed J. 2019; 42: 141–54.
30. Feng YH, Li X, Zeng R, Gorodeski GI. Endogenously expressed truncated P2X7 receptor lacking the C-terminus is preferentially upregulated in epithelial cancer cells and fails to mediate ligand-induced pore formation and apoptosis. Nucleosides, Nucleotides and Nucleic Acids. 2006; 25: 1271–6.
31. Adinolfi E, Cirillo M, Woltersdorf R, Falzoni S, Chiozzi P, Pellegatti P, et al. Trophic activity of a naturally occurring truncated isoform of the P2X7 receptor. FASEB J. 2010; 24: 3393–404.
32. Giuliani AL, Colognesi D, Ricco T, Roncato C, Capece M, Amoroso F, et al. Trophic activity of human P2X7 receptor isoforms A and B in osteosarcoma. PLoS One. 2014; 9.
33. Ulrich H, Ratajczak MZ, Schneider G, Adinolfi E, Orioli E, Ferrazoli EG, et al. Kinin and purine signaling contributes to neuroblastoma metastasis. Front Pharmacol. 2018; 9.
34. Boldrini L, Giordano M, Ali G, Servadio A, Pelliccioni S, Niccoli C, et al. P2X7 protein expression and polymorphism in non-small cell lung cancer (NSCLC). J Negat Results Biomed. 2014; 13.
35. Homerin G, Jawhara S, Dezitter X, Baudelet D, Dufrénoy P, Rigo B, et al. Pyroglutamide-based P2X7 receptor antagonists targeting inflammatory bowel disease. J Med Chem. 2020; 63: 2074–94.
36. Adinolfi E, Raffaghello L, Giuliani AL, Cavazzini L, Capece M, Chiozzi P, et al. Expression of P2X7 receptor increases *in vivo* tumor growth. Cancer Res. 2012; 72: 2957–69.
37. Amoroso F, Capece M, Rotondo A, Cangelosi D, Ferracin M, Franceschini A, et al. The P2X7 receptor is a key modulator of the PI3K/GSK3β/VEGF signaling network: evidence in experimental neuroblastoma. Oncogene. 2015; 34: 5240–51.
38. Amoroso F, Salaro E, Falzoni S, Chiozzi P, Giuliani AL, Cavallesco G, et al. P2X7 targeting inhibits growth of human mesothelioma. Oncotarget. 2016; 7.
39. Qiu Y, Li WH, Zhang HQ, Liu Y, Tian XX, Fang WG. P2X7 mediates ATP-driven invasiveness in prostate cancer cells. Kanellopoulos J, Ed. PLoS One. 2014; 9: e114371.
40. Gilbert S, Oliphant C, Hassan S, Peille A, Bronsert P, Falzoni S, et al. ATP in the tumour microenvironment drives expression of nfP2X7, a key mediator of cancer cell survival. Oncogene. 2019; 38: 194–208.
41. Gyorffy B, Surowiak P, Budczies J, Lánczky A. Online survival analysis software to assess the prognostic value of biomarkers using transcriptomic data in non-small-cell lung cancer. Chellappan SP, Ed. PLoS One. 2013; 8: e82241.

Supplementary Figure 1: Separation of cell populations from LUAD tissues

A. Graphical representation of the isolation of cell populations. B. Quality control after cell separation. Sorted $CD45^+$ and $CD45^-$ cells from non-tumor (N) and tumor (T) areas of LUAD tissues were stained with an anti-CD45 antibody and analyzed by flow cytometry. n=3 independent experiments.

Supplementary Figure 2: Expression of the homo-P2RX7A trimer

hP2RX7 HEK or purified $CD45^-$ cells were permeabilized or not with 1% triton and stained with the conformational anti-P2RX7 antibody to characterize intracellular (intra) and membrane expression (Mb) of P2RX7. This result showed that $CD45^-$ cells from a tumor area of LUAD patients did not retained P2RX7 within the cytoplasm.

Supplementary Figure 3: Characterization of P2RX7 activity

A. Representative dot plots are shown. hP2RX7 HEK cells were stimulated for 5 min with the indicated doses of BzATP (a stable analogue of ATP) and stained with both TO-PRO-3 (APC) and Fluo-4-AM (FITC) to assay for large pore opening and intracellular Ca^{2+} variations, respectively. B. Dose response curves showing large pore opening (TO-PRO-3 uptake) and Ca^{2+} channel activation in response to BzATP in live cells. n=3 independent experiments.

Supplementary Figure 4: P2RX7 activity in LUAD patients

Representative dot plot showing a time course of macropore opening in purified $CD45^+$ cells (A) or $CD45^-$ cells (B) isolated from LUAD tissue. The percentage of TO-PRO-3 positive cells in response to BzATP (250 µM) is shown. To demonstrate that P2RX7 is involved in the TO-PRO-3 uptake, cells were pretreated with a specific P2RX7 antagonist (GSK13700319A) 30 min before adding BzATP for an additional 30 min.

Supplementary Figure 5 : *P2RX7* splice variant expression in human peripheral blood mononuclear cells

A. Primers used to analyze *P2RX7* splice variant expression in human peripheral blood mononuclear cells (PBMC). **B.** Representative image showing qualitative PCR. We were unable to generate primers specific for *P2RX7D* and *E*.

Supplementary Figure 6 : Primers used in quantitative PCR experiments

A. Primers used to analyze *P2RX7* splice variant expression by qPCR. **B.** Expression vectors coding for human *P2RX7A*, *P2RX7B*, *P2RX7H* and *P2RX7J* were used to produce specific amplicons of each *P2RX7* mRNA. The number of molecules was calculated and serial dilutions, to verify the linear amplification of each mRNA after qPCR, were performed.

Supplementary Figure 7: *P2RX7* expression in LUAD

P2RX7 expression obtained from the TCGA database showing down-regulation of P2RX7 in LUAD tissues (T) versus non-tumor tissues (N). *P2RX7* expression was in compared LUAD tissues and adjacent non-tumor tissues. All stage: 57 LUAD tissues and paired non-tumor tissues; Stage I-II: 42 LUAD tissues and paired non-tumor tissues; Stage III-IV: 15 LUAD tissues and paired non-tumor tissues (unpaired Student's *t* test).

Supplementary Figure 8: Characterization of tagged P2RXA and P2RXA AB receptors

A. Hemi-venus expressing cells are not GFP positive. HEK cells were transiently transfected with P2RX7A and P2RX7B tagged with venus 1 or venus 2 sequences. Representative images of P2RX7B-v1, P2RX7B-v2, P2RX7A-v1 and P2RX7A-v2 showing that only cells expressing the trimeric conformation of P2RX7A are stained with the anti-P2RX7. P2RX7 (red), v1-v2 complementation (green), nucleus (blue). **B.** Representative illustration of the quantification of v1-v2 (GFP) and P2RX7A (red) positive cells. The distance between tagged-P2RX7 and P2RX7A was calculated using Image J software.

Supplementary Figure 9: Characterization of P2RX7B isoform in HEK transfected cells

A. HEK cells were transfected with empty vector, P2RX7A or P2RX7B. 50 ug of total protein were analyzed by western blotting using the anti-extracellular loop anti P2RX7 antibody. In cells transfected with P2RX7A we observed a band of 70 kDa. In cells transfected with P2RX7B, we observed two bands, one of 55 kDa which corresponds to P2RX7B and one at lower molecular which likely corresponds to

non-glycosylated protein. Expression of two bands in cells transfected with P2RX7B were previously observed in Adinolfi et al, 2010. **B.** Immunofluorescence analysis of HEK cells expressing either P2RX7A or P2RX7B. Cells were stained with the conformational anti-P2RX7 antibody (left panel). These results showed that P2RX7B is not recognized by the conformational antibody. The right panel illustrates HEK cells transfected with v1+v2-P2RX7B showing GFP fluorescence at the membrane (asterisk). **C.** P2RX7B expressed in HEK cells is activated by BzATP and induced increased Ca^{2+} concentration but not large pore opening. n=4 independent experiments.

Supplementary Figure 1

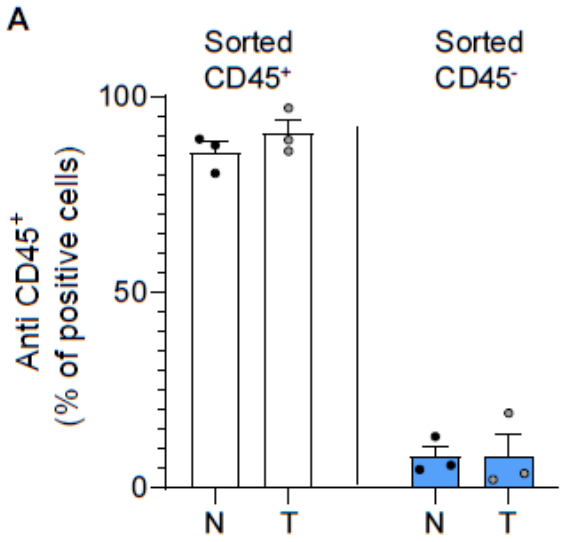

Supplementary Figure 2

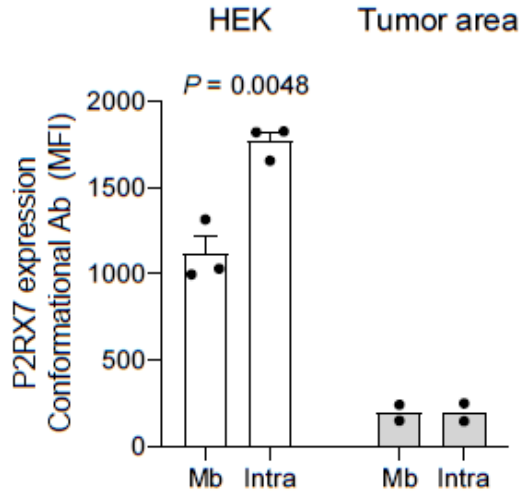

Supplementary Figure 3

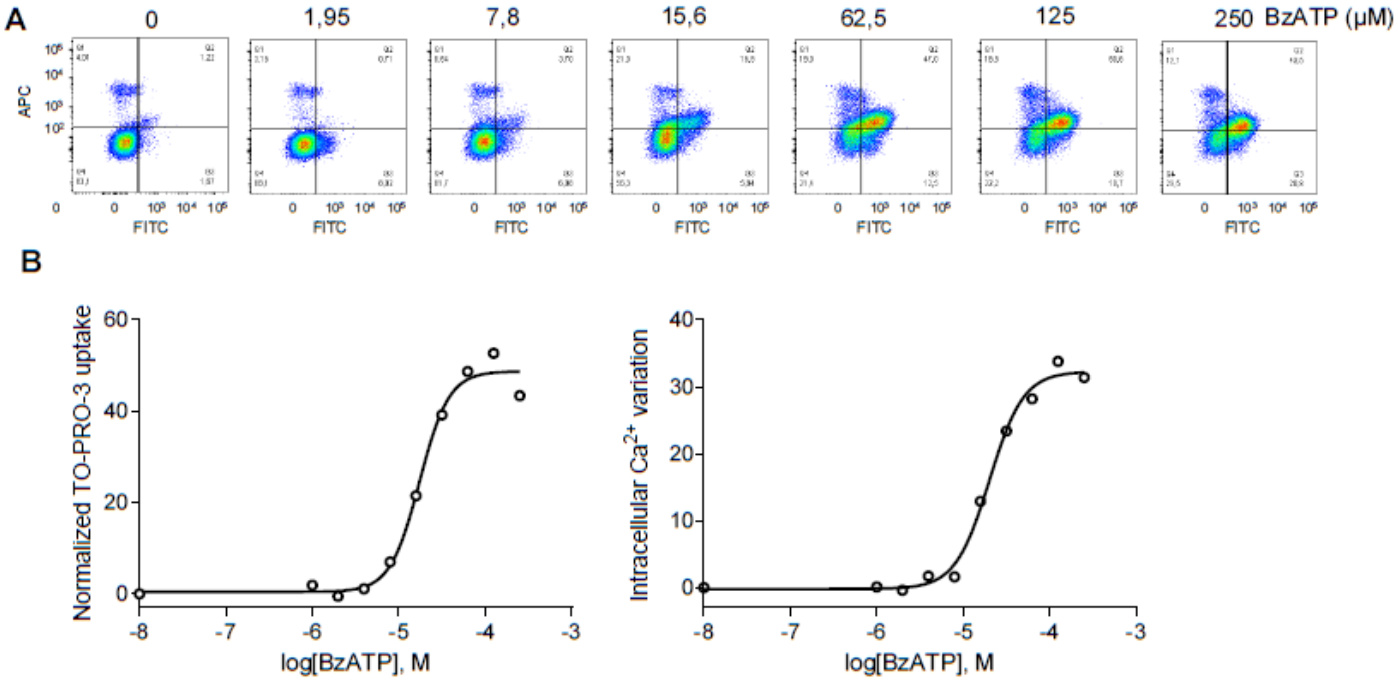

Supplementary Figure 4

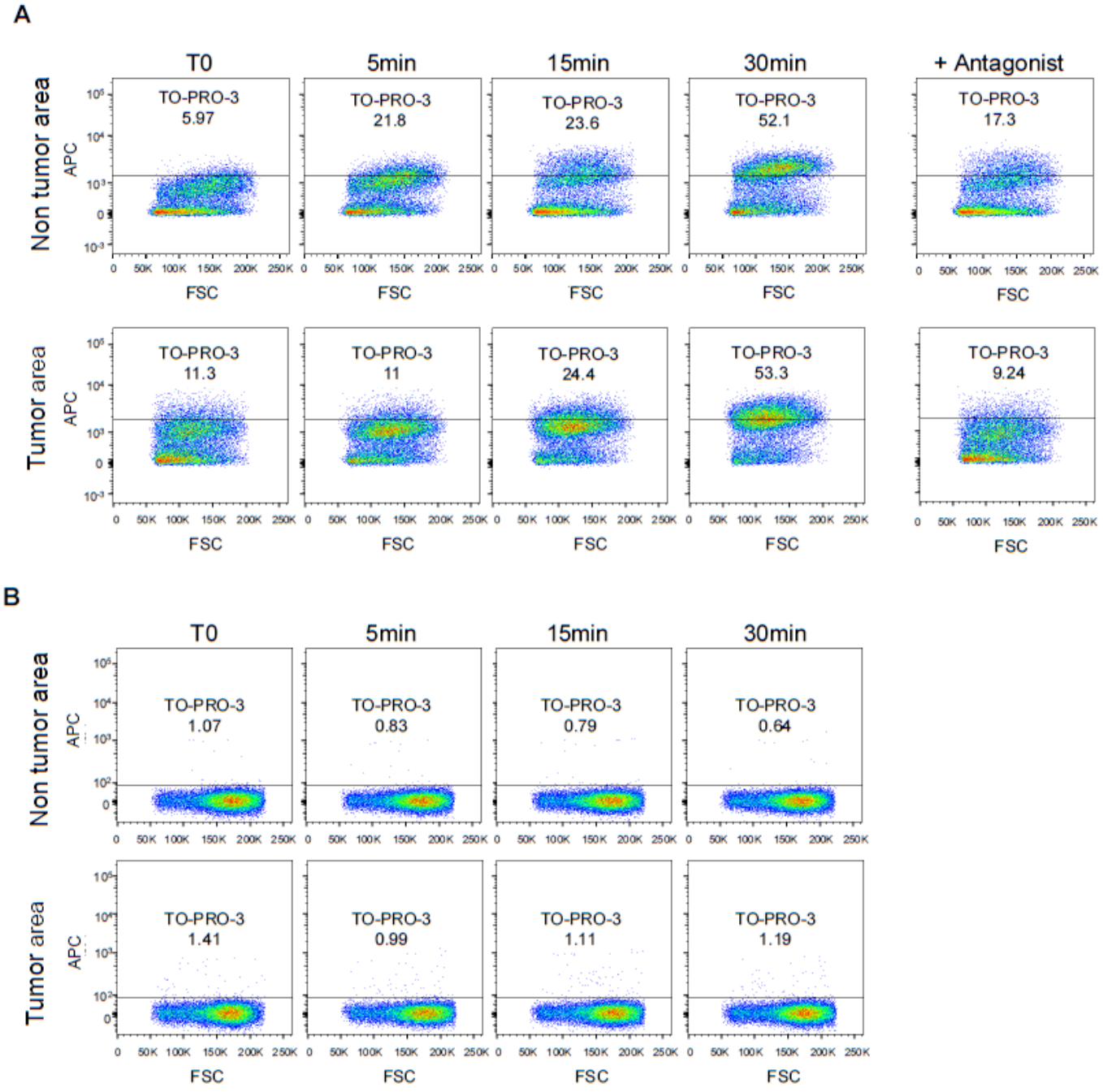

Supplementary Figure 5

A

Specificity	Forward primer	Reverse primer	MW
P2RX7(A, B, H)	GAACCAGCAGCTACTAGGGAGAAG	GAACCAGCAGCTACTAGGGAGAAG	476
P2RX7B	CGGCCACAACTACACCACGAG	CGGCCACAACTACACCACGAG	527
P2RX7H	CAAGGTCAGCCGAGATTCAG	CAAGGTCAGCCGAGATTCAG	850
P2RX7J	TTTCAGATGTGGCAATTCAGATA	TTTCAGATGTGGCAATTCAGATA	150

B

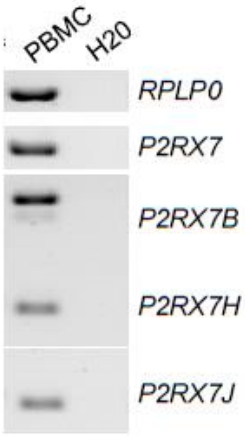

Supplementary Figure 6

A

Specificity	Forward primer	Reverse primer	MW
P2RX7 (A, B, H)	ATACAGTTTCCGTCGCCTTG	AACGGATCCCGAAGACTTTT	133
P2RX7B	GACATTATCCAGCTGGTTG	GACAAGCGCTGCGTTAGTCAC	125
P2RX7H	CAAGGTCAGCCGAGATTCAG	CAAGGTCAGCCGAGATTCAG	111
P2RX7J	TTTCAGATGTGGCAATTCAGATA	TTTCAGATGTGGCAATTCAGATA	150

B

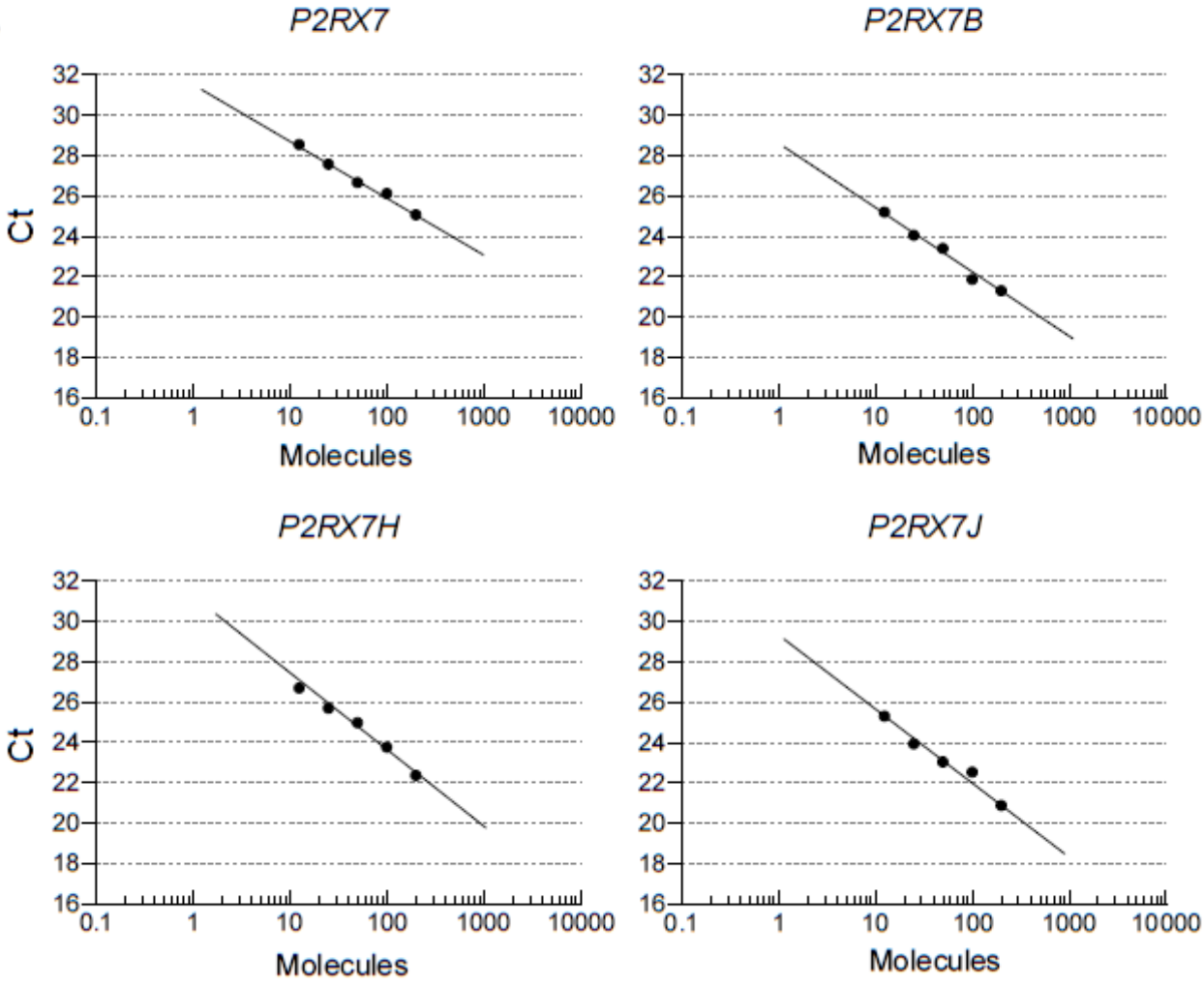

Supplementary Figure 7

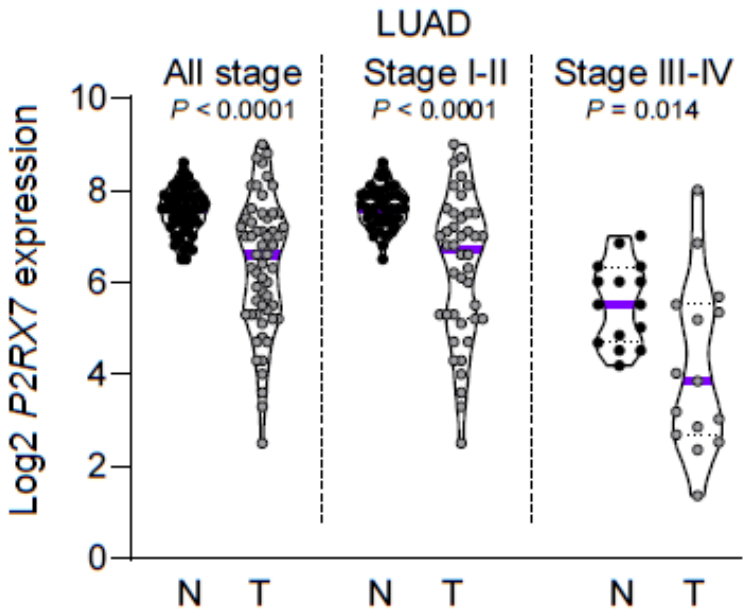

Supplementary Figure 8

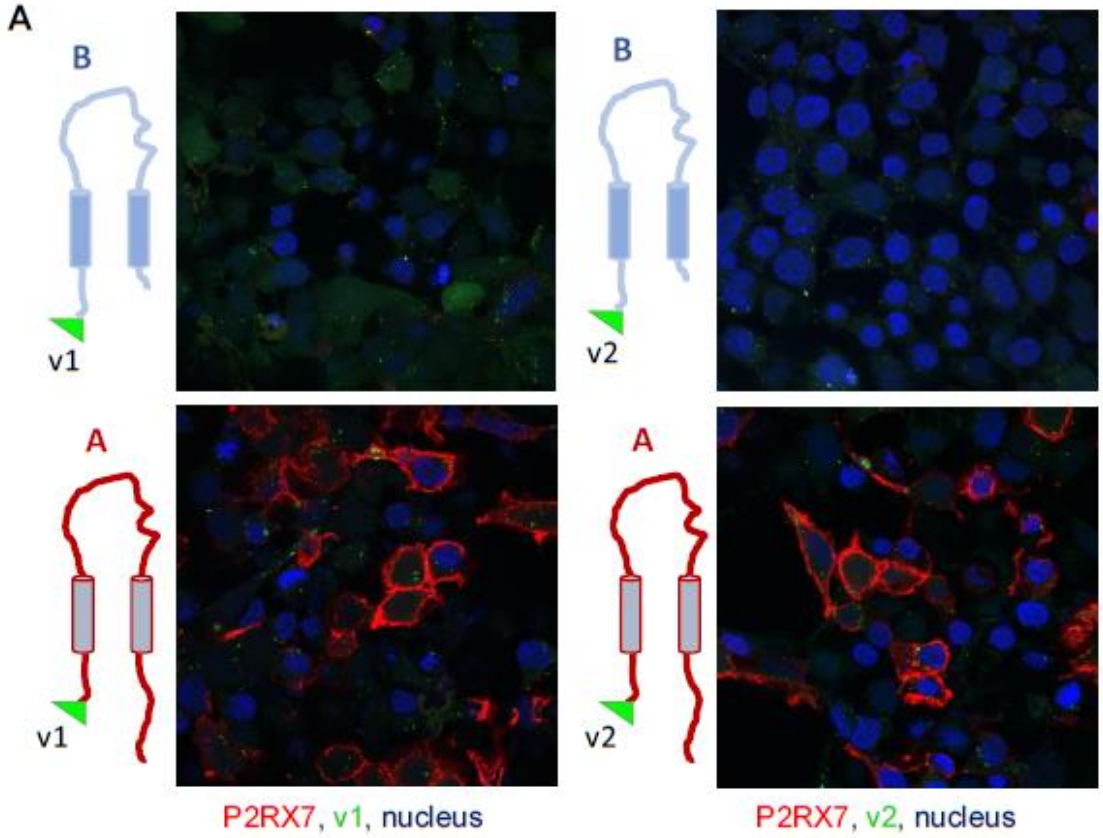

B

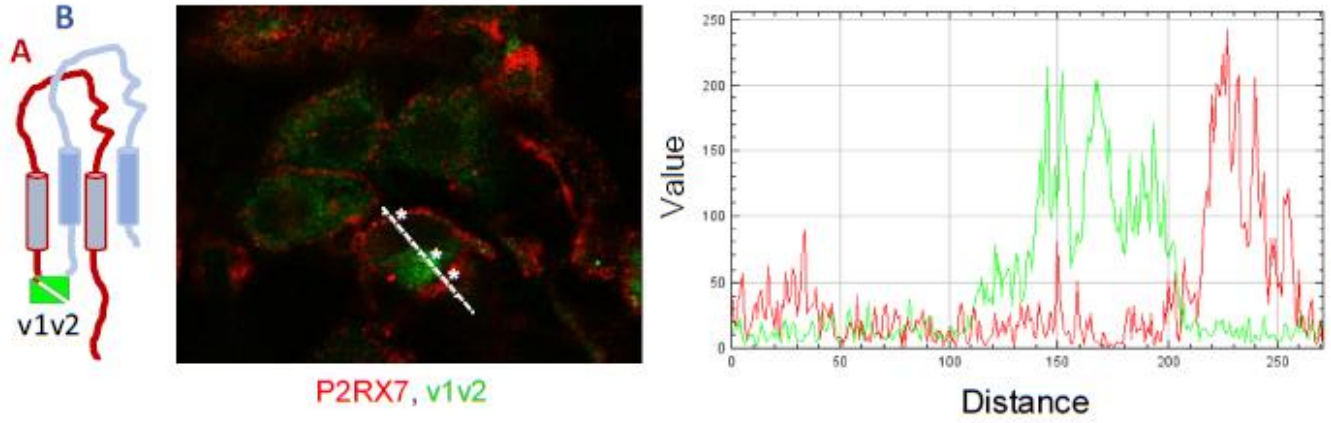

Supplementary Figure 9

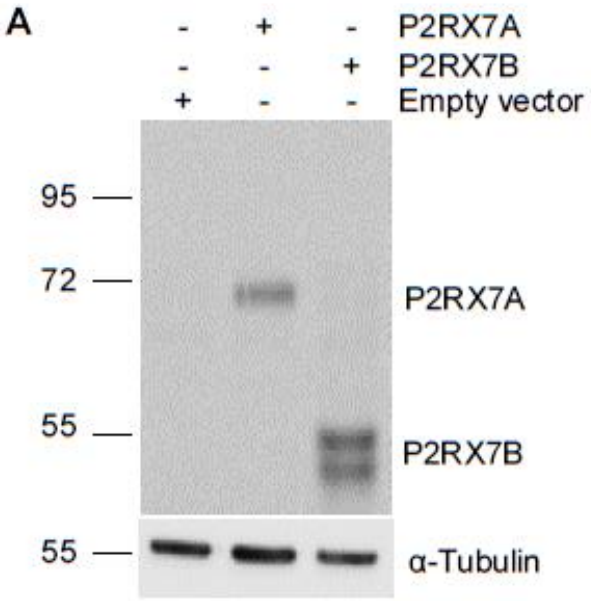

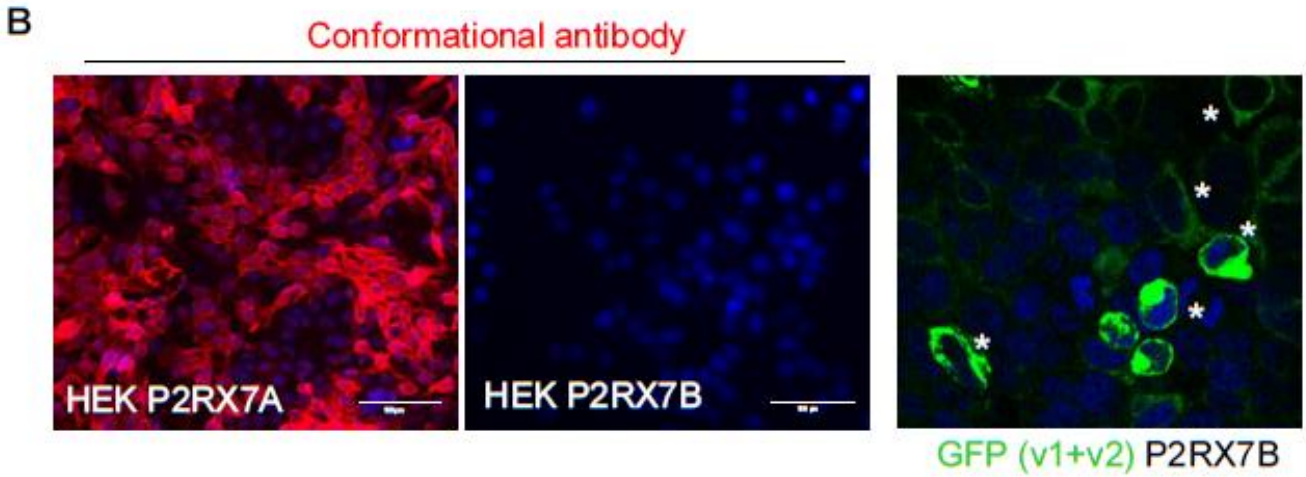

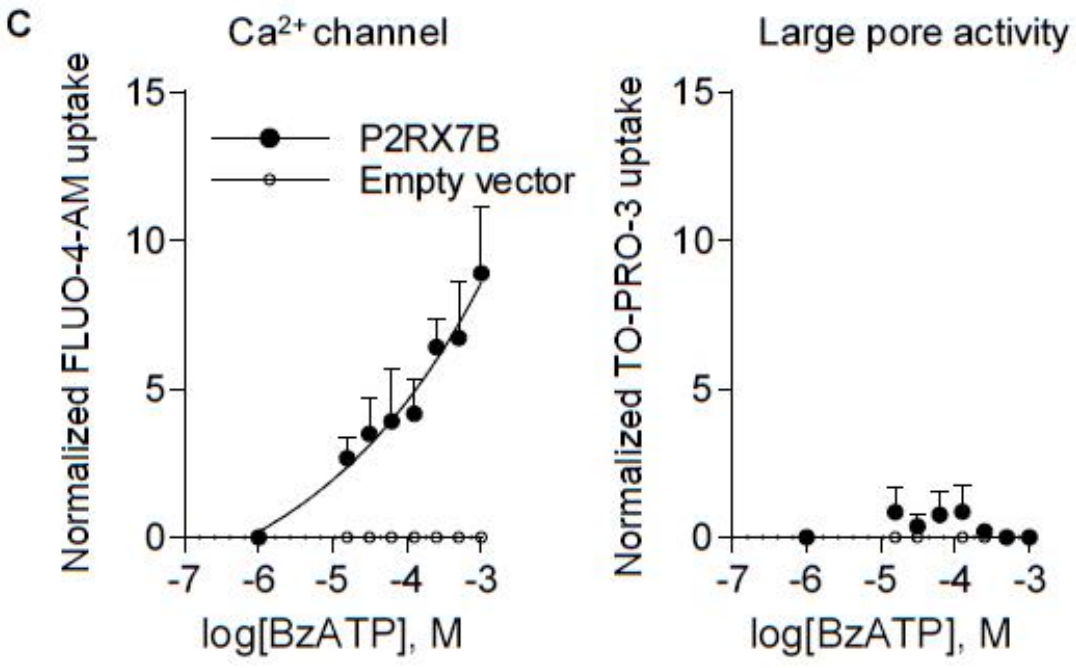

B. Publication scientifique N°2. La modulation positive de P2RX7 potentialise l'immunothérapie par inhibition de checkpoint de l'immunité chez la souris, et induit une réponse immunologique mémoire.

Article accepté (Nature Communications 2020)

Dans cet article, nous présentons une nouvelle molécule modulatrice chimique positive de P2RX7, qui potentialise le traitement par anti-PD1 dans le CNPC dans un modèle de souris transplantées ainsi que dans un modèle de souris induites par oncogène. Cette association thérapeutique induit des réponses immunitaires antitumorales durables par un mécanisme impliquant les cellules dendritiques exprimant P2RX7 et générant de l'interleukine 18 conduisant à la production d'interféron γ par les cellules NK et les lymphocytes T CD4. Les souris guéries présentent une protection à long terme de type T CD8 mémoire.

Cette nouvelle molécule représente une stratégie prometteuse dans le traitement du CNPC.

Ma participation pour cette publication, qui ne constituait pas le cœur de mon travail de thèse, a constitué en pratique à l'élaboration des outils d'analyses de l'expression et de la fonction de P2RX7 ainsi qu'aux analyses *in silico* de son expression.

Small-molecule P2RX7 activator sensitizes tumor to immunotherapy and vaccinates mouse against tumor re-challenge

Laetitia Douguet [1*], Serena Janho dit Hreich [1,4,5*], Jonathan Benzaquen [1,4,5], Laetitia Seguin [1,4], Thierry Juhel [1], Xavier Dezitter [7,9], Christophe Duranton [6], Bernhard Ryffel[12], Jean Kanellopoulos[13], Cecile Delarasse[14], Nicolas Renault [7,9], Christophe Furman [7,9], Germain Homerin [7,8], Chloé Féral [1,4], Julien Cherfils-Vicini [1], Régis Millet [7,9], Sahil Adriouch [10], Alina Ghinet [7,8,11], Paul Hofman [1,2,3,4] and Valérie Vouret-Craviari [1,4,5]

1. Université Côte d'Azur, CNRS, INSERM, IRCAN, 06108 Nice, France

2. Laboratory of Clinical and Experimental Pathology and Biobank, Pasteur Hospital, Nice, France

3. Hospital-Related Biobank (BB-0033-00025), Pasteur Hospital, Nice, France

4. FHU OncoAge, Nice, France

5. Centre Antoine Lacassagne, 06107 Nice, France

6. Université Côte d'Azur, CNRS, INSERM, LP2M, 06108 Nice, France

7. Univ. Lille, Inserm, CHU Lille, U1286 – Infinite – Institute for Translational Research in Inflammation, F-59000 Lille, France

8. Hautes Etudes d'Ingénieur (HEI), Yncréa Hauts-de-France, UC Lille, Laboratoire de chimie durable et santé, 13 rue de Toul, F-59046 Lille, France

9. Institut de Chimie Pharmaceutique Albert Lespagnol, IFR114, 3 rue du Pr Laguesse, F-59006 Lille, France

10. Normandie University, Institute for Research and Innovation in Biomedicine, F-76183 Rouen, France

11. 'Al. I. Cuza' University of Iasi, Faculty of Chemistry, Bd. Carol I, nr. 11, 700506 Iasi, Romania

12. INEM - UMR7355, Institute of Molecular Immunology and Neurogenetic, University and CNRS, Orleans, France

13. Institute for Integrative Biology of the Cell (I2BC), CEA, CNRS, Université Paris-Saclay, 91198, Gif-sur-Yvette cedex, France

14. Sorbonne Université, INSERM, CNRS, Institut de la Vision, 17 rue Moreau, F-75012 Paris, France

*Equal contribution

Corresponding authors:

Dr. Valérie Vouret-Craviari or Laetitia Douguet

Running title: P2RX7 activation to fight lung cancer

ABSTRACT

Only a subpopulation of non-small cell lung cancer (NSCLC) patients respond to immunotherapies, highlighting the urgent need to develop new therapeutic strategies to improve patient outcome. We developed a new chemical positive modulator (HEI3090) of the purinergic P2RX7 receptor that potentiates αPD-1 treatment to effectively control the growth of lung tumors in transplantable and oncogene-induced mouse models and triggers long lasting antitumor immune responses. Mechanistically, the molecule stimulates dendritic P2RX7 expressing cells to generate IL-18 which leads to the production of IFN-γ by Natural Killer and $CD4^+$ T cells within tumors. Combined with immune checkpoint inhibitor, the molecule induces a complete tumor regression in 80% of LLC tumor bearing mice. Cured mice are also protected against tumor re-challenge due to a CD8-dependent protective response. Hence, combination treatment of small-molecule P2RX7 activator followed by immune checkpoint inhibitor represents a promising novel strategy that may be active against NSCLC.

KEYWORDS: Purinergic receptors, ATP, immune checkpoint inhibitor, immunosurveillance

Introduction

Despite new biological insights and recent therapeutic advances, many tumors remain resistant to treatments, leading to premature death of the patient. This is particularly true for lung cancer which is the leading cause of cancer death for men and women worldwide. The 5-year survival rate for patients with any type of lung cancer is around 20%, which dramatically drops to 6% for metastatic lung cancers. Recent advances in new effective therapies such as targeted therapies and immunotherapies have revolutionized lung cancer treatments [1]. However, it is limited to a small percentage of patients and new approaches are urgently needed to improve patient outcome.

The P2RX7 receptor (also called P2X7R) is an ATP-gated ion channel composed of three protein subunits (encoded by the *P2RX7* gene), which is expressed predominantly in immune cells and in some tumor cells [2]. Activation of P2RX7 by high doses of extracellular ATP (eATP) leads to Na^+ and Ca^{2+} influx, and, after prolonged activation, to the opening of a larger conductance membrane pore. One consequence of this large pore opening, a unique characteristic of P2RX7, is to induce cell death in eATP rich microenvironments. Noteworthy, such high doses of eATP are present in the inflammatory and tumor microenvironments [3]. P2RX7 functions are largely described in immune cells, where it is involved in NLRP3 activation to induce the maturation and secretion of IL-1β and IL-18 pro-inflammatory cytokines by macrophages and dendritic cells (DC) [4]. In line, several P2RX7 inhibitors have been developed with the aim to treat inflammatory diseases. In addition to its ability to finely tune the amplitude of the inflammatory response [5], P2RX7 has been shown to orchestrate immunogenic cell death and to potentiate DC activation and ability to present tumor antigens to T cells [6]. Among immune cells, regulatory T cells (Treg) are highly sensitive to P2RX7-induced cell death and, in the presence of eATP, P2RX7 negatively regulates their number and their suppressive function [7]. Such response can participate in P2RX7-dependent immune surveillance by unleashing the effector functions of adaptive immune T cells [8]. Therefore, P2RX7 has been proposed to represent a new positive modulator of antitumor immune response. This is in agreement with data from our group showing that P2RX7-deficient mice are more sensitive to colitis-associated cancer [9]. Also, in this model, we noticed that transplanted Lewis Lung Carcinoma tumors grew faster in line with the findings of Adinolfi and collaborators using transplanted B16 melanoma and CT26 colon carcinoma tumors [10]. Collectively, these results support the notion that P2RX7 expression by host immune cells coordinates antitumor immune response.

Capture of tumor antigens by antigen-presenting DC is a key step in immune surveillance. Activated DCs present tumor

antigens to naïve T cells leading to their activation and differentiation in effector T cells. Tumor infiltrated effector T cells and NK cells can recognize and kill tumor cells resulting in the release of additional tumor antigens and amplification of the immune response. However, this response is often inhibited by immunosuppressive mechanisms present within the tumor microenvironment (TME). Different mechanisms sustain tumor escape as the reduced immune recognition of tumors due to the absence of tumor antigens, or the loss of MHC-I and related molecules, the increased resistance of tumor cells edited by the immune responses, and the development of a favorable TME associated with the presence of immunosuppressive cytokines and growth factors (such as VEGF, TGF-β) or the expression of checkpoint inhibitors such as PD-1/PD-L1 [11]. Inhibitory checkpoint inhibitors (αPD-1/PD-L1 and anti-CTLA-4) are used in daily practice for the treatment of advanced malignancies, including melanoma and non-small-cell lung cancer (NSCLC) [12]. These antibodies reduce immunosuppression and reactivate cytotoxic effector cell functions to elicit robust antitumor responses [13,14]. High response rate to αPD-1/PD-L1 therapy is often associated with immune inflamed cancer phenotype characterized by the presence in the TME of both $CD4^+$ and $CD8^+$ T cells, PD-L1 expression on infiltrating immune and tumor cells and many proinflammatory and effector cytokines, such as IFN-γ [15]. Noteworthy, only few cancer patients achieve a response with anti-immune checkpoint administered as single-agent [16], suggesting that strategies based on combined therapies would likely enhance antitumor efficacy and immunity.

Despite the role of P2RX7 in stimulating antitumor immunity and the observation that tumor development is more aggressive in *p2rx7* deficient animals [9], it is currently not known whether P2RX7 activation can modulate tumor progression *in vivo*. The purpose of this study is to investigate the effect of a positive modulator (PM) of P2RX7 on lung tumor fate. To do so, we use syngeneic immunocompetent tumor mice models and show that activation of P2RX7 improved mice survival. Mechanistically, activation of P2RX7 leads to increased production of IL-18 in a NLRP3-dependent manner, which in turn activates NK and $CD4^+$ T cells to produce IFN-γ and consequently increases tumor immunogenicity. Finally, activation of P2RX7 combined with αPD-1 immune checkpoint inhibitor allows tumor regression, followed by the establishment of a robust immunological memory response.

Results

HEI3090 is a positive modulator of P2RX7

In order to identify positive modulator of P2RX7, 120 compounds from the HEI's proprietary chemical library were screened for their ability to increase P2RX7-mediated intracellular calcium concentration during external ATP exposure. We first produced an HEK cell line expressing the cDNA encoding for *P2RX7* from C57BL/6 origin (HEK mP2RX7) and determined the minimal dose of ATP that should be used to initiate an increase in Ca^{2+} concentration. This dose corresponds to 333 µM (not shown). We tested 5 promising compounds and identified HEI3090 as a hit (patent WO2019185868A1). HEI3090 corresponds to a pyrrolidin-2-one derivative decorated with a 6-chloropyridin-3-yl-amide in position 1 and with a 2,4-dichlorobenzylamide moiety in position 5 (Fig. 1A). HEI3090 alone showed no toxic activity (data not shown), was unable to induce intracellular Ca^{2+} variation and required the presence of eATP to rapidly and dose dependently enhance the P2RX7 mediated intracellular calcium concentration (Fig. 1B and 1C). The maximum effect of HEI3090 was observed at 250 nM, which is in the range of doses identified in pharmacokinetic analysis (Fig. 1G). HEI3090 action required the expression of P2RX7, since HEK cells transfected with empty plasmid (pcDNA6) showed no increase in intracellular calcium concentration (Fig. 1C). P2RX7 has the unique capacity to form a large pore under eATP stimulation. Large pore opening of P2RX7 was assayed with the quantification of the uptake of the fluorescent TO-PRO-3 dye. As expected, HEI3090 alone had no effect and required eATP stimulation to enhance TO-PRO-3 entry within the cells. HEI3090 increased by 2.5-fold the large pore opening (Fig. 1D). The

rapid uptake of TO-PRO-3 was consistent with direct P2RX7 activation rather than ATP/P2RX7-induced cell death (Fig. 1E). We also tested HEI3090's effect on splenocytes expressing physiologic levels of P2RX7 (Fig 1F). In these immune cells, HEI3090 alone did not affect Fluo-4-AM nor TO-PRO-3 uptake. However, in the presence of eATP, HEI3090 enhanced Ca^{2+} influx and TO-PRO-3 uptake. We also showed that HEI3090 required the expression of P2RX7, since its effect was lost in splenocytes isolated from *p2rx7*$^{-/-}$ mice.

Collectively these results demonstrate that HEI3090 requires P2RX7 expression to be active and enhances eATP-induced P2RX7 activation.

HEI3090 inhibits tumor growth and enhances antitumor efficacy of αPD-1 treatment

We previously suggested that P2RX7 expression might favor the activation of immune responses [9]. We therefore evaluated the immuno-stimulatory effect and antitumor efficacy of HEI3090 *in vivo*, hypothesizing that the high level of eATP contained within the TME [17] would be sufficient to stimulate P2RX7. To do so, we used the subcutaneous Lewis Lung Carcinoma (LLC) syngeneic mouse model. Vehicle or HEI3090 (1.5mg/kg) were administered concomitantly to tumor cell injection and mice were treated daily for 11 days. Mice treated with HEI3090 displayed significantly reduced tumor growth and more than 4-fold decrease in tumor weight (Fig. 2A and Supplementary Fig. 2). We next tested the efficacy of HEI3090 to inhibit tumor growth in a therapeutic model, in which treatment started when tumor reached 10 to 15 mm^2 in volume. HEI3090 (3mg/kg), inhibited tumor growth and increased by 2-fold the median survival (Fig 2B). We also tested the effect of HEI3090 in the melanoma B16-F10 tumor mouse model and observed the same efficacy (Supplementary Fig. 3A-B).

Given the efficacy of HEI3090 to inhibit tumor growth, we next evaluated the combination of HEI3090 and αPD-1-1 antibody. After tumor inoculations, mice were treated daily with HEI3090 or vehicle and αPD-1 was administered at days 4, 7, 10, 13 and 16. While only 1 mouse out of the 16 mice treated with the αPD-1 alone showed a tumor regression, 13 out of the 16 mice treated with HEI3090+αPD-1 were tumor-free, suggesting that this molecule increased the efficacy of immune checkpoint inhibitor to induce effective antitumor immune responses and tumor regression (Fig. 2C). Importantly, only the combo treatment allows a long-lasting improved survival of at least 340 days (Fig. 2C, right panel). The combo treatment also increased the survival of mice grafted with B16-F10 tumors (Supplementary Fig. 3C) As illustrated in Fig 2D, we tested the combo treatment on the Kras-driven lung cancer (LSL *Kras*^{G12D}) model, which leads to adenocarcinomas 4 months after instillation of adenoviruses expressing the Cre recombinase [18]. Whereas αPD-1 treatment reduced the number of ADC (Fig. 2D), HEI3090 was able to enhance αPD-1's effects in this mouse model. Indeed, tumor burden in mice treated with the combo treatment is reduced by 60% compared to mice treated with αPD-1 alone. Accordingly, the cell number per mm^2 and the number of cells positively stained for the proliferation marker Ki67 were decreased by 50% in lesion areas (Supplementary Fig. 3D). One mouse out of the 6 treated with HEI3090 and αPD-1 was protected against adenocarcinoma formation.

Dendritic cells mediate the antitumor effect of HEI3090

LLC tumor cells express an active P2RX7 since the presence of high doses of eATP leads to an increase in intracellular Ca^{2+} concentration, which is blocked by the GSK1370319A P2RX7 inhibitor [19] (Supplementary Fig. 1). To functionally investigate which cells are targeted by HEI3090, we inoculated LLC in *p2rx7*$^{-/-}$ mice and treated them with HEI3090. Whereas HEI3090 efficiently blocked LLC tumor growth in WT mice (Fig. 2A), the same treatment was inefficient in *p2rx7*$^{-/-}$ mice, as tumor growth was indistinguishable in treated or non-treated groups (Fig. 3A). This result suggests that HEI3090 requires P2RX7 expression by mouse host cells to inhibit tumor growth. The importance of immune cells was further

confirmed by the demonstration that the antitumor efficacy of HEI3090 was restored after adoptive transfer of WT splenocytes into *p2rx7*$^{-/-}$ mice. Dendritic cells (DC) express P2RX7 and orchestrate antitumor immunity. Purified DC from WT spleens transferred into *p2rx7*$^{-/-}$ mice were able to restore the antitumor effect of HEI3090 (Fig. 3B). This experiment was further supported by the fact that phagocytic cells (macrophages and DC) were required for HEI3090's antitumor effect (Extended data and Supplementary Fig.4B) and that macrophages are less implicated in HEI3090's effect *in vivo* (Supplementary Fig.4C).

Flow cytometry analyses revealed that the TME of mice treated with HEI3090 were more infiltrated by immune cells than control mice (Fig. 3D). An increased infiltration of CD8$^+$ T cells was also observed in the LSL *Kras*^{G12D} lung tumor mouse model (Fig. 3E). Furthermore, we showed that HEI3090-treated mice showed higher levels of P2RX7 on DC (Supplementary Fig. 4A). Deeper characterization of immune cell infiltrate in the LLC tumor model revealed that anti-CD3 staining of tumors from HEI3090-treated mice contained 4 times more CD3$^+$ T cells than tumors from vehicle-treated mice (Fig. 3F). Whereas the proportion of CD4$^+$FOXP3$^+$ regulatory T cells was comparable between treated or non-treated mice (Fig. 3G), we found fewer myeloid derived suppressor cells (PMN-MDSCs) after HEI3090 therapy (Fig. 3H) and higher NK/PMN-MDSC and CD4/PMN-MDSC ratios (Fig. 3I) but the treatment failed to consistently increase the CD8/MDSC ratio. We also showed that HEI3090 targets immune cells in the low immunogenic B16-F10 melanoma syngeneic mouse model, where it was able to increase anti-tumor effector cells and decrease M-MDSCs infiltration (extended data and Supplementary Fig. 5).

P2RX7 expressed by DC has been shown to link innate and adaptive immune responses against dying tumor cells upon chemotherapy–induced immunogenic cell death (ICD) and facilitate tumor antigens presentation to T cells [6]. We evaluated the capacity of HEI3090 treatment to kill tumor cells and concomitant stimulation of DC maturation. Our results showed that HEI3090 is not an immunogenic cell death inducer (see Extended data and Supplementary Fig. 6).

The two tumor cell lines used in this study express different levels of P2RX7 (Supplementary Fig. 1), yet HEI3090 required P2RX7's expressing immune cells to inhibit tumor growth in both tumor mouse models. These results demonstrate that HEI3090 controls tumor growth by recruiting and activating P2RX7-expressing immune cells, especially DC, within the TME to initiate an effective antitumor immune response.

IL-18 is produced in response to HEI3090 treatment and is required to mediate its antitumor activity

We then investigated how the activation of P2RX7 enhanced antitumor immune responses. In addition to increasing intracellular Ca^{2+} concentration and stimulating the formation of a large membrane pore (see Fig. 1), P2RX7's activation is also known to activate the NLRP3 inflammasome that leads to the activation of caspase-1 and consequently to the maturation and release of the pro-inflammatory cytokines IL-1β and IL-18. We showed that HEI3090 enhanced caspase-1 cleavage (Supplementary Fig. 7). Whereas neutralization of IL-1β did not impact HEI3090's antitumor activity, neutralization of IL-18 suppressed the antitumor effect of HEI3090 (Fig. 4A). This result was confirmed using *il18* $^{-/-}$ mice in which HEI3090 had no impact on tumor growth (Fig. 4B). IHC staining of LLC tumors from HEI3090 treated mice showed a significant intratumor amount of IL-18 compared to mice treated with the vehicle (Fig. 4C), whereas staining of tumors from *il18*$^{-/-}$ mice revealed no staining (Supplementary Fig. 8A). Concordantly, serum levels of IL-18 were statistically more abundant in mice treated with HEI3090 than in vehicle mice (Fig. 4D), and no IL-18 was detected in the serum of mice that received IL-18 neutralizing antibody. In addition, HEI3090 was unable to modulate the levels of IL-18 in *p2rx7*$^{-/-}$ mice. Finally, primary peritoneal macrophages from WT mice cultured *ex vivo* with ATP and HEI3090 produce 1.5-fold more IL-18 than cells cultured with ATP and vehicle (Fig. 4E). IL-18 release by HEI3090

required the NLRP3 inflammasome, since its production is inhibited by the NLRP3 inflammasome-specific inhibitor (MCC950) (Fig. 4E). Moreover, we showed that HEI3090 enhanced caspase-1 cleavage (Supplementary Fig. 7) meaning that HEI3090 was able to increase IL-18 production by enhancing the activation of the NLRP3 inflammasome. Activation of P2RX7 by HEI3090 in macrophages from *p2rx7*$^{-/-}$ mice failed to increase IL-18 secretion (Supplementary Fig. 8B) and no staining was observed in LLC tumors from HEI3090 treated *p2rx7*$^{-/-}$ mice (Supplementary Fig. 8A). In agreement with the observation that HEI3090 retained its antitumor activity in mice treated with IL-1β neutralizing antibody, HEI3090 did not modify IL-1β protein levels in serum (Fig. 4D) and did not modulate IL-1β secretion in macrophages cultured *ex vivo* (Supplementary Fig. 8D).

Increased production of IL-18 was also observed in the LSL *Kras*^{G12D} lung tumor mouse model. Indeed, cells within lesions of mice treated with HEI3090 combined with αPD-1 expressed more IL-18 than mice treated with αPD-1 alone (Fig.4F). IL-18 protein levels in serum of mice that received the combo treatment were also increased by 6-fold (Fig. 4F and Supplementary Fig. 8C). As described with the LLC tumor model, HEI3090 did not impact the levels of IL-1β in this *in situ* genetic tumor mouse model (Supplementary Fig. 8F).

Collectively, these results demonstrate the antitumor effect of HEI3090 is highly dependent on P2RX7 expression and on its capacity to induce the production of mature IL-18 in the presence of eATP.

IL-18 is required to increase antitumor functions of NK and CD4$^+$ T cells

To identify which immune cells were involved in the HEI3090-induced antitumor response, we performed antibody specific cell depletion experiments. While NK and CD4$^+$ T cells depletions prevented HEI3090 treatment from inhibiting tumor growth (Fig. 5A and B), CD8$^+$ T cells depletion had no impact on HEI3090 treatment efficacy (Fig. 5A). To further study the effect of HEI3090 treatment on these subsets, we assessed their cytokine production within the TME. Analyses of tumor infiltrating immune cells first revealed that HEI3090 treatment significantly increased their capacity to produce IFN-γ (Fig. 5C). To precisely evaluate which cells in the TME produce IFN-γ, we studied the TIL sub-population and determined the ratios of IFN-γ to IL-10 production in each subset (Fig. 5D). NK and CD4$^+$ T cells were more biased to produce IFN-γ than the IL-10 immunosuppressive cytokine. CD8$^+$ T cells were relatively less prone to modification in this cytokine ratio profile upon HEI3090 treatment. In addition, two-fold more NK cells from mice treated with HEI3090 degranulate after *ex vivo* re-stimulation with LLC compared to NK from control mice (Fig. 5E), confirming their activation state, while no effect was noticeable on CD8$^+$ T cells. These phenotypic and functional analyses of intratumor immune infiltration suggested furthermore that treatment with HEI3090 stimulates CD4$^+$ T cells and NK cells' activation in the TME. Importantly, IL-18 neutralization abrogated the increase of the IFN-γ/IL-10 ratio by CD4$^+$ T cells and NK cells (Fig. 5F), suggesting that its production is a direct consequence of IL-18 release and signaling. We showed that DC and IL-18 were necessary for HEI3090's activity (Figs. 3B, 4A and B). *In vitro* stimulation of splenocytes treated with BzATP and HEI3090 did not increase IFN-γ production by T cells and NK cells indicating that its higher production in the tumor of treated mice is rather an indirect consequence of the therapy (Supplementary Fig. 9A). Concordantly, CD45$^+$ cells, CD8 and NK cells in the TME of *p2rx7*$^{-/-}$ mice supplemented with WT DC showed an increase in the IFN-γ/IL-10 ratio in the HEI3090-treated mice (Supplementary Fig. 9B). This result indicates that WT DC were able to produce IL-18 after the adoptive transfer, since anti-tumor effector cells were more prone to produce IFN-γ than the IL-10 immunosuppressive cytokine.

Finally, we uncovered that HEI3090 treatment of LLC tumor bearing mice *in vivo* increased the expression of MHC-I and PD-L1 by 2.2-fold (Fig. 5G). However, when LLC cells were treated *in vitro* with HEI3090, neither MHC-I nor PD-L1 expression were increased. By contrast, IFN-γ induced the expression of these

two proteins (Supplementary Fig. 9C). Taken together, our results suggest that the *in vivo* increase of MHC-I and PD-L1 expression is a consequence of IFN-γ upregulation driven by IL-18. Finally, using the LSL *Kras*^{G12D} tumor mouse model, we showed that tumor cells from mice that received both HEI3090 and αPD-1 expressed more PD-L1 than tumor cells from mice treated with αPD-1 only (Fig. 5H). Altogether, our results indicate that HEI3090 increases IL-18 production allowing the recruitment and activation of NK and CD4$^+$ T cells and the production of IFN-γ. In turn, IFN-γ stimulates expression of MHC-I and PD-L1 on cancer cells, leading to an increased-tumor immunogenicity and an increased sensitivity to anti-immune checkpoint inhibitors.

Combined with αPD-1 antibody, HEI3090 cures mice carrying LLC tumors and allows memory immune response

Combined with an αPD-1 antibody, HEI3090 cured 80% of LLC tumor bearing mice (Fig. 2D). To determine whether cured mice developed an antitumor immune memory response, they were re-challenged with LLC tumor cells 90 days after the first inoculation and were maintained without any therapy as illustrated in Fig. 6A. All long-term recovered mice were protected from LLC re-challenge, whereas all age-matched control mice developed tumors (Fig. 6B). The re-challenged mice were still alive 150 days after the initial challenge (Fig. 6C), sustaining the hypothesis that combo treatment effectively promoted an efficient antitumor memory immune response. Our results suggested that CD8$^+$ T cells are not directly involved in the primary antitumor effect of HEI3090 (see Fig. 5A). Nevertheless, it is well characterized that these cells play a pivotal role in the host's ability to mount an antitumoral adaptative immune response [20]. To evaluate the involvement of secondary memory CD8$^+$ T cells response in these mice, we sorted CD8$^+$ cells from age-matched naïve mice or 5 months (day 150) surviving re-challenged mice (see Fig 6A) and injected them to naïve mice prior to inoculation of LLC tumor cell in a 1/1 ratio. No treatment was given to mice. In this experimental condition, tumor growth was reduced by 2-fold in mice that received CD8$^+$ T cells isolated from cured mice (Fig. 6D), indicating that the combo therapy promoted a functional immune memory response that partly depends on CD8$^+$ T cells.

We next characterized the mice that were cured for a very long period (300 days), as illustrated in Fig. 6E. First, to discriminate between dormancy and eradication of tumor cells, we depleted CD8$^+$ T cells from 300 days-old cured mice and followed mice welfare in the absence of treatment (Fig. 6F). In this condition, no tumor relapse was observed during the 40 days of the experiment and the weight of the mice remained constant, revealing that the combo treatment efficiently eliminated tumor cells. Second, since circulating CD8$^+$ T cells are actively involved in the immune memory response [20] and participated in the HEI3090-induced antitumor response (see Fig. 6D), we investigated their involvement in the long-term memory immune response. To do so, 340 days-old cured or age-matched naïve mice were inoculated with LLC tumor cells in the absence of CD8$^+$ T cells. Both naïve- and cured- age-matched mice developed tumors (Fig 6G and 6H). However, the tumor growth was significantly reduced in cured mice and 3 out of the 6 mice did not have tumors (Fig. 6G, right panel). Cured mice survival was also significantly increased in comparison to naïve mice (Fig. 6I). Collectively, these results suggest that circulating CD8$^+$ T cells participate in the antitumor immune response induced by HEI3090.

P2RX7 is positively correlated with high infiltration of antitumor immune cells in NSCLC patients

Using the lung adenocarcinomas (LUAD) TCGA dataset, we analyzed the effect of *P2RX7* expression levels on the recruitment of cytotoxic immune cells. We clustered tumors of 80 patients with all stage (I-IV) of lung adenocarcinoma according to *P2RX7* expression and showed that high levels of *P2RX7* expression correlated with an increased-immune response in LUAD patients, characterized by a high mRNA expression of *CD274* (*PD-L1*), *IL1B*, *IL18*, a signature of

primed cytotoxic T cells (defined by *CD8A, CD8B, IFN-G, GZMA, GZMB, PRF1)* (Fig. 7A). Accordingly, Gene set enrichment analysis (GSEA) demonstrated a positive correlation between high *P2RX7* expression and the well characterized established signatures of "adaptive immune response", "T cell mediated immunity", "cytokine production" (Fig. 7B). Furthermore, high *P2RX7* expression is correlated with high levels of *CD274 (PD-L1),* independently of the stage of the disease (Fig. 7C). Consistently, a significant reduced overall survival is observed for *P2RX7* hi, *CD274* hi and *P2RX7* hi+*CD274* hi LUAD patients (Fig. 7D), suggesting that high expression levels of *P2RX7* is sufficient to bypass immune responses in the presence of high levels of *CD274*. Such a situation is considered to benefit from anti-checkpoint blockade and/or strategies aiming to reactivate immune responses, e.g. with an activator of P2RX7. Indeed, only few cancer patients achieve a response with anti-immune checkpoint administered as single-agent and combined therapies to enhance antitumor immunity and bring a clinical benefit for patients are actively tested. We showed in this study that the combination of HEI3090 and αPD-1 is more efficient to inhibit lung tumor growth than αPD-1 alone (see Fig.2C).

Discussion

This study demonstrates for the first time that activation of the purinergic P2RX7 receptor represents a promising strategy to control tumor growth. We developed a new positive modulator of P2RX7, called HEI3090, that stimulates antitumor immunity. HEI3090, induces production of IL-18 by P2RX7 expressing immune cells, by mainly targeting DC. IL-18 drives IFN-γ production to increase tumor immunogenicity and reinforces NK and $CD4^+$ T cells immune responses and generate protective $CD8^+$ T cells responses from recidivism. Noteworthy, therapeutic association of HEI3090 with αPD-1 antibody synergizes to cure mice in the LLC syngeneic model of lung cancer and elicits an antitumor immunity. We also observed that the combo treatment is more efficient than αPD-1 alone to inhibit tumor growth in the LSL-*KRas*^{G12D} lung tumor genetic mouse model. Lung tumor regression correlates with an increased immune cell infiltration, more secretion of IL-18 within the TME and higher expression of PD-L1 by tumor cells. Furthermore, this mode of action was confirmed using the B16-F10 melanoma tumor model (Supplementary Fig 5). Collectively these results demonstrate that the antitumor activity of HEI3090 follows the same rules in all tumor models tested and highlight the strength of HEI3090 to reactivate antitumor immunity.

The design of P2RX7's modulators was based on a ligand-based approach allowing the generation of a pharmacophore model. One hundred and twenty compounds were generated and were tested for their ability to enhance P2RX7's activities; five of them were able to do so. HEI3090 was the most promising and effective compound of the five and was therefore chosen for our study. Other natural or synthetic molecules, have been described to facilitate P2RX7 response to ATP [21–23]. However, until now, these molecules have not been tested in cancer models. Moreover, attempt to facilitate P2RX7 activation in the field of oncology has been limited by the finding that P2RX7 variants expressed by some tumor cells may sustain their proliferation and metabolic activity [2]. To explore this question, we analyzed P2RX7's functional features in *ex vivo* lung cancer samples [24] and showed that P2RX7 is functional in leukocytes whereas it is nonfunctional in tumor cells. Considering that P2RX7 is a pro-apoptotic receptor, it makes sense that tumor cells express a nonfunctional receptor. Whether this non-functional receptor corresponds to the non-conformational P2RX7 (nfP2RX7), described to be expressed by tumor cells [25], remains to be determined as well as the effect of HEI3090 on nfP2RX7.

Despite the finding that P2RX7 expression by immune cells restrains tumor growth [9,10], the use of specific P2RX7 antagonists has been promoted to treat cancers on the basis that inhibition of tumor cell proliferation would be more efficient [26,27]. Considerable effort has been made to engineer specific P2RX7 antagonists [28] and two of them (A74003 and AZ10606120) inhibited B16 tumor growth in immunocompetent mice [10]. However, to our

knowledge, these compounds have not been tested to treat cancer and have failed in the first clinical trials to treat inflammatory and pain-related diseases [28]. In addition, in the preclinical mouse model, we were unable to inhibit LLC and B16-F10 tumor growth when we tested the GSK1370319A compound, a well characterized P2RX7 antagonist [19] (data not shown). In line with this finding, our present results suggest that facilitation of P2XR7 is associated with efficient antitumor immunity in two different models of transplantable tumor (expressing moderate or higher level of P2RX7) as well as in the LSL-*KRas*^{G12D} genetic lung cancer mouse model. These results illustrate the view that P2RX7 activation, rather than inhibition, represent a promising strategy in cancer immunotherapy to unleash the immune responses, notably in conjunction with anti-checkpoint blockade. Therapeutic antibody represents another promising field of investigation to treat cancer. In particular, Gilbert and collaborators described an antibody against a non-functional P2RX7 variant that is promising to treat basal cell carcinoma [29]. It would be interesting to combine HEI3090 with the therapeutic P2RX7 antibody and assay the efficacy of this new combo treatment.

Antineoplastic action of eATP was previously explored using ATP administration in cancer patients and abandoned for lack of convincing results [30,31]. Extracellular ATP is naturally degraded to adenosine by ectoenzymes and adenosine is an immunosuppressive molecule [32]. To inhibit the production of adenosine, blocking antibodies against CD39 and CD73 ectoenzymes were produced and tested in mouse cancer models but also in ongoing clinical trials (NCT03454451). This strategy seems to be promising, at least in mice tumor models. In a first study, Perrot and collaborators showed that antibodies targeting human CD39 and CD73 promoted antitumor immunity by stimulating DC and macrophages which, in turn, restored the activation of effector T cells [33]. The authors also reported that the combination of anti-CD39 monoclonal antibody with oxaliplatin increased the survival of tumor bearing mice, at least for 50 days. In a second study, an independent anti-CD39 antibody was generated and tested on different mouse tumor models. This antibody alone dampened tumor growth and when combined with αPD-1, it further slowed tumor progression and 50% of the mice showed a complete rejection [34]. Mechanistically, the anti-CD39 antibody treatment led to increased eATP levels via the P2RX7/NLRP3/IL-18 to stimulate myeloid cells. Next, the authors demonstrated that anti-CD39 antibody sensitized αPD-1 resistant tumors by increasing CD8$^+$ T cells infiltration. Our results confirm these findings but also bring new highlights. First, we showed that activation of the eATP/P2RX7/NLRP3/IL-18 pathway by HEI3090 increased long lasting immune responses when combined with αPD-1 antibody. Second, we demonstrated that the endogenous eATP levels present in the TME was sufficient to enhance P2RX7 activation in the presence of HEI3090. These conditions are ideal to allow P2RX7 activation where it is needed and avoid the possible adverse effects associated with a systemic increase of ATP levels, such as the one observed in response to anti-CD39 and -CD73 antibodies.

It was shown that eATP attracts DC precursors towards the TME and promotes their activation state and their capacity to present antigen [35,36]. During the course of this study, we showed that HEI3090 targets P2RX7 expressing immune cells, especially DCs (Fig 4B) and observed that cDC CD4$^+$ T from mice treated with HEI3090 expressed higher levels of P2RX7 (Supplementary Fig. 4A). We also showed that HEI3090 treatment enhanced IL-18 production in a NLRP3-dependent manner but did not enhance the production of mature IL-1β (Fig. 4D) This was unexpected as secretion of mature IL-1β depends on the ATP/P2RX7-induced NLRP3 inflammasome activation as well [37]. However, unlike IL-1β, the inactive precursor form of IL-18 is constitutively expressed in most human and animal cells. Whether this explanation is sufficient alone to account for this differential IL-1β/IL-18 production is currently not known.

Whereas IL-1β is described to induce immune escape [38], IL-18 is involved in Th1 polarization and NK cell activation. We showed

here that IL-18 produced in response to HEI3090 treatment orchestrated the antitumor immune response by driving IFN-γ production by NK and $CD4^+$ T cells. This is in line with the well-known IFN-γ stimulating activity of IL-18 (originally designated IFN-γ-inducing factor), and with its Th1 and NK cells stimulating activity [39,40]. Protective effect of IL-18, but also the activation of NLRP3, have been previously reported in various mouse cancer models [41,42] NLRP3 activation in DCs as well as IL-18 have been linked to better prognosis, to drive anti-tumor immunity and to enhance the efficacy of immunotherapies in different tumor models [43]. In fact, when we combined HEI3090 with an αPD-1 antibody, we observed that the combo therapy efficiently controlled tumor burden in the 3 cancer models studied. Notably, the combo treatment cured 80% of LLC tumor bearing mice and very interestingly, cured mice developed an antitumor memory response.

CD8 memory T cells, comprising the circulating memory pool – composed of effector memory (T_{EM}) and central memory (T_{CM}) cells - and the tissue resident (T_{RM}) pool, play crucial roles in antitumor memory responses [44]. We showed that circulating $CD8^+$ T cells participated in cancer immunosurveillance after HEI3090 treatment (Fig. 6D). However, this $CD8^+$ T cells pool cannot be responsible for the entire response, since antitumor responses were still effective when $CD8^+$ T cells were depleted (Fig. 6G). These results suggest that other immune cells participate in local cancer surveillance. Possible candidates are the non-recirculating $CD8^+$ T_{RM} cells. The persistence of T_{RM} cells in tissues has been shown to depend on signaling programs driven by TGFβ and Notch-dependent signaling signature. Whether HEI3090 directly stimulates those programs remains to be determined but we observed, using HEK mP2RX7 cells, that HEI3090 enhanced ATP-stimulated ERK pathways (data not shown). Our results are also compatible with a role for $CD4^+$ T memory cells and the setup of a humoral response, in which B lymphocytes produce antibody against tumor cells.

Therapy with different αPD-1/PDL1 antibodies was approved in NSCLC in the first- and second-line settings. However, a significant fraction of patients does not benefit from the treatment (primary resistance), and some responders relapse after a period of response (acquired resistance) [45]. Expression of PD-L1 *per se* is not a robust biomarker with a predictive value since the αPD-L1 response has also been observed in some patients with PD-L1-negative tumors. Improvement of patient management for immunotherapy undoubtedly relies on the identification of such predictive markers. Using TCGA data set, we uncovered that *P2RX7* expression is correlated to *CD274* (PD-L1) expression and "hot" immunophenotype signatures in NSCLC patients. In addition, patients with high *P2RX7* and low *CD274* or high *CD274* and *low P2RX7* have a better overall survival than patients with high *CD274* and high *P2RX7*. This result suggests that immunotherapies may be efficient in double positive patients and questions the ability of P2RX7 to represent a valuable biomarker for αPD-1/PD-L1 therapies. In this context, we showed in another study [24] that the expression of *P2RX7B* splice variant in tumor immune cells is associated with less infiltrated tumors in lung adenocarcinoma. Mechanistically, we observed that the differential expression of the *P2RX7B* splice variant in immune cells within tumor area correlates with the expression of a less functional P2RX7 and lower leukocytes recruitment into LUAD.

To our knowledge, this is the first study demonstrating that a small-molecule activator of P2RX7 boosts immune surveillance by unleashing the effector functions of adaptive immune T cells and improving the efficacy of αPD-1treatment. This therapeutic strategy holds new hopes for cancer patients. By increasing tumor immunogenicity, it could first increase the number of patients eligible to immunotherapies and second, it could also be used as a neoadjuvant or adjuvant therapies of locally advanced lung tumors.

Methods section

Mice

This study was approved by the Institutional Care and Use Committee of the University of

Nice-Sophia Antipolis. Animal protocols were approved by the committee for Research and Ethics of the PACA region (CIEPAL azur) and followed the European directive 2010/63/UE, in agreement with the ARRIVE guidelines. *P2rx7*$^{-/-}$ (B6.129P2-*P2rx7*^{tm1Gab}/J) and *il18*$^{-/-}$ mice were from the Jackson Laboratory. LSL-*KRas*^{G12D} tumor lung model has been described in [18]. The generation of C57BL/6 mice harboring constitutive and myeloid specific targeted disruption of the *p2rx7* gene is described in the extended data section. Control C57BL/6J OlaHsD female (WT mouse) were supplied from Envigo (Gannat, France).

In vivo treatments

We used Lewis Lung carcinoma (ATCC CRL-1642) and the melanoma B16-F10 (ATCC CRL-6475) tumor cell lines. Cells were routinely checked for mycoplasma contamination and used between passages 7 to 15. Five x 10^5 tumors cells were injected s.c. into the left flank of WT mice. Pharmacokinetic analysis (Figure 1G), to characterize the clearance of HEI3090 showed that after a period of 18 h HEI3090 concentration is < 10 nM. Therefore, we have decided to inject HEI3090 daily. Mice were treated i.p. with vehicle (PBS, 10% DMSO) or with HEI3090 (1.5 mg/kg in PBS, 10% DMSO) which corresponds to the highest soluble dose. For therapeutic settings treatment started at day 3, when tumor reached approximately 10 to 15 mm^2, for a maximum of 20 days and mice received vehicle or HEI3090 (3 mg/kg in PBS, 10% DMSO) daily. Depleting and neutralizing antibodies from BioXCell were given i.p. in the right flank at days -1, 3, 7 and 10. We used anti-IL-1β (clone B122, 200 µg per injection), anti-IL-18 (clone YIGIF74-1G7, 200 µg per injection), anti-CD8 (clone 53-6.7 200 µg/injection), anti-CD4 (clone GK1.5, 200 µg per injection) and anti-NK1.1 (clone PK136, 300 µg per injection). αPD-1antibody (clone RPM1-4, BioXCell) was given i.p. at 200 µg per injection at days 4, 7, 10 and 13 (or as stated in the legend of the figure) post tumor cell inoculation. αPD-1and HEI3090 were injected separately, with at least 30 min delay between the two injections. 200 µL liposome clodronate (Liposoma) were injected i.p. 3 days before LLC tumor cell inocµation in WT mice and then every 3 days, at least 1 hour before HEI3090 treatment after the treatment started. CD8$^+$ T cells were sorted from peripheral lymph nodes of cured or naïve WT mice with Dynabeads® Untouched™ Mouse CD8 Cells (Invitrogen) according to the supplier's instructions. 5.10^5 CD8$^+$ T cells were adoptively transferred into 8 weeks-old naïve WT mice (i.v.) one day before tumor inoculation. 5.10^5 LLC cells were injected s.c. into the left flank of these mice and given no further treatment.

Adoptive transfer in *p2rx7* deficient mice

Spleens from WT C57BL/6J female mice were collected and digested in RPMI 1640 medium containing 5% FCS, 1 mg/ml collagenase IV (Sigma-Aldrich), and 50 U/ml DNase I (Roche) for 7 min at 37°C. Single-cell suspensions of spleens were prepared by passage through 100 µm cell strainers (BD Biosciences) and counted. For WT DCs isolation, spleens were digested with the spleen dissociation kit (Miltenyi Biotech) and isolated with the CD11c Microbeads UltraPure (Miltenyi biotech) according to the supplier's instructions. 5.10^6 splenocytes or $1.2.10^6$ DCs were injected i.v. in *p2rx7*$^{-/-}$ mice one day before subcutaneous injection of 5.10^5 LLC cells into the left flank. Mice were treated i.p. every day for 12 days with vehicle (PBS, 10% DMSO) or with HEI3090 (1.5 mg/kg in PBS, 10% DMSO). At day 12, tumors were collected, weighted and digested, when flow cytometry analyses were done.

Flow cytometry and antibodies

Tumors were mechanically dissociated and digested with 1 mg mL^{-1} collagenase A and 0.1 mg mL^{-1} DNase I for 20 min at 37°C. Then single cell suspensions of tumors were prepared by passage through 100 µM cell strainers (BD Biosciences). Surface staining was performed by incubating cells on ice, for 20 min, with saturating concentrations of labeled Abs in PBS, 5% FCS and 0.5% EDTA. After blocking Fc receptors using anti-CD16/32 (2.4G2) antibodies, cells were stained with the appropriate combination of antibodies (see Supplementary Table 1). The transcription factor staining Buffer Set (eBioscience) was used for the FoxP3 staining. For intracellular cytokines, staining was performed after stimulation of single-cell suspensions with

Phorbol 12-myristate 13-acetate (PMA at 50 ng mL^{-1}, Sigma), ionomycin (0.5 µg mL^{-1}, Sigma) and 1 µL mL^{-1} Golgi Plug™ (BD Biosciences) for 4 h at 37°C 5% CO2. Cells were incubated with Live/Dead Blue stain (Invitrogen), according to the manufacturer's protocol prior to Ab surface staining. Then, intracellular staining was performed using Cytofix/Cytoperm™ kit (BD biosciences) following the manufacturer's instructions. The production of IFN-γ and IL-10 was simultaneously analyzed in $CD45^+$, NK, $CD4^+$ T or $CD8^+$ T cells. Data files were acquired and analyzed on Aria III using Diva software (BD Biosciences) or on the CytoFlex LX (Beckman Coulter) and analyzed using FlowJo software (LLC).

Immunohistological analysis of tumors

Collected tumors or lungs were processed as previously described [9]. We used the following antibodies: anti-CD3 and anti-CD8 (Roche, 790-4341, 750-4460 respectively), anti-IL-18 (BioVision, dil 1/200), and αPD-L1 (Dako, clone 22C3, dil 1/50), anti-Ki67 (Abcam, clone sp6, dil 1/100). After staining, slides were captured and analyzed using NDP view2 software. For the analyses, 5 zones per tumor were randomly selected and cells were counted using Figdi software. Results are expressed as number of positive cells per total cell number.

Characterization of lesions in the LSL *KRas^{G12D}* mouse model

At the end of the treatment mice were sacrificed, exsanguinated and lungs processed for histologic and immunological analyses as described here [46]. After deparaffinization, HE stains were performed and slides were captured and analyzed using NDP view2 software. Tumor burden was calculated by determining total tumor area and dividing by total lung area. To count the cells and determine de percentage of Ki67 positive cells within lesions, 10 lesions per lung, from grade 2 to 5 according to the Sutherland scoring [47], were randomly selected, their perimeter was determined, and positive and negative nuclei were counted using Figdi software. Results are expressed as number of cells per mm^2 and the percentage of Ki67 positive cells.

***Ex vivo* macrophages stimulation**

Peritoneal lavage was done with RPMI 1640 medium on WT or *p2rx7*$^{-/-}$ mice. 4.10^5 macrophages were seeded in a 96 well plate overnight in RPMI 1640 containing 10% FBS, 2% sodium pyruvate, 1% penicillin/streptomycin and 50 µM β-mercaptoethanol. After 2 washes with the complete medium, cells were primed for 4 hours with 100 ng/ml LPS (Sigma-Aldrich) at 37 °C and then stimulated for 30 minutes at 37 °C with ATP (Sigma-Aldrich) with or without 50 µM of HEI3090 or with 10 µM nigericin. When indicated, NLRP3 inflammasome was inhibited with 1 µM of MCC950 (Invivogen) for 1 hour at 37 °C before cell stimulation.

Supernatants were collected and stored at -80°C before cytokine detection by ELISA using mouse IL-1 beta/IL-1F2 (R&D) and IL-18 (MBL) according to the supplier's instructions.

Cells were lysed with Laemmli buffer (10% glycerol, 3% SDS, 10 mM Na_2HPO_4) with protease inhibitor cocktail (Roche). Proteins were separated on a 12% SDS-PAGE gel and electro transferred onto PVDF membranes which were blocked for 30 minutes at RT with 3% bovine serum albumin (BSA). Membranes were incubated with primary antibodies diluted 1/1000 at 4°C overnight. The following antibodies were used: anti-NLRP3 (clone Cryo-2, Adipogen) anti-ASC (clone AL177, Adipogen), anti-caspase-1 (clone Casper-1, Adipogen) and anti-β-actin (Biorad). Secondary antibodies (Sigma-Aldrich) were incubated for 1 hour at RT. Immunoblot detection was achieved by exposure with a chemiluminescence imaging system (PXI Syngene, Ozyme) after membrane incubation with ECL (Immobilon Western, Millopore). The bands intensity values were normalized to that of β-actin using the GeneTools (Syngene) software.

Calcium uptake assay

20.10^3 HEK293T-mP2RX7$^{C57BL/6J}$ or HEK293T-pcDNA6 cells were seeded per well on a poly-L-Lysine (Sigma-Aldrich) 96 well-coated plate in complete medium. 24 hours later, cells were washed in sucrose buffer (300 mM sucrose, 5 mM KCl, 1mM $MgCl_2$, 1mM $CaCl_2$, 10 mM Glucose, 20 mM HEPES, pH 7-7.4) and incubated for 1 hour at 37 °C with 1 µM of Fluo-4 AM (Life Technologies). Cells were washed once with PBS+5% FBS then twice with the

sucrose buffer. Fluo-4 AM fluorescence was read on a Xenius, microplate reader (SAFAS) at 485/528 nm at 37 °C. After 3 minutes of baseline readings, 333 µM of ATP (Sigma-Aldrich) were added with or without various concentrations of HEI3090. For the assay on splenocytes, spleens were digested with the spleen dissociation kit (Miltenyi Biotech). 5.10^5 splenocytes were seeded per well on a 96-well plate in sucrose buffer and incubated for 30 minutes at RT with 1 µM of Fluo-4-AM.

TO-PRO-3 uptake assay

30.10^3 HEK293T-mP2RX7$^{C57BL/6J}$ or HEK293T-pcDNA6 cells were seeded per well on a poly-L-Lysine (Sigma-Aldrich) black clear bottom 96 well-coated plate (Perkin Elmer) in complete medium. 24 hours later, cells were washed twice in sucrose buffer (300 mM sucrose, 5 mM KCl, 1mM $MgCl_2$, 1mM $CaCl_2$, 10 mM Glucose, 20 mM HEPES, pH 7-7.4). 1 µM of TO-PRO-3 (Life Technologies) was added in the sucrose buffer. TO-PRO-3 fluorescence was read on a Xenius, microplate reader (SAFAS) at 550/660 nm at 37°C. After 10 minutes of baseline readings, 250 µM of ATP (Sigma-Aldrich) were added with or without various concentrations of HEI3090. Alternatively, percentage of TO-PRO-3$^+$ cells was analyzed on non-adherent cells by flow cytometry.

Cell viability

Colorimetric assay based on XTT (Roche) was used to quantify the viability of tumor cells treated with 1 mM of BzATP and 50 µM of HEI3090. LLC cells were treated for 16h and B16-F10 for 3h. Cellular viability was determined as described in the supplier's protocol.

***In vivo* assay for immunogenic cell death**

B16-F10 were exposed to 3mM ATP and 50 µM HEI3090 for 3 hours at 37 °C. Cells were then washed and resuspended in PBS and cell death was determined with trypan blue. Dying B16-F10 cells reached 97% in this assay. One.10^5 dying cells were injected *s.c.* into the right flank of WT mice (in 200 µL PBS). Control mice received 200 µL PBS into the right flank. Seven days later, mice were challenged with live $5x10^5$ B16-F10 cells into the left flank. Tumor growth was routinely monitored at both injection sites.

Synthesis of HEI3090

Starting materials are commercially available and were used without further purification (suppliers: Carlo Erba Reagents S.A.S., Thermo Fisher Scientific Inc., and Sigma-Aldrich Co.). Intermediates were synthesized according to the methods described in the literature [28]. Melting points were measured on the MPA 100 OptiMelt® apparatus and are uncorrected. Nuclear magnetic resonance (NMR) spectra were acquired at 400 MHz for ^{1}H NMR and at 100 MHz for ^{13}C NMR, on a Varian 400-MR spectrometer with tetramethylsilane (TMS) as internal standard, at 25 °C. Chemical shifts (δ) are expressed in ppm relative to TMS. Splitting patterns are designed: s, singlet; d, doublet; dd, doublet of doublet; t, triplet; m, multiplet; sym m, symmetric multiplet; br s, broaden singlet; br t, broaden triplet. Coupling constants (J) are reported in Hertz (Hz). Thin layer chromatography (TLC) was realized on Macherey Nagel silica gel plates with fluorescent indicator and were visualized under a UV-lamp at 254 nm and 365 nm. Column chromatography was performed with a CombiFlash Rf Companion (Teledyne-Isco System) using RediSep packed columns. IR spectra were recorded on a Varian 640-IR FT-IR Spectrometer. Elemental analyses (C, H, N) of new compounds were determined on a Thermo Electron apparatus by 'Pôle Chimie Moléculaire-Welience', Faculté de Sciences Mirande, Université de Bourgogne, Dijon, France. LC-MS was accomplished using an HPLC combined with a Surveyor MSQ (Thermo Electron) equipped with APCI source.

The synthesis of the title compound was accomplished starting from L-pyroglutamic acid also known as the "forgotten amino acid", bio-sourced affordable raw material (Fig. 1A). After simple esterification of the L-pyroglutamic acid, the resulting methyl pyroglutamate was reacted with 2,4-dichlorobenzylamine in presence of catalytic amount or zirconium (IV) chloride in solvent-less conditions to provide pyroglutamide (HEI2313) in 90% yield. To obtain *(S)-N^1-(6-chloropyridin-3-yl)-N^2-(2,4-dichlorobenzyl)-5-oxopyrrolidine-1,2-dicarboxamide* (HEI3090), a

mixture of pyroglutamide (HEI2313) (1.86 g, 6.48 mmol) and 2-chloro-5-isocyanatopyridine (1.00 g, 6.48 mmol) in toluene was refluxed for 24 hours under nitrogen atmosphere and magnetic stirring. After cooling to rt, the mixture has been concentrated *in vacuo* and the resulting crude has been purified by column chromatography (CH_2Cl_2 / MeOH: 1/0 to 9/1) to afford pure HEI3090 as a white powder in 54% yield (1.62 g, 3.51 mmol). mp 187-190 °C (MeOH); TLC R*f* (CH_2Cl_2/MeOH: 95/5) 0.8; ^{1}H NMR ($CDCl_3$, 400 MHz) δ ppm 2.21-2.37 (m, 2H, C*H*$_2$CH$_2$CH), 2.59-2.68 (m, 1H, CH$_2$C*H*$_2$CH), 2.99-3.10 (m, 1H, CH$_2$C*H*$_2$CH), 4.49 (dd, *J* = 15.2, 6.2 Hz, 1H NHC*H*$_2$), 4.55 (dd, *J* = 15.2, 6.2 Hz, 1H, NHC*H*$_2$), 4.77 (dd, *J* = 7.2, 2.8 Hz, 1H, CH$_2$CH$_2$CH), 6.65 (br t, *J* = 6.2 Hz, 1H, N*H*CH$_2$), 7.22 (dd, *J* = 8.1, 2.0 Hz, 1H, Ar*H*), 7.29 (d, *J* = 8.6 Hz, 1H, Ar*H*), 7.33 (d, *J* = 8.1 Hz, 1H, Ar*H*), 7.38 (d, *J* = 2.0 Hz, 1H, Ar*H*), 7.92 (dd, *J* = 8.6, 2.5 Hz, 1H, Ar*H*), 8.49 (d, *J* = 2.5 Hz, 1H, Ar*H*), 10.66 (br s, 1H, N*H*Ar); ^{13}C NMR ($CDCl_3$,100 MHz) δ ppm 21.4 (CH_2), 32.4 (CH_2), 41.4 (CH_2), 59.2 (CH), 124.3 (CH), 127.5 (CH), 129.5 (CH), 130.2 (CH), 130.9 (CH), 133.1 (C), 133.6 (2 C), 134.2 (C), 141.3 (CH), 146.2 (C), 150.3 (C), 170.0 (C), 177.7 (C); IR (neat): ν cm^{-1} 3271, 3095, 1720, 1655, 1594, 1542, 1464, 1217, 1104, 829.

Statistical analyses

All analyses were carried out using Prism software (GraphPad). Mouse experiments were performed on at least n = 5 individuals, as indicated in Fig legends. Mice were equally divided for treatments and controls. Data were represented as mean values and error bars represent SEM. Mann-Whitney t test and Mantel Cox test were used to evaluate the statistical significance between groups. The corresponding tests and P -values were mentioned in the legend of each Figure. For survival analysis, patients were separated based on optimal cut-off of the expression value of the marker determined using KMplot.

Data Availability

All relevant data are available from the authors

Acknowledgments

The authors wish to thank Prof L. Counillon for valuable discussions, Anne Laure Rossi for technical expertise and graphical art. The authors greatly acknowledge the IRCAN's Animal core facility and IRCAN's Flow Cytometry Facility that is supported by FEDER, Ministère de l'Enseignement Supérieur, Région Provence Alpes-Côte d'Azur, Conseil Départemental 06, ITMO Cancer Aviesan (plan cancer), Cancéropole PACA, CNRS and Inserm.

Disclosure of potential conflicts of interest

We have no conflict of interest.

Funding

The funding sources for this work were Institut National du Cancer (INCa), Canceropole PACA, Bristol-Myers Squibb Foundation for Research in Immuno-Oncology, the "Ligue Nationale Contre le Cancer", the French Government (National Research Agency, ANR through the "Investments for the Future": program reference #ANR-11-LABX-0028-01) and the Centre National de la Recherche Scientifique (CNRS),the Institut National de la Santé et Recherche Médicale (INSERM) and the University of Orleans, The Region Centre Val de Loire (2003-00085470), the Conseil Général du Loiret and European Regional Development Fund (FEDER No. 2016-00110366 and EX005756).

Figure legends

Figure 1: HEI3090 enhances ATP-induced receptor channel activity

A. Representation of HEI3090's synthesis steps.

B. Modulation of ATP-induced intracellular Ca^{2+} variation (F1/F0) in HEK mP2RX7 cells (C57Bl/6 origin). After 10 baseline cycles, ATP (333 µm) and HEI3090 (250 nM) were injected.

C. Average Fluo-4-AM fluorescence intensities in HEK mP2RX7 or control HEK pcDNA6 measured 315s after stimulation with ATP (330 µM) and HEI3090 at concentrations ranging from 25 nM to 2.5 µM, as indicating in the color code. Means ± SEM (n=3 independent experiments and 6 replicates).

D. Modulation of ATP-induced TO-PRO-3 uptake in HEK mP2RX7 cells (F1/F0) in cells treated with ATP and HEI3090 (25nM).

E. Average fluorescence intensities in HEK mP2RX7 or control HEK pcDNA6 measured 10 min after stimulation. Means ± SEM (n=3 independent experiments and 6 replicates).

F. Left: Average fluo-4-AM fluorescence intensities in WT or *p2rx7*$^{-/-}$ splenocytes stimulated with 50 µM ATP. Means ± SEM (n=2 independent experiments and 4 replicates). Right: Graph represents the percentage of TO-PRO-3 positive cells in splenocytes isolated from naïve WT or *p2rx7*$^{-/-}$ mice. Data are means ± SEM (n=3 independent experiments in duplicate).

G. Pharmacokinetic analysis of HEI3090 intraperitoneally injected in WT mice. Data are means ± SEM (n=3 independent experiments in duplicate). Bars are mean ± SEM. *p<0.05, **p<0.01 ***p<0.001, ****p<0.0001 (Mann-Whitney test). Source data are provided as a Source Data file.

Figure 2: HEI3090 inhibits tumor growth and combined with immunotherapy ameliorates mice survival

A. Prophylactic administration. Average tumor area and weight of LLC allograft after daily treatment with HEI3090. Curves are mean ± SEM.

B. Therapeutic administration. Average tumor area and survival curves of LLC allograft. HEI3090 started when tumors reached 10 to 15 mm^2 of size. Curves are mean ± SEM.

C. Combo treatment. Average tumor area of LLC allograft after HEI3090 and αPD-1 treatment. Spaghetti plots and survival curves of animals are shown.

D. Schematic illustration of treatment given to LSL *Kras*^{G12D} mice. Representative images showing lung tumor burden. (Bar=2mm upper panel and 500 µm lower panel) with tumor histopathology. Average tumor burden of LSL *Kras*G12D mice in response to treatments were studied as the number of ADC per mouse and the surface of ADC lesions per lung. Each point represents one mouse. *p<0.05, **p<0.01 ***p<0.001, ****p<0.0001 (Mann-Whitney or Mantel Cox (B and C) tests). Source data are provided as a Source Data file.

Figure 3: Immune cells mediate the antitumor activity induced by HEI3090

LLC cells were used in all panels except in E.

A. Average tumor area of LLC allograft in *p2rx7* deficient mice (*p2rx7*$^{-/-}$) after daily treatment with HEI3090 or after adoptive transfer of WT splenocytes and daily treatment with HEI3090

B. Average tumor area of LLC allograft in *p2rx7* deficient mice (*p2rx7*$^{-/-}$) after adoptive transfer of WT DCs and daily treatment with HEI3090.

C. Tumor weight of animals from the study shown in A and B.

D. Characterization of immune infiltrate at day 12. Percentage of $CD45^+$ analyzed by flow cytometry among living cells within TME.

E. Representative picture of $CD8^+$ cells recruitment in LSL *Kras*G12D mice. (340X magnification) and quantification.

F. Representative images of CD3 staining in LLC tumors and quantification.

G. Percentage of regulatory T cells determined by flow cytometry as $FOXP3^+$ $CD4^+$ among $CD3^+$ within LLC tumors.

H. Proportion of PMN-MDSC among $CD45^+$ within LLC tumors

I. Gating strategy (left panel) and ratio of NK, $CD4^+$ or $CD8^+$ T cells on PMN-MDSC within LLC tumors (right panel). data are mean ± SEM. *p<0.05, **p<0.01 ***p<0.001, ****p<0.0001

(Mann-Whitney or two-way Anova (C) tests). Each point represents one individual mouse. Source data are provided as a Source Data file.

Figure 4: HEI3090-induced IL-18 production is required to inhibit tumor growth

A. Average tumor area of LLC allograft in WT mice injected with IL-1β and IL-18 neutralizing antibodies and daily treatment with HEI3090.

B. Average tumor area and tumor weight of LLC allograft in *il-18* deficient mice (*il-18*$^{-/-}$) and daily treatment with HEI3090.

C. Representative images of IL-18 staining in LLC tumors.

D. Production of IL-18 and IL-1β in serum of treated mice determined by ELISA.

E. *Ex vivo* production of IL-18 in primary peritoneal macrophages.

F. Representative images of IL-18 staining in lung tumor lesions from LSL *Kras*^{G12D} mice (Bar = 30 µm) and production of IL-18 in serum of LSL *Kras*^{G12D} mice. Data are mean ± SEM. *p<0.05, **p<0.01 ***p<0.001, ****p<0.0001 (Mann-Whitney or Mantel Cox (C) tests or t-test (E). Each point represents one individual mouse. Source data are provided as a Source Data file.

Figure 5: HEI3090 triggers antitumor responses mediated by IL-18-induced NK and CD4$^+$ T cells

A. Average tumor weight of LLC allograft in WT mice injected with depleting antibody and daily treated with HEI3090.

B. Spaghetti plots of LLC allograft in WT mice injected with depleting antibody and daily treated with HEI3090.

C. Average of IFN-γ$^+$ cells among CD45$^+$ cells in LLC tumors.

D. Representative dot plots of IFN-γ and IL-10 staining on TILs (left panel) and ratios of IFN-γ on IL-10 in the same positive cells of each TILs (right panel).

E. *Ex vivo* degranulation assay of splenocytes from LLC tumor bearing mice. CD107a positive cells in NK, CD4$^+$ and CD8$^+$ T cells are shown.

F. Ratios of IFN-γ on IL-10 in the same positive cells of each TILs of IL-18 neutralized mice.

G. Flow cytometry analyses of MHC-I and PD-L1 expression on CD45$^-$ cells in LLC tumors

H. Representative images of PD-L1 staining in cancer lesion of LSL *KRas*^{G12D} mice. (Bar = 30 µm) and quantification. Bars are mean ± SEM. Each point represents one individual mouse. *p<0.05, **p<0.01 ***p<0.001, ****p<0.0001 (Mann-Whitney test). Source data are provided as a Source Data file.

Figure 6: HEI3090 combined with αPD-1 induces antitumor memory immune response

A. Schematic illustration of treatments with transfer of CD8 cells.

B. Average tumor area of LLC allograft in 90 days-old WT and 90 days-old cured mice in absence of treatment.

C. Survival curves of animals from the study shown in B

D. Average tumor area of LLC allograft in WT mice injected with CD8$^+$ T cells isolated from re challenged cured mice as shown in A

E. Long lasting antitumor immune response: schematic illustration of treatments

F. Mouse body weight follow up of 300 days-old cured mice injected with anti-isotype (black circle) or depleting αCD8 antibodies (blue circle).

G. Individual survival curves of 340 days-old WT and cured animals injected with anti-CD8 antibody and re challenge with LLC in absence of treatment.

H. Average tumor area from animals shown in G.

I. Survival curves from animals shown in G. Data are mean ± SEM. *p<0.05, **p<0.01 ***p<0.001, ****p<0.0001 Mann-Whitney, two-way Anova or Mantel Cox tests. Source data are provided as a Source Data file.

Figure 7: P2RX7 expression in LUAD is associated with "Hot" immunophenotype signature

A. Association of *P2RX7* mRNA expression with a cluster of inflammatory genes (heatmap).

B. GSEA plot associating *P2RX7* high mRNA levels from LUAD patients (TCGA) with three inflammatory signatures.

C. Correlation curves of *P2RX7* and *CD274* expression from LUAD patients (TCGA) of all stage (left panel), low stage (middle panel) and high stage (right panel). Mann-Whitney or Mantel Cox (C and E) tests were used to performed statistical analyses.

D. Kaplan Meyer plot (http://kmplot.com) showing survival curves of *P2RX7* high vs *P2RX7* low patients (left panel), *CD274* high vs *CD274* low (middle panel) and *P2RX7* high or low vs *CD274* high or low (right panel). For all panels, the optimal cut-off is determined on KMplot. The *P*-value (log-rank (Mantel Cox) test), the hazard ratio and number of patients are indicated. Source data are provided as a Source Data file.

References

1. Schrank, Z. *et al.* Current molecular-targeted therapies in NSCLC and their mechanism of resistance. *Cancers (Basel).* **10**, E224 (2018).
2. Benzaquen, J. *et al.* Alternative splicing of P2RX7 pre-messenger RNA in health and diseases: Myth or reality? *Biomed. J.* **42**, 141–154 (2019).
3. Pellegatti, P. *et al.* Increased level of extracellular ATP at tumor sites: In vivo imaging with plasma membrane luciferase. *PLoS One* **3**, 1–9 (2008).
4. Perregaux, D. G., McNiff, P., Laliberte, R., Conklyn, M. & Gabel, C. A. ATP Acts as an Agonist to Promote Stimulus-Induced Secretion of IL-1β and IL-18 in Human Blood. *J. Immunol.* **165**, 4615–4623 (2000).
5. Cesaro, A. *et al.* Amplification loop of the inflammatory process is induced by P2X 7R activation in intestinal epithelial cells in response to neutrophil transepithelial migration. *Am. J. Physiol. - Gastrointest. Liver Physiol.* **299**, G32-42 (2010).
6. Ghiringhelli, F. *et al.* Activation of the NLRP3 inflammasome in dendritic cells induces IL-1B-dependent adaptive immunity against tumors. *Nat. Med.* **15**, 1170–1178 (2009).
7. Rissiek, B., Haag, F., Boyer, O., Koch-Nolte, F. & Adriouch, S. ADP-ribosylation of P2X7: A matter of life and death for regulatory T cells and natural killer T cells. *Curr. Top. Microbiol. Immunol.* **384**, 107–126 (2014).
8. Hubert, S. *et al.* Extracellular NAD+ shapes the Foxp3+ regulatory T cell compartment through the ART2-P2X7 pathway. *J. Exp. Med.* **207**, 2561–2568 (2010).
9. Hofman, P. *et al.* Genetic and pharmacological inactivation of the purinergic P2RX7 receptor dampens inflammation but increases tumor incidence in a mouse model of colitis-associated cancer. *Cancer Res.* **75**, 835–845 (2015).
10. Adinolfi, E. *et al.* Accelerated tumor progression in mice lacking the ATP receptor P2X7. *Cancer Res.* **75**, 635–644 (2015).
11. Vesely, M. D., Kershaw, M. H., Schreiber, R. D. & Smyth, M. J. Natural Innate and Adaptive Immunity to Cancer. *Annu. Rev. Immunol.* **29**, 235–271 (2011).
12. Hughes, P. E., Caenepeel, S. & Wu, L. C. Targeted Therapy and Checkpoint Immunotherapy Combinations for the Treatment of Cancer. *Trends Immunol.* **37**, 462–476 (2016).
13. Postow, M. A. *et al.* Peripheral T cell receptor diversity is associated with clinical outcomes following ipilimumab treatment in metastatic melanoma. *J. Immunother. Cancer* **3**, 23 (2015).
14. Topalian, S. L. *et al.* Immunotherapy: The path to win the war on cancer? *Cell* **161**, 185–186 (2015).
15. Chen, D. S. & Mellman, I. Elements of cancer immunity and the cancer-immune set point. *Nature* **541**, 321–330 (2017).
16. Eggermont, A. M. M., Maio, M. & Robert, C. Immune checkpoint inhibitors in melanoma provide the cornerstones for curative therapies. *Semin. Oncol.* **42**, 429–435 (2015).

17. Di Virgilio, F., Sarti, A. C., Falzoni, S., De Marchi, E. & Adinolfi, E. Extracellular ATP and P2 purinergic signalling in the tumour microenvironment. *Nat. Rev. Cancer* **18**, 601–618 (2018).
18. DuPage, M., Dooley, A. L. & Jacks, T. Conditional mouse lung cancer models using adenoviral or lentiviral delivery of Cre recombinase. *Nat. Protoc.* **4**, 1064–1072 (2009).
19. Homerin, G. *et al.* Pyroglutamide-Based P2X7 Receptor Antagonists Targeting Inflammatory Bowel Disease. *J. Med. Chem.* **63**, 2074–2094 (2020).
20. Mittal, D., Gubin, M. M., Schreiber, R. D. & Smyth, M. J. New insights into cancer immunoediting and its three component phases-elimination, equilibrium and escape. *Curr. Opin. Immunol.* **27**, 16–25 (2014).
21. Fischer, W., Urban, N., Immig, K., Franke, H. & Schaefer, M. Natural compounds with P2X7 receptor-modulating properties. *Purinergic Signal.* **10**, 313–326 (2014).
22. Di Virgilio, F., Giuliani, A. L., Vultaggio-Poma, V., Falzoni, S. & Sarti, A. C. Non-nucleotide agonists triggering P2X7 receptor activation and pore formation. *Front. Pharmacol.* **9**, 39 (2018).
23. Bidula, S. M., Cromer, B. A., Walpole, S., Angulo, J. & Stokes, L. Mapping a novel positive allosteric modulator binding site in the central vestibule region of human P2X7. *Sci. Rep.* **9**, 1–11 (2019).
24. Jonathan Benzaquen, Serena Janho Dit Hreich, Simon Heeke, Thierry Juhel, Salomé Lalvee, Serge Bauwens, Simona Saccani, Philippe Lenormand, Véronique Hofman, Mathilde Butori, Sylvie Leroy, Jean-Philippe Berthet, Charles-Hugo Marquette, Paul Hofman, Valerie. P2RX7B is a new theranostic marker for lung adenocarcinoma patients. *Theranostics* **in press**, (2020).
25. Gilbert, S. *et al.* ATP in the tumour microenvironment drives expression of nfP2X 7 , a key mediator of cancer cell survival. *Oncogene* **38**, 194–208 (2019).
26. Di Virgilio, F. P2RX7: A receptor with a split personality in inflammation and cancer. *Mol. Cell. Oncol.* **3**, (2016).
27. Young, C. N. J. & Górecki, D. C. P2RX7 purinoceptor as a therapeutic target-The second coming? *Front. Chem.* **6**, 248 (2018).
28. Park, J. H. & Kim, Y. C. P2X7 receptor antagonists: a patent review (2010–2015). *Expert Opin. Ther. Pat.* **27**, 257–267 (2017).
29. Gilbert, S. M. *et al.* A phase I clinical trial demonstrates that nfP2X7-targeted antibodies provide a novel, safe and tolerable topical therapy for basal cell carcinoma. *Br. J. Dermatol.* **177**, 117–124 (2017).
30. Agteresch, H. J., Burgers, S. A., Van Der Gaast, A., Wilson, J. H. P. & Dagnelie, P. C. Randomized clinical trial of adenosine 5′-triphosphate on tumor growth and survival in advanced lung cancer patients. *Anticancer. Drugs* **14**, 639–644 (2003).
31. Beijer, S. *et al.* Effect of adenosine 5′-triphosphate infusions on the nutritional status and survival of preterminal cancer patients. *Anticancer. Drugs* **20**, 625–633 (2009).
32. Vijayan, D., Young, A., Teng, M. W. L. & Smyth, M. J. Targeting immunosuppressive adenosine in cancer. *Nat. Rev. Cancer* **17**, 709–724 (2017).
33. Perrot, I. *et al.* Blocking Antibodies Targeting the CD39/CD73 Immunosuppressive Pathway Unleash Immune Responses in Combination Cancer Therapies. *Cell Rep.* **27**, 2411-2425.e9 (2019).
34. Li, X. Y. *et al.* Targeting CD39 in cancer reveals an extracellular ATP-and inflammasome-driven tumor immunity. *Cancer Discov.* **9**, 1754–1773 (2019).
35. Mutini, C. *et al.* Mouse dendritic cells express the P2X7 purinergic receptor: characterization and possible participation in antigen presentation. *J.*

Immunol. **163**, 1958–65 (1999).

36. Ma, Y. *et al.* ATP-dependent recruitment, survival and differentiation of dendritic cell precursors in the tumor bed after anticancer chemotherapy. *Oncoimmunology* **2**, 5–7 (2013).

37. Bours, M. J. L., Swennen, E. L. R., Di Virgilio, F., Cronstein, B. N. & Dagnelie, P. C. Adenosine 5′-triphosphate and adenosine as endogenous signaling molecules in immunity and inflammation. *Pharmacol. Ther.* **112**, 358–404 (2006).

38. Kaplanov, I. *et al.* Blocking IL-1β reverses the immunosuppression in mouse breast cancer and synergizes with anti–PD-1 for tumor abrogation. *Proc. Natl. Acad. Sci. U. S. A.* **116**, 1361–1369 (2019).

39. Okamura, H. *et al.* A novel costimulatory factor for gamma interferon induction found in the livers of mice causes endotoxic shock. *Infect. Immun.* **63**, 3966–3972 (1995).

40. Ushio, S. *et al.* Cloning of the cDNA for human IFN-gamma-inducing factor, expression in Escherichia coli, and studies on the biologic activities of the protein. *J. Immunol.* **156**, 4274–9 (1996).

41. Fabbi, M., Carbotti, G. & Ferrini, S. Context-dependent role of IL-18 in cancer biology and counter-regulation by IL-18BP. *J. Leukoc. Biol.* **97**, 665–675 (2015).

42. Segovia, M. *et al.* Targeting TMEM176B Enhances Antitumor Immunity and Augments the Efficacy of Immune Checkpoint Blockers by Unleashing Inflammasome Activation. *Cancer Cell* **35**, 767-781.e6 (2019).

43. Zhou, T. *et al.* IL-18BP is a secreted immune checkpoint and barrier to IL-18 immunotherapy. *Nature* (2020). doi:10.1038/s41586-020-2422-6

44. Park, S. L., Gebhardt, T. & Mackay, L. K. Tissue-Resident Memory T Cells in Cancer Immunosurveillance. *Trends Immunol.* **40**, 735–747 (2019).

45. Sharma, P., Hu-Lieskovan, S., Wargo, J. A. & Ribas, A. Primary, Adaptive, and Acquired Resistance to Cancer Immunotherapy. *Cell* **168**, 707–723 (2017).

46. Regala, R. P. *et al.* Atypical protein kinase Cι is required for bronchioalveolar stem cell expansion and lung tumorigenesis. *Cancer Res.* **69**, 7603–7611 (2009).

47. Sutherland, K. D. *et al.* Multiple cells-of-origin of mutant K-Ras-induced mouse lung adenocarcinoma. *Proc. Natl. Acad. Sci. U. S. A.* **111**, 4952–4957 (2014).

Table 1: Antibodies used to phenotype immune cells

Antibody	Company	Clone	Species
CD16/CD32 Fc Block	BD Biosciences	2.4G2	Rat SD (outbred
CD3ε	BD Biosciences	145-2611	Armenian Hams
CD4	Biolegend	GK1.5	Rat
CD4	BD Biosciences	GK1.5	Rat LEW
CD4	BD Biosciences	RM4-5	Rat DA
CD8α	Biolegend	53-6.7	Rat
CD8α	BD Biosciences	53-6.7	Rat LOU
γδ TCR	BD Biosciences	GL3	Armenian Hams
CD25	BD Biosciences	PC61	Rat OFA
CD44	BD Biosciences	IM7	Rat
CD44	BD Biosciences	IM7	Rat
CCR7	BD Biosciences	4B12	Rat LOU
CD107a	BD Biosciences	1D4B	Rat SD (outbred
NK1.1	BD Biosciences	PK136	Mouse C3H x BA
B220	eBiosciences	RA3-6B2	Rat
CD19	BD Biosciences	ID3	Rat LEW
CD45.2	BD Biosciences	104	Mouse SJL
CD11b	eBiosciences	M1/70	Rat
CD11c	BD Biosciences	HL3	Armenian Hams
Ly6C	BD Biosciences	AL-21	Rat
Ly6G	BD Biosciences	1A8	Rat LEW
Ly6G	BD Biosciences	1A8	Rat LEW
CD80	Biolegend	16-10A1	Armenian Hams
CD86	BD Biosciences	GL1	Rat LOU
CD86	BD Biosciences	GL1	Rat LOU
I-A/I-E	Biolegend	M5/114.5.2	Rat
H-2K^{b}/H-2D^{b}	Biolegend	28-8-6	Mouse (C3H)
IL-10	BD Biosciences	JES5-16E3	Rat
Foxp3	eBiosciences	FJK16S	Rat
CD103	Biolegend	2E7	Armenian Hams
IFN-γ	BD Biosciences	XMG1.2	Rat
IL-17A	BD Biosciences	TC11-18H10	Armenian Hams
IL-4	BD Biosciences	11B11	Rat
IL-13	eBiosciences	eBio13A	Rat
GATA3	BD Biosciences	L50-823	Mouse BALB/c
CD279 (PD-1)	BD Biosciences	J43	Rat
CD274 (PD-L1)	Biolegend	10F.9G2	Rat
CD274 (PD-L1)	Biolegend	10F.9G2	Rat
CD273 (PD-L2)	Biolegend	TY25	Rat
CTLA-4	BD Biosciences	UC10-4F10-11	Armenian Hams
TIM-3	BD Biosciences	5D12/TIM-3	Mouse
P2RX7	Biolegend	1F11	Rat

Figure 1

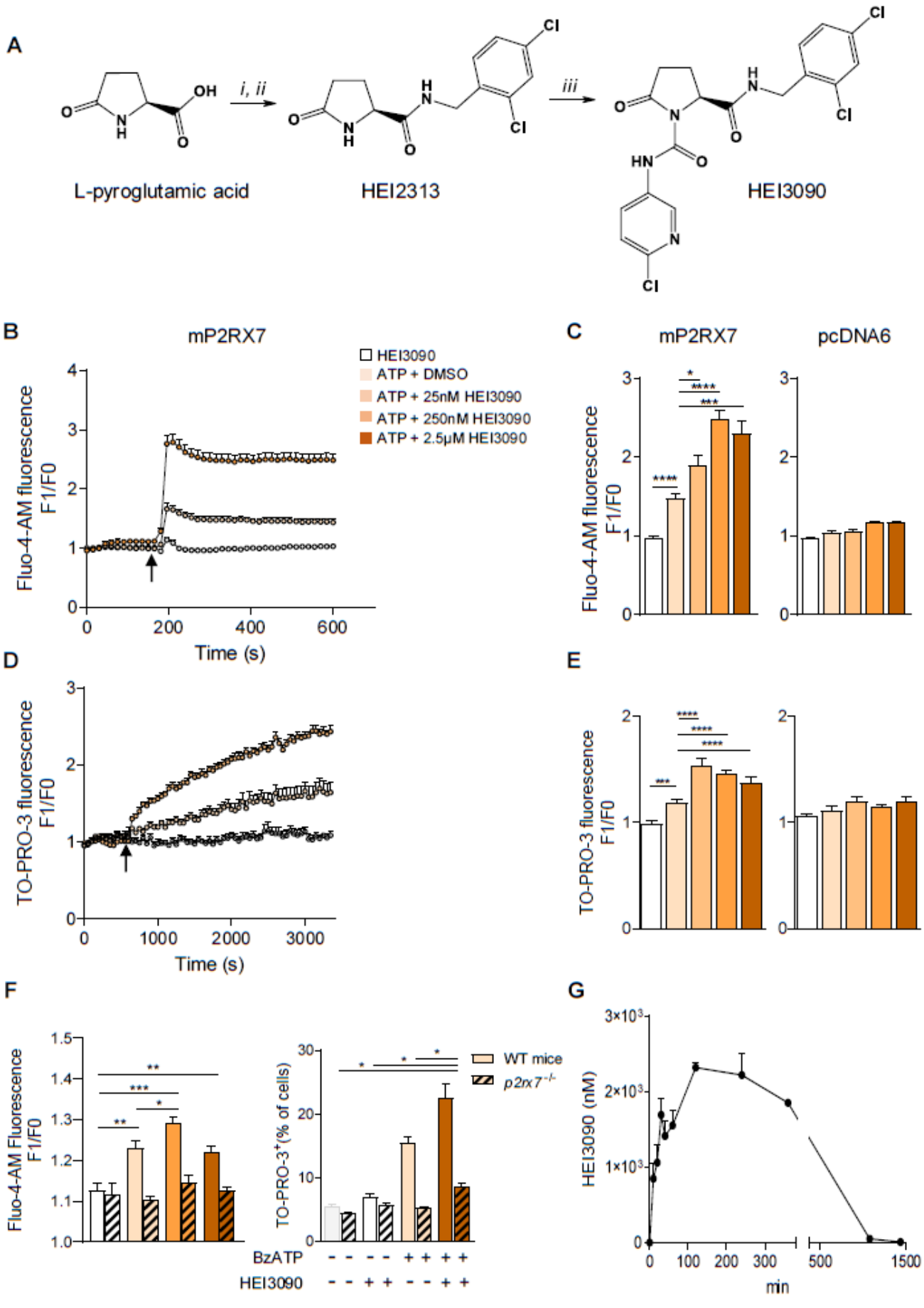
A
L-pyroglutamic acid
HEI2313
HEI3090
i, ii
iii
B
mP2RX7
HEI3090
ATP + DMSO
ATP + 25nM HEI3090
ATP + 250nM HEI3090
ATP + 2.5µM HEI3090
Fluo-4-AM fluorescence F1/F0
Time (s)
C
mP2RX7
pcDNA6
Fluo-4-AM fluorescence F1/F0
D
TO-PRO-3 fluorescence F1/F0
Time (s)
E
TO-PRO-3 fluorescence F1/F0
F
Fluo-4-AM Fluorescence F1/F0
TO-PRO-3+(% of cells)
WT mice
p2rx7-/-
BzATP
HEI3090
G
HEI3090 (nM)
min

Figure 2

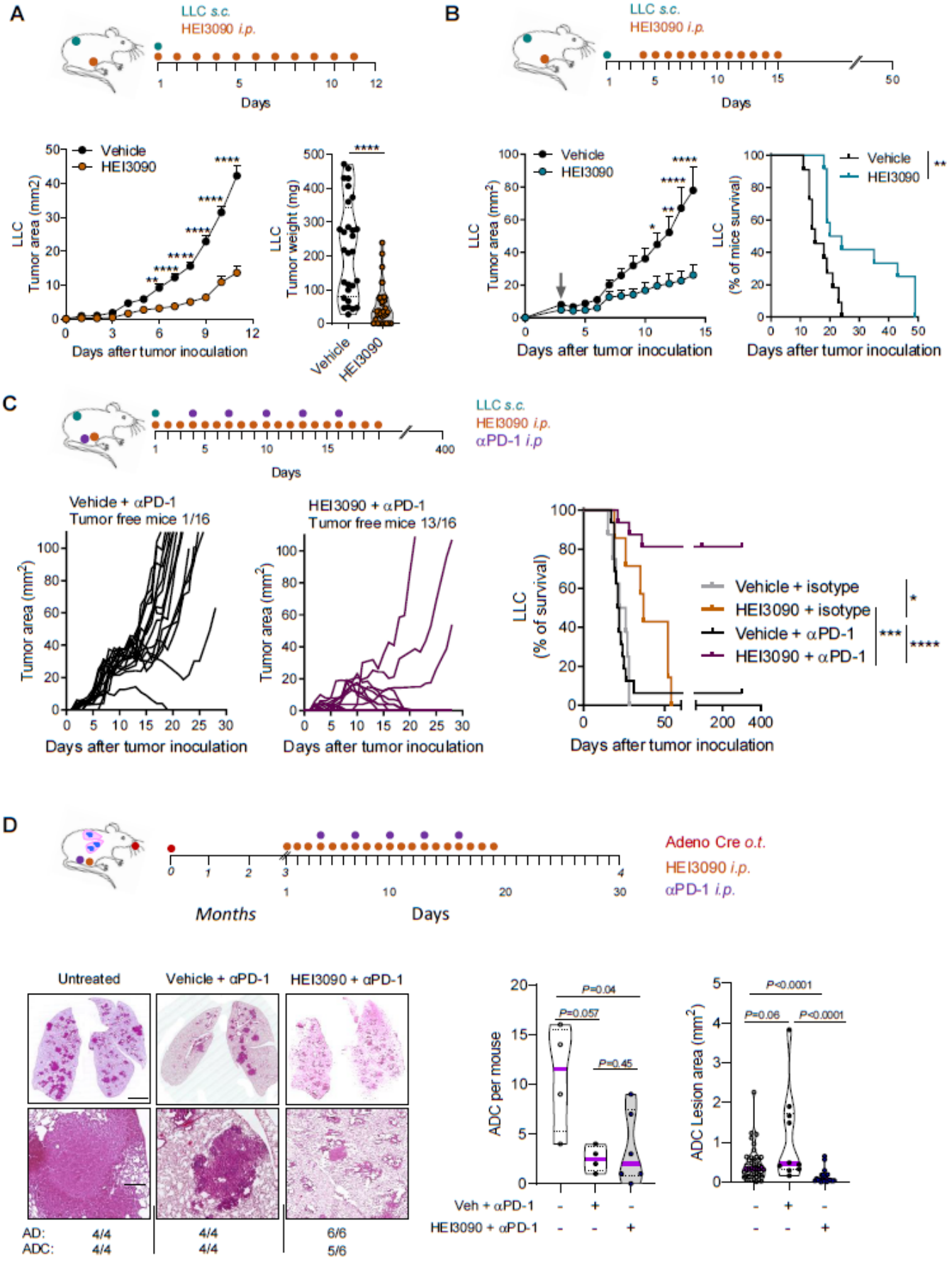
A
LLC s.c.
HEI3090 i.p.
Days
Vehicle
HEI3090
LLC Tumor area (mm2)
Days after tumor inoculation
LLC Tumor weight (mg)
B
LLC s.c.
HEI3090 i.p.
Days
Vehicle
HEI3090
LLC Tumor area (mm²)
Days after tumor inoculation
LLC (% of mice survival)
Days after tumor inoculation
C
LLC s.c.
HEI3090 i.p.
αPD-1 i.p
Days
Vehicle + αPD-1
Tumor free mice 1/16
HEI3090 + αPD-1
Tumor free mice 13/16
Tumor area (mm²)
Days after tumor inoculation
LLC (% of survival)
Vehicle + isotype
HEI3090 + isotype
Vehicle + αPD-1
HEI3090 + αPD-1
Days after tumor inoculation
D
Adeno Cre o.t.
HEI3090 i.p.
αPD-1 i.p.
Months
Days
Untreated
Vehicle + αPD-1
HEI3090 + αPD-1
AD:
ADC:
4/4
4/4
4/4
4/4
6/6
5/6
ADC per mouse
P=0.04
P=0.057
P=0.45
Veh + αPD-1
HEI3090 + αPD-1
ADC Lesion area (mm²)
P<0.0001
P=0.06
P<0.0001

Figure 3

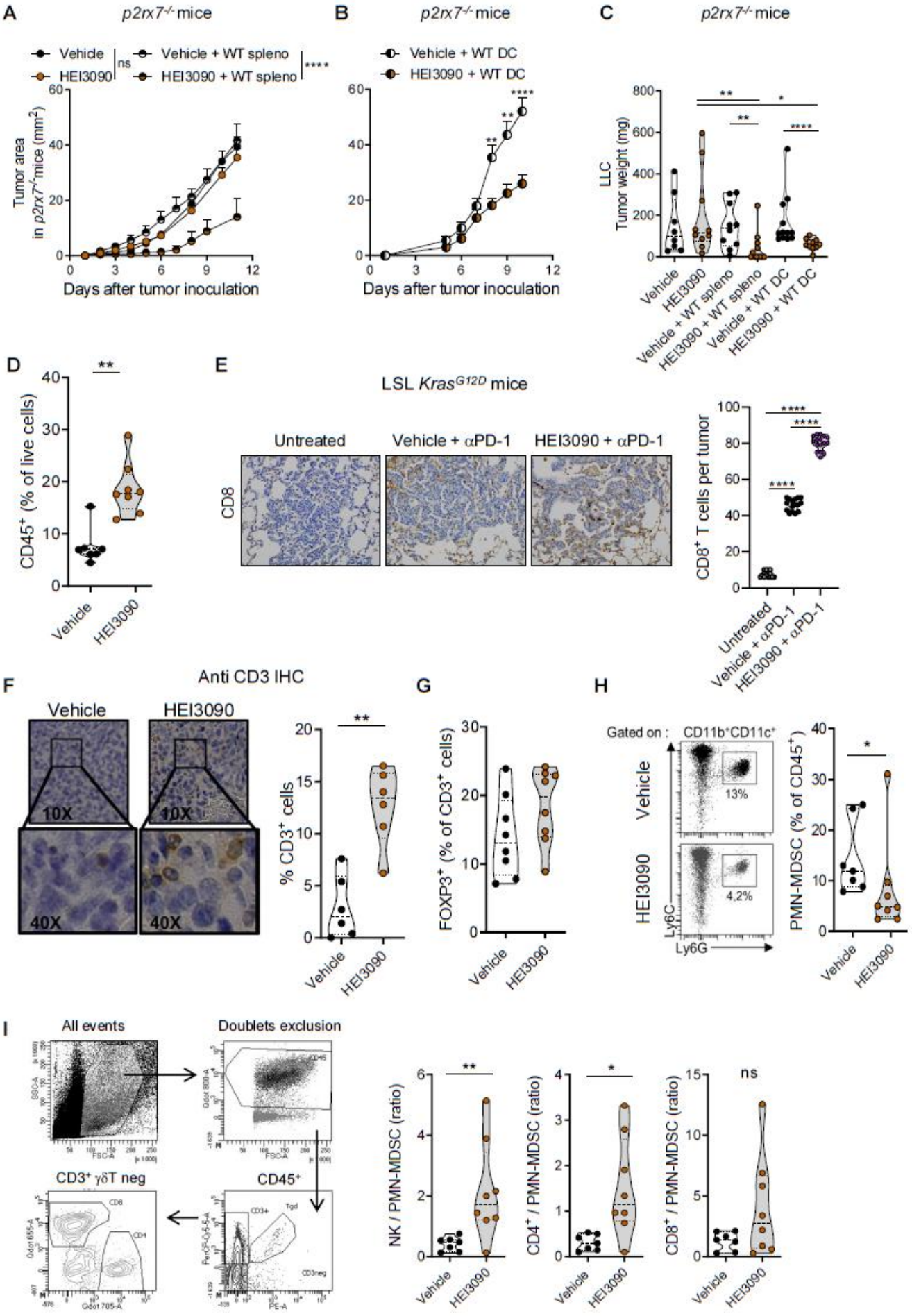
A
p2rx7-/- mice
Vehicle
HEI3090
ns
Vehicle + WT spleno
HEI3090 + WT spleno
****
Tumor area in p2rx7-/- mice (mm2)
Days after tumor inoculation
B
p2rx7-/- mice
Vehicle + WT DC
HEI3090 + WT DC
Days after tumor inoculation
C
p2rx7-/- mice
LLC Tumor weight (mg)
Vehicle
HEI3090
Vehicle + WT spleno
HEI3090 + WT spleno
Vehicle + WT DC
HEI3090 + WT DC
D
CD45+ (% of live cells)
Vehicle
HEI3090
E
LSL KrasG12D mice
Untreated
Vehicle + αPD-1
HEI3090 + αPD-1
CD8
CD8+ T cells per tumor
F
Anti CD3 IHC
Vehicle
HEI3090
10X
40X
% CD3+ cells
G
FOXP3+ (% of CD3+ cells)
H
Gated on : CD11b+CD11c+
13%
4,2%
Ly6C
Ly6G
PMN-MDSC (% of CD45+)
I
All events
Doublets exclusion
CD3+ γδT neg
CD45+
NK / PMN-MDSC (ratio)
CD4+ / PMN-MDSC (ratio)
CD8+ / PMN-MDSC (ratio)

Figure 4

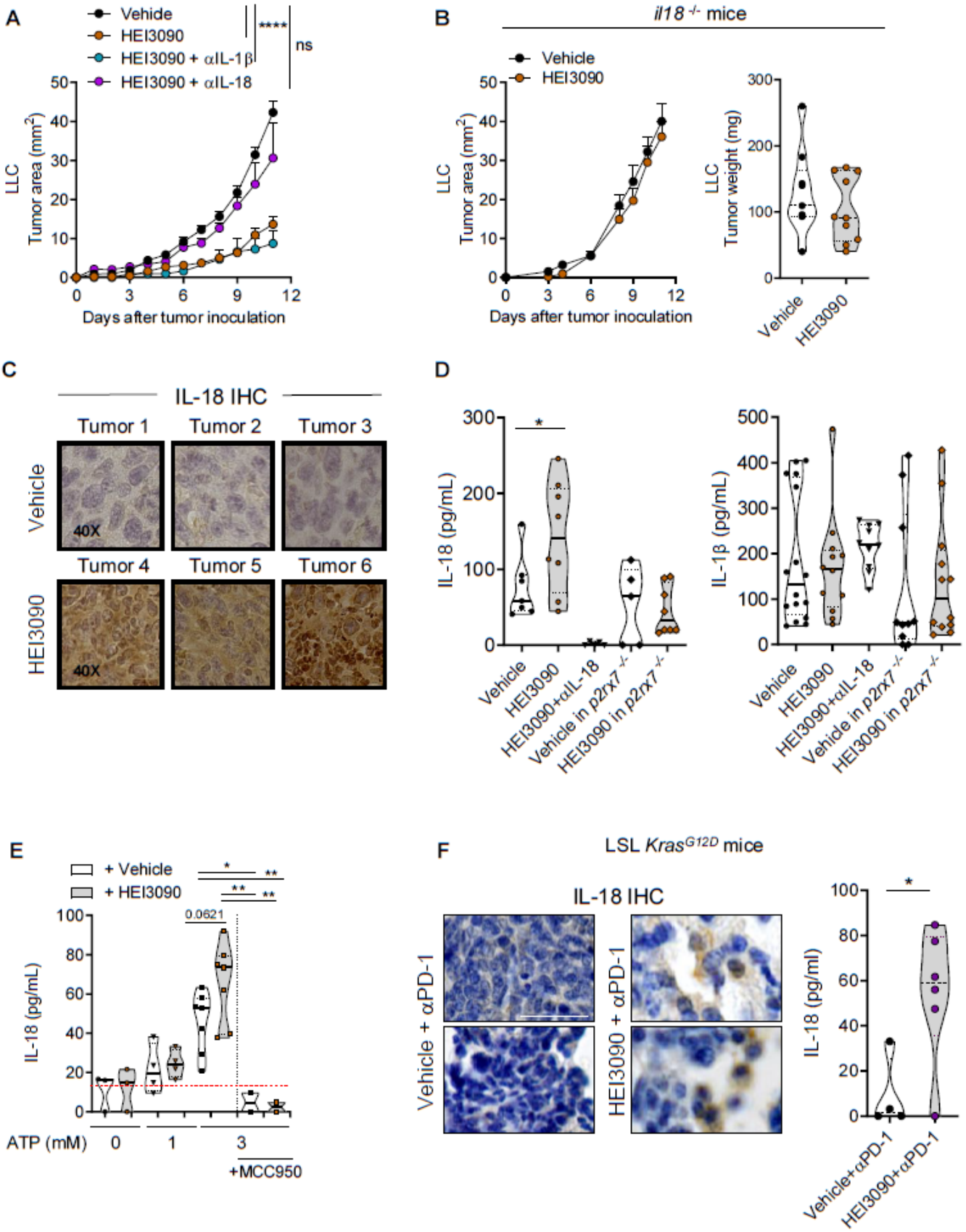
A
Vehicle
HEI3090
HEI3090 + αIL-1β
HEI3090 + αIL-18
****
ns
LLC Tumor area (mm²)
Days after tumor inoculation
B
il18 -/- mice
Vehicle
HEI3090
LLC Tumor area (mm²)
Days after tumor inoculation
LLC Tumor weight (mg)
Vehicle
HEI3090
C
IL-18 IHC
Tumor 1
Tumor 2
Tumor 3
Vehicle
40X
Tumor 4
Tumor 5
Tumor 6
HEI3090
40X
D
IL-18 (pg/mL)
IL-1β (pg/mL)
Vehicle
HEI3090
HEI3090+αIL-18
Vehicle in p2rx7 -/-
HEI3090 in p2rx7 -/-
E
+ Vehicle
+ HEI3090
0.0621
IL-18 (pg/mL)
ATP (mM)
0
1
3
+MCC950
F
LSL KrasG12D mice
IL-18 IHC
Vehicle + αPD-1
HEI3090 + αPD-1
IL-18 (pg/ml)
Vehicle+αPD-1
HEI3090+αPD-1

Figure 5

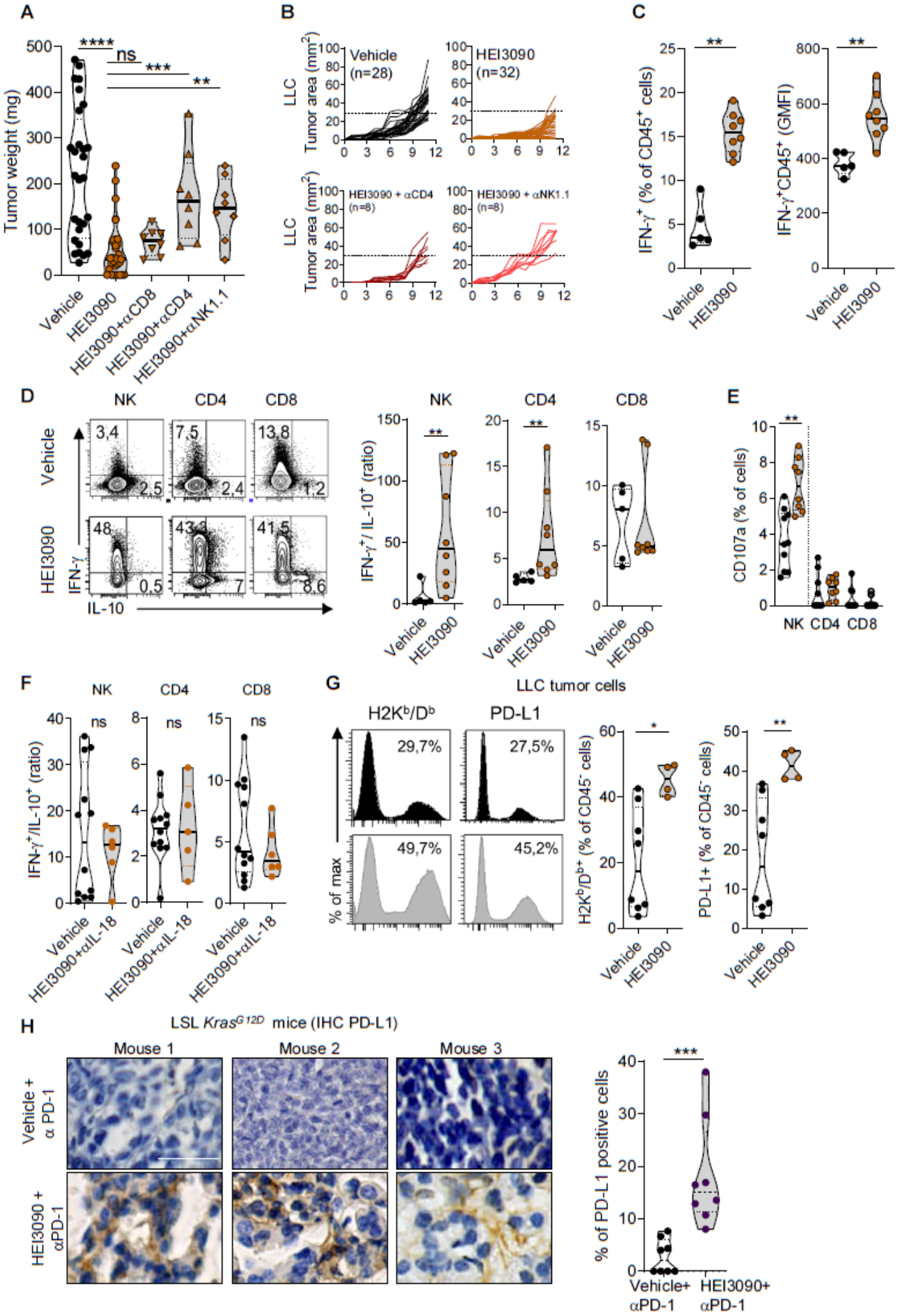
A
Tumor weight (mg)
****
ns
***
**
Vehicle
HEI3090
HEI3090+αCD8
HEI3090+αCD4
HEI3090+αNK1.1
B
LLC Tumor area (mm²)
Vehicle (n=28)
HEI3090 (n=32)
HEI3090 + αCD4 (n=8)
HEI3090 + αNK1.1 (n=8)
C
IFN-γ⁺ (% of CD45⁺ cells)
IFN-γ⁺CD45⁺ (GMFI)
D
NK
CD4
CD8
Vehicle
HEI3090
IFN-γ
IL-10
3,4
2.5
7.5
2.4
13.8
1.2
48
0.5
43.3
7
41.5
8.6
IFN-γ⁺/ IL-10⁺ (ratio)
E
CD107a (% of cells)
F
IFN-γ⁺/IL-10⁺ (ratio)
ns
Vehicle
HEI3090+αIL-18
G
LLC tumor cells
H2K^b/D^b
PD-L1
29,7%
27,5%
49,7%
45,2%
% of max
H2K^b/D^b⁺ (% of CD45⁻ cells)
PD-L1+ (% of CD45⁻ cells)
H
LSL Kras^G12D mice (IHC PD-L1)
Mouse 1
Mouse 2
Mouse 3
Vehicle + α PD-1
HEI3090 + αPD-1
% of PD-L1 positive cells
Vehicle+ αPD-1
HEI3090+ αPD-1

Figure 6

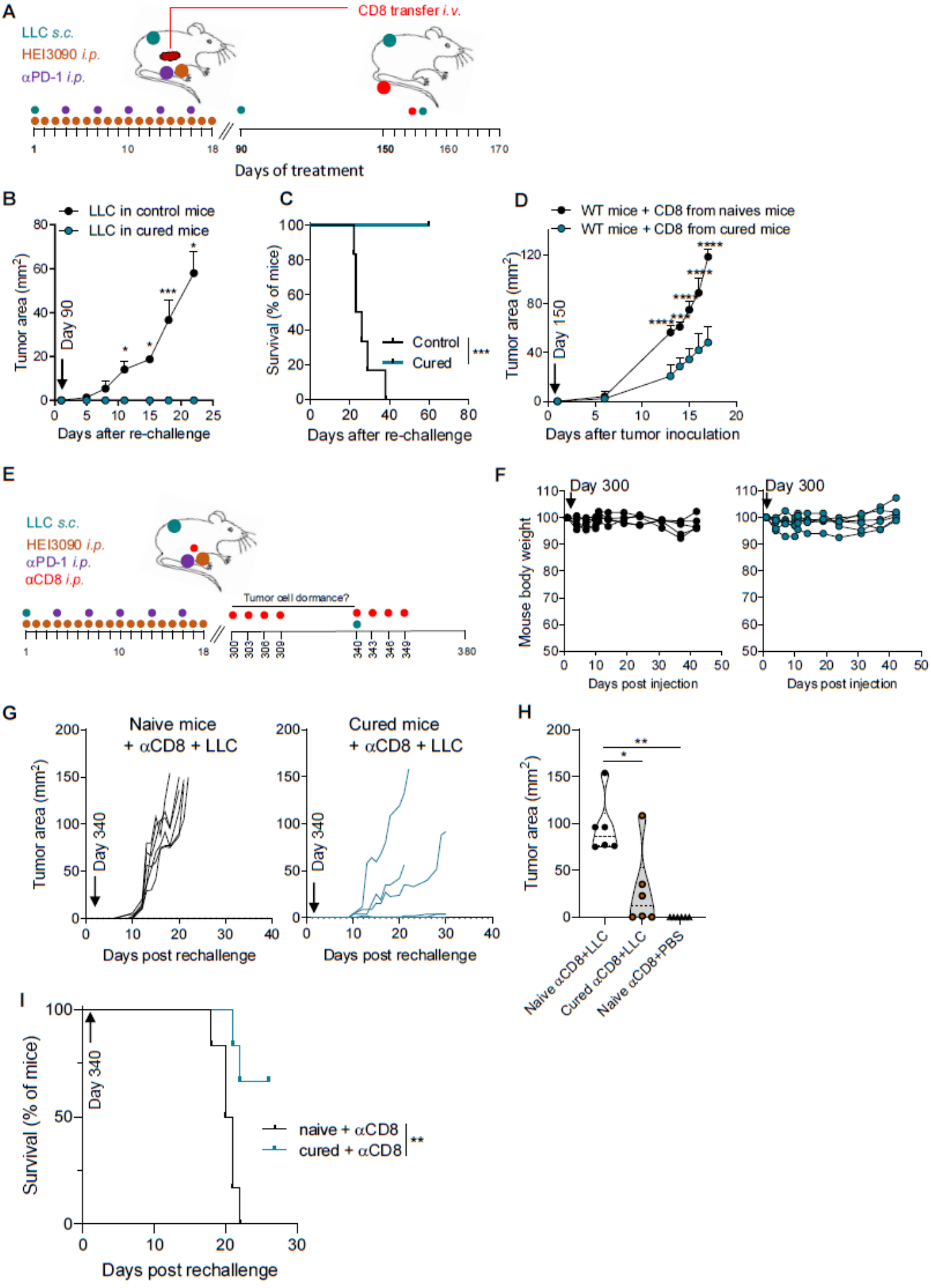
A
CD8 transfer i.v.
LLC s.c.
HEI3090 i.p.
αPD-1 i.p.
Days of treatment
B
LLC in control mice
LLC in cured mice
Tumor area (mm²)
Day 90
Days after re-challenge
C
Survival (% of mice)
Control
Cured
Days after re-challenge
D
WT mice + CD8 from naives mice
WT mice + CD8 from cured mice
Tumor area (mm²)
Day 150
Days after tumor inoculation
E
LLC s.c.
HEI3090 i.p.
αPD-1 i.p.
αCD8 i.p.
Tumor cell dormance?
F
Day 300
Mouse body weight
Days post injection
G
Naive mice
+ αCD8 + LLC
Cured mice
+ αCD8 + LLC
Tumor area (mm²)
Day 340
Days post rechallenge
H
Tumor area (mm²)
Naive αCD8+LLC
Cured αCD8+LLC
Naive αCD8+PBS
I
Survival (% of mice)
Day 340
naive + αCD8
cured + αCD8
Days post rechallenge

Figure 7

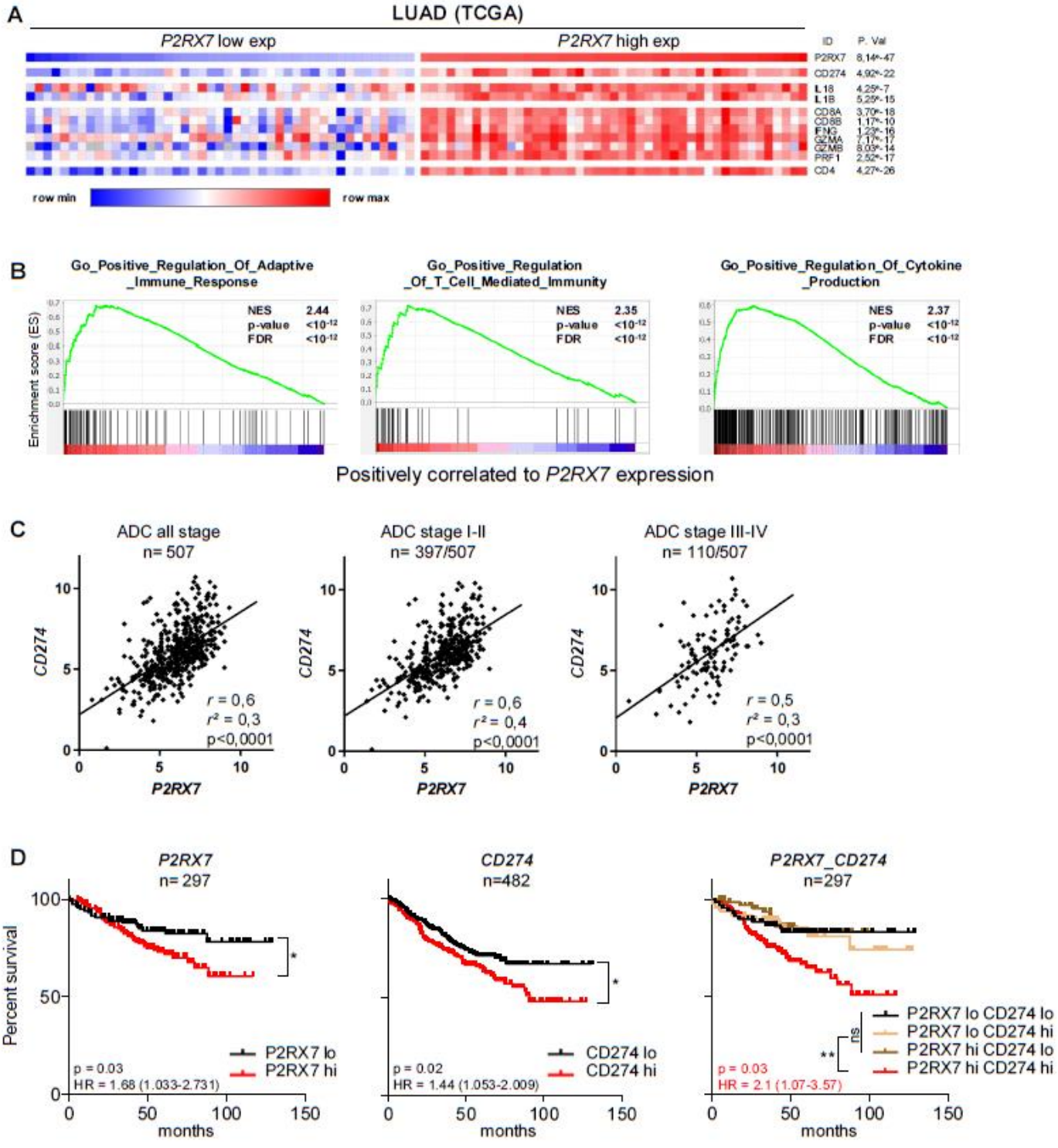
A
LUAD (TCGA)
P2RX7 low exp
P2RX7 high exp
ID
P. Val
P2RX7 8,14E-47
CD274 4,92E-22
IL18 4,25E-7
IL1B 5,25E-15
CD8A 3,70E-18
CD8B 1,17E-10
IFNG 1,23E-16
GZMA 7,17E-17
GZMB 8,03E-14
PRF1 2,52E-17
CD4 4,27E-26
row min
row max
B
Go_Positive_Regulation_Of_Adaptive_Immune_Response
NES 2.44
p-value <10-12
FDR <10-12
Go_Positive_Regulation_Of_T_Cell_Mediated_Immunity
NES 2.35
p-value <10-12
FDR <10-12
Go_Positive_Regulation_Of_Cytokine_Production
NES 2.37
p-value <10-12
FDR <10-12
Enrichment score (ES)
Positively correlated to P2RX7 expression
C
ADC all stage
n= 507
ADC stage I-II
n= 397/507
ADC stage III-IV
n= 110/507
CD274
P2RX7
r = 0,6
r² = 0,3
p<0,0001
r = 0,6
r² = 0,4
p<0,0001
r = 0,5
r² = 0,3
p<0,0001
D
P2RX7
n= 297
CD274
n=482
P2RX7_CD274
n=297
Percent survival
months
P2RX7 lo
P2RX7 hi
p = 0.03
HR = 1.68 (1.033-2.731)
CD274 lo
CD274 hi
p = 0.02
HR = 1.44 (1.053-2.009)
P2RX7 lo CD274 lo
P2RX7 lo CD274 hi
P2RX7 hi CD274 lo
P2RX7 hi CD274 hi
ns
p = 0.03
HR = 2.1 (1.07-3.57)

Extended data

Generation of *p2rx7*$^{fl/fl}$ mice

P2rx7-flox mice were engineered as follow: ES clones (C57/BL/6) containing a construct for the conditional elimination or re-expression of P2RX7 (purchased from The European Conditional Mouse Mutagenesis Program, EUCOMM) were injected into blastocytes of C57Bl6/N, chimeric mice were selected and crossed with deleter mice that are transgenic for the Flip-recombinase under the control of the ubiquitous actin promoter to produce *p2rx7* $^{loxP/loxP}$ mice.

Our *p2rx7* $^{loxP/loxP}$ mice, with loxP sequence floxing the second exon of *p2rx7*, were crossed with (C57BL/6NTacGt(ROSA)26Sor<tm1(ACTB-Cre,-EGFP) transgenic mice which express the Cre-recombinase under the control of the b-actin promoter to produce p2rx7$^{exon2-/-}$ mice or with LysM-Cre mice (B6.129P2-Lys2tm1(cre)Ifo from the Jackson Laboratories (obtained from Dr B. Chazaud, France) to generate myeloid cell conditional p2rx7 knockout and WT control (*p2rx7*$^{loxp/loxp}$) mice.

HEI3090 enhances the efficacy of anti-PD-1 antibody to inhibit melanoma growth in immunocompetent mice

To go further, we tested the efficacy of HEI3090 to inhibit the low immunogenic B16-F10 melanoma tumor growth. In the first setting of experiments, HEI3090 (1.5 mg/kg) or vehicle were administered daily for 11 days starting the day of tumor cell inoculations (Supplementary Fig. 3A). Mice treated with HEI3090 displayed significantly reduced tumor growth (left panel) and tumor weight (right panel). Flow cytometry analyses indicated that, as with LLC tumor cells, the success of HEI3090 treatment was associated with a better infiltration of immune cells within the tumor microenvironment (Supplementary Fig. 5A to D). The importance of mouse host cells to mediate HEI3090's antitumor effect was confirmed in experiment where *p2rx7*$^{-/-}$ mice were inoculated with B16-F10 cells. As described in the lung tumor model, HEI3090 was unable to inhibit melanoma growth when host cells were devoid of P2RX7 expression (Supplementary Fig. 4A). In the second setting of experiments, treatment started 3 days after tumor cell inoculation (at 2-8 mm^2 of tumor size). HEI3090 (3 mg/kg) was also able to inhibit tumor growth (Supplementary Fig. 3B), despite a lower efficacy than the one observed with LLC tumor cells (Fig. 2B). Of interest, HEI3090 treatment increases the median survival of 3 days (19 d. with HEI3090 vs 16 d. with vehicle). We also combined HEI3090 treatment with the anti-PD-1 immune checkpoint inhibitor and observed that HEI3090 enhanced the effect of the anti-PD-1 treatment. In particular, 2 out of 8 mice that were treated with HEI3090 combined to anti-PD-1 doubled their lifetime (Supplementary Fig. 3C).

HEI3090 targets phagocytic cells, mainly dendritic cells, for its anti-tumor activity

We have shown that HEI3090 requires immune cells to inhibit tumor growth (Fig 3A). It was of interest to see if HEI3090 targeted phagocytic cells to inhibit tumor growth, since they express high levels of P2RX7 and are able to kill tumor cells either directly or by inducing an immune response. To do so, we used several approaches. First, we depleted phagocytic cells by several administrations of clodronate liposome that has been described to deplete mainly macrophages and DCs. HEI3090's activity was lost in clodronate-liposome treated mice (Supplementary Fig4B) meaning that phagocytic cells are targeted by HEI3090. In order to specifically identify HEI3090-targeted cell, we conducted two complementary experiments using myeloid-specific P2RX7 deficiency (*p2rx7*$^{fl/fl}$-*LysM*) mice (Supplementary Fig4C) where P2RX7 was essentially lost in macrophages, and adoptive transfer of WT DCs into *p2rx7*$^{-/-}$ mice (Fig. 3B). HEI3090's anti-tumor activity was restored after adoptive transfer of WT DCs and was still efficient in *p2rx7*$^{fl/fl}$-*LysM* mice. The three experiments combined show that DCs are the major cell type targeted by HEI3090 to inhibit tumor growth. However, macrophages could still be involved in HEI3090-antitumor effect as a minor or secondary population but are not absolutely required like DCs.

We have also shown that IL-18 was necessary for HEI3090 anti-tumor effect (Fig 4). In order to see whether DCs produced IL-18, we quantified IL-18 in mice sera at the end of the WT DCs adoptive transfer experiment (D12). We can indeed see a slight increase in IL-18 release in sera of HEI3090-treated mice (Supplementary Fig9B). It is not that surprising not to see a major difference since mice received once WT DCs at the beginning of the experiment (D-1) and the IL-18 produced will be degraded since then. However, we can see that CD45$^+$ cells, CD8 and NK cells in the TME show an increase in the IFN-γ/IL-10 ratio in the HEI3090-treated mice (Supplementary Fig. 9B), showing that immune cells are differentiated into anti-tumor effector cells and suggesting that IL-18 produced by WT DCs was efficient during the experiment.

Collectively, these results suggest that the copresence of DCs, live tumor cells, ATP and HEI3090 represent the perfect microenvironment where DCs are primed by tumor antigens and activated by the ATP/P2RX7 axis to release IL-18 and inhibit tumor growth.

HEI3090 does not favor immunogenic cell death

P2RX7 expressed by DC has been shown to link innate and adaptive immune responses against dying tumor cells upon chemotherapy–induced ICD and facilitate tumor antigens presentation to T cells by the

DC (6). In this study we choose two transplantable tumor models with different levels of P2RX7 expression. B16-F10 cells expressed higher level of P2RX7 than LLC cells (Supplementary Fig. 1B). To evaluate the capacity of HEI3090 treatment to induce ICD of tumor cells and concomitant stimulation of DC maturation, we first characterized whether HEI3090 induced tumor cell death. We observed that *in vitro* treatment of tumor cell lines (LLC and B16-F10) with BzATP (a stable agonist of P2RX7) and HEI3090 induced cell death (Supplementary Fig. 6A and B). We also noticed that HEI3090 treatment slightly increased P2RX7 expression in DC $CD4^+$ cells (Supplementary Fig. 4A). Second, we tested the HEI3090-induced ICD and DC stimulation hypothesis by inoculating WT mice with dying tumor cells and challenged them with live tumor cells, 7 days later. We used B16-F10 cells since they were more efficiently killed *in vitro* when stimulated by ATP and HEI3090 than LLC cells. Tumor growth was similar in mice vaccinated with *in vitro* treated tumors cells and in control mice (Supplementary Fig. 6C), indicating that the main antitumor effect of HEI3090 is not solely dependent on direct tumor ICD and the concomitant stimulation of DC maturation.

Supplementary Figure legends

Figure 1: Active P2RX7 is expressed on LLC and B16-F10 tumor cells

A. P2RX7 expression and activity in Lewis Lung carcinoma (LLC) cell line. P2RX7 expression was assayed by flow cytometry using the anti P2RX7 (clone 1F11, left panel) or by western blotting using an anti-extracellular loop of P2RX7 antibody (APR-008, Alomone Labs) that recognizes a band of 70kDa, the expected size for P2RX7 (middle panel). To assay P2RX7's activity we measured the ATP-induced increase of intracellular Ca^{2+} concentration (Fluo-4-AM uptake) in the presence of the P2RX7's inhibitor (GSK1370319A), using a plate reader (right panel). B. P2RX7 expression and activity in melanoma (B16-F10) cell line. These results demonstrated that both cell lines expressed an active P2RX7, with B16-F10 cells expressing higher P2RX7 levels than LLC cells.

Figure 2: Picture of HEI3090 effect on LLC tumor size

Figure 3: HEI3090 inhibits the growth of melanoma B16-F10 tumor cells and increased mice survival when combined with anti-PD-1 antibody

A. $5x10^5$ B16-F10 were injected s.c. into the flank of C57BL6/J mice. Mice were injected i.p every day with vehicle or HEI3090 (1.5 mg/kg) from day 1 to day 12. Curves showed mean tumor area in mm^2 (left panel) and graph showed mean tumor weight the day of sacrifice (right panel). B. Effect of HEI3090 in therapeutic administration. Mice were treated

i.p. with vehicle or HEI3090 (3 mg/kg) from days 5 (when tumors reached a volume of approximatively 5-10 mm^2) to 15. Curves showed mean tumor area (left panel) and survival of B16-F10 tumor bearing mice (right panel). **C.** Effect of HEI3090 and αPD-1 checkpoint inhibitor on survival of B16-F10 tumor bearing mice. $5x10^5$ B16-F10 were injected s.c. into the flank of WT mice. Mice were treated i.p. with vehicle or with HEI3090 (3 mg/kg) from days 1 to day 18. Each mouse received 200 µg of αPD-1 i.p. at day 4, 7, 10, 12 and 16. Mice were sacrificed when tumor reached 100 mm^2. Bars are mean ± SEM. *p<0.05, **p<0.01 ***p<0.001, (Mann-Whitney or Mantel Cox (C) tests) Each point represents one mouse. **D.** Efficacy of the combo treatment in the *in situ* (LSL $KRas^{G12D}$) genetic lung tumor mouse model. Ten lung lesions per mouse (5 large, 5 small) were selected. Average cell number/mm^2 and $Ki67^+$ cells are shown. Bars are mean ± SEM. *p<0.05, **p<0.01 ***p<0.001, ****p<0.0001 (Mann-Whitney or Mantel Cox (C and E) tests). Each point represents one individual mouse.

Figure 4: HEI3090 targets P2RX7-expressing dendritic cells.

A. P2RX7 expression by DC $CD4^+$ cells was increased in response to HEI3090. **B.** Three days prior to tumor cell inoculation, liposome clodronate (200 µl) was injected ip to mice. Then mice were injected every 3 days with liposome clodronate 1h before HEI3090 treatment. 5.10^5 LLC cells were inoculated s.c. and mice were treated daily with 1.5 mg/kg of HEI3090 or vehicle. Tumor area was measured with a caliper. At the end of the experiment, tumors were weighted. **C.** Cells from the myeloid lineage did not support HEI3090-induced antitumor response. $5x10^5$ LLC cells were injected s.c. to $p2rx7^{fl/fl}$ -LysM mice and mice were daily treated with HEI3090 or vehicle, as detailed in the method section. Curves showed mean tumor area in mm^2 (left panel) and graph showed mean tumor weight the day of sacrifice (right panel).

Figure 5: Immune cells mediate the antitumor activity induced by HEI3090 in the B16-F10 tumor mouse model

A. Effect of HEI3090 on B16-F10 tumor growth in $p2rx7^{-/-}$mice. $5x10^5$ cells were injected s.c. into the flank of $p2rx7^{-/-}$ mice. Mice were treated i.p. with vehicle or with HEI3090 as indicated in A. Curves represent daily follow up of tumor area (left panel) and graph corresponds to the weight of tumors the day of sacrifice (right panel). **B.** Effect of HEI3090 on the recruitment of immune cells within the TME. $5x10^5$ B16-F10 cells were injected s.c. into the flank of WT mice. Mice were injected i.p every day with vehicle or HEI3090 (1.5 mg/kg). At day 12, tumors were collected for flow cytometry analyses. **C.** Proportion of M-MDSC within the TME among $CD45^+$ within LLC tumors from mice treated with vehicle or HEI3090. In this tumor model PMN-MDSC

were not affected by HEI3090 treatment (not shown). **D.** Ratio of NK, $CD4^+$ or $CD8^+$ T cells on M-MDSC within the TME. *p<0.05, **p<0.01 ***p<0.001, ****p<0.0001 (Mann-Whitney or two-way Anova (C) tests). Each point represents one individual mouse.

Figure 6: HEI3090 does not promote immunogenic cell death

HEI3090-induced LLC (**A**) and B16-F10 (**B**) tumor cell toxicity as described above. **C.** *In vivo* assay for the evaluation of HEI3090 as an inducer of immunogenic cell death. B16-F10 were exposed to 3mM ATP and 50µM HEI3090. WT mice were inoculated s.c. with 1.10^5 dying B16-F10 cells in the right flank (n=6) or PBS as control (n=4). 7 days later, 5.10^5 live B16-F10 cells were injected s.c. in the contralateral flank. The details of the ICD experiment are provided in the methods section. Curves shown mean of tumor growth in the contralateral site. Bars are mean ± SEM. *p<0.05, **p<0.01 ***p<0.001, (Mann-Whitney test).

Figure 7: HEI3090 increased eATP-induced caspase-1 cleavage in macrophages

4.10^5 peritoneal macrophages from WT mice were primed for 4h at 37°C with 100 ng/ml LPS and then stimulated for 30 minutes with 10 µM nigericin or 3 mM ATP with 50 µM HEI3090 or DMSO. Whole cell protein extracts were analyzed by western blotting by using antibodies recognizing NLRP3, ASC, pro-caspase-1 and active form caspase-1, and β-actin as a loading control. Relative band intensities of each protein were assessed to that of β-actin.

Figure 8: HEI3090-induced IL18 production required P2RX7 expression

A. IL-18 staining of LLC tumors collected from WT, *p2rx7*$^{-/-}$ or *il18*$^{-/-}$ mice, demonstrated the specificity of IL-18 antibody **B.** Production of IL-18 (ELISA) by splenocytes isolated from *p2rx7*$^{-/-}$ mice, demonstrated that without P2RX7 expression, HEI3090 was unable to increase IL-18 levels. **C.** IL-18 staining from lung of LSL *KRas*^{G12D}, illustrating that IL-18 expression was increased in lung macrophages of HEI3090 + αPD-1 treated mice. **D.** Production of IL-1β (ELISA) by peritoneal macrophages isolated from WT mice, demonstrated that HEI3090 was unable to increase IL-1β levels. The specific inhibitor of NLRP3 (MCC950 compound) efficiently inhibits IL-1β production. **E.** Quantification of IL-1β levels from serum of indicated mice confirming that HEI3090 did not modulate the production of IL-1β in *p2rx7*$^{-/-}$ complemented with WT DC. **F.** Quantification of IL-1β levels from serum of LSL *KRas*^{G12D} mice treated with HEI3090 and anti PD-1 antibody. Each point represents one mouse. Bars are mean ± SEM. *p<0.05, **p<0.01 (Mann-Whitney or two-way anova (B, C and D) tests.

Figure 9: Indirect effect of HEI3090 on IFN-γ production by antitumor immune cells

A. *Ex vivo* IFN-γ production. Splenocytes from WT mice were treated as indicated and IFN-γ production was assayed by flow cytometry in NK, $CD4^+$ and $CD8^+$ T cells. **B.** Purified WT DC were inoculated to *p2rx7*$^{-/-}$ mice i.v. at D-1. At D0, $5x10^5$ LLC cells were injected s.c.. Mice were treated i.p. with vehicle or with HEI3090 daily for 11 days. At D12, mice were sacrificed, sera and tumors were collected for ELISA and flow cytometry analyses respectively. The ratio of IFN-γ on IL-10 in indicated cells (left panel) and the concentration of IL-18 in the sera (right panel) are shown. **C.** MHC-I and PD-L1 expression induced by HEI3090 on LLC *in vitro*. LLC were stimulated as indicated for 24h and expression of MHC-I ($H2K^d/D^b$) and PD-L1 were assayed by flow cytometry analyses. This data revealed that P2RX7 activation indirectly led to increased tumor immunogenicity.

Supplementary Figure 1

Lung tumor cells (LLC)

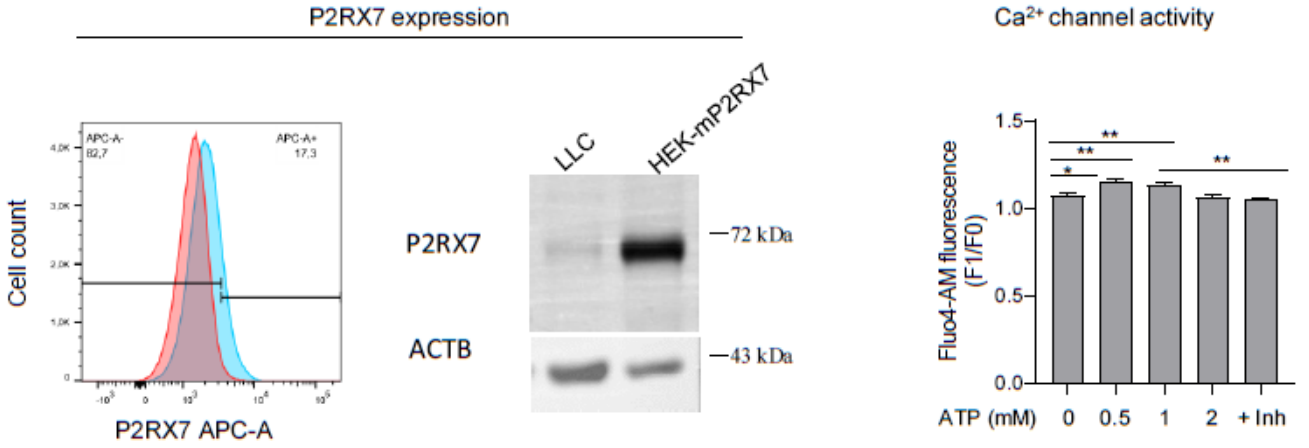

Melanoma tumor cells (B16-F10)

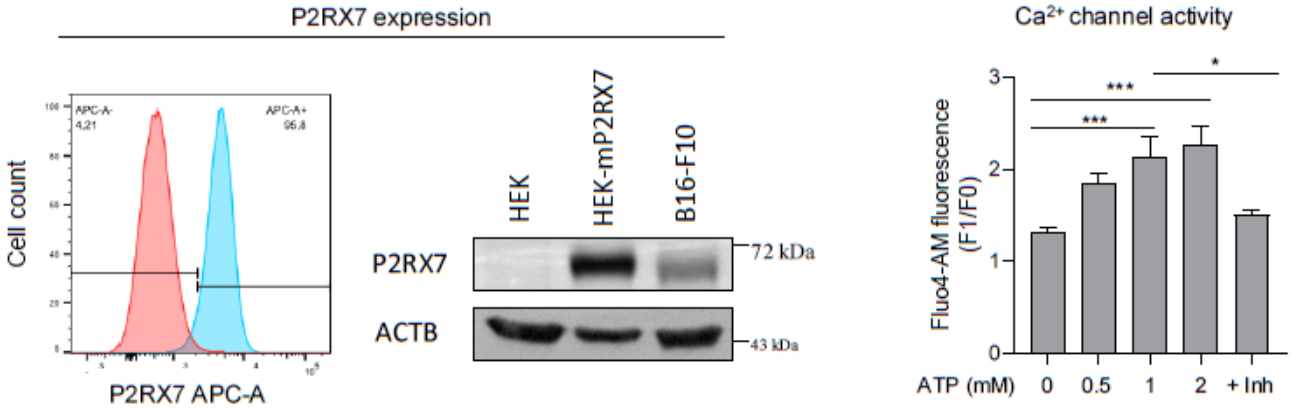

Supplementary Figure 2

Supplementary Figure 3

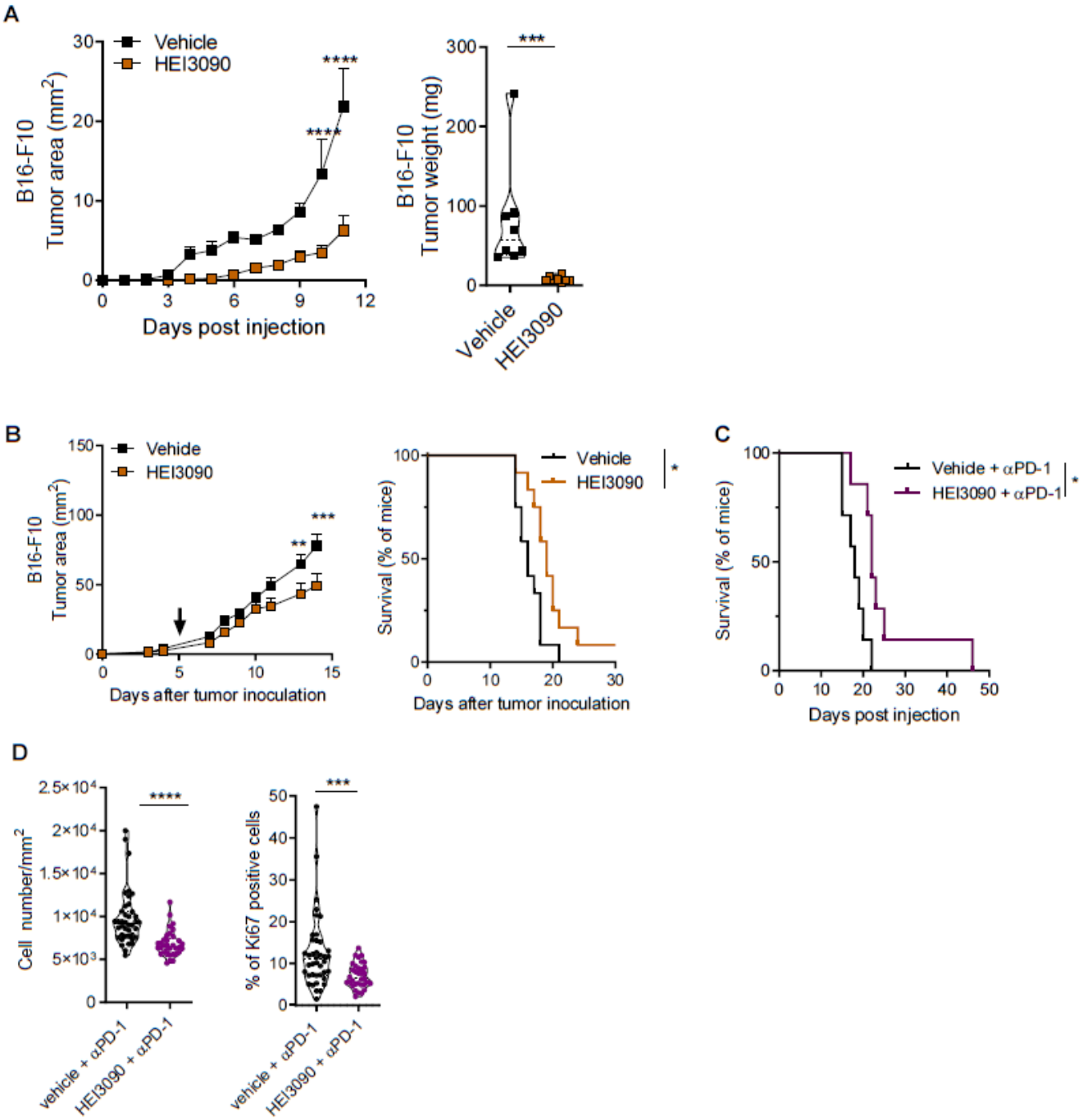

Supplementary Figure 4

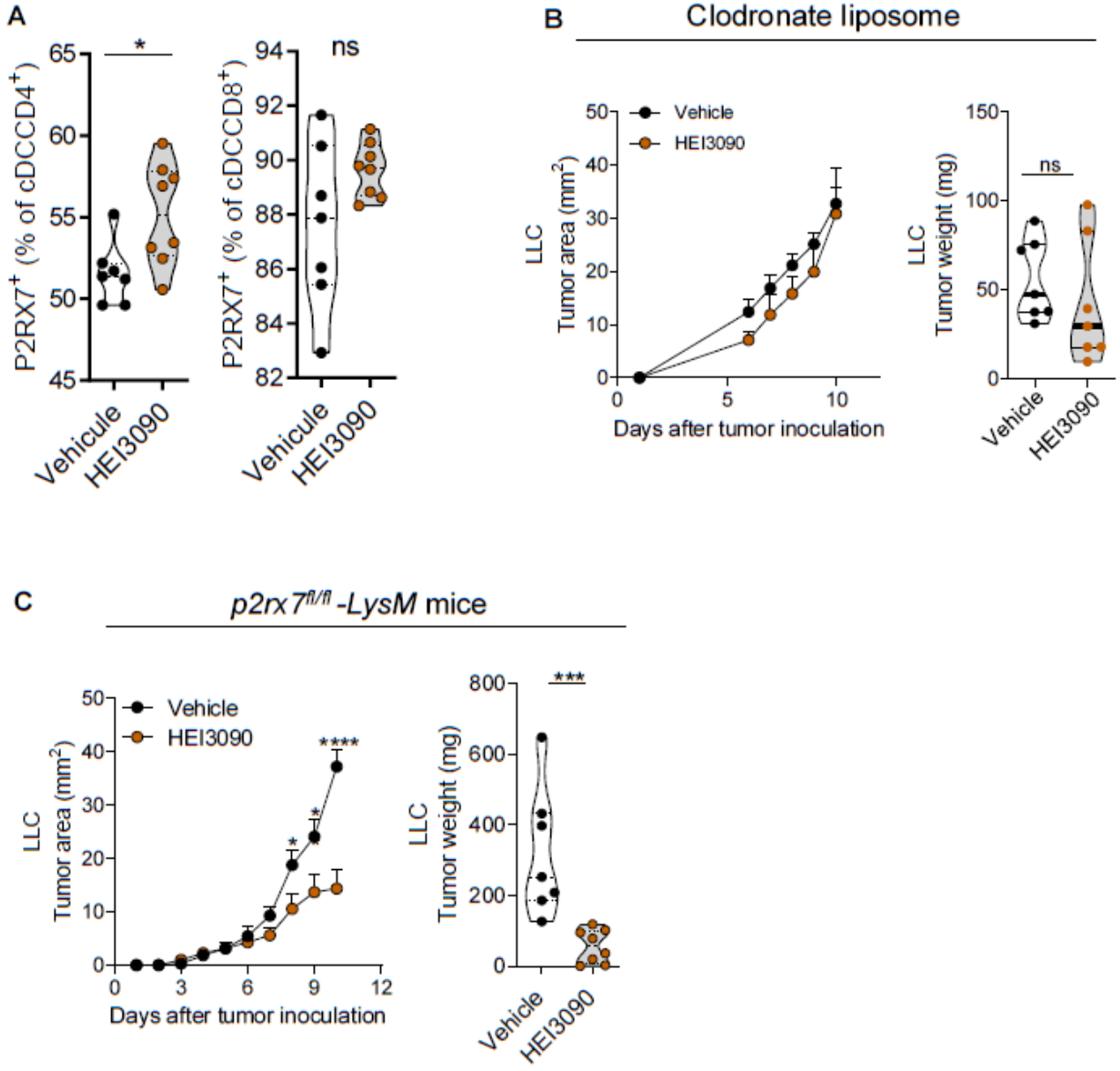

Supplementary Figure 5

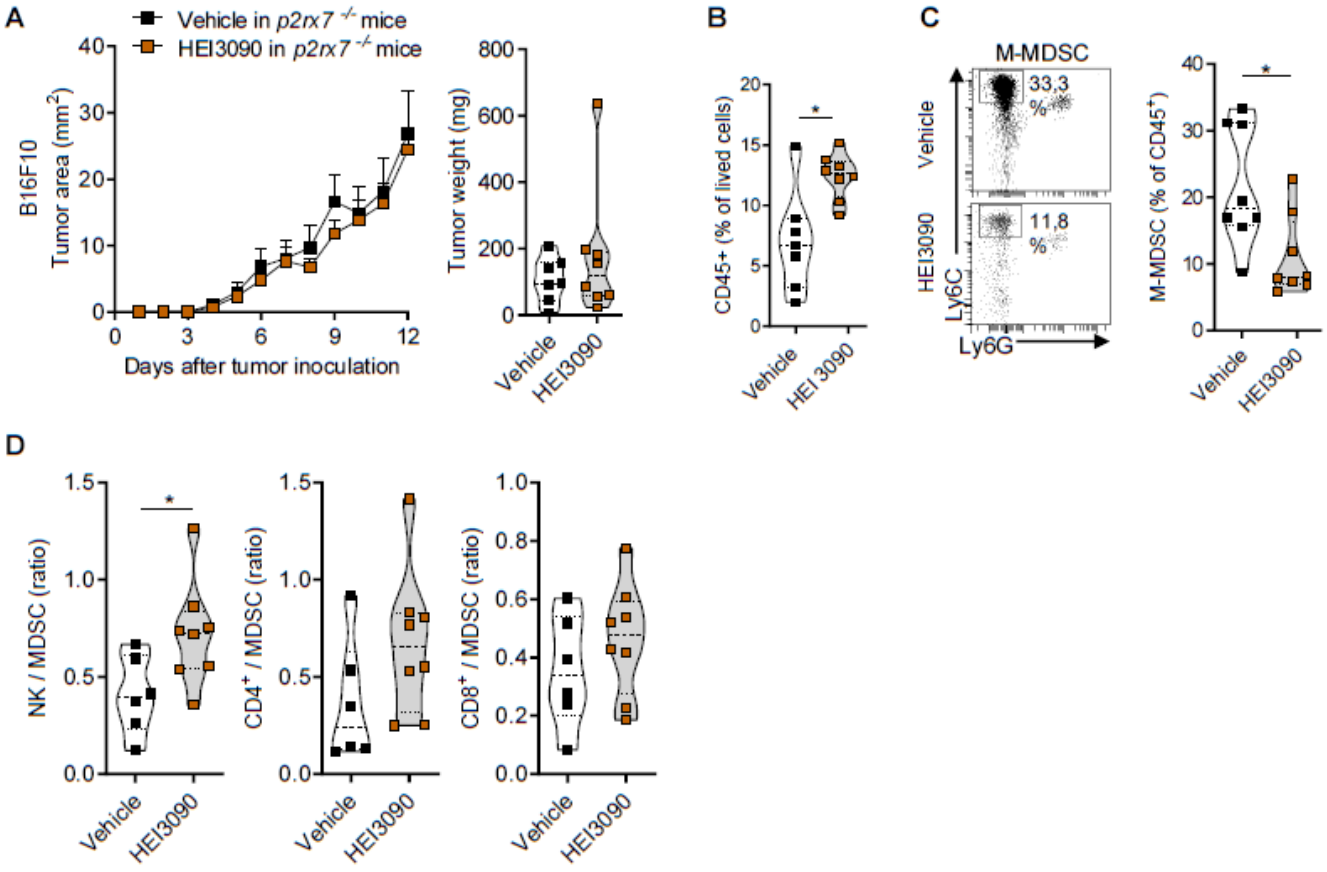

Supplementary Figure 6

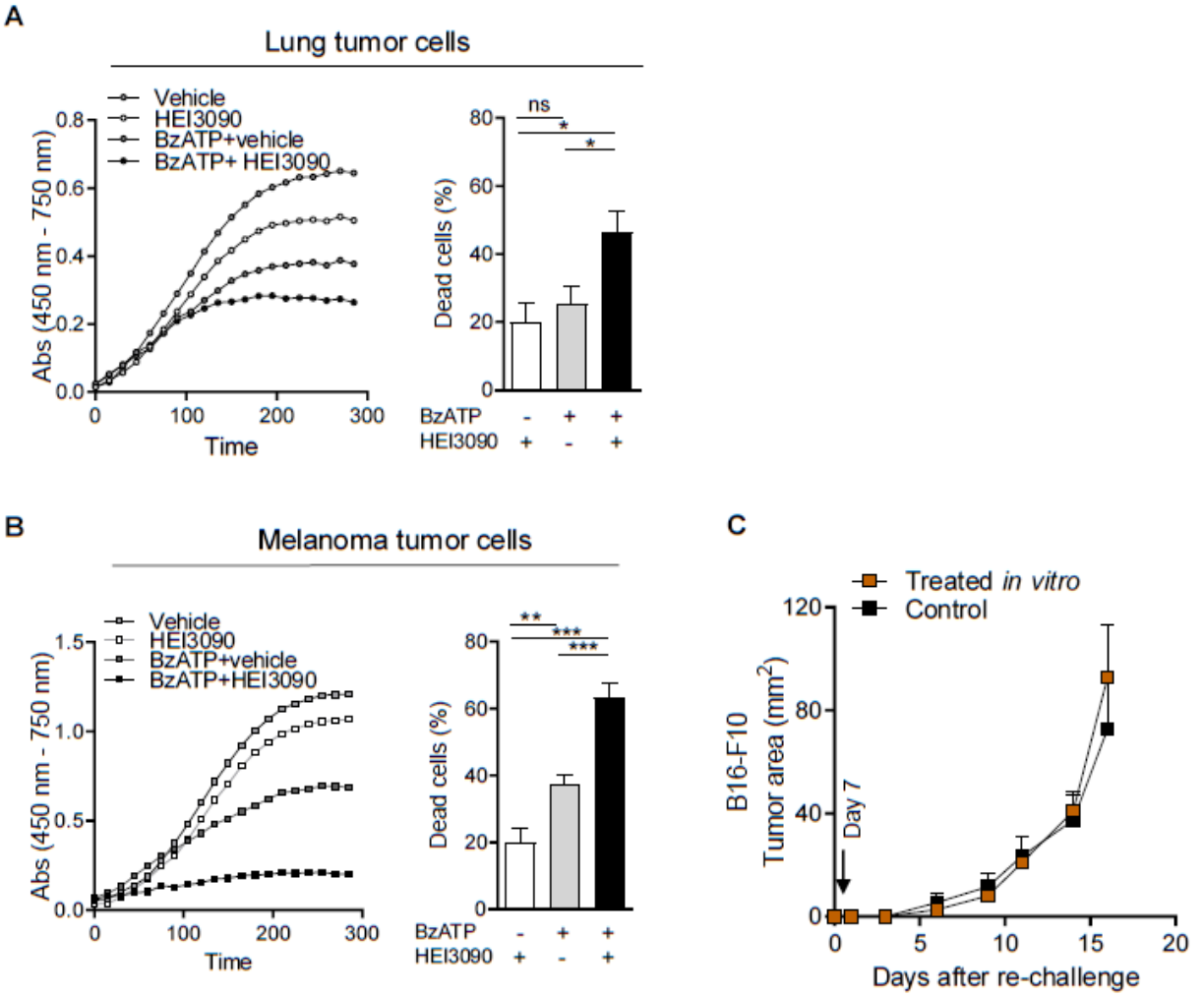

Supplementary Figure 7

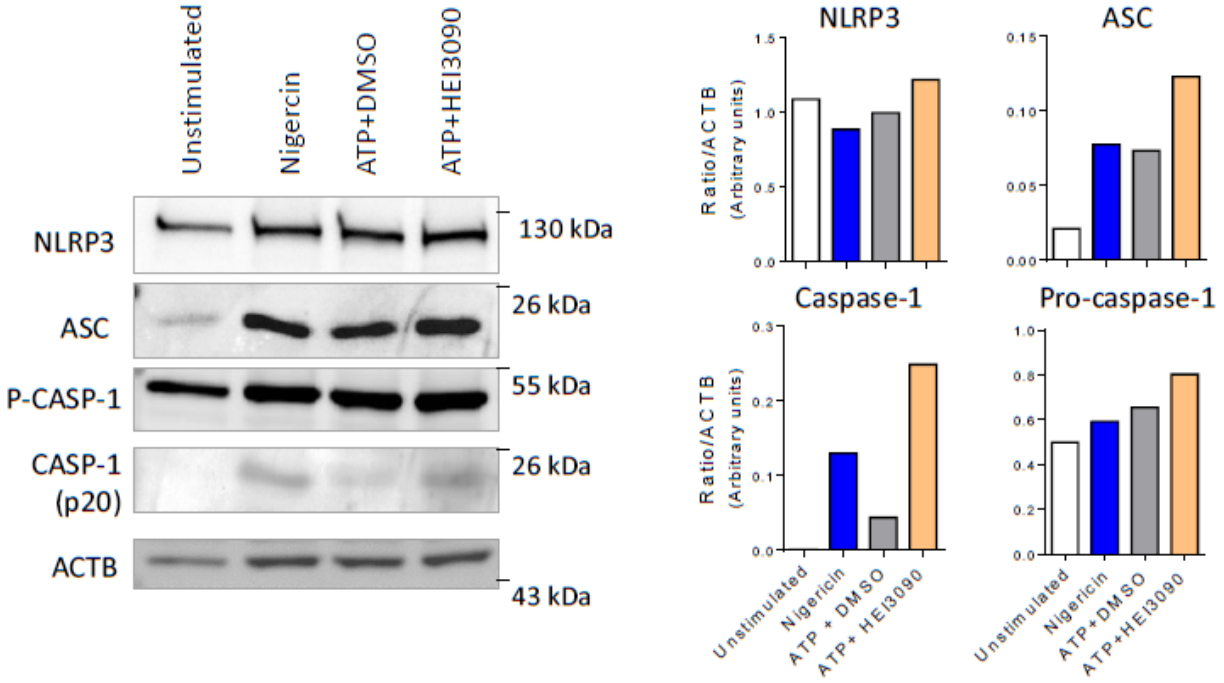

Supplementary Figure 8

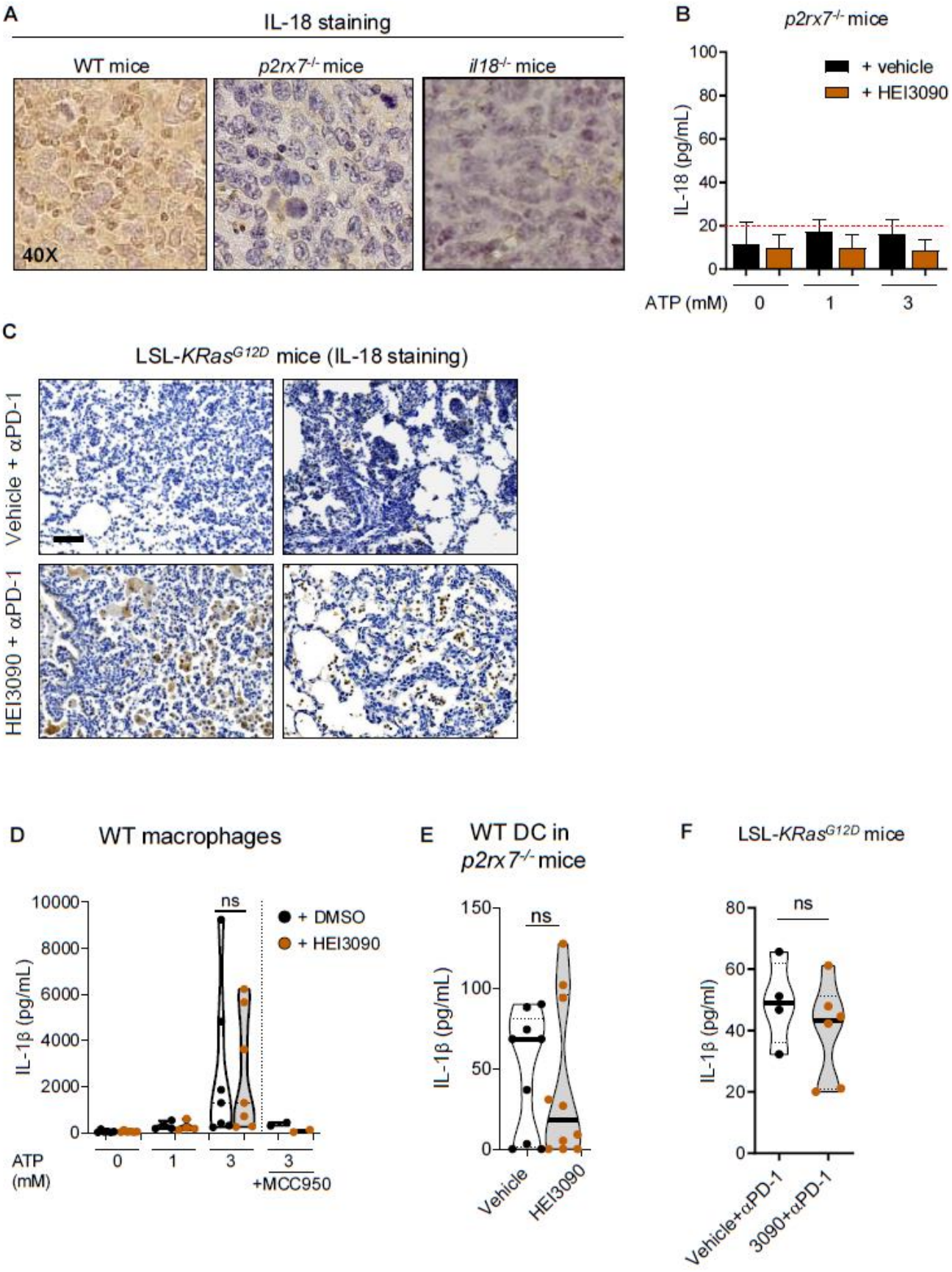

Supplementary Figure 9

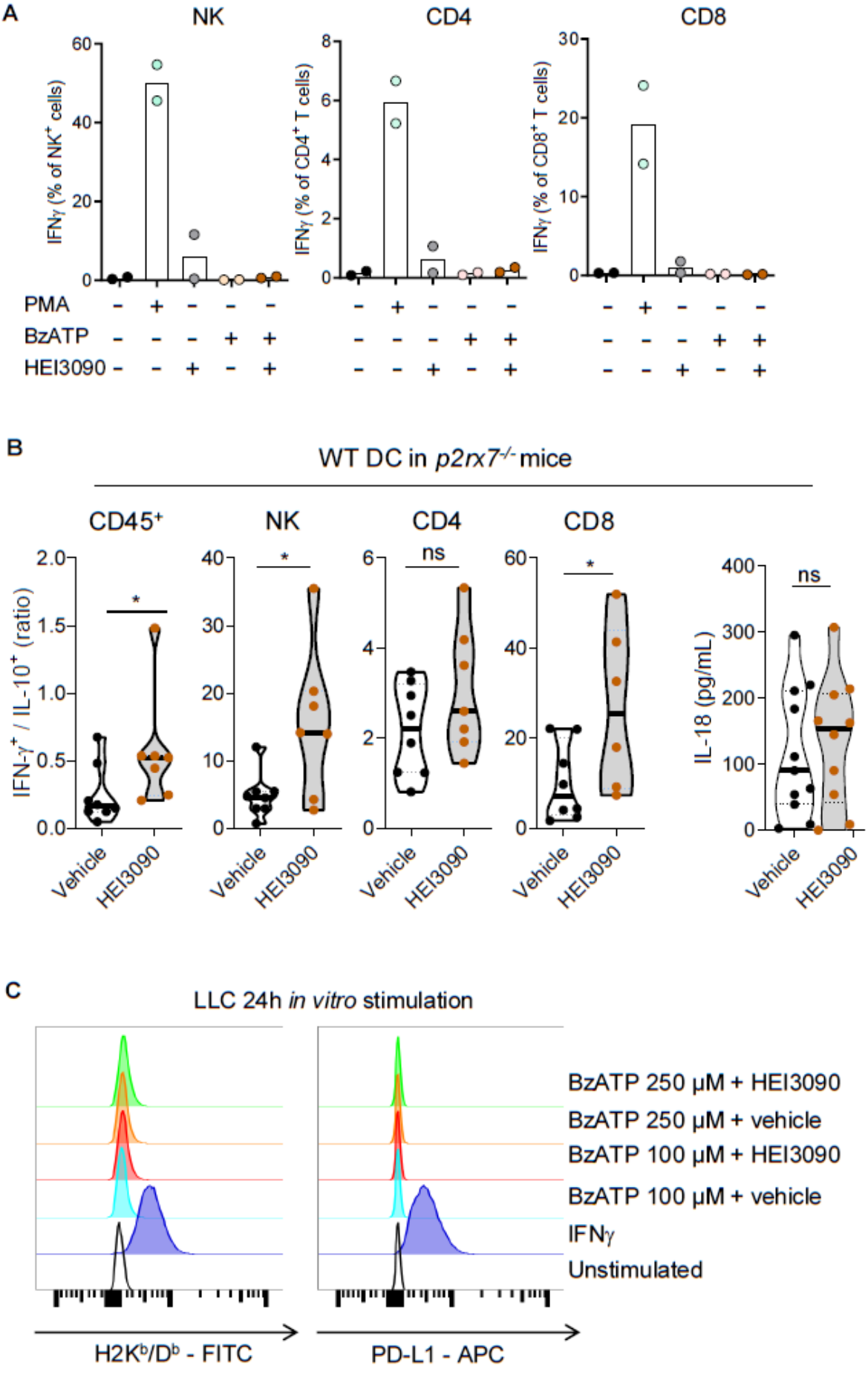

VI. Discussion

Le cancer du poumon est un cancer fréquent et particulièrement grave lorsqu'il est découvert à un stade tardif. La découverte de nouveaux outils théranostiques est d'une importance majeure. Le récepteur P2RX7, particulièrement exprimé dans les tissus tumoraux et par les cellules de l'immunité, a été récemment défini comme un immunomodulateur des réponses antitumorales. L'expression d'un récepteur P2RX7 par les cellules tumorales, capable de les perméabiliser en présence du ligand endogène présent à forte concentration dans ces tissus, nous apparaissait contre-intuitif. L'objectif de cette thèse était de définir l'expression de P2RX7 dans le CNPC en émettant l'hypothèse que des variants d'épissage pourraient impacter les fonctions biologiques de P2RX7 dans cette pathologie.

L'étude présentée en III.D. est une revue de la littérature dans laquelle nous avons discuté les rôles de l'épissage alternatif de *P2RX7* en pathologie humaine. Nous avons résumé les connaissances actuelles concernant les SNPs affectant la fonction biologique de P2RX7, et n'avons notamment pas relevé d'étude retrouvant une association entre un SNP et la condition tumorale du CNPC, ni de données en faveur d'un outil pronostic représenté par les SNPs dans cette pathologie. Nous avons fait la liste des épissages alternatifs connus pour affecter les fonctions de P2RX7, et avons analysé les sites de fixation des protéines régulant l'épissage de l'ARNm. Certains SNPs étaient identifiés dans ces zones régulant l'épissage de *P2RX7*, mais la fréquence de distribution dans les analyses bioinformatiques était si basse que nous ne pensons pas qu'ils puissent réguler l'épissage alternatif de *P2RX7* et avoir une traduction physiopathologique chez l'humain. Il est à noter que, postérieurement à cette revue, la mise en évidence d'une régulation par le SNP rs208307 du variant d'épissage *P2RX7L*, a été rapportée comme vu en section III.C.g.iii.3.

L'étude présentée en V.A. a constitué les principaux travaux de ma thèse. Nous avons caractérisé les niveaux d'expression et la fonctionnalité *ex vivo* de P2RX7 chez les patients atteints de LUAD, couplée à l'analyse des variants d'épissage du récepteur. A cette fin, la mise au point d'outils durant la première année de cette thèse, permettant d'analyser spécifiquement P2RX7 dans cette pathologie, a représenté une étape majeure et

indispensable. En effet nous avons établi un protocole de dissociation des tissus pulmonaires adénocarcinomateux et adjacents non tumoraux prélevés à l'état frais suivi d'un tri des fractions cellulaires immunitaires et non immunitaires dans ces tissus. Nous avons sélectionné des amorces spécifiques permettant d'étudier l'expression des messagers de *P2RX7, P2RX7B*, *P2RX7H* et *P2RX7J* dans ces fractions cellulaires. Seuls ces variants ont été étudiés car nous avions mis en évidence ces seuls variants dans les cellules mononucléées du sang périphérique humain. Il est à noter que, concernant l'isoforme pleine taille *P2RX7A* il n'a pas été possible de produire un outil n'amplifiant spécifiquement que cet isoforme, du fait de l'absence de zone propre de cet épissage alternatif permettant le couplage des amorces de qPCR, ce qui impose certaines limites dont nous avons tenu compte pour l'analyse de nos données.

Nous avons choisi dans cette étude de démontrer non seulement l'expression du récepteur dans le LUAD mais surtout sa fonction biologique. En effet, de nombreuses études se sont attachées à mettre en évidence l'expression du récepteur avec des techniques d'IHC, certaines utilisant des méthodes soustractives avec des anticorps reconnaissant différents domaines du récepteur afin d'en déduire les variants d'épissage exprimés et même l'impact fonctionnel. Cependant comme nous le discutons, ces méthodes ne permettent pas d'être formel sur la nature du récepteur exprimé dans les tissus analysés, puisque le signal de fluorescence dépend de la spécificité de chaque anticorps, rendant peu commode l'usage de méthodes soustractives. Nous avons donc choisi d'utiliser un protocole de test fonctionnel en cytométrie de flux optimisé pour les tissus pulmonaires humains, permettant d'étudier l'ouverture du large pore membranaire dépendant spécifiquement de P2RX7. En effet, la détection d'un signal dépendant spécifiquement de P2RX7 signe sa présence dans les compartiments cellulaires étudiés, cette approche étant appropriée pour la mise en évidence de l'expression fonctionnelle de P2RX7 dans le LUAD. Cette technique a aussi été adaptée pour étudier simultanément les fonctions d'ouverture du large pore et d'influx calcique dépendant de P2RX7 dans un modèle d'expression hétérologue sur la lignée HEK293T décrite pour ne pas exprimer de récepteur P2RX. Une limite importante est liée au fait que le test fonctionnel de P2RX7 dans ces travaux concerne des cellules en suspension, et il serait également important de caractériser ces fonctions sur des cellules adhérées à une matrice.

Alors que P2RX7 est exprimé à la fois dans les cellules tumorales et immunitaires, seules les cellules immunitaires exprimaient un récepteur fonctionnel dans le LUAD. Cette donnée est

d'autant plus importante que P2RX7 est avant tout exprimé par les cellules de l'immunité, ce qui corrobore son implication dans l'immunomodulation du MET soulignée par de nombreux travaux. Nous avons ensuite analysé l'expression différentielle des variants d'épissage de *P2RX7* et avons montré que l'épissage alternatif *P2RX7B* est particulièrement exprimé dans les cellules immunitaires infiltrant la tumeur, et est associé de façon intéressante à un désert immunitaire chez les patients présentant les plus hauts niveaux d'expression de *P2RX7B*. Cette donnée pourrait conduire à proposer l'analyse de l'expression de *P2RX7B* par les cellules immunitaires intratumorales en tant que biomarqueur prédictif d'un désert immunitaire tumoral et d'une possible non-réponse à l'immunothérapie par ICI, qui reste cependant à objectiver.

Sur un plan mécanistique, nous avons montré que P2RX7B impacte négativement la localisation membranaire de P2RX7 et sa fonction d'ouverture du large pore du fait d'une part de l'expression vraisemblable d'homotrimères P2RX7B dans une même cellule, et d'autre part de l'hétéro-oligomérisation de P2RX7AB. La séquence conduisant au désert immunologique observé chez les forts expresseurs de *P2RX7B* pose en revanche question. En effet nous n'expliquons pas pourquoi des cellules immunitaires exprimant l'hétéro-oligomère P2RX7AB - dont la susceptibilité à la lyse cellulaire induite par l'ATPe est moindre - se trouvent en plus faible abondance dans la zone tumorale. Nous pourrions présumer que la forme P2RX7AB impacterait les capacités de différenciation des cellules qui l'expriment. Pour adresser cette question, il conviendrait de définir exactement les populations immunitaires qui expriment particulièrement ce variant d'épissage dans la zone tumorale ; en effet notre protocole expérimental dichotomisait les populations cellulaires immunitaires et non immunitaires selon l'expression du $CD45^{+}$, et cela ne renseigne pas sur le type de cellules immunitaires impliquées. S'il s'agit de cellules immunitaires suppressives, on peut aisément imaginer que la surexpression de ce variant par ces dernières aura une conséquence péjorative sur l'évolution tumorale, en revanche s'il s'agit de cellules immunitaires antitumorales alors l'expression de *P2RX7B* serait providentielle puisque les épargnant de la cytolyse dépendante de l'ATPe. L'analyse de l'infiltrat immunitaire tumoral et de l'expression par les sous types de cellules immunitaires de *P2RX7B*, pourrait apporter des éléments de réponse quant à l'absence d'infiltrat immunitaire tumoral chez les patients surexprimant ce variant.

L'étude présentée en V.B., qui n'était pas le cœur de mon travail de thèse, avait pour objectif d'étudier l'effet d'une nouvelle molécule activatrice de P2RX7, le HEI3090, sur l'évolution des tumeurs pulmonaires dans un modèle murin. Nous avons utilisé des modèles de souris immunocompétentes syngéniques de tumeurs et avons montré que l'utilisation de cette molécule améliorait la SG. Le mécanisme qui conduit à cet effet est associé à l'augmentation de la production d'IL-18 dépendamment de l'inflammasome NLRP3 en aval de l'activation de P2RX7, NLRP3 qui à son tour active les cellules T NK et $CD4^+$ pour produire de l'interféron gamma augmentant ainsi l'immunogénicité tumorale. Enfin, l'activation de P2RX7 combinée à l'inhibiteur de point de contrôle immunitaire PD-1 permet la régression de la tumeur, suivie par l'établissement d'une réponse immunologique mémoire.

Les données de l'étude V.A. montrant que P2RX7 est exprimé et fonctionnel sur les cellules immunitaires pulmonaires essentiellement, et les données de l'étude V.B. montrant que les fonctions anti-tumorales de HEI3090 dépendent d'une mise en jeu de réponses immunitaires anti-tumorales par les cellules de l'hôte et non d'une activation directe du P2RX7 tumoral, sont en adéquation sur un plan mécanistique. La question de l'action éventuelle du HEI3090 sur P2RX7B exprimé par les cellules immunitaires intratumorales, demeurse ouverte.

VII. Perspectives

Cette thèse a permis de positionner *P2RX7B* comme un nouveau marqueur prometteur dans le LUAD. L'expression de ce variant par les cellules immunitaires intratumorales est associée à des tumeurs peu infiltrées et ainsi, nous pouvons présumer que l'expression de *P2RX7B* pourrait être associée à un défaut de réponse immunitaire anti-tumorale dans le LUAD.

D'un point de vue diagnostique et pronostique, ces résultats pourraient constituer un support intéressant pour évaluer le pronostic des patients et éventuellement inclure ces données dans le cadre des biomarqueurs de réponse aux immunothérapies.

A visée thérapeutique, l'utilisation de modulateurs pharmacologiques ciblant P2RX7 semble prometteuse pour cibler le MET, cependant nous ne pouvons pas préjuger si P2RX7B doit être modulé positivement ou négativement, puisqu'il s'agit d'un variant "perte de fonction". Nous

pourrions imaginer que P2RX7B devrait être activé pour restaurer la fonction du récepteur dans la tumeur, mais cela est hautement spéculatif en l'absence de données étayant cette question. A court terme, il serait intéressant de caractériser précisément l'infiltrat immunitaire tumoral du LUAD en identifiant quelles cellules expriment particulièrement *P2RX7B*, puis de réaliser des expériences mettant en jeu des modulateurs positifs comme le HEI3090 pour tenter de réactiver les fonctions d'ouverture du large pore de P2RX7B *in vitro* et d'en étudier les voies de signalisation d'aval et les conséquences biologiques. A plus long terme nous pourrions envisager de cultiver les tumeurs humaines par technique en trois dimensions avec un maintien du flux. Cette approche permet d'assurer la survie des cellules qui composent la tumeur mais également d'étudier leur évolution (immunitaires, stromales et cancéreuses) en réponse à des molécules comme le HEI3090. Enfin, nous pourrions envisager d'étudier l'efficacité de telles molécules sur un modèle de souris immunodéprimées puis reconstituées d'un système immunitaire humain et transplantée avec une tumeur humaine, dans une perspective translationnelle.

VIII. Publications annexes

A. Revue de la littérature annexe N°1. Rationnel biologique de l'immunothérapie des cancers

Article publié (Revue des Maladies Respiratoires 2018 Feb;35(2):206-222. doi: 10.1016/j.rmr.2017.11.008.)

Rationnel biologique de l'immunothérapie des cancers

J. Benzaquen (a), C.-H. Marquette (a), N. Glaichenhaus (b), S. Leroy (a), P. Hofman (c), M. Ilié (c)

(a) Department of Pulmonary Medicine and Oncology, CHU de Nice, FHU OncoAge, 06100 Nice, France

(b) Université Côte-d'Azur, CNRS, Inserm, institut de pharmacologie moleculaire et cellulaire, FHU-OncoAge, 06560 Valbonne, France

(c) Laboratory of Clinical and Experimental Pathology and Hospital-related Biobank (BB-0033-00025), IRCAN, FHU OncoAge, 06100 Nice, France

Résumé

Introduction. — L'immunothérapie vise à promouvoir la réponse immunitaire anticancéreuse via une réponse immune contre certains antigènes tumoraux. État des connaissances. — L'immunosurveillance module l'immunogénicité des tumeurs. Pour être efficace, elle doit comporter l'activation de lymphocytes T CD4+ et CD8+ et de l'immunité innée. Des molécules de costimulation activatrices et inhibitrices régulent l'activation lymphocytaire T au niveau de checkpoints de l'immunité notamment PD-1/PDL1 et CTLA-4. La résistance immunitaire adaptative est un mode de résistance des tumeurs à l'immunosurveillance par le biais de ces checkpoints. Perspectives. — La combinaison de plusieurs immunothérapies entre elles ou avec la chimiothérapie et la radiothérapie et des anticorps contre d'autres molécules de costimulation sont en développement. Le développement de biomarqueurs capables de sélectionner une population cible et de prédire cette réponse thérapeutique représente un défi majeur. Le séquenc¸age haut débit des tumeurs pourrait permettre d'affiner « l'immunoscore ». Le TCR intratumoral semble représenter un biomarqueur prometteur. Conclusions. — Le développement de l'immunothérapie pose de nombreux défis et nécessitera de s'appuyer sur des données de recherche préclinique et translationnelle.

Mots clés

Carcinome bronchique ; Immunothérapie ; Immunosurveillance ; Échappement ; PD-1 ; PD-L1

I. INTRODUCTION

L'immunothérapie vise à déclencher la réponse immunitaire antitumorale naturelle contre les cancers via une réponse lymphocytaire effectrice et mémoire contre certains antigènes dominants du cancer du patient. Pour être efficace, cette immunité doit comporter l'activation spécifique de lymphocytes T CD4+ et CD8+ soit l'immunité « acquise », et probablement la stimulation de l'immunité « innée » [1, 2]. Cette avancée thérapeutique dans le domaine de l'oncologie est majeure, c'est une approche originale puisque ce n'est plus exclusivement la cellule tumorale qui est ciblée, comme le permettent les traitements classiques, mais aussi son microenvironnement inflammatoire.

Le système immunitaire est constitué de plusieurs types cellulaires capables d'entrer en interaction avec des antigènes pathogènes du « non soi » (comme un agent infectieux), mais aussi avec des cellules « anormales » telles que les cellules cancéreuses. Ces cellules se répartissent en deux classes : celles de l'immunité innée et celles de l'immunité adaptative.

Les cellules de l'immunité innée (cellules Natural Killer [NK], macrophages, neutrophiles) ont la particularité de réagir très rapidement et constituent donc la première ligne de défense de l'organisme. Une fois activées, ces cellules peuvent mobiliser les cellules de l'immunité adaptative. La réponse immunitaire innée fait intervenir en particulier les cellules NK, qui reconnaissent les cellules tumorales des cellules saines par le biais d'un processus complexe d'expression de différentes molécules stimulatrices et inhibitrices. Elles expriment des récepteurs cytotoxiques naturels à leur surface (NKp46, NKp30, NKp44, et NKG2D) qui se lient au complexe majeur d'histocompatibilité (CMH) de classe 1. Lorsqu'il y a liaison entre le récepteur sur la cellule NK et le CMH1 sur une cellule cible, cette dernière n'est pas menacée par la cellule NK. Si cette liaison n'a pas lieu, la cellule cible est lysée. Les molécules du stress cytoplasmiques comprennent les motifs moléculaires associés aux dégâts cellulaires (DAMPs) comme les protéines du choc thermique, les bêta-défensines, l'acide urique, qui sont des éléments reconnus par des récepteurs, qui peuvent être sur la surface cellulaire, cytoplasmiques, ou solubles [3]. La libération de ces molécules du stress cytoplasmique active les macrophages et les cellules dendritiques, entraînant en particulier la production d'IL-12, sous la dépendance des « Toll Like Receptors » (TLR), et la transition vers le système d'immunité adaptative [4].

Les cellules de l'immunité adaptative, lymphocytes B (LB) et lymphocytes T (LT), ont la particularité de pouvoir persister dans l'organisme pendant des mois, et même des années, après avoir été activées. Ce sont ces cellules qui sont responsables de la « mémoire immunitaire », un phénomène essentiel sur lequel repose l'efficacité des vaccins [5]. Contrairement aux cellules de l'immunité innée qui reconnaissent des structures moléculaires présentes exclusivement chez les microorganismes ou dans des cellules ayant subi un « stress », les lymphocytes T reconnaissent des peptides antigéniques issus de la dégradation – par les cellules de l'immunité innée – de protéines cellulaires ou microbiennes, mais également de la dégradation cellulaire non médiée par le système immunitaire. Ces peptides antigéniques du « soi » sont présentés à la surface cellulaire par des molécules du Complexe Majeur Histocompatibilité (HLA chez l'homme). Une fois activés, les lymphocytes T prolifèrent et se différencient en différentes cellules « effectrices » : lymphocytes cytotoxiques, lymphocytes auxiliaires, ou lymphocytes régulateurs. Afin de limiter leur expansion et leur activité, ces cellules sont équipées de mécanismes de rétrocontrôle négatif, les « verrous immunologiques » (« immune checkpoints ») qui permettent de limiter dans le temps la réponse immunitaire et éviter ainsi les dommages tissulaires qui pourraient en résulter [6].

Des données expérimentales montrent que les cellules de l'immunité innée et de l'immunité adaptative exercent une surveillance du processus tumoral. Cette immunosurveillance met en jeu à la fois la reconnaissance d'antigènes tumoraux par les LT et l'activation des cellules de l'immunité innée. Lorsqu'il est efficace, ce processus permet la détection des cellules tumorales dès qu'elles apparaissent et soit leur destruction avant toute manifestation clinique, soit leur maintien à l'état de tumeurs dormantes non évolutives. C'est le principe autour duquel s'organise l'immunothérapie en tant que stratégie thérapeutique [1, 2, 7].

Le traitement du cancer bronchique a significativement évolué lors des quinze dernières années, notamment suite au développement de thérapies ciblant des voies de signalisations oncogéniques, en particulier les inhibiteurs de tyrosine kinase de la voie de l'EGFR (récepteur du facteur de croissance épidermique) et les inhibiteurs d'ALK (anaplastic lymphoma kinase) [8, 9]. Ces molécules peuvent induire des réponses cliniques majeures dans certains types tumoraux exprimant ces cibles oncogéniques. Cependant, ces réponses sont transitoires, avec un échappement tumoral constant et une rechute [10]. De plus, elles bénéficient à un nombre restreint de malades dont la tumeur présente une anomalie spécifique de l'EGFR (environ 10 à 15 %) ou d'ALK (3 à 5 %) [11, 12].

Jusqu'à ces dernières années, le cancer bronchique n'était pas considéré comme un cancer particulièrement « immunogène », alors que la présence de cellules immunitaires dans son microenvironnement a été mise en évidence depuis de nombreuses années [13]. C'est la découverte d'antigènes associés aux tumeurs bronchopulmonaires [1, 2] et la reconnaissance des antigènes tumoraux par ces dernières, qui a permis d'étayer et de soutenir l'hypothèse d'un cancer bronchique « immunogène ». Le développement et les succès de l'immunothérapie du cancer ont conduit à une meilleure compréhension de l'immunité anti-tumorale. Il existe une relation triangulaire entre les cellules tumorales, le système immunitaire de l'hôte, et le

microenvironnement tumoral, et cette relation détermine les mécanismes de contrôle et d'échappement tumoral au cours de l'histoire naturelle de la maladie [1, 2]. Cette dynamique peut être modifiée favorablement par les immunothérapies ciblant la tumeur et/ou son microenvironnement. Différentes molécules ont été récemment évaluées chez des patients présentant des tumeurs bronchiques de stade avancé et/ou résistantes aux traitements classiquement utilisés, et montrent des résultats remarquables avec en particulier des réponses prolongées dans le temps [14].

II. RÔLE DU SYSTÈME IMMUNITAIRE DANS LE CONTRÔLE TUMORAL

Les étapes clefs impliquées dans une réponse immune antitumorale efficace ont été décrites et illustrées par Chen et Mellman, constituant « le cycle de l'immunité contre le cancer » [15] (Figure 1).

Brièvement, les antigènes du « soi » tumoraux qui apparaissent sont capturés par les cellules dendritiques du microenvironnement tumoral. Suite à leur activation, ces cellules dendritiques migrent via les vaisseaux lymphatiques vers les ganglions lymphatiques qui drainent la tumeur. C'est dans ces ganglions qu'elles présentent les antigènes tumoraux aux lymphocytes T ce qui conduit à leur activation et à leur différenciation en lymphocytes T effecteurs. Ces lymphocytes T effecteurs quittent les ganglions lymphatiques via les vaisseaux lymphatiques efférents pour se retrouver dans la circulation sanguine, puis dans les vaisseaux sanguins irriguant les tumeurs. Ils peuvent ainsi infiltrer le lit tumoral au travers de multiples processus impliquant des interactions intriquées entre les lymphocytes T et les cellules endothéliales, puis migrent dans la tumeur par voie trans-endothéliale [16].

Une fois que les lymphocytes T anti-tumoraux ont infiltré le lit tumoral, ils peuvent reconnaître et détruire les cellules tumorales, ce qui a pour conséquence le relargage d'antigènes tumoraux supplémentaires et l'amplification de la réponse immunitaire [7, 17]. La lyse des cellules tumorales par les lymphocytes T anti-tumoraux met en jeu plusieurs mécanismes moléculaires, parmi lesquels i) la libération de molécules cytotoxiques (perforine, granzyme, etc.) à partir de granules préformés et ii) l'activation des voies de signalisation en aval des récepteurs de molécules de la famille du TNF (facteur de nécrose tumorale) et notamment Fas et Trail [7].

Les modèles murins ont clairement démontré que les lymphocytes T jouaient un rôle déterminant dans le contrôle de la croissance des tumeurs, que celles-ci apparaissent spontanément ou consécutivement à une exposition à des carcinogènes [18].

Sur le plan clinique, les données obtenues en caractérisant les cellules immunitaires intra-tumorales ont montré que la présence de lymphocytes T mémoires, de lymphocytes T helper type 1 (qui correspondent à des lymphocytes T CD4+ non cytotoxiques sécrétant principalement de l'interféron gamma et de l'IL1 et qui ont pour rôle de potentialiser la réponse T cytotoxique), de lymphocytes cytotoxiques CD8+ et de cellules NK CD57+ était associée à une survie plus importante des patients. Ceci démontre le rôle déterminant de ces cellules dans le contrôle de la progression tumorale [19-22].

Les études fonctionnelles de la réponse immunitaire impliquée dans l'immunosurveillance des cancers ont montré que cette réponse met en jeu un réseau complexe de cellules intervenant dans la réponse immunitaire innée, dont les cellules NK et les macrophages, et dans la réponse immunitaire adaptative, dont les lymphocytes T CD8+ ou CD4+ exprimant le récepteur αβ et les cellules NKT. Les lymphocytes T γδ sont des lymphocytes T non conventionnels impliqués à la fois dans la réponse innée et adaptative de l'organisme, ils possèdent un TCR composé des chaînes γ et δ, n'ont pas besoin que les molécules du CMH présentent l'antigène afin qu'il soit reconnu, et sont activés en présence d'IL-2 [23]. Ils ne sont donc pas influencés par la résistance à l'immunoediting conférée par la perte du CMH des cellules tumorales, ce qui en fait des outils potentiellement intéressants sur un plan thérapeutique. Contrairement aux lymphocytes T pouvant identifier les cellules tumorales en reconnaissant les antigènes tumoraux présentés par les molécules du CMH, les cellules NK ne reconnaissent pas ces antigènes, mais peuvent être activées par des signaux de stress ou de danger. Ces protéines sont exprimées par les cellules tumorales en réponse aux altérations de leur ADN et reconnues par des récepteurs activés des NK dont le récepteur NKG2D [24].

La réponse immune joue un rôle majeur dans la défense de l'organisme contre les tumeurs, et est probablement responsable du contrôle de la croissance tumorale dans

une grande majorité de tumeurs, en particulier lors de la phase initiale de tumorigenèse.

Cependant, sous l'effet des mutations génétiques liées à l'instabilité génomique, et des modifications épigénétiques de l'ADN et des histones, les cellules tumorales, dont l'origine est monoclonale, se diversifient en sous-populations hétérogènes. Cette propension à se diversifier dépend de leur capacité invasive propre, de leur sensibilité et de leur résistance au traitement entrepris. Leur capacité à induire une réponse immunitaire et leur sensibilité à cette réponse dépend également des variations génétiques et épigénétiques qui leurs sont propres [25].

L'immunosurveillance peut moduler (« éditer ») l'immunogénicité des tumeurs en supprimant sélectivement les cellules exprimant fortement les antigènes reconnus par les lymphocytes T et de ce fait les plus sensibles à la réponse immunitaire, et en sélectionnant les clones cellulaires les plus résistants à l'immunosurveillance. Ainsi, les tumeurs développées chez des patients immunocompétents sont des tumeurs éditées, provenant de cellules ayant résisté à l'immunosurveillance et dont la descendance a hérité de cette résistance immunitaire adaptative [26].

Les relations complexes entre l'immunosurveillance et l'échappement des cellules tumorales à la destruction médiée par le système immunitaire peuvent aboutir à trois scénarios que le groupe de Schreiber a classifiés comme constituant les trois « E » de l'immunosurveillance : Élimination – Équilibre – Échappement (Figure 2) [27, 28].

La première phase est celle de l'élimination des cellules tumorales. Cette destruction survient généralement à un stade précoce de l'oncogenèse, avant que la tumeur soit détectable cliniquement [29]. Des cas exceptionnels de régression complète spontanée de cancers établis ou même métastatiques ont été rapportés, notamment dans les mélanomes [30].

La seconde phase est l'instauration d'un équilibre entre le renouvellement des cellules tumorales et leur élimination par le système immunitaire. Cette étape peut se prolonger pendant plusieurs années de latence, durant lesquelles la tumeur peut être contrôlée et maintenue à son site d'origine. Mais cet équilibre peut être aboli par une évolution des clones cellulaires du fait de la plasticité de leur génome, conférant une résistance progressive envers l'action suppressive du système immunitaire ou par une défaillance des mécanismes d'immunosurveillance [27].

La troisième phase est représentée par l'échappement des cellules tumorales qui s'évadent du contrôle de l'immunosurveillance, se multiplient et envahissent les tissus environnants ou disséminent à distance [27]. Cette étape induit un climat d'immunotolérance favorable à la croissance tumorale. La tumorigenèse est alors enclenchée, et la tumeur devient détectable et symptomatique cliniquement. Des travaux récents ont permis de mettre en évidence le rôle clef du microenvironnement tumoral et des caractéristiques biologiques de son architecture dans l'évolution vers une dissémination métastatique [31, 32].

Le dialogue établi entre les cellules tumorales et leur microenvironnement pendant la période de développement et croissance d'une tumeur produit une empreinte qui est reproduite aux différents sites de développement du cancer [33].

Il faut noter que chaque type de tumeur a son individualité immunologique et sa propre réponse à l'immunosurveillance, conduisant à une grande variabilité de la réponse ou la résistance des cancers à l'immunosurveillance et ainsi à l'immunothérapie [34, 35].

III. MECANISMES D'ECHAPPEMENT À L'IMMUNOSURVEILLANCE

Plusieurs acteurs sont impliqués dans l'échappement tumoral à l'immunosurveillance : la cellule tumorale elle-même, les cellules immunitaires et les cellules du stroma [1, 25].

Les cellules tumorales ont une identité moléculaire antigénique propre. Cette identité correspond aux antigènes tumoraux. Ces derniers sont relargués lors de la lyse cellulaire tumorale (phase 1 du cycle du cancer de Chen et Mellman), interceptés par les cellules présentatrices d'antigène (phase 2 du cycle du cancer) puis présentés aux lymphocytes T qui se polarisent et s'activent (phase 3 du cycle du cancer) [15, 36]. Ces lymphocytes activés migrent au niveau du site tumoral (phase 4 du cycle du cancer), infiltrent la tumeur (phase 5 du cycle du cancer) puis reconnaissent les cellules tumorales (phase 6 du cycle du cancer) pour les tuer (phase 7 du cycle du cancer) [15].

Nombre de ces antigènes sont exprimés à certains niveaux dans les tissus sains, notamment dans les cellules immunes périphériques et dans le thymus, ce qui conduit à une tolérance immunologique dans le cadre d'interactions majeures entre : peptide, CMH, et récepteur T pour l'antigène (T-cell receptor ou TCR). La tolérisation de ces lymphocytes T engendre une spécificité d'interaction plus faible, ce qui a pour effet de limiter l'efficacité de la réponse immune anticancéreuse. D'autres antigènes résultent des mutations génétiques aléatoires affectant les cellules tumorales au cours de l'oncogenèse. Ces néo-antigènes « du soi modifié » sont restreints à des tumeurs individuelles et peuvent générer des réponses immunitaires plus importantes que les antigènes communs « du soi », mais leur détection est rendue plus difficile du fait de leur caractère plus spécifique, en effet cette interaction nécessite une spécificité optimale entre l'épitope de l'antigène et son site de liaison sans quoi la détection antigénique ne peut pas avoir lieu [37]. La stimulation prolongée des lymphocytes T provoquée par leur exposition permanente aux antigènes tumoraux peut induire un état d'immunotolérance consécutif à la disparition ou à l'inactivation des lymphocytes T capables de reconnaître ces antigènes ou à leur conversion en lymphocytes T régulateurs (Treg) immunosuppresseurs [38, 39]. Le phénotype des cellules tumorales est modifié par pression de sélection du système immunitaire qui va sélectionner des variants de résistance à l'attaque immunologique par différents mécanismes (perte de l'expression de molécules impliquées dans la présentation de l'antigène HLA ou de l'antigène reconnu par les lymphocytes T) [40-42]. Elles peuvent aussi réduire l'expression des ligands de NKG2D (natural killer groupe 2 D) ou diminuer l'expression du récepteur NKG2D à la surface des cellules NK, récepteur activateur de la cytolyse antitumorale des Natural Killer, sous la dépendance de ligands, dont certains sont exprimés par les cellules tumorales [43].

Les cellules tumorales peuvent échapper à la lyse induite par le système immunitaire en augmentant l'expression de protéines anti-apoptotiques [44]. Les cellules tumorales vont modifier le phénotype des lymphocytes T qui vont devenir anergiques ou non fonctionnels et ne seront plus capables d'exercer un rôle cytotoxique vis-à-vis de la cellule tumorale. Elles peuvent exprimer l'indoleamine-2,3-dioxygénase (IDO), une enzyme permettant la dégradation active du tryptophane, un acide aminé nécessaire à la survie des lymphocytes T, et génère la kinurénine qui altère les fonctions antitumorales de ces lymphocytes [45].

Les caractéristiques biologiques définissant l'état tumoral d'une cellule, décrites en 2000 par Hanahan et Weinberg, sont au nombre de six et ont initialement été considérées comme indépendantes les unes des autres. Il s'agit de : l'indépendance vis-à-vis des signaux de prolifération, l'échappement à l'inhibition de la prolifération, la résistance à la mort cellulaire, une capacité de réplication infinie, une néoangiogenèse induite, et une activation des mécanismes d'invasion locorégionale et à distance [46]. De nouvelles « caractéristiques» ont secondairement été ajoutées à cette description, notamment : la capacité de la cellule à échapper au système immunitaire, le rôle potentiel de l'inflammation chronique, les mutations et l'instabilité génétique, et la dérégulation du métabolisme cellulaire énergétique [47]. C'est alors que ces « caractéristiques» ont été considérées comme dépendantes les unes des autres mais également dépendantes du système immunitaire de l'hôte, du microenvironnement tumoral et du métabolisme énergétique. La déprivation en nutriments et l'hypoxie tissulaire est capable de modifier les caractéristiques des compartiments immunitaires et tumoraux. La compréhension de l'immunité anti-tumorale ne repose ainsi pas exclusivement sur le déchiffrage de l'onco-immunologie et des checkpoint de l'immunité, mais également sur la connaissance de l'influence du micro-environnement tumoral, de son métabolisme, et de ses caractéristiques.

En situation physiologique, les antigènes tumoraux sont reconnus par les TCR (Phase 3 du cycle du cancer) [15]. L'activation de ces récepteurs nécessite des molécules de costimulation activatrices (CD27, CD28, etc.) et ce processus est régulé par des molécules de costimulation inhibitrices (PD-1, Tim-3, CTLA-4, Lag-3) qui, après liaison avec leurs ligands respectifs (PD-L1, Galectine-9, CD80, molécules du CMH de classe 2) inhibent l'activation des lymphocytes T. Dans une tumeur, cette inhibition des lymphocytes T persiste de façon pathologique sous forme de costimulation inhibitrice chronique, freinant l'immunité antitumorale. C'est ainsi que la levée d'inhibition par les nouveaux traitements d'immunothérapie bloquant PD-1 ou PD-L1, permet de rétablir l'activité antitumorale des lymphocytes T en leur faisant quitter leur état quiescent [48-50].

Les cellules tumorales peuvent exprimer à leur surface d'autres molécules inhibant l'action cytotoxique des lymphocytes T et des cellules NK, comme HLA-G ou HLA-E [51, 52].

Les cellules tumorales peuvent créer un environnement favorable à la tolérisation des lymphocytes en produisant ou en induisant la sécrétion de molécules immunosuppressives à large spectre (IL-10, TGF-β, récepteur soluble à l'IL-2 ou à l'IL-15, etc.), qui suppriment les fonctions antitumorales des lymphocytes T et des cellules NK [53-55].

L'échappement des cellules tumorales à l'immunosurveillance peut être favorisé par le recrutement dans le microenvironnement tumoral de cellules immunosuppressives (Treg, cellules myéloïdes suppressives ou « myeloid derived suppressor cells » en anglais (MDSC), certaines cellules dendritiques tolérogènes, macrophages de type M2, neutrophiles de type N2) [25, 48, 56, 57].

Il existe une association entre la présence d'une infiltration tumorale par ce type de cellules immunes et le pronostic défavorable des patients atteints de cancer broncho-pulmonaire [56, 58-61].

En présence d'IL-6, le TGF-β produit par les cellules tumorales, favorise le développement de lymphocytes T régulateurs caractérisés par l'expression des molécules de surface CD4 et CD25 et du facteur de transcription Foxp3 [62].

Leur stimulation inhibe les fonctions des lymphocytes T cytotoxiques, mais aussi celles d'autres cellules immunitaires antitumorales comme les NK, les macrophages, les cellules dendritiques et les lymphocytes B, pour prévenir la destruction des cellules tumorales. Les Treg expriment constitutivement des molécules co-stimulatrices inhibitrices dont notamment CTLA-4, un récepteur des molécules B7 apparenté au co-récepteur CD28, mais aussi PD-1 et PD-L1. L'expression de CTLA-4 peut être aussi induite sur les lymphocytes T CD4+ et CD8 effecteurs et contribuer à leur anergie [63].

Les MDSC sont des cellules myéloïdes immatures induites par les cytokines pro-inflammatoires produites par les cellules tumorales, telles que le GM-CSF, l'IL-1β, l'IL-6, la PGE, et le VEGF. Les MDSC constituent une population hétérogène rassemblant des monocytes et des polynucléaires neutrophiles capables d'inhiber les fonctions des lymphocytes T effecteurs et favorisent la génération des Treg à partir de lymphocytes T indifférenciés [64].

Pour exercer leur activité immunosuppressive, les MDSC ne doivent pas seulement s'accumuler dans le lit tumoral, mais également être activées. Plusieurs facteurs, dont la plupart sont produits par les cellules du stroma tumoral et par les lymphocytes T, comme l'INF-γ, l'IL-4, l'IL-13, le TGFβ, mais aussi certaines fractions du complément, sont capables d'activer différentes voies de signalisation dans les MDSC, s'appuyant en général sur les facteurs de transcription STAT1, STAT3 et STAT6, et NF-κB [65].

La compréhension de ces différents mécanismes a conduit récemment à des avancées thérapeutiques importantes en immunothérapie. Plusieurs approches sont actuellement en cours de développement ou de validation clinique [7]:

- Les anticorps anti – « immune checkpoints », notamment le blocage de CTLA-4 et de la voie PD-1/PD-L1, dont les indications thérapeutiques validées pour certains cancers tendent à s'élargir.

- Les vaccins anti tumoraux consistent en une injection d'antigène tumoraux, et relèvent davantage aujourd'hui du domaine de la recherche, bien que le vaccin « sipuleucel » contre le cancer de la prostate bénéficie d'une autorisation de mise sur le marché par la Food and Drug Administration mais dont le coût reste prohibitif en rapport avec un bénéfice modéré sur la survie ;

- Le transfert de lymphocytes T spécifiques d'antigènes, appelé thérapie adoptive, qui relève du domaine de la recherche ;

- L'association de différentes immunothérapies entre elles ou avec des chimiothérapies conventionnelles ou avec la radiothérapie, avec de nombreux essais en cours (https://clinicaltrials.gov/).

Des réponses thérapeutiques durables ont été obtenues grâce aux traitements par anticorps anti-PD-1/D-L1 dans plusieurs types de cancers en phase métastatique (poumon, mélanome, vessie, rein, prostate, sein, côlon, tête et cou, lymphomes) [66-73].

Dans des modèles murins, l'inhibition combinée de CTLA-4 et de PD-L1, ou de LAG-3 et PD-1, ou la déplétion de

cellules Treg combinée à la réduction de leur prolifération homéostatique pour inhiber l'anergie des lymphocytes T, ont démontré leur potentiel de synergie d'action [74]. L'association d'immunothérapies ciblant les checkpoints est actuellement une piste prioritaire dans les essais cliniques pour la prise en charge thérapeutique des patients atteints de cancer broncho-pulmonaire.

IV. VOIE PD-1/PD-L1

PD-1 est une protéine transmembranaire de type I immunorégulatrice appartenant à la superfamille des immunoglobulines (SFIg) (« famille CD28 et B7 »), qui est codée par le gène PDCD1 [75]. Il est l'un des plus importants récepteurs co-inhibiteurs exprimés par les lymphocytes T. Sa structure comporte un domaine IgV extracellulaire (qui partage 21 à 33 % de sa séquence génétique avec CTLA4, CD28 et ICOS), un domaine transmembranaire hydrophobe, et un domaine intracellulaire basé sur un motif de tyrosine kinase inhibitrice et un motif de tyrosine kinase régulatrice. PD-1 a deux ligands : PD-L1 (B7-H1/CD274) et PD-L2 (B7-CD/CD273). PD-L1 est exprimé par les lymphocytes T et B, les cellules dendritiques, les macrophages, les cellules endothéliales, et les cellules des îlots pancréatiques. PD-1 et son ligand PD-L1 jouent un rôle clef dans l'échappement tumoral et dans l'entretien d'un microenvironnement tumoral et de l'évolution de la tumeur.

Deux isoformes de PD-L1, dépendant de variants d'épissage, existent chez l'homme [75]. Un variant d'épissage dont l'isoforme est localisée au niveau du système endomembranaire, a une fonction inconnue mais cette isoforme semble avoir la particularité d'être incapable de se lier au récepteur PD-1 [76]. L'isoforme complète de PD-L1 lui permet quant à elle de se fixer à son récepteur PD-1 [75, 77].

À l'état physiologique, PD-L1 et PD-L2 sont exprimés sur les cellules présentatrices de l'antigène, les lymphocytes T activés, et de nombreux types tissulaires avec une expression spontanée dans le cœur, le poumon, le foie, le placenta, et un niveau faible d'expression dans la rate, les ganglions lymphatiques, le thymus, et une absence d'expression dans le cerveau [78, 79]. Cette expression partagée par les organes lymphoïdes et non lymphoïdes suggère que l'axe PD1-PD-L1/2 est impliqué dans une modulation de la réponse immunitaire dans les organes lymphoïdes secondaires et dans les organes concernés par cette expression [80].

Dans le tissu tumoral, la distribution de PD-L1 et PD-L2 a pu être dichotomisée en fonction des différents types tumoraux. Les cancers du poumon, peau, côlon, vessie, sein, cancers épidermoïdes de la tête et du cou, rein, estomac, gliaux, surexpriment PD-L1. Les cancers de l'œsophage, de l'ovaire, et du pancréas surexpriment soit PD-L1 soit PD-L2 [80]. Les cancers surexprimant le plus PD-L1 sont en premier lieu : le mélanome, le cancer du poumon non à petites cellules-CNPC, et le cancer du rein [49, 81-83]. Dans ces tumeurs, PD-L2 est moins exprimé que PD-L1.

Environ 20 à 40 % des patients atteints de CNPC ont une forte expression de PD-L1, défini par une expression membranaire sur au moins 50 % des cellules tumorales, seuil choisi dans les essais cliniques récents évaluant le pembrolizumab, anticorps ciblant la voie PD-1/PD-L1 [66, 70].

Le couple PD-1/PD-L1 a pour rôle physiologique de réguler négativement la réponse immunitaire. Il agit à différents stades de la maturation lymphocytaire intra-thymique. PD-1 est impliqué dans le développement d'un pool lymphocytaire T matures et dans la tolérogenèse d'origine centrale, en exerçant une pression de sélection négative sur le complexe pré-TCR/CD3 des thymocytes CD4-/CD8- [84].

PD-1 agit également en périphérie à plusieurs niveaux, et notamment sur les clones lymphocytaires auto-réactifs ayant survécu à cette pression de sélection, en supprimant le signal immunitaire activateur. Les cellules présentatrices de l'antigène vont exercer un pouvoir tolérogène par délétion ou anergie des lymphocytes T naïfs, sous la dépendance de l'axe PD-1/PD-L1. Le déficit en PD-1 entraîne a contrario une hyperactivation lymphocytaire T auto-réactive [85].

PD-1/PD-L1 sont exprimés par les lymphocytes T reg CD4+Foxp3+. Le TGF-β induit une différentiation de ces CD4+Foxp3+ naïfs en lymphocytes T régulateurs, et l'interaction entre PD-1 et PD-L1 favorise leur survie dans le temps [86].

PD-1 régule par ailleurs la fonction effectrice et le maintien des lymphocyte B activés, en permettant le maintien fonctionnel des plasmocytes médullaires IgG+, et en agissant sur la commutation des classes

d'immunoglobulines et l'hyper mutation somatique [87, 88].

L'expression physiopathologique de PD-L1 est sous la dépendance de mécanismes de contrôle intrinsèque et extrinsèque [48].

Les mécanismes de contrôle intrinsèque comprennent l'inactivation du gène suppresseur de tumeur PTEN conduisant à l'activation de la voie PI3K/AKT et du facteur de transcription STAT3, l'activation de la voie de signalisation de l'oncoprotéine EML4-ALK, via STAT3 et ERK [89-91]. L'activation simultanée de KRAS et l'inactivation de Lkb1/STK11 (kinase hépatique B1, aussi nommée sérine-thréonine kinase 11, correspondant à un gène suppresseur de tumeur présent chez tous les eucaryotes) sont impliquées dans la formation des carcinomes épidermoïdes pulmonaires, tandis que l'inactivation de PTEN et de Lkb1 conduisent au développement de carcinomes épidermoïdes pulmonaires avec une surexpression de PD-L1 [91].

La stimulation du TCR et du BCR (B cell receptor) induit l'expression de PD-L1 sur les lymphocytes T et B. Les interleukines IL-2, IL-7, et IL-15 induisent l'expression de PD-L1 sur les monocytes. L'interleukine IL-21 accentue l'expression de PD-L1 sur les monocytes mais pas sur les lymphocytes T. L'IL-21 est la seule à favoriser l'expression de PD-L1 sur les lymphocytes B. L'IFN-γ induit l'expression de PD-L1 sur les lymphocytes T CD8+, les monocytes, et les cellules dendritiques [92, 93].

Il a été démontré que l'hypoxie tissulaire induit une surexpression de PD-L1 sur les cellules tumorales et sur les cellules dendritiques myéloïdes, en empruntant les voies de signalisation médiées par HIF-1α. Dans une tumeur, la néoangiogenèse erratique, le développement du stroma, et la croissance tumorale, sont propices à cette hypoxie [94, 95].

Un modèle murin a été utilisé pour étayer la notion d'échappement tumoral dans les adénocarcinomes pulmonaires. Il a été récemment montré que l'activation de la signalisation dépendante d'EGFR induit la surexpression de PD-L1 [96]. Dans ce modèle, un traitement inhibiteur spécifique d'EGFR était administré, ce qui diminuait l'expression de PD-L1 induite par mutation activatrice d'EGFR, et a permis de restaurer la fonction des lymphocytes T et d'assister à une survie prolongée des souris atteintes d'adénocarcinome pulmonaire exprimant une mutation d'EGFR [96]. Cette étude a démontré pour la première fois l'existence d'un mécanisme d'induction de l'expression de PD-L1 oncogène-dépendante, pouvant jouer un rôle dans l'échappement tumoral des adénocarcinomes pulmonaires. Cependant il a été également montré récemment, lors d'une étude clinique, que les altérations de l'EGFR ou de ALK sont associées une expression moindre de PD-L1 et à un infiltrat en CD8 plus faible [97].

Les cellules cancéreuses surexpriment PD-L1 et PD-L2, lesquels se lient au récepteur PD-1 des lymphocytes T, inhibant leur activation et induisant l'échappement immunitaire de la tumeur. La voie PD-1/PD-L1 régule l'immunosuppression par plusieurs mécanismes : induction de l'apoptose des lymphocytes T activés ; anergie lymphocytaire T ; stimulation des cellules T régulatrices ; inhibition de la prolifération des lymphocytes T ; inhibition de l'activation des lymphocytes T ainsi que de la production de l'IL-2.

Les anticorps bloquant PD-1 ou PD-L1 ont fait leur apparition dans l'arsenal thérapeutique du cancer broncho-pulmonaire avancé. L'activité clinique de ces traitements est liée à l'expression de PD-L1 et de l'infiltration T CD8 dans le microenvironnement tumoral [69].

Le blocage thérapeutique de la voie PD-1/PD-L1 modifie le microenvironnement tumoral et stimule la réponse auto-immune endogène antitumorale (Figure 3) [98]. Plusieurs anticorps ciblant PD-1 sont actuellement disponibles : nivolumab (Bristol-Meyers Squibb), qui est un anticorps monoclonal humain de IgG4 ; le pembrolizumab (Merck) qui est un anticorps monoclonal humanisé hautement sélectif ayant une activité contre PD-1 et contenant une mutation à C228P. En 2e ligne de traitement, le nivolumab a montré un taux de réponse de 19 % dans les CNPC prétraités avec une survie globale à 1 an de 51 % versus 39 % avec le docetaxel, et à 18 mois de 39 % versus 23 % avec le docétaxel [99].

Récemment, un essai clinique multicentrique de phase III a validé l'utilisation du pembrolizumab pour le traitement en 1e ligne des patients atteints de CBNPC avancé exprimant PD-L1 [70].

Une autre approche basée sur des anticorps bloquant PD-L1, notamment l'atézolizumab (Roche/Genentech) et le durvalumab (AstraZeneca) font également l'objet de

développement clinique avec des résultats prometteurs [100, 101].

L'hypothèse est que l'utilisation de PD-L1 comme cible thérapeutique pourrait être accompagnée de moins de toxicité en partie en modulant sélectivement la réponse immunitaire dans le microenvironnement tumoral, cependant les résultats d'une méta-analyse de 2016 ne montrait pas de différence de toxicité entre ces deux traitements chez des patients traités pour un CNPC [46].

Les anti-CTLA-4 constituent une autre approche d'immunothérapie ciblant les checkpoint de l'immunité : le CD28 situé à la surface du lymphocyte interagit avec ses ligands B7-1 et B7-2 exprimés sur les CPA. CTLA-4, exprimé sur les lymphocytes T auxiliaires, se lie à B7 et exerce un signal de costimulation inhibiteur sur les lymphocytes T cytotoxiques, le CTLA-4 ayant une bien meilleure affinité avec ce ligand que le CD28. Le blocage thérapeutique par Ipilimumab de la voie CTLA-4-B7 a fait ses preuves d'efficacité en traitement du mélanome métastatique [102, 103]. Le tremelimumab est placé en tant que molécule orpheline pour la prise en charge du mésothéliome [104]. L'utilisation des anti-CTLA-4 dans le cancer du poumon fait l'objet d'essais cliniques, notamment en association avec les anti-PD-1, afin de combiner la levée d'inhibition sur les lymphocytes T cytotoxiques par synergie d'action sur les checkpoints, et de favoriser la mort cellulaire des lymphocytes T régulateurs qui peut s'observer avec certaines molécules anti-CTLA-4 [105-107].

Le blocage thérapeutique de la voie PD-1/PD-L1 dans les CPNPC ne s'avère efficace (en première ligne ou en deuxième ligne de traitement) que pour certains patients. Le défi actuel est de pouvoir distinguer la population des patients répondant à une telle approche thérapeutique. Ainsi se pose la question d'utiliser des biomarqueurs capables de prédire cette réponse thérapeutique. Ces biomarqueurs pourraient être utilisés comme test « compagnon » ou comme test « complémentaire » d'une molécule thérapeutique [108]. De plus, l'efficacité du blocage de la voie PD-1/PD-L1 est tempérée par la survenue d'effets indésirables rares mais potentiellement graves. Par ailleurs, le coût très élevé des anticorps monoclonaux lance un défi éthique et les enjeux économiques sont réels, ce qui impose de préciser des biomarqueurs prédictifs du blocage PD-1/PD-L1 afin de sélectionner au mieux les patients cibles [1, 2].

L'expression tumorale de PD-L1 analysée par immunohistochimie représente à ce jour la seule approche à court terme à proposer en oncologie thoracique comme biomarqueur prédictif de l'immunothérapie ciblant l'axe PD-1/PD-L1 [109-111].

Cependant, certains patients ne présentant pas d'expression de PD-L1 peuvent parfois répondre aux anti-PD-1/PD-L1 et à l'inverse il existe un pourcentage assez important de patients exprimant fortement PD-L1 avec d'emblée une résistance au traitement. Un autre écueil est certainement la grande hétérogénéité d'expression tissulaire de PD-L1 qui peut faire sous-estimer le statut PD-L1 sur un échantillonnage biopsique par rapport à l'ensemble de la tumeur [112, 113].

Ainsi ces tests compagnons ou complémentaires basés sur l'immunohistochimie ne sont pas parfaits mais devront être probablement largement utilisés, en particulier lorsque les différentes molécules vont obtenir une AMM, notamment pour une première ligne de traitement [109].

V. PERSPECTIVES

Longtemps restée marginale, avec ses adeptes et ses détracteurs, l'immunothérapie fait aujourd'hui la preuve tangible de son efficacité. Alors que l'importance de la charge mutationnelle des tumeurs a longtemps été associée à l'idée conceptuelle d'un caractère pronostic péjoratif, l'immunothérapie utilise cette charge mutationnelle pour activer la réponse immune adaptative, boostée par la diversité antigénique tumorale [114]. Cette efficacité reste intrinsèquement liée à l'état d'immunogénicité de la tumeur. La tumeur devrait donc être considérée non plus comme une entité propre, mais devrait être étudiée dans son microenvironnement et dans sa relation avec le système immunitaire de l'hôte, intégrée dans l'histoire clinique et thérapeutique du malade. La mise en évidence de biomarqueurs prédictifs intégrés afin d'établir un « immunoscore » représente un facteur pronostique majeur prédictif de réponse thérapeutique et de survie des patients [2]. Différents marqueurs reflétant une immunité antitumorale préexistante au traitement tels l'infiltration par les lymphocytes T CD8+ exprimant PD-1 et l'expression intra-tumorale d'IFN-γ semblent être également corrélés à une meilleure réponse clinique aux anticorps anti-PD-1/PD-L1 [115]. L'équipe de Galon a défini un immunoscore

appliqué à la pathologie tumorale colique, dont l'impact pronostique pourrait être plus important que celui de la classification TNM seule, s'intéressant en particulier aux composantes de l'infiltrat immun du micro-environnement tumoral [47]. L'équipe de Teng a étudié l'infiltrat lymphocytaire tumoral (TIL) et son association ou non à l'expression de PD-L1, afin de distinguer quatre types de micro-environnements tumoraux : PD-L1+/TIL+, PD-L1-/TIL-, PD-L1+/TIL-, PD-L1-/TIL+, associés à une valeur prédictive de réponse (tumeur dite « chaude ») ou de non-réponse (tumeur dite « froide ») à l'immunothérapie [116]. Le séquençage génomique à haut débit des tumeurs est quant à lui en passe de bouleverser le paysage oncothéranostique et pourrait permettre d'affiner davantage « l'immunoscore ». Une grande hétérogénéité génétique a été observée entre les tumeurs bronchiques des patients fumeurs et non-fumeurs, et cette différence de profils mutationnels semble prédire la sensibilité au blocage de l'axe PD-1/PD-L1 chez des patients atteints de CNPC [117, 118]. Concernant les nouvelles modalités d'immunothérapie, les recherches actuelles portent sur la combinaison de plusieurs immunothérapies entre elles, ou avec la chimiothérapie, ainsi que sur l'association entre inhibiteurs de PD-1/PD-L1 et radiothérapie [119, 120]. Le risque de ces approches combinées est la toxicité, à l'image de ce qui a été observé avec les combinaisons de thérapies ciblées. Cependant, les rationnels biologiques pour de telles combinaisons sont forts [121]. Des anticorps contre d'autres molécules de costimulation inhibitrices (Lag3, Tim-3, etc.) ou activatrices (OX40) sont en cours de développement clinique seuls ou en association avec le blocage de la voie PD-1/PD-L1 [122]. L'immunothérapie active, par vaccination antitumorale permet, par injection d'antigènes spécifiques, un afflux de lymphocytes T CD8+ au siège de la tumeur. Cette piste thérapeutique nécessite néanmoins de définir les antigènes pertinents. La preuve d'efficacité existe en pratique clinique, le vaccin sipuleucel bénéficiant d'une autorisation de la FDA. Cependant, le coup reste prohibitif lorsqu'il est mis en rapport avec le bénéfice relatif sur la survie. Les associations de traitement par vaccination et immunothérapie passive nécessitent des modèles précliniques pour anticiper les effets secondaires potentiels [2]. Le développement des CAR-T cells (chimeric antigen receptor T cell), véritables « lymphocytes T armés » par un anticorps reconnaissant un antigène des lymphocytes B, pourrait ouvrir de nouvelles voies thérapeutiques pour les patients non répondeurs à l'immunothérapie passive, par le biais d'une immunothérapie adoptive. Les travaux de Carl June ont démontré l'efficacité de ce traitement pour la prise en charge de certaines leucémies lymphoblastiques et lymphoïdes chroniques. L'extension de ce type de traitement à d'autres cibles tumorales est une piste majeure de recherche. Les enjeux économiques seront cependant à considérer attentivement [123, 124].

En conclusion, le développement de l'immunothérapie pose de nombreux défis afin de l'utiliser au mieux dans la stratégie de lutte contre le cancer et nécessitera de s'appuyer sur des données de recherche préclinique et translationnelle encore insuffisantes.

Références

1. Lawrence MS, Stojanov P, Polak P, et al. Mutational heterogeneity in cancer and the search for new cancer-associated genes. Nature 2013-6-16;499:214-8.
2. Zitvogel L, Hannani D, François M. Immunothérapie des cancers au troisième millénaire: Edp Sciences; 2015.
3. Panayi GS, Corrigall VM, Henderson B. Stress cytokines: pivotal proteins in immune regulatory networks; Opinion. Curr Opin Immunol. 2004 Aug;16(4):531-4.
4. Medzhitov R, Preston-Hurlburt P, Janeway CA. A human homologue of the Drosophila Toll protein signals activation of adaptive immunity. Nature 1997;388:394-7.
5. Janeway CA. Approaching the asymptote? Evolution and revolution in immunology. Cold Spring Harb Symp Quant Biol 1989;54:1-13.
6. Steinman RM. Decisions About Dendritic Cells: Past, Present, and Future. Annu Rev Immunol. 2012 2012-04-23;30:1-22.
7. Granier C, Karaki S, Roussel H, et al. Immunothérapie des cancers : rationnel et avancées récentes. Rev Med Interne 2016;37:694-700.
8. Shaw AT, Kim D-W, Nakagawa K, et al. Crizotinib versus Chemotherapy in Advanced ALK -Positive Lung Cancer. N Engl J Med 2013;368:2385-94.
9. Sandler A, Gray R, Perry MC, et al. Paclitaxel–carboplatin alone or with bevacizumab for non–small-cell lung cancer. N Engl J Med 2006;355:2542–50.
10. van der Wekken AJ, Saber A, Hiltermann TJN, et al. Resistance mechanisms after tyrosine kinase inhibitors

afatinib and crizotinib in non-small cell lung cancer, a review of the literature. Crit Rev Oncol Hematol 2016 ;100:107-16.
11. Keedy VL, Temin S, Somerfield MR, et al. American Society of Clinical Oncology Provisional Clinical Opinion: Epidermal Growth Factor Receptor (EGFR) Mutation Testing for Patients With Advanced Non-Small-Cell Lung Cancer Considering First-Line EGFR Tyrosine Kinase Inhibitor Therapy. J Clin Oncol 2011;29:2121-7.
12. Soda M, Choi YL, Enomoto M, et al. Identification of the transforming EML4-ALK fusion gene in non-small-cell lung cancer. Nature 2007 ;448:561-6.
13. Balkwill F, Mantovani A. Inflammation and cancer: back to Virchow? Lancet 2001 ;357:539-45.
14. Hughes PE, Caenepeel S, Wu LC. Targeted Therapy and Checkpoint Immunotherapy Combinations for the Treatment of Cancer. Trends Immunol 2016 ;37:462-76.
15. Chen Daniel S, Mellman I. Oncology Meets Immunology: The Cancer-Immunity Cycle. Immunity 2013;39:1-10.
16. Muller WA. Localized signals that regulate transendothelial migration. Curr Opin Immunol 2016 ;38:24-9.
17. Schumacher TN, Schreiber RD. Neoantigens in cancer immunotherapy. Science. 2015 April 2, 2015;348:69.
18. Shankaran V, Ikeda H, Bruce AT, et al. IFNgamma and lymphocytes prevent primary tumour development and shape tumour immunogenicity. Nature. 2001 Apr 26, 2001;410:1107-11.
19. Djenidi F, Adam J, Goubar A, et al. CD8+CD103+ tumor-infiltrating lymphocytes are tumor-specific tissue-resident memory T cells and a prognostic factor for survival in lung cancer patients. Journal of Immunology (Baltimore, Md: 1950). 2015 Apr 01, 2015;194:3475-86.
20. Kawai O, Ishii G, Kubota K, et al. Predominant infiltration of macrophages and CD8(+) T Cells in cancer nests is a significant predictor of survival in stage IV nonsmall cell lung cancer. Cancer. 2008 Sep 15, 2008;113:1387-95.
21. Villegas FR, Coca S, Villarrubia VG, et al. Prognostic significance of tumor infiltrating natural killer cells subset CD57 in patients with squamous cell lung cancer. Lung Cancer. 2002 Jan 2002;35:23-8.
22. Fridman WH, Pagès F, Sautès-Fridman C, et al. The immune contexture in human tumours: impact on clinical outcome. Nature Reviews Cancer. 2012 Mar 15, 2012;12:298-306.
23. Catros V, Toutirais O, Bouet F, et al. [Tgammadelta lymphocytes in oncology: unconventional killer lymphocytes]. Med Sci (Paris). 2010 Feb;26(2):185-91.
24. Bryceson YT, Ljunggren H-G. Tumor cell recognition by the NK cell activating receptor NKG2D. Eur J Immunol. 2008 Nov 2008;38:2957-61.
25. Schreiber RD, Old LJ, Smyth MJ. Cancer immunoediting: integrating immunity's roles in cancer suppression and promotion. Science. 2011 2011;331:1565–70.
26. Matsushita H, Vesely MD, Koboldt DC, et al. Cancer exome analysis reveals a T-cell-dependent mechanism of cancer immunoediting. Nature. 2012 Feb 08, 2012;482:400-4.
27. Dunn GP, Bruce AT, Ikeda H, et al. Cancer immunoediting: from immunosurveillance to tumor escape. Nat Immunol. 2002 November 2002;3:991-8.
28. Dunn GP, Old LJ, Schreiber RD. The three Es of cancer immunoediting. Annu Rev Immunol. 2004 2004;22:329-60.
29. Pardoll D. Does the immune system see tumors as foreign or self? Annu Rev Immunol. 2003 2003;21:807-39.
30. Maio M. Melanoma as a model tumour for immuno-oncology. Ann Oncol. 2012 Sep 2012;23 Suppl 8:viii10-4.
31. Giraldo NA, Becht E, Remark R, et al. The immune contexture of primary and metastatic human tumours. Curr Opin Immunol. 2014 Apr 2014;27:8-15.
32. Joyce JA, Pollard JW. Microenvironmental regulation of metastasis. Nature Reviews Cancer. 2009 Apr 2009;9:239-52.
33. Carlini MJ, De Lorenzo MS, Puricelli L. Cross-talk between tumor cells and the microenvironment at the metastatic niche. Curr Pharm Biothecno. 2011 Nov 2011;12:1900-8.
34. McGranahan N, Furness AJS, Rosenthal R, et al. Clonal neoantigens elicit T cell immunoreactivity and sensitivity to immune checkpoint blockade. Science (New York, NY). 2016 Mar 25, 2016;351:1463-9.
35. Hölzel M, Bovier A, Tüting T. Plasticity of tumour and immune cells: a source of heterogeneity and a cause for therapy resistance? Nature Reviews Cancer. 2013 May 2013;13:365-76.
36. Spranger S, Spaapen RM, Zha Y, et al. Up-Regulation of PD-L1, IDO, and T(regs) in the Melanoma Tumor Microenvironment Is Driven by CD8(+) T Cells. Sci Transl Med. 2013 August 28, 2013;5:200ra116-200ra116.

37. Bos R, Marquardt KL, Cheung J, et al. Functional differences between low- and high-affinity CD8 + T cells in the tumor environment. OncoImmunology. 2012 11/2012;1:1239-47.
38. Fridman W-H, Dieu-Nosjean M-C, Pagès F, et al. The Immune Microenvironment of Human Tumors: General Significance and Clinical Impact. Cancer Microenviron. 2013 8/2013;6:117-22.
39. Willimsky G, Blankenstein T. Sporadic immunogenic tumours avoid destruction by inducing T-cell tolerance. Nature. 2005 Sep 01, 2005;437:141-6.
40. Cerezo-Wallis D, Soengas MS. Understanding Tumor-Antigen Presentation in the New Era of Cancer Immunotherapy. Curr Pharm Des. 2016;22(41):6234-50.
41. Yu F, Sharma S, Edwards J, et al. Dynamic expression of transcription factors T-bet and GATA-3 by regulatory T cells maintains immunotolerance. Nat Immunol. 2015 Feb;16(2):197-206.
42. Lu B, Finn OJ. T-cell death and cancer immune tolerance. Cell Death Differ. 2008 Jan;15(1):70-9.
43. Waldhauer I, Steinle A. NK cells and cancer immunosurveillance. Oncogene. 2008 2008-10-06;27:5932-43.
44. Bauer C, Hees C, Sterzik A, et al. Proapoptotic and antiapoptotic proteins of the Bcl-2 family regulate sensitivity of pancreatic cancer cells toward gemcitabine and T-cell-mediated cytotoxicity. Journal of Immunotherapy (Hagerstown, Md: 1997). 2015 Apr 2015;38:116-26.
45. Prendergast GC, Smith C, Thomas S, et al. Indoleamine 2,3-dioxygenase pathways of pathogenic inflammation and immune escape in cancer. Cancer Immunol Immunother. 2014 Jul 2014;63:721-35.
46. Pillai RN, Behera M, Owonikoko TK, et al. Evaluation of toxicity profile of PD-1 versus PD-L1 inhibitors in non-small cell lung cancer (NSCLC). J Clin Oncol. 2016;34(15_suppl):9035-.
47. Galon J, Mlecnik B, Bindea G, et al. Towards the introduction of the 'Immunoscore' in the classification of malignant tumours. The Journal of Pathology. 2014;232(2):199-209.
48. Pardoll DM. The blockade of immune checkpoints in cancer immunotherapy. Nat Rev Cancer. 2012 2012-3-22;12:252-64.
49. Taube JM, Klein A, Brahmer JR, et al. Association of PD-1, PD-1 Ligands, and Other Features of the Tumor Immune Microenvironment with Response to Anti-PD-1 Therapy. Clin Cancer Res. 2014 2014-10-01;20:5064-74.
50. Topalian SL, Hodi FS, Brahmer JR, et al. Safety, Activity, and Immune Correlates of Anti–PD-1 Antibody in Cancer. N Engl J Med. 2012 2012-06-28;366:2443-54.
51. Carosella ED, Rouas-Freiss N, Tronik-Le Roux D, et al. HLA-G: An Immune Checkpoint Molecule. Adv Immunol. 2015 2015;127:33-144.
52. Sasaki T, Kanaseki T, Shionoya Y, et al. Microenvironmental stresses induce HLA-E/Qa-1 surface expression and thereby reduce CD8(+) T-cell recognition of stressed cells. Eur J Immunol. 2016 Apr 2016;46:929-40.
53. Whiteside TL. The tumor microenvironment and its role in promoting tumor growth. Oncogene. 2008 2008-10-06;27:5904-12.
54. Teicher BA. Transforming growth factor-beta and the immune response to malignant disease. Clin Cancer Res. 2007 Nov 01, 2007;13:6247-51.
55. Domagala-Kulawik J, Osinska I, Hoser G. Mechanisms of immune response regulation in lung cancer. Transl Lung Cancer Res. 2014 Feb 2014;3:15-22.
56. Cortez-Retamozo V, Etzrodt M, Newton A, et al. Origins of tumor-associated macrophages and neutrophils. Proc Natl Acad Sci. 2012 2012-02-14;109:2491-6.
57. Srivastava MK, Andersson Å, Zhu L, et al. Myeloid suppressor cells and immune modulation in lung cancer. Immunotherapy. 2012 Mar 2012;4:291-304.
58. Hattar K, Franz K, Ludwig M, et al. Interactions between neutrophils and non-small cell lung cancer cells: enhancement of tumor proliferation and inflammatory mediator synthesis. Cancer Immunol Immunother. 2014 12/2014;63:1297-306.
59. Ilie M, Hofman V, Ortholan C, et al. Predictive clinical outcome of the intratumoral CD66b-positive neutrophil-to-CD8-positive T-cell ratio in patients with resectable nonsmall cell lung cancer. Cancer. 2012 2012-03-15;118:1726-37.
60. Kim J, Bae J-S. Tumor-Associated Macrophages and Neutrophils in Tumor Microenvironment. Mediators Inflamm. 2016 2016;2016:1-11.
61. Shih J-Y, Yuan A, Chen JJ-W, et al. Tumor-associated macrophage: its role in cancer invasion and metastasis. J Cancer Mol. 2006 2006;2:101–6.
62. Moo-Young TA, Larson JW, Belt BA, et al. Tumor-derived TGF-beta mediates conversion of CD4+Foxp3+ regulatory T cells in a murine model of pancreas cancer. Journal of Immunotherapy (Hagerstown, Md: 1997). 2009 Jan 2009;32:12-21.

63. Pedicord VA, Montalvo W, Leiner IM, et al. Single dose of anti-CTLA-4 enhances CD8+ T-cell memory formation, function, and maintenance. Proc Natl Acad Sci U S A. 2011 Jan 04, 2011;108:266-71.
64. Ortiz ML, Lu L, Ramachandran I, et al. Myeloid-derived suppressor cells in the development of lung cancer. Cancer Immunol Res. 2014 Jan 2014;2:50-8.
65. Gabrilovich DI, Nagaraj S. Myeloid-derived suppressor cells as regulators of the immune system. Nature Reviews Immunology. 2009 Mar 2009;9:162-74.
66. Herbst RS, Soria J-C, Kowanetz M, et al. Predictive correlates of response to the anti-PD-L1 antibody MPDL3280A in cancer patients. Nature. 2014 2014-11-26;515:563-7.
67. Ibrahim R, Stewart R, Shalabi A. PD-L1 Blockade for Cancer Treatment: MEDI4736. Semin Oncol. 2015 06/2015;42:474-83.
68. Soria J-C, Marabelle A, Brahmer JR, et al. Immune Checkpoint Modulation for Non-Small Cell Lung Cancer. Clin Cancer Res. 2015 2015-05-15;21:2256-62.
69. Sunshine J, Taube JM. PD-1/PD-L1 inhibitors. Curr Opin Pharmacol. 2015 08/2015;23:32-8.
70. Reck M, Rodríguez-Abreu D, Robinson AG, et al. Pembrolizumab versus Chemotherapy for PD-L1-Positive Non-Small-Cell Lung Cancer. N Engl J Med. 2016 Nov 10, 2016;375:1823-33.
71. Robert C, Long GV, Brady B, et al. Nivolumab in Previously Untreated Melanoma without BRAF Mutation. N Engl J Med. 2015 2015-01-22;372:320-30.
72. Fehrenbacher L, Spira A, Ballinger M, et al. Atezolizumab versus docetaxel for patients with previously treated non-small-cell lung cancer (POPLAR): a multicentre, open-label, phase 2 randomised controlled trial. Lancet. 2016 04/2016;387:1837-46.
73. Rosenberg JE, Hoffman-Censits J, Powles T, et al. Atezolizumab in patients with locally advanced and metastatic urothelial carcinoma who have progressed following treatment with platinum-based chemotherapy: a single-arm, multicentre, phase 2 trial. Lancet. 2016 05/2016;387:1909-20.
74. Gajewski TF, Schreiber H, Fu Y-X. Innate and adaptive immune cells in the tumor microenvironment. Nat Immunol. 2013 2013-9-18;14:1014-22.
75. Keir ME, Butte MJ, Freeman GJ, et al. PD-1 and Its Ligands in Tolerance and Immunity. Annu Rev Immunol. 2008 04/2008;26:677-704.
76. He J, Hu Y, Hu M, et al. Development of PD-1/PD-L1 Pathway in Tumor Immune Microenvironment and Treatment for Non-Small Cell Lung Cancer. Sci Rep. 2015 2015-8-17;5:13110.
77. Zak Krzysztof M, Kitel R, Przetocka S, et al. Structure of the Complex of Human Programmed Death 1, PD-1, and Its Ligand PD-L1. Structure. 2015 12/2015;23:2341-8.
78. Dong H, Strome SE, Salomao DR, et al. Tumor-associated B7-H1 promotes T-cell apoptosis: A potential mechanism of immune evasion. Nat Med. 2002 2002-6-24.
79. Freeman GJ, Long AJ, Iwai Y, et al. Engagement of the PD-1 immunoinhibitory receptor by a novel B7 family member leads to negative regulation of lymphocyte activation. J Exp Med. 2000 2000;192:1027–34.
80. Okazaki T, Honjo T. PD-1 and PD-1 ligands: from discovery to clinical application. Int Immunol. 2007 2007-06-22;19:813-24.
81. Fourcade J, Sun Z, Benallaoua M, et al. Upregulation of Tim-3 and PD-1 expression is associated with tumor antigen–specific CD8 + T cell dysfunction in melanoma patients. J Exp Med. 2010 2010-09-27;207:2175-86.
82. Konishi J, Yamazaki K, Azuma M, et al. B7-H1 expression on non-small cell lung cancer cells and its relationship with tumor-infiltrating lymphocytes and their PD-1 expression. Clin Cancer Res. 2004 2004;10:5094–100.
83. Parsa AT, Waldron JS, Panner A, et al. Loss of tumor suppressor PTEN function increases B7-H1 expression and immunoresistance in glioma. Nat Med. 2007 1/2007;13:84-8.
84. Nishimura H, Honjo T, Minato N. Facilitation of β selection and modification of positive selection in the thymus of PD-1–deficient mice. J Exp Med. 2000 2000;191:891–8.
85. Martin-Orozco N, Wang Y-H, Yagita H, et al. Cutting Edge: Programed Death (PD) Ligand-1/PD-1 Interaction Is Required for CD8+ T Cell Tolerance to Tissue Antigens. J Immunol. 2006 2006-12-15;177:8291-5.
86. Francisco LM, Salinas VH, Brown KE, et al. PD-L1 regulates the development, maintenance, and function of induced regulatory T cells. J Exp Med. 2009 2009-12-21;206:3015-29.
87. Good-Jacobson KL, Szumilas CG, Chen L, et al. PD-1 regulates germinal center B cell survival and the formation and affinity of long-lived plasma cells. Nat Immunol. 2010 6/2010;11:535-42.
88. Okazaki T, Okazaki I-m, Wang J, et al. PD-1 and LAG-3 inhibitory co-receptors act synergistically to prevent

autoimmunity in mice. J Exp Med. 2011 2011-02-14;208:395-407.
89. Cumberbatch M, Tang X, Beran G, et al. Identification of a Subset of Human Non-Small Cell Lung Cancer Patients with High PI3K and Low PTEN Expression, More Prevalent in Squamous Cell Carcinoma. Clin Cancer Res. 2014 2014-02-01;20:595-603.
90. Ota K, Azuma K, Kawahara A, et al. Induction of PD-L1 Expression by the EML4-ALK Oncoprotein and Downstream Signaling Pathways in Non-Small Cell Lung Cancer. Clin Cancer Res. 2015 2015-09-01;21:4014-21.
91. Xu C, Fillmore Christine M, et al. Loss of Lkb1 and Pten Leads to Lung Squamous Cell Carcinoma with Elevated PD-L1 Expression. Cancer Cell. 2014 05/2014;25:590-604.
92. Bennett F, Luxenberg D, Ling V, et al. Program Death-1 Engagement Upon TCR Activation Has Distinct Effects on Costimulation and Cytokine-Driven Proliferation: Attenuation of ICOS, IL-4, and IL-21, But Not CD28, IL-7, and IL-15 Responses. J Immunol. 2003 2003-01-15;170:711-8.
93. Kinter AL, Godbout EJ, McNally JP, et al. The common γ-chain cytokines IL-2, IL-7, IL-15, and IL-21 induce the expression of programmed death-1 and its ligands. J Immunol. 2008 2008;181:6738–46.
94. Barsoum IB, Smallwood CA, Siemens DR, et al. A Mechanism of Hypoxia-Mediated Escape from Adaptive Immunity in Cancer Cells. Cancer Res. 2014 2014-02-01;74:665-74.
95. Noman MZ, Desantis G, Janji B, et al. PD-L1 is a novel direct target of HIF-1α, and its blockade under hypoxia enhanced MDSC-mediated T cell activation. J Exp Med. 2014 2014-05-05;211:781-90.
96. Akbay EA, Koyama S, Carretero J, et al. Activation of the PD-1 Pathway Contributes to Immune Escape in EGFR-Driven Lung Tumors. Cancer discov. 2013 2013-12-01;3:1355-63.
97. Gainor JF, Shaw AT, Sequist LV, et al. EGFR Mutations and ALK Rearrangements Are Associated with Low Response Rates to PD-1 Pathway Blockade in Non-Small Cell Lung Cancer: A Retrospective Analysis. Clin Cancer Res. 2016 Sep 15;22(18):4585-93.
98. Byun DJ, Wolchok JD, Rosenberg LM, et al. Cancer immunotherapy - immune checkpoint blockade and associated endocrinopathies. Nat Rev Endocrinol. 2017 Jan 20.
99. Borghaei H, Paz-Ares L, Horn L, et al. Nivolumab versus Docetaxel in Advanced Nonsquamous Non–Small-Cell Lung Cancer. N Engl J Med. 2015 2015-10-22;373:1627-39.
100. Rittmeyer A, Barlesi F, Waterkamp D, et al. Atezolizumab versus docetaxel in patients with previously treated non-small-cell lung cancer (OAK): a phase 3, open-label, multicentre randomised controlled trial. Lancet. 2016 12/2016.
101. Planchard D, Yokoi T, McCleod MJ, et al. A Phase III Study of Durvalumab (MEDI4736) With or Without Tremelimumab for Previously Treated Patients With Advanced NSCLC: Rationale and Protocol Design of the ARCTIC Study. Clin Lung Cancer. 2016 May 2016;17:232-6.e1.
102. Hodi FS, O'Day SJ, McDermott DF, et al. Improved survival with ipilimumab in patients with metastatic melanoma. N Engl J Med. 2010 Aug 19;363(8):711-23.
103. Robert C, Thomas L, Bondarenko I, et al. Ipilimumab plus dacarbazine for previously untreated metastatic melanoma. N Engl J Med. 2011 Jun 30;364(26):2517-26.
104. Guazzelli A, Hussain M, Krstic-Demonacos M, et al. Tremelimumab for the treatment of malignant mesothelioma. Expert Opin Biol Ther. 2015;15(12):1819-29.
105. Romano E, Kusio-Kobialka M, Foukas PG, et al. Ipilimumab-dependent cell-mediated cytotoxicity of regulatory T cells ex vivo by nonclassical monocytes in melanoma patients. Proc Natl Acad Sci U S A. 2015 May 12;112(19):6140-5.
106. Antonia SJ, Lopez-Martin JA, Bendell J, et al. Nivolumab alone and nivolumab plus ipilimumab in recurrent small-cell lung cancer (CheckMate 032): a multicentre, open-label, phase 1/2 trial. Lancet Oncol. 2016 Jul;17(7):883-95.
107. Hellmann MD, Rizvi NA, Goldman JW, et al. Nivolumab plus ipilimumab as first-line treatment for advanced non-small-cell lung cancer (CheckMate 012): results of an open-label, phase 1, multicohort study. Lancet Oncol. 2017 Jan;18(1):31-41.
108. Ilie M, Hofman V, Dietel M, et al. Assessment of the PD-L1 status by immunohistochemistry: challenges and perspectives for therapeutic strategies in lung cancer patients. Virchows Arch. 2016 May 2016;468:511-25.
109. Hofman V, Ilie M, Long E, et al. [Issues and current limits for immunohistochemical assessment of PD-L1 status in bronchial biopsies]. Bull Cancer (Paris). 2016 Apr 2016;103:368-80.

110. Grigg C, Rizvi NA. PD-L1 biomarker testing for non-small cell lung cancer: truth or fiction? J Immunother Cancer. 2016 12/2016;4.
111. Shien K, Papadimitrakopoulou VA, Wistuba II. Predictive biomarkers of response to PD-1/PD-L1 immune checkpoint inhibitors in non–small cell lung cancer. Lung Cancer. 2016 09/2016;99:79-87.
112. Ilie M, Long-Mira E, Bence C, et al. Comparative study of the PD-L1 status between surgically resected specimens and matched biopsies of NSCLC patients reveal major discordances: a potential issue for anti-PD-L1 therapeutic strategies. Ann Oncol. 2016 Jan 2016;27:147-53.
113. McLaughlin J, Han G, Schalper KA, et al. Quantitative Assessment of the Heterogeneity of PD-L1 Expression in Non-Small-Cell Lung Cancer. JAMA Oncol. 2016 Jan 2016;2:46-54.
114. Lyford-Pike S, Peng S, Young GD, et al. Evidence for a role of the PD-1:PD-L1 pathway in immune resistance of HPV-associated head and neck squamous cell carcinoma. Cancer Res. 2013 March 15, 2013;73:1733-41.
115. Tumeh PC, Harview CL, Yearley JH, et al. PD-1 blockade induces responses by inhibiting adaptive immune resistance. Nature. 2014 2014-11-26;515:568-71.
116. Teng MW, Ngiow SF, Ribas A, et al. Classifying Cancers Based on T-cell Infiltration and PD-L1. Cancer Res. 2015 Jun 01;75(11):2139-45.
117. Bossé Y, Postma DS, Sin DD, et al. Molecular Signature of Smoking in Human Lung Tissues. Cancer Res. 2012 July 31, 2012;72:3753.
118. Rizvi NA, Hellmann MD, Snyder A, et al. Mutational landscape determines sensitivity to PD-1 blockade in non–small cell lung cancer. Science (New York, NY). 2015 April 3, 2015;348:124-8.
119. Rizvi NA, Hellmann MD, Brahmer JR, et al. Nivolumab in Combination With Platinum-Based Doublet Chemotherapy for First-Line Treatment of Advanced Non-Small-Cell Lung Cancer. J Clin Oncol. 2016 2016-09-01;34:2969-79.
120. Seyedin SN, Schoenhals JE, Lee DA, et al. Strategies for combining immunotherapy with radiation for anticancer therapy. Immunotherapy. 2015 2015;7:967-80.
121. Mellman I, Coukos G, Dranoff G. Cancer immunotherapy comes of age. Nature. 2011 2011-12-21;480:480-9.
122. Thomas LJ, Vitale L, O'Neill T, et al. Development of a Novel Antibody-Drug Conjugate for the Potential Treatment of Ovarian, Lung, and Renal Cell Carcinoma Expressing TIM-1. Mol Cancer Ther. 2016 Dec 2016;15:2946-54.
123. Fraietta JA, Beckwith KA, Patel PR, et al. Ibrutinib enhances chimeric antigen receptor T-cell engraftment and efficacy in leukemia. Blood. 2016 2016;127:1117–27.
124. June CH. Remote Controlled CARs: Towards a Safer Therapy for Leukemia. Cancer Immunol Res. 2016 2016-08-01;4:643-.

LEGENDES DES FIGURES

Figure 1. Le cycle de l'immunité contre le cancer (d'après Chen et Mellman [13])

1) Les antigènes tumoraux (en rouge) sont relargués dans la circulation par des cellules tumorales immunogènes (en gris). 2) Ces antigènes sont interceptés par les cellules présentatrices d'antigène (CPA) qui rejoignent les organes lymphoïdes secondaires. 3) La présentation antigénique aux lymphocytes T naïfs permet leur maturation intra-ganglionnaire pour devenir des lymphocytes T cytotoxiques CD8 spécifiques. 4) Ces lymphocytes T CD8 cytotoxiques (en violet) migrent dans le lit tumoral, 5) infiltrent le microenvironnement tumoral, 6) lorsqu'ils reconnaissent spécifiquement les cellules tumorales, et 7) les éliminent (en magenta). La cytolyse tumorale induit le relargage de nouveaux antigènes tumoraux ce qui amplifie la présentation antigénique et la poursuite du cycle de l'immunité contre le cancer. A la marge de ce cycle certaines cellules tumorales peu immunogènes (en beige) ne sont pas détectées par le système immunitaire et échappent à l'immunosurveillance.

Figure 2. La théorie constituant les 3 « E » de l'immunosurveillance [d'après Dunn et coll. (24, 25)].

- ELIMINATION : Le système immunitaire est capable de distinguer les cellules tumorales (en gris) des cellules

saines (en bleu clair) et de les éliminer, alors que la tumeur est encore indétectable cliniquement. Les cellules immunes (ex ; NK, CD8, CD4, T γδ) infiltrent le microenvironnement tumoral. Les cellules NK appartiennent à l'immunité innée, elles expriment des récepteurs cytotoxiques et ont la capacité de mobiliser les cellules de l'immunité adaptative. La réponse lymphocytaire adaptative T médiée, sur le socle de l'interaction antigène-CD4-CD8, induit une cytotoxicité CD8 antitumorale spécifique et efficace. Certaines cellules tumorales peu immunogènes (en vert), demeurent invisibles au système immunitaire, tout en restant en dormance.

- EQUILIBRE : Une pression de sélection s'exerce sur le contingent tumoral et des cellules tumorales résistantes à l'immunosurveillance (en rouge) émergent, par le biais de mutations et /ou de défaillance du processus d'immunosurveillance. Le système immunitaire ne parvient pas à détecter ces cellules.

- ECHAPPEMENT : Un climat d'immunotolérance s'installe suite au recrutement par les cellules tumorales de cellules inflammatoires immunosuppressives telles que les cellules myéloïdes suppressives, T régulatrices, neutrophiles type N2, macrophages types M2, lymphocytes T γδ propices à la tumorigenèse. La tumeur devient détectable cliniquement.

Figure 3. Mécanismes d'action des agents anti-CTLA4, PD-1 et PD-L1 [D'après Byun et coll. (98)].

Le récepteur des cellules T (TCR) se lie au complexe majeur d'histocompatibilité (CMH) au contact d'une cellule présentatrice d'antigène (CPA), afin d'activer le lymphocyte T CD8 (panel supérieur). B7, ligand co-stimulateur, se lie au récepteur CD28 exprimé par le lymphocyte T CD8. L'interaction entre B7 et CTLA-4 implique un rétrocontrôle négatif sur l'activation du lymphocyte T CD8 médiée par le couple CMH-TCR. Le blocage thérapeutique de CTLA-4 par l'Ipilimumab (panel inférieur) permet de supprimer le rétrocontrôle négatif et d'augmenter indirectement l'activation des lymphocytes T.

Le récepteur de costimulation inhibiteur PD-1, après liaison avec son ligand PD-L1, inhibe l'activation des lymphocytes T (panel supérieur). Le blocage de PD-1 (Pembrolizumab, Nivolumab) ou de PD-L1 (Atezolizumab, Durvalumab) stimule la réponse auto-immune endogène antitumorale (panel inférieur).

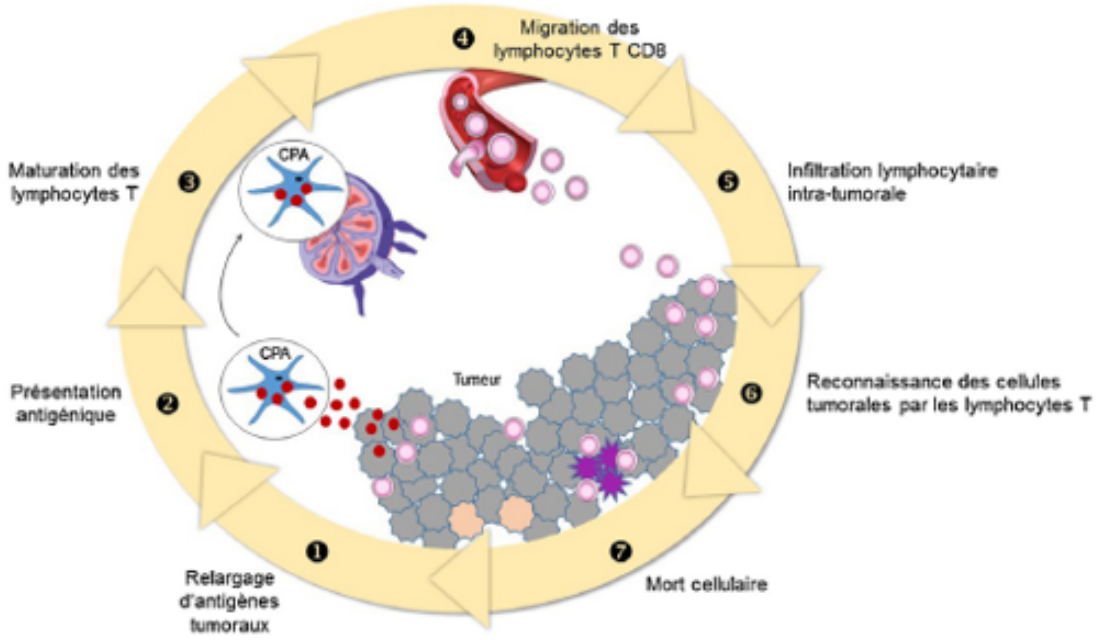

Figure 1

Figure 2

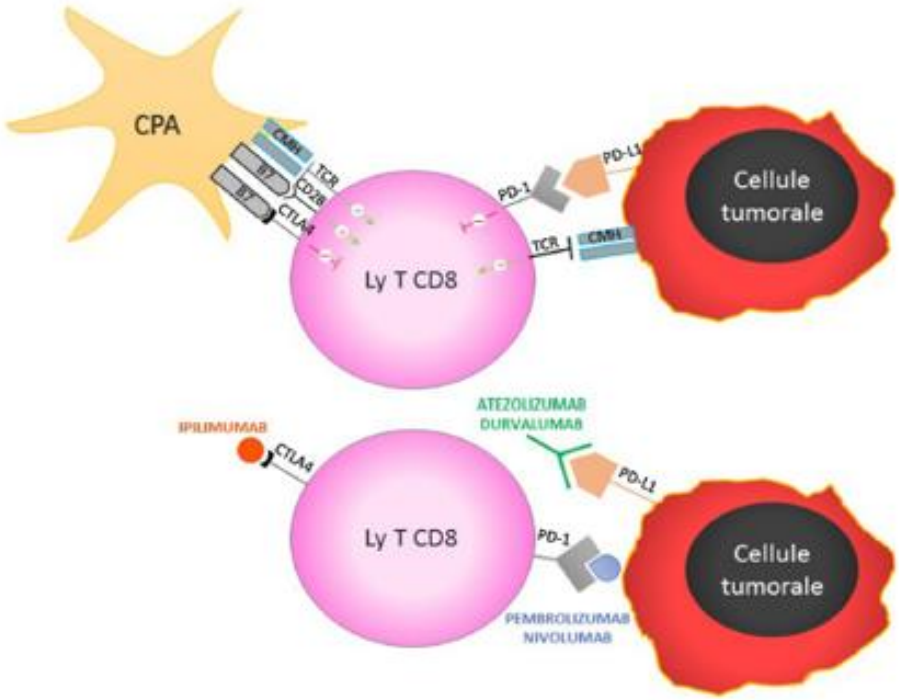

Figure 3

B. Revue de la littérature annexe N°2. Rationnel biologique de l'immunothérapie du cancer bronchique non à petites cellules

Articlé publié (Current Molecular Medecine 2017;17(8):527-540. doi: 10.2174/1566524018666180222114038)

Immunotherapy in solid tumors: Biological principles and future opportunities

Marius Ilie*[a,b], Jonathan Benzaquen*[b,c], Veronique Hofman[a,b], Sandra Lassalle[a,b], Nathalie Yazbeck [b], Sylvie Leroy[c], Simon Heeke [b], Coraline Bence[a], Baharia Mograbi[b], Nicolas Glaichenhaus[d], Charles-Hugo Marquette[b,c] and Paul Hofman[a,b]

[a]University Cote d'Azur, Nice Hospital, FHU OncoAge, Laboratory of Clinical and Experimental Pathology and Hospital-related Biobank (BB-0033-00025), 06001 Nice, France
[b]University Cote d'Azur, Inserm U1081/CNRS UMR 7284, Institute for Research on Cancer and Aging, Comprehensive Cancer Center Antoine Lacassagne, Nice, France
[c]University Cote d'Azur, Nice Hospital, FHU OncoAge, Pneumology Department, 06000 Nice, France
[d]University Cote d'Azur, FHU OncoAge, Cellular and Molecular Pharmacology Institute CNRS, INSERM, Valbonne, France

*Equally contribution

Abstract

Immunotherapy aims to amplify the anticancer immune response through activation of the lymphocytic response raised against several tumor antigens. Immunosurveillance may modify the immunogenicity of tumors. Regulatory and inhibitory costimulatory molecules regulate the activation of anti-tumor T lymphocytes. PD-1/PD-L1 blockade restores the anti-tumor activity of T-cells, forcing them to leave their quiescent state. Identifying biomarkers that could be used for predicting response to immunotherapy represents a major challenge. Highthroughput sequencing of tumors could refine the "immunoscore." Intra-tumor T-cell receptors, in particular the CD3 variable domain are promising biomarkers. Therapies combining several immunotherapies without or with chemotherapy and radiotherapy, and antibodies against other co-stimulatory molecules, are under development. Active immunotherapy by anti-tumor vaccination and adoptive immunotherapy by development of CAR–T cells could open new therapeutic ways for patients who do not exhibit a clinical response to passive immunotherapy. Numerous challenges still remain in developing research approaches that lead to the elaboration of novel immunotherapies.

Key Words: NSCLC, immunotherapy, immunosurveillance, immune escape, PD-1, PD-L1

Introduction :

The treatment of lung cancer has evolved substantially over the past fifteen years, notably as the result of the development of inhibitors targeting oncogenic signaling pathways, in particular tyrosine kinase inhibitors of the EGFR (epidermal growth factor receptor) pathway and inhibitors of ALK [1, 2] These molecules can induce a major clinical response in certain types of tumors expressing oncogenic targets. However, these responses are transitory, eventually resulting in tumor escape and disease relapse [3]. In addition, only a limited number of patients with tumors who exhibit specific EGFR (approximately 10 to 15%) or ALK (3 to 5%) anomalies have shown a beneficial response [4, 5]. While lung cancer was not considered to be an « immunogenic » cancer until recently, the discovery of antigens associated to lung tumors has demonstrated its « immunogenic » character [6, 7]. The demonstration that immune cells were present in the tumor microenvironment and that some of them recognized tumor antigens has underpinned and supported the hypothesis that bronchial cancer is « immunogenic ». A triangular relationship exists between the tumor, the immune system and the tumor microenvironment, a relationship that determines the tumor's control and escape mechanisms throughout the course of the disease [6, 7]. This dynamic situation can be favorably modified by immunotherapies targeting the tumor microenvironment. For example, various molecules have been administered to patients with advanced stage non-small cell lung cancer (NSCLC) who were resistant to several lines of chemotherapy, and have resulted in remarkable response rates with, in particular, long-term responses [8]. Immunotherapy aims to amplify the normal anti-tumor immune response directed against cancer through an effector memory lymphocyte response directed against dominant antigens of cancer patients. To be effective, the immunity must include activation of specific CD4+ and CD8+ lymphocytes and probably the stimulation of innate immunity [6, 7]. The immune system is composed of several types of cells that can react - and eventually eliminate - not only infectious agents but also « abnormal » cells such as cancer cells. The cells of the immune system are divided into two classes: those of innate and adaptive immunity. Innate immune cells, including Natural Killer (NK) cells, macrophages and neutrophils, react very quickly and thus constitute the first line of defense of human body. Among innate immune cells, NK cells play a critical role in the destruction of tumor cells. NK cell activation is regulated by various activating, inhibitory, chemotactic, cytokine and adhesion receptors. When activated, NK cells can kill tumor cells and induce the release of cytoplasmic stress molecules that eventually induce the production of IL-12 by macrophages and dendritic cells and further activate the adaptive immune system [9]. Activated B and T lymphocytes are adaptive immune cells that can persist in an organism for months and even years and are therefore responsible of immunological memory [10]. In exchange, innate immune cells that recognize molecular structures present exclusively on microorganisms or on "stressed" cells, T lymphocytes recognize protein-derived antigenic peptides presented at the cell surface by the molecules of the major histocompatibility complex (MHC). Once activated, T lymphocytes proliferate and differentiate into effector cells such as cytotoxic T lymphocytes CD8+, memory T cells (CD4+/CD8+CCR7+CD45RO) or regulatory T lymphocytes (Treg; CD4+Foxp3+CD25+). In order to limit their expansion and their activity these cells possess negative feedback mechanisms, « immune checkpoints », which restrain their activity over time and thereby avoiding tissue damage [11]. Experimental data have shown that innate and adaptive immune cells monitor tumor development [12]. This immune surveillance involves not only the recognition by T lymphocytes of tumor antigens but also the activation of innate immune cells. When efficient, this process detects tumor cells as soon as they appear and results in either destruction before any clinical revelation or the maintenance in a dormant unchanged state. However, tumors can escape this surveillance through a process of selection of « edited » tumor cells that are poorly immunogenic or resistant to immunosurveillance. Strategies to enhance the efficacy of immunotherapy consider immune escape mechanisms exploited by cancer [6, 7, 13]. Finally, considering the strengths and weaknesses of target therapy and immunotherapy in the fight against cancer development and progression, it is obvious that their combination may be synergistic to destroy cancer cells. In this context, different properties of targeted therapy can enhance the effects of immunotherapy, such as 1) an increase in the expression of death receptors and a diminution of survival signals that sensitizes malignant cells to immune-mediated death, 2) trigger activation of memory T-cells, 3) induce differentiation of T-cells, and 4) promote of dendritic cell maturation. Targeted therapies can break the oncogene addiction and then induce a potentiation of the immune response against cancer cells and facilitate tumor clearance

by T cells. However, responses to combination of both immunotherapy and targeted therapy in cancer patients are under evaluation, considering that the intensification of the response might lead to higher toxicity, and that the appropriate dose of the different molecules, timing and best sequence for treatment scheme are mandatory in order to achieve successful results [14].

The role of the immune system in tumor control

The key steps of an efficient anti-tumor immune response have been first described and illustrated by Dan Chen and Ira Mellman as the « cancer immunity cycle » (Figure 1) [15, 16]. Briefly, tumor antigens that are expressed during oncogenesis are captured by dendritic cells in the tumor microenvironment. Once activated, dendritic cells migrate through efferent lymphatic vessels to tumor draining lymphatic nodes, present tumor antigens to T lymphocytes, resulting in their activation and differentiation into effector T lymphocytes. Effector T lymphocytes exit lymphatic nodes through efferent lymphatic vessels, enter the blood flow, and eventually the tumor bed by extravasation through the blood vessels that irrigate the tumor [17]. Once mature activated T lymphocytes have infiltrated the tumor bed, they can recognize and destroy the tumor cells. This results in the release of additional tumor antigens and immune response amplification [13, 18]. Tumor cell lysis by T lymphocytes brings into play several molecular mechanisms including: i) shedding of cytotoxic molecules (perforin, granzyme) from preformed granules and ii) activation of signaling pathways downstream of members of the TNF receptor family, notably of Fas and Trail [13]. Murine experimental models have shown that T lymphocytes play a fundamental role in regulating tumor growth, whether it occurs spontaneously or subsequent to exposure to a carcinogen [19]. In addition, clinical studies have shown that the presence of tumor-infiltrating memory T lymphocytes, Th1 lymphocytes, cytotoxic CD8+ lymphocytes and CD57+ NK cells is associated with longer survival of cancer patients, including NSCLC, therefore suggesting that these cells play a critical role in controlling tumor progression [20-23]. Studies aimed at investigating the role of immune cells in cancer surveillance have pointed out the critical role of immune cells types involved in innate immune response, including NK cells, macrophages, dendritic cells, and in adaptive immune response, including NK T cells, CD8+ and CD4+ T lymphocytes expressing the γδ or αβ receptors [24]. In contrast to T lymphocytes, which react to tumor antigen-derived peptides presented by MHC molecules, NK cells do not recognize these antigens but are activated by stress or danger signals such as the surface proteins MICA and MICB. These proteins are absent on normal cell but are expressed by tumor cells in response to alterations to their DNA and are recognized by activated receptors of NK cells such as the NKG2D receptor [25]. The immune response plays a major role in the defense of the organism against cancers and is probably responsible for control over tumor growth for a large majority of tumors, in particular during the initial phase of tumorigenesis. However, due to genetic mutations related to genomic instability, and to epigenetic modifications of DNA and histones, tumor cells, which have a monoclonal origin, differentiate into different subpopulations according to their invasive ability, their tendency to generate metastases, their sensitivity and resistance to treatment, but also their capability to induce an immune response as well as their sensitivity to this response [26]. Immunosurveillance can modify ("edit") tumor immunogenicity by selectively suppressing cells expressing high levels of the antigens recognized by T lymphocytes, and thus those that are the most sensitive to the immune response, and by selecting the cell clones the most resistant to immunosurveillance. Thus, tumors that develop in immuno-incompetent patients have been edited and are derived from cells which have evaded immunosurveillance [24]. The complex relationship between immunosurveillance and the escape of tumor cells from destruction mediated by the immune system can give rise to three scenarios that Schreiber's group classified as being constituted of three « Es » of immunosurveillance: Elimination-Equilibrium-Escape [12, 27]. The first phase is the elimination of tumor cells. Destruction generally arises at an early stage in oncogenesis, before the tumor is clinically detectable [28]. Exceptional cases of spontaneous total regression of an established cancer or even of metastases have been reported, particularly for melanomas [29]. The second phase is the development of a balance between the replacement of tumor cells and their elimination by the immune system. This phase can last several years during which tumor is controlled and maintained at its original site. However, this equilibrium can be abolished by the development of clonal cells resulting from the plasticity of their genome, which confers progressive resistance to the suppressive action of the immune system, or by a defect of immunosurveillance [12]. The third phase is the escape of tumor cells from immunosurveillance and their proliferation and

invasion into the surrounding tissue or spread to a distant site [12]. This phase induces a state of immune tolerance that favors tumor growth. Tumorigenesis is initiated and tumor becomes detectable, resulting in clinical symptoms development. Recent studies have shown that at a metastatic stage the tumor are no longer able to escape from the favorable or unfavorable control of the microenvironment [30, 31]. The dialogue established between the tumor cells and their microenvironment during the period of development and growth, produces a footprint that is reproduced at the distant sites of development of the cancer [32]. It should be pointed out that each type of tumor has its specific immunological profile and its own response to immunosurveillance, resulting in a large spectrum of responses or in resistance of cancers to immunosurveillance and thus to immunotherapy [33, 34].

Mechanisms of escape from immunosurveillance

Several components are involved in the escape of tumors from immunosurveillance: the tumor cells themselves, immune cells and stromal cells [6, 26]. The tumor cells have their own molecular antigenic identity that is recognized by T lymphocytes [35]. Several of these antigens are expressed in normal tissues, including the thymus, therefore resulting in immune T cell tolerance and weak anticancer immune response. Other antigens arising from random genetic mutations occur during oncogenesis. These neo-antigens are restricted to individual tumors and can generate a stronger immune response than the common antigens, but their detection is made difficult due to their increased specificity [36]. Prolonged stimulation of T lymphocytes due to constant exposure to tumor antigens can induce an immune tolerant state subsequent to the disappearance or inactivation of T lymphocytes that recognize these antigens or when they become immunosuppressive Treg [37, 38]. The phenotype of tumor cells is modified by the selection pressure of the immune system, which selects variants that resist immunological attack by different mechanisms (loss of expression of molecules involved in the presentation of the antigen–HLA or antigens recognized by T lymphocytes). They can also decrease the expression of NKG2D ligands or diminish the expression of the NKG2D receptor at the surface of NK cells [39]. By expressing higher levels of the anti-apoptosis proteins BCL-XL and FLIP, tumor cells can escape lysis by immune cells [40]. In some cases, tumor cells have been shown to render T lymphocytes anergic or non-functional, therefore inhibiting their ability to lyse tumor cell. They can do so by expressing indoleamine-2,3-dioxygenase (IDO), an enzyme that actively degrades tryptophan, required for T lymphocytes survival [41]. T cell activation does not only require the recognition of tumor antigen-derived peptides by the TCR, but also the engagement of co-stimulatory receptors including CD27 and CD28. In addition, T cell activation is regulated by the inhibitory receptors PD-1, Tim-3, CTLA-4 and Lag-3 that bind MHC class II molecules such as PD-L1, Galectine-9, CD80 and CD86. Several of these inhibitory receptors are engaged when T cells infiltrate tumors, therefore preventing tumor cell destruction. Immunotherapies that block PD-1 or PD-L1 are aimed at alleviating these inhibitory processes therefore restoring their ability to lyse tumor cells [42-44]. Tumor cells can express on their surface other molecules that inhibit the cytotoxic action of T lymphocytes and of NK cells, such as HLA-G or HLA-E [45, 46]. Tumor cells can create a favorable environment for lymphocyte tolerance by producing or inducing the secretion of a large spectrum of immunosuppressive molecules (IL-10, TGF-β, IL-2 or IL-15 soluble receptors, etc.), which suppress the anti-tumor function of T lymphocytes and NK cells [47-49]. The recruitment into the tumor microenvironment of immunosuppressive cells (Treg, myeloid-derived suppressor cells or MDSC, certain tolerogenic dendritic cells, pro-tumor macrophages type M2, pro-tumor neutrophils type N2) also favors escape of tumor cells from immunosurveillance [26, 42, 50, 51]. An association between the presence of these immune cells within tumors and decreased survival of patients with lung cancer has been shown [50, 52-55]. The stimulation of Treg inhibits not only the function of cytotoxic T lymphocytes but also that of anti-tumor immune cells such as NK cell, macrophages, dendritic cells and B lymphocytes, which prevent the destruction of tumor cells. Treg constitutively express inhibitory co-stimulatory molecules such as CTLA-4, a receptor of B7 molecules of the co-receptor CD28, but also PD-1 and PD-L1. The expression of CTLA-4 can also be induced on CD4+ T lymphocytes and CD8 effectors, which contributes to their anergy [56]. MDSCs are immature myeloid cells induced by proinflammatory cytokines, such as GM-CSF, IL-1β, IL-6, PGE, and VEGF, produced by tumor cells. MDSCs constitute a heterogeneous population of monocytes and neutrophils that can inhibit the function of effector T lymphocytes and can favor the generation of Treg from undifferentiated T lymphocytes [57]. To play

their immunosuppressive role, MDSCs must not only accumulate in the tumor bed but also be activated. Several factors, most of which are produced by tumor stromal cells and T lymphocytes, such as INF-γ, IL-4, IL-13, TGF-β but also certain fractions of the complement system, can activate MDSCs by inducing different signaling pathways, in generally regulated by the transcription factors STAT1, STAT3 and STAT6, and NF-κB [58]. Thus, solid tumors contain a variable proportion of MDSCs that maintain an immunosuppressive network in the tumor microenvironment and compromise the efficacy of cancer immunotherapy. In addition, MDSCs can also strongly affect tumor progression by producing high levels of MMPs and TGF-β and thus contributing to tumor growth, neovascularization and cancer cells dissemination [59]. Finally, regulation of myeloid cells by activated T cells may determine the efficacy of PD-1 blockade [60]. Substantial advances in immunotherapy have been made subsequent to a better understanding of the different mechanisms involved. Several approaches are presently being developed or validated in the clinics [13, 61]: − Antibodies against « immune checkpoints », notably inhibition of CTLA-4 and of the PD-1/PD-L1 pathway. The therapeutic use of which has been validated for certain cancers and is being extended to other cancers. − Anti-tumor vaccines composed of tumor antigens, which are still mostly at the research stage, with the exception of the « sipuleucel » vaccine, which has received FDA approval for prostate cancer but at a cost that is prohibitive and results in only a moderate improvement in survival. − The transfer of T lymphocyte specific antigens, termed adoptive therapy, is presently at a preclinical research stage. − Association of several immunotherapies or immunotherapy with or without conventional chemotherapy or radiotherapy; many trials are underway (https://clinicaltrials.gov/). Durable therapeutic responses have been obtained with anti-PD-1/D-L1 antibodies used to treat several types of cancers in a metastatic phase (lung, melanoma, bladder, kidney, prostate, breast, colon, head and neck and lymphoma) [62-69]. Combined inhibition of CTLA-4 and PD-L1, or LAG-3 and PD-1 or depletion of Treg cells together with a decrease in their homeostatic proliferation to inhibit the anergy of T lymphocytes, have shown potential synergy of action in murine model systems [70]. Currently, combination strategies with immunotherapies targeting checkpoints is a high-priority approach of clinical trials [71, 72].

The PD1-/PD-L1 pathway

PD-1 is a transmembrane protein of the superfamily of immunoglobulins (SFIg) (« family CD28 and B7 »), encoded by the PDCD1 gene [73]. It is one of the co-inhibitor receptors expressed by T lymphocytes. It is composed of an extracellular IgV domain (which shares 21-33% gene sequence homology with CTLA-4, CD28 and ICOS), a hydrophobic transmembrane domain, an intracellular domain based on an inhibiting tyrosine kinase domain and an intracellular regulating tyrosine kinase domain. PD-1 has two ligands: PD-L1 (B7-H1 / CD274) and PD-L2 (B7-CD / CD273). PD-L1 is expressed by T and B lymphocytes, dendritic cells, macrophages, endothelial cells and pancreatic islet cells. PD-1 and its ligand PD-L1 play a key role in tumor escape, in maintenance of the tumor environment and in development of the tumor [73]. Two PD-L1 splice variant isoforms exist in humans, one contains 290 amino acids and the other 176 amino acids [73]. A splice variant lacking the IgV domain encoded by exon 2 exists in humans and is localized to the endomembrane system. While the function of this isoform is unknown it appears not to be able to bind the PD- 1 receptor [74]. The full length isoform of PD-L1 contains an extracellular domain that allows binding to the PD-1 receptor [73, 75]. PD-L1 and PD-L2 are expressed on antigen presenting cells, on activated T lymphocytes and cells of a number of tissue types including heart, lung, liver, placenta; while they are expressed at a low level in spleen, lymph nodes, thymus, the brain shows no expression [76, 77]. The shared expression of lymphoid and nonlymphoid organs suggests that the PD1-PD-L1/2 couple is involved in the modulation of the immune response in secondary lymphoid organs and in organs showing expression [78]. The distribution of PD-L1 and PD-L2 in tumor tissues can be divided into two groups depending of the type of tumor. PD-L1 is over-expressed in cancers of the lung, skin, colon, bladder, breast, epidermoid head and neck, kidney, stomach and brain. Cancers of the esophagus, ovaries and pancreas over-express either PDL1 or PD-L2 [78]. Melanomas, non-small cell lung cancer (NSCLC) and kidney cancer express the highest levels of PD-L1 [43, 79-81]. The expression of PD-L2 is lower than PD-L1 in these types of tumors. About 20 to 40% of patients with NSCLC show high level of expression of PDL1 in the membrane of at least 50% of tumor cells, the threshold selected in recent clinical trials that evaluate antibodies targeting the PD-1/PD-L1 pathway [62, 66]. The physiological role of the PD-1/PD-L1 couple is to negatively regulate the natural

immune response. It acts at different stages of maturation of lymphocytes within the thymus. PD-1 is involved in the development of a pool of mature T lymphocytes and in the process of central tolerance by applying negative selection on the pre-TCR/CD3 complex of CD4-/CD8- thymocytes [82]. PD-1 also acts in the periphery at several levels, and in particular on the autoreactive lymphocyte clones that have experienced this selection pressure, by suppressing the activator immune signal. The antigen presenting cells exert a tolerogenic modulation or anergy on naive T lymphocytes, under the control of the PD-1/PD-L1 couple. In contrast a defect in PD-1 leads to hyper-activation of autoreactive T lymphocytes [83]. PD-1 and PD-L1 are expressed by CD4+Foxp3+ Treg lymphocytes. TGF-β induces differentiation of these naive Treg and the interaction between PD-1 and PD-L1 favors their survival [84]. PD-1 also regulates the effector function and maintains active B lymphocytes, by allowing functional maintenance of central IgG+ plasmocytes and by acting on the commutation of immunoglobulin classes and on somatic hyper-mutation [85, 86]. The pathophysiological expression of PD-L1 depends on intrinsic and extrinsic control mechanisms [42]. The intrinsic control mechanisms concern the inactivation of the tumor suppressor gene PTEN, resulting in the activation of the PI3K/AKT pathway, of the transcription factor STAT3 and activation of the oncoprotein signaling pathway EML4-ALK, via STAT3 and ERK [87-89]. Simultaneous activation of KRAS and inactivation of Lkb1/STK11 are involved in the formation of pulmonary squamous cell carcinomas, whilst inactivation of PTEN and Lkb1 lead to the development of pulmonary squamous cell carcinomas overexpressing PD-L1 [89]. The stimulation of TCR and BCR (B cell receptor) induces PD-L1 expression on T and B lymphocytes. The interleukins IL-2, IL-7, and IL-15 induce expression of PD-L1 on monocytes. IL-21 increases the expression of PD-L1 on monocytes but not on T lymphocytes. IL-21 is the only interleukin that favors expression of PD-L1 on B lymphocytes. IFN-γ induces the expression of PD-L1 on CD8+ T lymphocytes, monocytes and dendritic cells [90, 91]. It has been shown that tissue hypoxia induces the over-expression of PD-L1 on tumor cells and on myeloid dendritic cells through activation of the HIF-1 signaling pathway. Hypoxia in tumors is produced by erratic neo-angiogenesis, the development of the stroma and the growth of the tumor [92, 93]. Finally, it was shown recently that activation of EGFR-dependent signaling induces the over-expression of PD-L1 [94]. Treatment of these mice with a specific EGFR inhibitor lead to a decrease in the PD-L1 expression induced by activating EGFR mutations and allowed restoration of the T lymphocyte function, resulting in prolonged survival of the mice with lung adenocarcinomas expressing an EGFR mutation [94]. This study demonstrated for the first time the existence of a mechanism inducing oncogene–dependent expression of PD-L1, which could play a role in tumor escape of lung adenocarcinomas. Cancer cells over-express PD-L1 and PD-L2, which then bind to PD-1 receptors on T lymphocytes, thus inhibiting their activation and inducing immune escape of the tumor. The PD-1/PD-L1 pathway regulates immunosuppression through several mechanisms: initiation of apoptosis of T activated lymphocytes; T lymphocyte anergy; stimulation of regulatory T cells; inhibition of proliferation of T lymphocytes; inhibition of T lymphocyte activation and of IL-2 production. Antibodies that block PD-1 or PD-L1 have emerged as part of the therapeutic arsenal for advanced lung cancer (Figure 2). The clinical response of this treatment is based on the expression of PD-L1 and the infiltration of CD8 T lymphocytes into the tumor microenvironment [65]. The therapeutic inhibition of the PD-1/PD-L1 pathway modifies the tumor microenvironment and stimulates the endogenous antitumor autoimmune response. Several antibodies targeting PD-1 are presently available: Nivolumab (Bristol-Myers Squibb), a human IgG4 monoclonal antibody; Pembrolizumab (Merck Inc.), a highly specific humanized monoclonal antibody with activity to PD-1 and containing a C228P mutation; Pidilizumab (Medivation Inc.), an IgG-1K recombinant anti-PD-1 humanized monoclonal antibody that showed antitumor activity in murine cancer model systems (Figure 2). As second line treatment, Nivolumab has a response rate of 19% in treatment of NSCLC with an overall oneyear survival of 51% versus 39% for docetaxel [95]. A multicenter phase III clinical trial recently validated the use of Pembrolizumab as first-line treatment of advanced NSCLC and strong PD-L1 expression (≥50%) in tumor cells [66]. Another approach based on antibodies to PD-L1, notably Atezolizumab (Roche/Genentech) and Durvalumab (AstraZeneca) are also being developed in the clinic and are giving promising results (Figure 2) [96, 97]. Therapeutic targeting of PD-L1 has been hypothesized to be associated with limited toxicity due to selective modulation of the immune response in the tumor environment [66]. Therapeutic inhibition of the PD-1/PD-L1 for NSCLC is only effective (as first or second line treatment) for some subsets of patients. The challenge today is to identify the population of

patients that respond to this therapeutic approach. Thus, the use of biomarkers predicting the therapeutic response is under investigation. These biomarkers could be used as « companion » or « complementary » tests for a therapeutic molecule [98]. In addition, the efficacy of inhibition of the PD-1/PD-L1 pathway is tempered by rare but potentially serious side effects. The prohibitive cost of the monoclonal antibodies is also an ethical challenge and the economic issues are real, which requires the application of predictive biomarkers of PD-1/PD-L1 inhibition to optimally select patients [6, 7]. Evaluation by immunohistochemistry of the tumor expression of PD-L1 is, to date, the only approach in thoracic oncology providing a predictive biomarker for immunotherapy targeting the PD-1/PD-L1 couple [99-101]. However, some patients lacking PD-L1 tumor expression sometimes respond to anti-PD-1/PD-L1 and a relatively significant percentage of patients showing expression resist treatment. Another pitfall lies in the large spectrum of expression of PD-L1 in tissues, which can lead to under estimation of the PD-L1 status in a biopsy sample compared to the overall tumor [102, 103]. Thus, companion or complementary tests based on immunohistochemistry are not perfect but will probably be used extensively, in particular when the different molecules will obtain marketing authorization, notably for first-line treatment [99].

Perspectives

For a long time, immunotherapy has remained marginal, attracting followers and opponents, but today tangible proof of its efficacy has been demonstrated. While the mutational characteristics of tumors have for a long time been associated with a conception of a negative prognostic character, immunotherapy uses this mutagenicity to activate the adaptive immune response, which is enhanced by diverse tumor antigens [104]. The efficiency remains intrinsic to the immunogenic status of the tumor. Tumors should no longer be considered as specific entities but should be studied in association with their microenvironment and in relationship to the immune system of the host, with consideration of the clinical and therapeutic history of the patient. The « immunoscore » is now defined as a prognostic tool to use for quantification of in situ immune cell infiltrates, which appears to be superior to the tumor-node-metastasis (TNM) classification in colorectal cancer. In NSCLC, no immunoscore has been established, but in situ tumor immunology is recognized as highly important. The question still open is the challenge of the “universal” character of the immunoscore [7, 105]. A number of markers such as infiltration by CD8+ T lymphocytes expressing PD-1 and intra-tumor expression of IFN-γ suggest the presence of preexisting antitumor immunity and seems to correlate to a better clinical response to anti-PD-1/PDL1 inhibitors [106]. High throughput genomic sequencing is in the process of changing the oncotheranostic landscape and may help to improve the value of the « immunoscore ». Substantial genetic heterogeneity was obtained when comparing lung tumors of smoking and non-smoking patients and the difference in the mutational profile seems to predict sensitivity to the inhibition of the PD-1/PD-L1 couple of patients with NSCLC [107, 108]. A study evaluating tumors of patients treated with Pembrolizumab, by next generation sequencing, with a smoker and a non-smoker arm, was able to highlight a « molecular smoking signature », which was significantly associated with better progression-free survival [108]. More recently, an association between the frequency of mutations in tumors and treatment response was identified, an association that may be explained by a higher increase in the frequency of CD8+ T lymphocytes directed against these mutations [109]. In addition, amplification of the PD-L1 gene seems to be complementary to the protein expression detected by immunohistochemistry, both approaches having shown significant correlation with survival of NSCLC patients [110]. Finally, recent studies have suggested that intra-tumor TCR, in particular the variable CDR3 domain evaluated by PCR, represents a potential biomarker for prediction of the therapeutic response to inhibition with anti-PD-1/PD-L1 inhibitors [111, 112]. Research into new protocols for immunotherapy concern combinations of several immunotherapies or combinations with chemotherapy, as well as association of inhibitors of PD-1/PD-L1 and radiotherapy [113, 114]. It has been hypothesized that radiotherapy sensitizes tumor cells to immunotherapy, even at distant irradiated sites, by an activation effect, and thereby optimizes the anti-PD-1/PD-L1 effect [70]. One of the risks of combined approaches is toxicity, as observed for combinations of targeted therapies. However, the biological rational behind such approaches is evident [115]. Other antibodies against other inhibitory co-stimulation molecules (Lag3, Tim- 3, etc.) or activators (OX40) are being evaluated in the clinic, alone or in association with inhibition of the PD-1/PD-L1 pathway [116]. Active immunotherapy by anti-tumor vaccination, by injection of specific antigens, generates an influx of CD8+ T lymphocytes into the tumor bed. However, this therapeutic approach needs to define the

relevant antigens. Proof of efficacy exists in practice in the clinic, the sipuleucel vaccine has received FDA approval. However, when considering the benefice in terms of survival the cost remains prohibitive. The association of vaccination and passive immunotherapy requires preclinical models to anticipate potential secondary effects [7]. The development of CAR-T cells (chimeric antigen receptor T cell), true « armed T lymphocytes », with an antibody recognizing a B lymphocyte antigen, may open up new therapeutic avenues for patients who do not respond to passive immunotherapy through adoptive immunotherapy. Studies by Carl June have demonstrated the efficacy of this treatment for the care of certain lymphoblastic and chronic lymphoid leukemias. Research projects are investigating the extension of this therapeutic approach to other types of tumors. Nonetheless the economics will need to be taken into serious consideration [117, 118]. The development of immunotherapy faces numerous challenges before implementation as a strategy in the fight against cancer and needs to rely on ongoing preclinical and translational research. Thus immune check point inhibition is a promising strategy in solid tumors which can induce durable response. There is a need to further improve the immunotherapy. Immune responses are regulated by various molecules and different immune cells, which have a role in modulating response to anti-PD1 and anti-PD-L1 monoclonal antibodies. PD-L1 expression in tumor cells is currently the candidate for predicting responses to anti-PD1/PD-L1 treatment. It is noteworthy that the lack of PD-L1 expression in solid tumors cannot be totally relied upon to exclude patients from immunotherapy. In this context, understanding the role of other components of microenvironment in modulating the response to anti-PD1/PD-L1 treatment is of strong interest. In this regard different new orientations of research may implicate several mechanisms. One can be the fact that the key factors modulating response to immune checkpoint inhibitors can be the TGF-β. This latter tolerogenic cytokine is frequently overexpressed in aggressive cancers [119]. This cytokine is well known to play a pivotal role in tumorigenesis and in the maintenance of immune homoeostasis. In this context, TGF-β affects antigen presentation by dendritic cells by modulating the expression of MHC II. Moreover, this cytokine induces upregulation of immune modulating molecules, including PD-L1 with the induction of immune tolerance and tumor evasion from immune response. Thus different opportunities for enhancing immunotherapy can be suggested considering the tight link between the immunologic system, acquisition of stemness properties, hypoxia and EMT induced by TGF-β. Even if some evidence strongly suggests a role of TGF-β in modulating response to anti-PD1/PD-L1 treatment because of its pleiotropic activity, its role in immune resistance is complex and needs to be explored in the future [119]. Another field of interest can be to explore the link between cancer immunology and stem cell research in order to develop new therapeutic approaches to prevent metastasis and development of therapy resistance [120]. In this regard, cancer stem cells are well characterized by immunosuppressive activity and low immunogenicity. These cells are able to defend themselves from the immune system and adapt to modifications in the microenvironment caused by chemo and/or radiotherapy [121]. The molecular identification of immune modeling treatments that can reverse and/or inhibit cancer stem cell escape from immunosurveillance should determine to set up new immunotherapy strategies targeting cancer stem cells. In conclusion, the success of immunotherapeutic approaches, in particular those targeting the PD-L1/PD1 couple will depend in the future on a better understanding of the basic biology and mechanisms of immune responses, more particularly the effect of microenvironment in shaping immune responses.

Conflict of interest

The authors declare to have no conflict of interest

Acknowledgements French Government (National Research Agency, ANR) through the "Investments for the Future" LABEX SIGNALIFE: program reference # ANR-11-LABX-0028-01; Fondation ARC pour la recherche sur le cancer – ARC SL220110603478; CANC'AIR Genexposomic project; Cancéropôle PACA; Conseil Général 06, France.

References

1. Shaw AT, Kim DW, Nakagawa K, Seto T, Crino L, Ahn MJ, et al. Crizotinib versus chemotherapy in advanced ALK-positive lung cancer. N Engl J Med 2013;368: 2385-94.
2. Sandler A, Gray R, Perry MC, Brahmer J, Schiller JH, Dowlati A, et al. Paclitaxel-carboplatin alone or with bevacizumab for non-small-cell lung cancer. N Engl J Med 2006;355: 2542-50.
3. van der Wekken AJ, Saber A, Hiltermann TJ, Kok K, van den Berg A, Groen HJ. Resistance mechanisms after tyrosine kinase inhibitors afatinib and crizotinib in non-small cell lung cancer, a review of the literature. Crit Rev Oncol Hematol 2016;100: 107-16.
4. Keedy VL, Temin S, Somerfield MR, Beasley MB, Johnson DH, McShane LM, et al. American Society of Clinical Oncology provisional clinical opinion: epidermal growth factor receptor (EGFR) Mutation testing for patients with advanced non-smallcell lung cancer considering first-line EGFR tyrosine kinase inhibitor therapy. J Clin Oncol 2011;29: 2121-7.
5. Soda M, Choi YL, Enomoto M, Takada S, Yamashita Y, Ishikawa S, et al. Identification of the transforming EML4-ALK fusion gene in non-small-cell lung cancer. Nature 2007;448: 561-6.
6. Lawrence MS, Stojanov P, Polak P, Kryukov GV, Cibulskis K, Sivachenko A, et al. Mutational heterogeneity in cancer and the search for new cancer-associated genes. Nature 2013;499: 214-8.
7. Zitvogel L, Hannani D, Martin F, editors. Immunothérapie des cancers au troisième millénaire EDP Sciences; 2015.
8. Hughes PE, Caenepeel S, Wu LC. Targeted Therapy and Checkpoint Immunotherapy Combinations for the Treatment of Cancer. Trends Immunol 2016;37: 462-76.
9. Medzhitov R, Preston-Hurlburt P, Janeway CA, Jr. A human homologue of the Drosophila Toll protein signals activation of adaptive immunity. Nature 1997;388: 394-7.
10. Janeway CA, Jr. Approaching the asymptote? Evolution and revolution in immunology. Cold Spring Harb Symp Quant Biol 1989;54 Pt 1: 1-13.
11. Steinman RM. Decisions about dendritic cells: past, present, and future. Annu Rev Immunol 2012;30: 1-22.
12. Dunn GP, Bruce AT, Ikeda H, Old LJ, Schreiber RD. Cancer immunoediting: from immunosurveillance to tumor escape. Nat Immunol 2002;3: 991-8.
13. Granier C, Karaki S, Roussel H, Badoual C, Tran T, Anson M, et al. [Cancer immunotherapy: Rational and recent breakthroughs]. Rev Med Interne 2016;37: 694-700.
14. Cortinovis D, Gregorc V, Migliorino MR, Abate MI, Manzo A, Malapelle U, et al. New perspectives in the second-line treatment of non squamous NSCLC patients: Results from a large Italian Lung Cancer Working Group. Crit Rev Oncol Hematol 2017;109: 35-41.
15. Chen DS, Mellman I. Oncology meets immunology: the cancer-immunity cycle. Immunity 2013;39: 1-10.
16. Chen DS, Mellman I. Elements of cancer immunity and the cancer-immune set point. Nature 2017;541: 321-30.
17. Muller WA. Localized signals that regulate transendothelial migration. Curr Opin Immunol 2016;38: 24-9.
18. Schumacher TN, Schreiber RD. Neoantigens in cancer immunotherapy. Science 2015;348: 69-74.
19. Shankaran V, Ikeda H, Bruce AT, White JM, Swanson PE, Old LJ, et al. IFNgamma and lymphocytes prevent primary tumour development and shape tumour immunogenicity. Nature 2001;410: 1107-11.
20. Djenidi F, Adam J, Goubar A, Durgeau A, Meurice G, de Montpreville V, et al. CD8+CD103+ tumor-infiltrating lymphocytes are tumor-specific tissue-resident memory T cells and a prognostic factor for survival in lung cancer patients. J Immunol 2015;194: 3475-86.
21. Kawai O, Ishii G, Kubota K, Murata Y, Naito Y, Mizuno T, et al. Predominant infiltration of macrophages and CD8(+) T Cells in cancer nests is a significant predictor of survival in stage IV nonsmall cell lung cancer. Cancer 2008;113: 1387- 95.
22. Villegas FR, Coca S, Villarrubia VG, Jimenez R, Chillon MJ, Jareno J, et al. Prognostic significance of tumor infiltrating natural killer cells subset CD57 in patients with squamous cell lung cancer. Lung Cancer 2002;35: 23-8.
23. Fridman WH, Pages F, Sautes-Fridman C, Galon J. The immune contexture in human tumours: impact on clinical outcome. Nat Rev Cancer 2012;12: 298-306.
24. Matsushita H, Vesely MD, Koboldt DC, Rickert CG, Uppaluri R, Magrini VJ, et al. Cancer exome analysis reveals a T-cell-dependent mechanism of cancer immunoediting. Nature 2012;482: 400-4.
25. Bryceson YT, Ljunggren HG. Tumor cell recognition by the NK cell activating receptor NKG2D. Eur J Immunol 2008;38: 2957-61.
26. Schreiber RD, Old LJ, Smyth MJ. Cancer immunoediting: integrating immunity's roles in cancer suppression and promotion. Science 2011;331: 1565-70.
27. Dunn GP, Old LJ, Schreiber RD. The three Es of cancer immunoediting. Annu Rev Immunol 2004;22: 329-60.
28. Pardoll D. Does the immune system see tumors as foreign or self? Annu Rev Immunol 2003;21: 807-39.
29. Kalialis LV, Drzewiecki KT, Klyver H. Spontaneous regression of metastases from melanoma: review of the literature. Melanoma Res 2009;19: 275-82.
30. Giraldo NA, Becht E, Remark R, Damotte D, Sautes-Fridman C, Fridman WH. The immune contexture of primary and metastatic human tumours. Curr Opin Immunol 2014;27: 8-15.
31. Joyce JA, Pollard JW. Microenvironmental regulation of metastasis. Nat Rev Cancer 2009;9: 239-52.
32. Carlini MJ, De Lorenzo MS, Puricelli L. Cross-talk between tumor cells and the microenvironment at the metastatic niche. Curr Pharm Biotechnol 2011;12: 1900-8.
33. McGranahan N, Furness AJ, Rosenthal R, Ramskov S, Lyngaa R, Saini SK, et al. Clonal neoantigens elicit T

cell immunoreactivity and sensitivity to immune checkpoint blockade. Science 2016;351: 1463-9.
34. Holzel M, Bovier A, Tuting T. Plasticity of tumour and immune cells: a source of heterogeneity and a cause for therapy resistance? Nat Rev Cancer 2013;13: 365- 76.
35. Spranger S, Spaapen RM, Zha Y, Williams J, Meng Y, Ha TT, et al. Upregulation of PD-L1, IDO, and T(regs) in the melanoma tumor microenvironment is driven by CD8(+) T cells. Sci Transl Med 2013;5: 200ra116.
36. Bos R, Marquardt KL, Cheung J, Sherman LA. Functional differences between low- and high-affinity CD8(+) T cells in the tumor environment. Oncoimmunology 2012;1: 1239-47.
37. Fridman WH, Dieu-Nosjean MC, Pages F, Cremer I, Damotte D, Sautes- Fridman C, et al. The immune microenvironment of human tumors: general significance and clinical impact. Cancer Microenviron 2013;6: 117-22.
38. Willimsky G, Blankenstein T. Sporadic immunogenic tumours avoid destruction by inducing T-cell tolerance. Nature 2005;437: 141-6.
39. Waldhauer I, Steinle A. NK cells and cancer immunosurveillance. Oncogene 2008;27: 5932-43.
40. Bauer C, Hees C, Sterzik A, Bauernfeind F, Mak'Anyengo R, Duewell P, et al. Proapoptotic and antiapoptotic proteins of the Bcl-2 family regulate sensitivity of pancreatic cancer cells toward gemcitabine and T-cell-mediated cytotoxicity. J Immunother 2015;38: 116-26.
41. Prendergast GC, Smith C, Thomas S, Mandik-Nayak L, Laury-Kleintop L, Metz R, et al. Indoleamine 2,3-dioxygenase pathways of pathogenic inflammation and immune escape in cancer. Cancer Immunol Immunother 2014;63: 721-35.
42. Pardoll DM. The blockade of immune checkpoints in cancer immunotherapy. Nat Rev Cancer 2012;12: 252-64.
43. Taube JM, Klein A, Brahmer JR, Xu H, Pan X, Kim JH, et al. Association of PD-1, PD-1 ligands, and other features of the tumor immune microenvironment with response to anti-PD-1 therapy. Clin Cancer Res 2014;20: 5064-74.
44. Topalian SL, Hodi FS, Brahmer JR, Gettinger SN, Smith DC, McDermott DF, et al. Safety, activity, and immune correlates of anti-PD-1 antibody in cancer. N Engl J Med 2012;366: 2443-54.
45. Carosella ED, Rouas-Freiss N, Tronik-Le Roux D, Moreau P, LeMaoult J. HLA-G: An Immune Checkpoint Molecule. Adv Immunol 2015;127: 33-144.
46. Sasaki T, Kanaseki T, Shionoya Y, Tokita S, Miyamoto S, Saka E, et al. Microenvironmental stresses induce HLA-E/Qa-1 surface expression and thereby reduce CD8(+) T-cell recognition of stressed cells. Eur J Immunol 2016;46: 929-40.
47. Whiteside TL. The tumor microenvironment and its role in promoting tumor growth. Oncogene 2008;27: 5904-12.
48. Teicher BA. Transforming growth factor-beta and the immune response to malignant disease. Clin Cancer Res 2007;13: 6247-51.
49. Domagala-Kulawik J, Osinska I, Hoser G. Mechanisms of immune response regulation in lung cancer. Transl Lung Cancer Res 2014;3: 15-22.
50. Cortez-Retamozo V, Etzrodt M, Newton A, Rauch PJ, Chudnovskiy A, Berger C, et al. Origins of tumor-associated macrophages and neutrophils. Proc Natl Acad Sci U S A 2012;109: 2491-6.
51. Srivastava MK, Andersson A, Zhu L, Harris-White M, Lee JM, Dubinett S, et al. Myeloid suppressor cells and immune modulation in lung cancer. Immunotherapy 2012;4: 291-304.
52. Hattar K, Franz K, Ludwig M, Sibelius U, Wilhelm J, Lohmeyer J, et al. Interactions between neutrophils and non-small cell lung cancer cells: enhancement of tumor proliferation and inflammatory mediator synthesis. Cancer Immunol Immunother 2014;63: 1297-306.
53. Ilie M, Hofman V, Ortholan C, Bonnetaud C, Coelle C, Mouroux J, et al. Predictive clinical outcome of the intratumoral CD66b-positive neutrophil-to-CD8- positive T-cell ratio in patients with resectable nonsmall cell lung cancer. Cancer 2012;118: 1726-37.
54. Kim J, Bae JS. Tumor-Associated Macrophages and Neutrophils in Tumor Microenvironment. Mediators Inflamm 2016;2016: 6058147.
55. Chen JJ, Lin YC, Yao PL, Yuan A, Chen HY, Shun CT, et al. Tumorassociated macrophages: the double-edged sword in cancer progression. J Clin Oncol 2005;23: 953-64.
56. Pedicord VA, Montalvo W, Leiner IM, Allison JP. Single dose of anti-CTLA-4 enhances CD8+ T-cell memory formation, function, and maintenance. Proc Natl Acad Sci U S A 2011;108: 266-71.
57. Ortiz ML, Lu L, Ramachandran I, Gabrilovich DI. Myeloid-derived suppressor cells in the development of lung cancer. Cancer Immunol Res 2014;2: 50-8.
58. Gabrilovich DI, Nagaraj S. Myeloid-derived suppressor cells as regulators of the immune system. Nat Rev Immunol 2009;9: 162-74.
59. Serafini P. Myeloid derived suppressor cells in physiological and pathological conditions: the good, the bad, and the ugly. Immunol Res 2013;57: 172-84.
60. Eissler N, Mao Y, Brodin D, Reutersward P, Andersson Svahn H, Johnsen JI, et al. Regulation of myeloid cells by activated T cells determines the efficacy of PD-1 blockade. Oncoimmunology 2016;5: e1232222.
61. Jeanbart L, Swartz MA. Engineering opportunities in cancer immunotherapy. Proc Natl Acad Sci U S A 2015;112: 14467-72.
62. Herbst RS, Soria JC, Kowanetz M, Fine GD, Hamid O, Gordon MS, et al. Predictive correlates of response to the anti-PD-L1 antibody MPDL3280A in cancer patients. Nature 2014;515: 563-7.
63. Ibrahim R, Stewart R, Shalabi A. PD-L1 blockade for cancer treatment: MEDI4736. Semin Oncol 2015;42: 474-83.
64. Soria JC, Marabelle A, Brahmer JR, Gettinger S. Immune checkpoint modulation for non-small cell lung cancer. Clin Cancer Res 2015;21: 2256-62.
65. Sunshine J, Taube JM. PD-1/PD-L1 inhibitors. Curr Opin Pharmacol 2015;23: 32-8.

66. Reck M, Rodriguez-Abreu D, Robinson AG, Hui R, Csoszi T, Fulop A, et al. Pembrolizumab versus Chemotherapy for PD-L1-Positive Non-Small-Cell Lung Cancer. N Engl J Med 2016;375: 1823-33.
67. Robert C, Long GV, Brady B, Dutriaux C, Maio M, Mortier L, et al. Nivolumab in previously untreated melanoma without BRAF mutation. N Engl J Med 2015;372: 320-30.
68. Fehrenbacher L, Spira A, Ballinger M, Kowanetz M, Vansteenkiste J, Mazieres J, et al. Atezolizumab versus docetaxel for patients with previously treated non-smallcell lung cancer (POPLAR): a multicentre, open-label, phase 2 randomised controlled trial. Lancet 2016;387: 1837-46.
69. Rosenberg JE, Hoffman-Censits J, Powles T, van der Heijden MS, Balar AV, Necchi A, et al. Atezolizumab in patients with locally advanced and metastatic urothelial carcinoma who have progressed following treatment with platinum-based chemotherapy: a single-arm, multicentre, phase 2 trial. Lancet 2016;387: 1909-20.
70. Gajewski TF, Schreiber H, Fu YX. Innate and adaptive immune cells in the tumor microenvironment. Nat Immunol 2013;14: 1014-22.
71. He Y, Yu H, Rozeboom L, Rivard CJ, Ellison K, Dziadziuszko R, et al. LAG-3 Protein Expression in Non-small Cell Lung Cancer and Its Relationship with PD-1/PD-L1 and Tumor-Infiltrating Lymphocytes. J Thorac Oncol 2017.
72. Seetharamu N, Budman DR, Sullivan KM. Immune checkpoint inhibitors in lung cancer: past, present and future. Future Oncol 2016;12: 1151-63.
73. Keir ME, Butte MJ, Freeman GJ, Sharpe AH. PD-1 and its ligands in tolerance and immunity. Annu Rev Immunol 2008;26: 677-704.
74. He J, Hu Y, Hu M, Li B. Development of PD-1/PD-L1 Pathway in Tumor Immune Microenvironment and Treatment for Non-Small Cell Lung Cancer. Sci Rep 2015;5: 13110.
75. Zak KM, Kitel R, Przetocka S, Golik P, Guzik K, Musielak B, et al. Structure of the Complex of Human Programmed Death 1, PD-1, and Its Ligand PD-L1. Structure 2015;23: 2341-8.
76. Dong H, Strome SE, Salomao DR, Tamura H, Hirano F, Flies DB, et al. Tumor-associated B7-H1 promotes T-cell apoptosis: a potential mechanism of immune evasion. Nat Med 2002;8: 793-800.
77. Freeman GJ, Long AJ, Iwai Y, Bourque K, Chernova T, Nishimura H, et al. Engagement of the PD-1 immunoinhibitory receptor by a novel B7 family member leads to negative regulation of lymphocyte activation. J Exp Med 2000;192: 1027-34.
78. Okazaki T, Honjo T. PD-1 and PD-1 ligands: from discovery to clinical application. Int Immunol 2007;19: 813-24.
79. Fourcade J, Sun Z, Benallaoua M, Guillaume P, Luescher IF, Sander C, et al. Upregulation of Tim-3 and PD-1 expression is associated with tumor antigen-specific CD8+ T cell dysfunction in melanoma patients. J Exp Med 2010;207: 2175-86.
80. Konishi J, Yamazaki K, Azuma M, Kinoshita I, Dosaka-Akita H, Nishimura M. B7-H1 expression on non-small cell lung cancer cells and its relationship with tumorinfiltrating lymphocytes and their PD-1 expression. Clin Cancer Res 2004;10: 5094- 100.
81. Parsa AT, Waldron JS, Panner A, Crane CA, Parney IF, Barry JJ, et al. Loss of tumor suppressor PTEN function increases B7-H1 expression and immunoresistance in glioma. Nat Med 2007;13: 84-8.
82. Nishimura H, Honjo T, Minato N. Facilitation of beta selection and modification of positive selection in the thymus of PD-1-deficient mice. J Exp Med 2000;191: 891-8.
83. Martin-Orozco N, Wang YH, Yagita H, Dong C. Cutting Edge: Programmed death (PD) ligand-1/PD-1 interaction is required for CD8+ T cell tolerance to tissue antigens. J Immunol 2006;177: 8291-5.
84. Francisco LM, Salinas VH, Brown KE, Vanguri VK, Freeman GJ, Kuchroo VK, et al. PD-L1 regulates the development, maintenance, and function of induced regulatory T cells. J Exp Med 2009;206: 3015-29.
85. Good-Jacobson KL, Szumilas CG, Chen L, Sharpe AH, Tomayko MM, Shlomchik MJ. PD-1 regulates germinal center B cell survival and the formation and affinity of long-lived plasma cells. Nat Immunol 2010;11: 535-42.
86. Okazaki T, Okazaki IM, Wang J, Sugiura D, Nakaki F, Yoshida T, et al. PD-1 and LAG-3 inhibitory co-receptors act synergistically to prevent autoimmunity in mice. J Exp Med 2011;208: 395-407.
87. Cumberbatch M, Tang X, Beran G, Eckersley S, Wang X, Ellston RP, et al. Identification of a subset of human non-small cell lung cancer patients with high PI3Kbeta and low PTEN expression, more prevalent in squamous cell carcinoma. Clin Cancer Res 2014;20: 595-603.
88. Ota K, Azuma K, Kawahara A, Hattori S, Iwama E, Tanizaki J, et al. Induction of PD-L1 Expression by the EML4-ALK Oncoprotein and Downstream Signaling Pathways in Non-Small Cell Lung Cancer. Clin Cancer Res 2015;21: 4014-21.
89. Xu C, Fillmore CM, Koyama S, Wu H, Zhao Y, Chen Z, et al. Loss of Lkb1 and Pten leads to lung squamous cell carcinoma with elevated PD-L1 expression. Cancer Cell 2014;25: 590-604.
90. Bennett F, Luxenberg D, Ling V, Wang IM, Marquette K, Lowe D, et al. Program death-1 engagement upon TCR activation has distinct effects on costimulation and cytokine-driven proliferation: attenuation of ICOS, IL-4, and IL-21, but not CD28, IL-7, and IL-15 responses. J Immunol 2003;170: 711-8.
91. Kinter AL, Godbout EJ, McNally JP, Sereti I, Roby GA, O'Shea MA, et al. The common gamma-chain cytokines IL-2, IL-7, IL-15, and IL-21 induce the expression of programmed death-1 and its ligands. J Immunol 2008;181: 6738-46.
92. Barsoum IB, Smallwood CA, Siemens DR, Graham CH. A mechanism of hypoxia-mediated escape from adaptive immunity in cancer cells. Cancer Res 2014;74: 665-74.

93. Noman MZ, Desantis G, Janji B, Hasmim M, Karray S, Dessen P, et al. PD-L1 is a novel direct target of HIF-1alpha, and its blockade under hypoxia enhanced MDSC-mediated T cell activation. J Exp Med 2014;211: 781-90.
94. Akbay EA, Koyama S, Carretero J, Altabef A, Tchaicha JH, Christensen CL, et al. Activation of the PD-1 pathway contributes to immune escape in EGFR-driven lung tumors. Cancer Discov 2013;3: 1355-63.
95. Borghaei H, Paz-Ares L, Horn L, Spigel DR, Steins M, Ready NE, et al. Nivolumab versus Docetaxel in Advanced Nonsquamous Non-Small-Cell Lung Cancer. N Engl J Med 2015;373: 1627-39.
96. Rittmeyer A, Barlesi F, Waterkamp D, Park K, Ciardiello F, von Pawel J, et al. Atezolizumab versus docetaxel in patients with previously treated non-small-cell lung cancer (OAK): a phase 3, open-label, multicentre randomised controlled trial. Lancet 2017;389: 255-65.
97. Planchard D, Yokoi T, McCleod MJ, Fischer JR, Kim YC, Ballas M, et al. A Phase III Study of Durvalumab (MEDI4736) With or Without Tremelimumab for Previously Treated Patients With Advanced NSCLC: Rationale and Protocol Design of the ARCTIC Study. Clin Lung Cancer 2016;17: 232-6 e1.
98. Ilie M, Hofman V, Dietel M, Soria JC, Hofman P. Assessment of the PD-L1 status by immunohistochemistry: challenges and perspectives for therapeutic strategies in lung cancer patients. Virchows Arch 2016;468: 511-25.
99. Hofman V, Ilie M, Long E, Butori C, Lassalle S, Washetine K, et al. [Issues and current limits for immunohistochemical assessment of PD-L1 status in bronchial biopsies]. Bull Cancer 2016;103: 368-80.
100. Grigg C, Rizvi NA. PD-L1 biomarker testing for non-small cell lung cancer: truth or fiction? J Immunother Cancer 2016;4: 48.
101. Shien K, Papadimitrakopoulou VA, Wistuba, II. Predictive biomarkers of response to PD-1/PD-L1 immune checkpoint inhibitors in non-small cell lung cancer. Lung Cancer 2016;99: 79-87.
102. Ilie M, Long-Mira E, Bence C, Butori C, Lassalle S, Bouhlel L, et al. Comparative study of the PD-L1 status between surgically resected specimens and matched biopsies of NSCLC patients reveal major discordances: a potential issue for anti-PD-L1 therapeutic strategies. Ann Oncol 2016;27: 147-53.
103. McLaughlin J, Han G, Schalper KA, Carvajal-Hausdorf D, Pelekanou V, Rehman J, et al. Quantitative Assessment of the Heterogeneity of PD-L1 Expression in Non-Small-Cell Lung Cancer. JAMA Oncol 2016;2: 46-54.
104. Lyford-Pike S, Peng S, Young GD, Taube JM, Westra WH, Akpeng B, et al. Evidence for a role of the PD-1:PD-L1 pathway in immune resistance of HPVassociated head and neck squamous cell carcinoma. Cancer Res 2013;73: 1733-41.
105. Galon J, Fox BA, Bifulco CB, Masucci G, Rau T, Botti G, et al. Immunoscore and Immunoprofiling in cancer: an update from the melanoma and immunotherapy bridge 2015. J Transl Med 2016;14: 273.
106. Tumeh PC, Harview CL, Yearley JH, Shintaku IP, Taylor EJ, Robert L, et al. PD-1 blockade induces responses by inhibiting adaptive immune resistance. Nature 2014;515: 568-71.
107. Bosse Y, Postma DS, Sin DD, Lamontagne M, Couture C, Gaudreault N, et al. Molecular signature of smoking in human lung tissues. Cancer Res 2012;72: 3753-63.
108. Rizvi NA, Hellmann MD, Snyder A, Kvistborg P, Makarov V, Havel JJ, et al. Cancer immunology. Mutational landscape determines sensitivity to PD-1 blockade in non-small cell lung cancer. Science 2015;348: 124-8.
109. Desrichard A, Snyder A, Chan TA. Cancer Neoantigens and Applications for Immunotherapy. Clin Cancer Res 2016;22: 807-12.
110. Inoue Y, Yoshimura K, Mori K, Kurabe N, Kahyo T, Mori H, et al. Clinical significance of PD-L1 and PD-L2 copy number gains in non-small-cell lung cancer. Oncotarget 2016;7: 32113-28.
111. Groenen PJ, Langerak AW, van Dongen JJ, van Krieken JH. Pitfalls in TCR gene clonality testing: teaching cases. J Hematop 2008;1: 97-109.
112. Khagi Y, Kurzrock R, Patel SP. Next generation predictive biomarkers for immune checkpoint inhibition. Cancer Metastasis Rev 2016.
113. Rizvi NA, Hellmann MD, Brahmer JR, Juergens RA, Borghaei H, Gettinger S, et al. Nivolumab in Combination With Platinum-Based Doublet Chemotherapy for First-Line Treatment of Advanced Non-Small-Cell Lung Cancer. J Clin Oncol
2016;34: 2969-79.
114. Seyedin SN, Schoenhals JE, Lee DA, Cortez MA, Wang X, Niknam S, et al. Strategies for combining immunotherapy with radiation for anticancer therapy. Immunotherapy 2015;7: 967-80.
115. Mellman I, Coukos G, Dranoff G. Cancer immunotherapy comes of age. Nature 2011;480: 480-9.
116. Thomas LJ, Vitale L, O'Neill T, Dolnick RY, Wallace PK, Minderman H, et al. Development of a Novel Antibody-Drug Conjugate for the Potential Treatment of Ovarian, Lung, and Renal Cell Carcinoma Expressing TIM-1. Mol Cancer Ther 2016;15: 2946-54.
117. Fraietta JA, Beckwith KA, Patel PR, Ruella M, Zheng Z, Barrett DM, et al. Ibrutinib enhances chimeric antigen receptor T-cell engraftment and efficacy in leukemia. Blood 2016;127: 1117-27.
118. June CH. Remote Controlled CARs: Towards a Safer Therapy for Leukemia. Cancer Immunol Res 2016;4: 643.
119. de Gramont A, Faivre S, Raymond E. Novel TGF-beta inhibitors ready for prime time in onco-immunology. Oncoimmunology 2017;6: e1257453.
120. Bruttel VS, Wischhusen J. Cancer stem cell immunology: key to understanding tumorigenesis and tumor immune escape? Front Immunol 2014;5: 360.

121. Codony-Servat J, Rosell R. Cancer stem cells and immunoresistance: clinical implications and solutions. Transl Lung Cancer Res 2015;4: 689-703.

Legend to Figures

Figure 1. Cancer immunity cycle. The cancer immunity cycle is a multistep process that involves (1) release of cancer cell antigens (magenta circles); (2) cancer antigen presentation to antigen-presenting cells (APC); (3) T cell priming and activation into lymph nodes; (4) trafficking of T cells to the tumor; (5) infiltration of T cells into the tumor; (6) recognition of cancer cells by T cells; and (7) killing of cancer target cells. The numerous factors that come into play in the cancer-immunity cycle provide a wide range of potential therapeutic targets. Adapted from Chen and Mellman [15, 16].

Figure 2. Principle of the anti-PD-1/PD-L1 immunotherapy. PD-1 is expressed by activated T lymphocytes; by binding to PD-L1, expressed on cancer cells, it mediates T-lymphocyte suppression (right). The use of anti-PD-1 (i.e.; Nivolumab, Pembrolizumab, Pidilizumab) or anti-PD-L1 inhibitors (i.e.; Atezolizumab, Durvalumab) leads to the interruption of this immunosuppression and potential cytotoxicity exerted by the re-activated T cells (left).

Figure 1

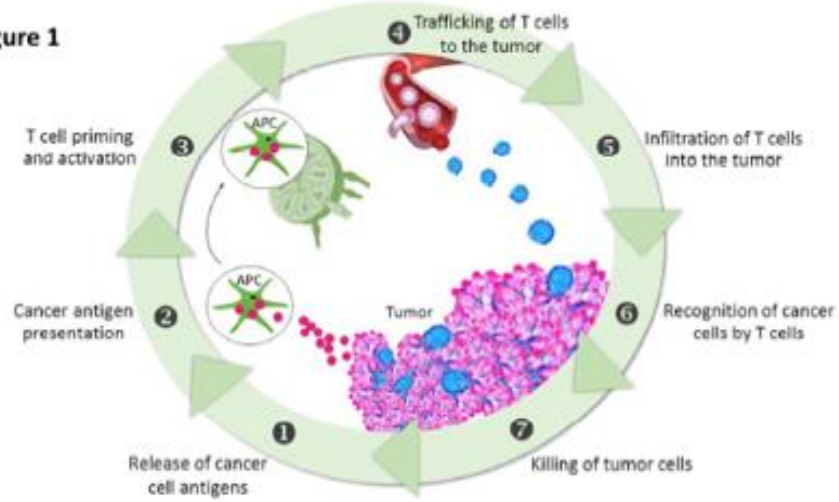

Figure 2

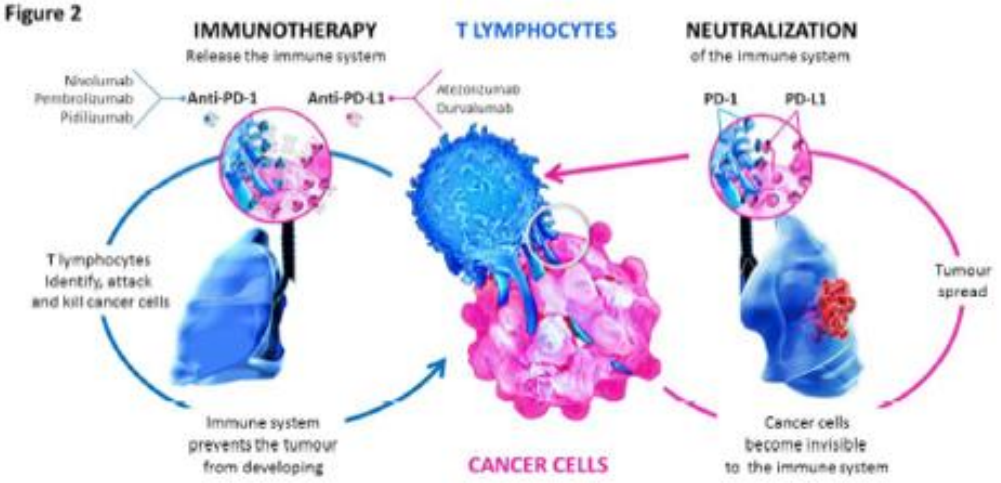

C. Autres publications

J. Benzaquen, Une BPCO trouée, La Lettre du Pneumologue 2017

M. Levraut, N. Martis, S. Leroy, JG. Fuzibet, J. Benzaquen, V. Queyrel, Atteinte pulmonaire associée à la MICI : une manifestation extradigestive mal connue. A propos de 2 cas, Société Nationale de Médecine Interne, 2017,

D. Makris, S. Leroy, J. Pradelli, J. Benzaquen, H. Guenard, J-M Perotin, S. Zakynthinos, E. Zakynthinos, G. Deslee, C.H. Marquette, Changes in dynamic lung mechanics after lung volume reduction coil treatment of severe emphysema, Thorax 2017, 73(6)

S. Leroy, J. Benzaquen, A. Mazzetta, S. Marchand-Adam, B. Padovani, D. Israel-Biet, C. Pison, P. Chanez, J. Cadranel, J. Mazières, V. Jounieaux, C. Cohen, V. Hofman, M. Ilie, P. Hofman, C.H. Marquette, Circulating tumour cells as a potential screening tool for lung cancer (the AIR study): protocol of a prospective multicentre cohort study in France, BMJ Open 2017, 7(12)

J. Benzaquen, J. Pradelli, B. Padovani, C.H. Marquette, S. Leroy, Emphysème, vous avez dit emphysème ? Revue des maladies respiratoires 2018, 35(1)

S. Heeke, V. Hofman, E. Long-Mira, V. Lespinet, S. Lalvée, O. Bordone, C. Ribeyre, V. Tanga, J. Benzaquen, S. Leroy, C. Cohen, J. Mouroux, C.H. Marquette, M. Ilié, P. Hofman, Use of the Ion PGM and the GeneReader NGS Systems in Daily Routine Practice for Advanced Lung Adenocarcinoma Patients: A Practical Point of View Reporting a Comparative Study and Assessment of 90 Patients, Cancers 2018 10(4)

J. Bulsei, S. Leroy, JM. Perotin, H. Mal, CH. Marquette, H. Dutau, A. Bourdin, JM. Vergnon, C. Pison, R. Kessler, V. Jounieaux, M. Salaün, A. Marceau, S. Dukic, C. Barbe, M. Bonnaire, G. Deslee, I. Durand-Zaleski & the REVOLENS study group, Cost-effectiveness of lung volume reduction coil treatment in patients with severe emphysema: results from the 2-year follow-up crossover REVOLENS study (REVOLENS-2 study) , Respiratory Research 2018, 19(1)

J. Benzaquen, J. Boutros, C.H. Marquette, H. Delingette, P. Hofman, Lung Cancer Screening, Towards a Multidimensional Approach: Why and How?, Cancers, 2019, 11(2)

S. Heeke, H. Delingette, Y Fanjat, E. Long-Mira, S. Lassalle, V. Hofman, J. Benzaquen, C.H. Marquette, P. Hofman, M. Ilié, La pathologie cancéreuse pulmonaire à l'heure de l'intelligence artificielle: entre espoir, désespoir et perspectives, Annales de pathologie 2019, 39(2)

Hofman V, Rouquette I, Long-Mira E, Piton N, Chamorey E, Heeke S, Vignaud JM, Yguel C, Mazières J, Lepage AL, Bibeau F, Begueret H, Lassalle S, Lalvée S, Zahaf K, Benzaquen J, Poudenx M, Marquette CH, Sabourin JC, Ilié M, Hofman P., Multicenter Evaluation of a Novel ROS1 Immunohistochemistry Assay (SP384) for Detection of ROS1 Rearrangements in a Large Cohort of Lung Adenocarcinoma Patients, J Thorac Oncol. 2019, 14(7)

Ilié M, Benzaquen J, Diascorn Y, Cohen C, Lésions pseudo tumorales induites par des agents pathogènes. Cas no 3, Annales de Pathologie, 2019, 39(4)

Ilié M, Benzaquen J, Diascorn Y, Cohen C, Lésions pseudo tumorales induites par des agents pathogènes. Cas no 4, Annales de Pathologie, 2019, 39(4)

Hofman V, Benzaquen J, Diascorn Y, Cohen C, Lésions pseudo tumorales induites par des agents pathogènes. Cas no 5, Annales de Pathologie, 2019, 39(4)

Hofman V, Benzaquen J, Diascorn Y, Cohen C, Lésions pseudo tumorales induites par des agents pathogènes. Cas no 6, Annales de Pathologie, 2019, 39(4)

Hofman P, Benzaquen J, Diascorn Y, Cohen C, Lésions pseudo tumorales induites par des agents pathogènes. Cas no 7, Annales de Pathologie, 2019, 39(4)

Hofman P, Benzaquen J, Lassalle S, Diascorn Y, Cohen C, Lésions pseudo tumorales induites par des agents pathogènes. Cas no 8, Annales de Pathologie, 2019, 39(4)

S. Heeke*, J. Benzaquen*, V. Hofman, M. Ilié, M. Allegra, E. Long-Mira, S. Lassalle, V. Tanga, C. Salacroup, C. Bonnetaud, J. Fayada, L. Gazoppi, L. Ribeyre, O. Castelnau, G. Garnier, F. Cattet, I. Nanni, F. de Fraipont, C. Cohen, JP. Berthet, S. Leroy, M. Poudenx, CH. Marquette, MG. Denis, F. Barlesi, P. Hofman, Critical Assessment in Routine Clinical Practice of Liquid Biopsy for EGFR Status Testing in Non-Small-Cell Lung Cancer: A Single-Laboratory Experience (LPCE, Nice, France), Clinical Lung Cancer 2019, 21(1)

S. Heeke, J. Benzaquen, E. Long-Mira, B. Audelan, V. Lespinet, O. Bordone, S. Lalvée, K. Zahaf, M. Poudenx, O. Humbert, H. Montaudié, PM. Dugourd, M. Chassang, T. Passeron, H. Delingette, CH Marquette, V. Hofman, A. Stenzinger, M. Ilié and P. Hofman, In-house Implementation of Tumor Mutational Burden Testing to Predict Durable Clinical Benefit in Non-small Cell Lung Cancer and Melanoma Patients, Cancers 2019, 11(9)

J. Boutros, M. Muzzone, J. Benzaquen, M. Levraut, CH. Marquette, F. Rocher, Y. Diascorn, B. Padovani, V. Hofman, S. Leroy, A case report of exogenous lipoid pneumonia associated with avocado/soybean unsaponifiables, BMC Pulmonary Medicine 2019, 19(1)

J. Pradelli, P. Verdoire, J. Boutros, AC. Frin, P. Follana, J. Duquesne, CH. Marquette, J. Benzaquen, M. Ben Hayoun, S. Leroy, Allergy Evaluation of Hypersensitivity to Platinum Salts and Taxanes: A Six-Year Experience, The Journal of Allergy and Clinical Immunology: In Practice 2019, 8(5)

S. Heeke, V. Hofman, M. Ilié, M. Allegra, V. Lespinet, O. Bordone, J. Benzaquen, J. Boutros, M. Poudenx, S. Lalvée, V. Tanga, C. Salacroup, C. Bonnetaud, CH. Marquette, P. Hofman, Prospective evaluation of NGS-based liquid biopsy in untreated late stage non-squamous lung carcinoma in a single institution, Journal of Translational Medicine 2020, 18(1)

J. Boutros, J. Benzaquen, M. Delin, B. Padovani, CH Marquette, S. Leroy, Exuberant cystic destruction of lung parenchyma, Respiratory Medicine and Research 2020, 78

S. Lassalle, V. Hofman, S. Heeke, J. Benzaquen, E. Long, M. Poudenx, E. Lantéri, J. Boutros, V. Tanga, K. Zahaf, S Lalvée, V. Lespinet, O. Bordone, JM. Félix, C. Bonnetaud, CH. Marquette, M. Ilie, P. Hofman, Targeted Assessment of the EGFR Status as Reflex Testing in Treatment-Naive Non-Squamous Cell Lung Carcinoma Patients: A Single Laboratory Experience (LPCE, Nice, France), Cancers 2020, 12(4)

V. Hofman, J. Benzaquen, S. Heeke, S. Lassalle, M. Poudenx, E. Long, E. Lantéri, O. Bordone, V. Lespinet, V. Tanga, C. Bonnetaud, Y. Bille, M. Ilié, CH. Marquette, F. Barlesi, J. Boutros, P. Hofman, Real-world assessment of the BRAF status in non-squamous cell lung carcinoma using VE1 immunohistochemistry: A single laboratory experience (LPCE, Nice, France), Lung Cancer 2020, 145

S. Heeke, J. Benzaquen, V. Hofman, E. Long-Mira, V. Lespinet, O. Bordone, CH. Marquette, H. Delingette, M. Ilié, P. Hofman, Comparison of Three Sequencing Panels Used for the Assessment of Tumor Mutational Burden in NSCLC Reveals Low Comparability, Journal of Thoracic Oncology 2020, 15(9)

P. Brest, J. Benzaquen, DJ. Klionsky, P. Hofman, B. Mograbi, Open questions for harnessing autophagy-modulating drugs in the SARS-CoV-2 war: hope or hype? Autophagy 2020, online

CH. Marquette, J. Boutros, J. Benzaquen, M. Ferreira, J. Pastre, C. Pison, B. Padovani, F. Bettayeb, V. Fallet, N. Guibert, D. Basille, M. Ilie, V. Hofman, P. Hofman, AIR project Study Group, Circulating tumour cells as a potential biomarker for lung cancer screening: a prospective cohort study, The Lancet Respiratory Medicine 2020, 8(7)

D. Chardin, M. Paquet, R. Schiappa, J. Darcourt, C. Bailleux, M. Poudenx, A. Sciazza, M. Ilie, J. Benzaquen, N. Martin, J. Otto, O. Humbert, Baseline metabolic tumor volume as a strong predictive and prognostic biomarker in patients with non-small cell lung cancer treated with PD1 inhibitors: a prospective study, Journal for ImmunoTherapy of Cancer 2020, 8(2)

L. Bouhlel, J. Doyen, E. Chamorey, M. Poudenx, M. Ilie, J. Gal, J. Guigay, J. Benzaquen, CH. Marquette, JP. Berthet, J. Mouroux, R. Schiappa, B. Padovani, P. Hofman, J. Otto, Occurrence and number of immune-related adverse events are independently associated with survival in advanced non-small-cell lung cancer treated by nivolumab, Bulletin du Cancer 2020, 107(9)

E. Nadal, S. Heeke, J. Benzaquen, N. Vilariño, A. Navarro, D. Azuara, M. Varela, J. Otto, N. Baixeras, D. Shahbazian, P. Puchois, S. Church, T. Smith, E. Lanteri, M. Ilié, P. Hofman, Two Patients With Advanced-Stage Lung Adenocarcinoma With Radiologic Complete Response to Nivolumab Treatment Harboring an STK11/LKB1 Mutation, Journal of Clinical Oncology (Precision Oncology) 2020, 4

P. Hofman, M. Ilié, E. Chamorey, P. Brest, R. Schiappa, V. Nakache, M. Antoine, M. Barberis, H. Begueret, F. Bibeau, C. Bonnetaud, P. Boström, P. Brousset, L. Bubendorf, L. Carvalho, G. Cathomas, A. Cazes, L. Chalabreysse, M.P. Chenard, M.C. Copin, J.F. Côté, D. Damotte, L. de Leval, P. Delongova, V. de Montpreville, A. de Muret, A. Dema, W. Dietmaier, M. Evert, A.

Fabre, F. Forest, A. Foulet, S. Garcia, M. Garcia-Martos, L. Gibault, G. Gorkiewicz, D. Jonigk, J. Gosney, A. Hofman, I. Kern, K. Kerr, M. Kossai, M. Kriegsmann, S. Lassalle, E. Long-Mira, A. Lupo, A. Mamilos, R. Matěj, J. Meilleroux, C. Ortiz-Villalón, L. Panico, A. Panizo, M. Papotti, P. Pauwels, G. Pelosi, F. Penault-Llorca, O. Pop, N. Poté, S. Ramon Y Cajal, J.C. Sabourin, I. Salmon, M. Sajin, S. Savic-Prince, H.U. Schildhaus, P. Schirmacher, I. Serre, E. Shaw, D. Sizaret, A. Stenzinger, J. Stojsic, E. Thunnissen, W. Timens, G. Troncone, C. Werlein, H. Wolff, J.P. Berthet, J. Benzaquen, C.H. Marquette, V Hofman, F Calabrese, Clinical and molecular practice of European thoracic pathology laboratories during the COVID-19 pandemic. The past and the near future. ESMO Open 2020, accepted.

IX. Bibliographie

1. Inca. Les cancers en France l'essentiel des faits et chiffres. E-CancerFr. 2019;
2. Scagliotti GV, Parikh P, von Pawel J, et al. Phase III Study Comparing Cisplatin Plus Gemcitabine With Cisplatin Plus Pemetrexed in Chemotherapy-Naive Patients With Advanced-Stage Non–Small-Cell Lung Cancer. J Clin Oncol [Internet]. 2008; 26: 3543–51. Available at: http://ascopubs.org/doi/10.1200/JCO.2007.15.0375
3. Sandler A, Gray R, Perry MC, et al. Paclitaxel–Carboplatin Alone or with Bevacizumab for Non–Small-Cell Lung Cancer. N Engl J Med [Internet]. 2006; 355: 2542–50. Available at: http://www.nejm.org/doi/abs/10.1056/NEJMoa061884
4. Yuan M, Huang LL, Chen JH, Wu J, Xu Q. The emerging treatment landscape of targeted therapy in non-small-cell lung cancer. Signal Transduct Target Ther [Internet]. 2019; 4: 61. Available at: http://www.nature.com/articles/s41392-019-0099-9
5. Havel JJ, Chowell D, Chan TA. The evolving landscape of biomarkers for checkpoint inhibitor immunotherapy. Nat Rev Cancer [Internet]. 2019; 19: 133–50. Available at: http://www.nature.com/articles/s41568-019-0116-x
6. Balkwill FR, Capasso M, Hagemann T. The tumor microenvironment at a glance. J Cell Sci [Internet]. 2012; 125: 5591–6. Available at: http://jcs.biologists.org/cgi/doi/10.1242/jcs.116392
7. Anderson NM, Simon MC. The tumor microenvironment. Curr Biol [Internet]. 2020; 30: R921–5. Available at: https://linkinghub.elsevier.com/retrieve/pii/S0960982220309337
8. Fox IH. Degradation of Purine Nucleotides. In 1978: 93–124. Available at: http://link.springer.com/10.1007/978-3-642-66867-8_5
9. Di Virgilio F, Sarti AC, Falzoni S, De Marchi E, Adinolfi E. Extracellular ATP and P2 purinergic signalling in the tumour microenvironment. Nat Rev Cancer [Internet]. 2018; 18: 601–18. Available at: http://www.nature.com/articles/s41568-018-0037-0
10. RAPAPORT E. Mechanisms of Anticancer Activities of Adenine Nucleotides in Tumor-Bearing Hosts. Ann N Y Acad Sci [Internet]. 1990; 603: 142–9. Available at: http://doi.wiley.com/10.1111/j.1749-6632.1990.tb37668.x
11. Kepp O, Loos F, Liu P, Kroemer G. Extracellular nucleosides and nucleotides as immunomodulators. Immunol Rev [Internet]. 2017; 280: 83–92. Available at: http://doi.wiley.com/10.1111/imr.12571
12. Di Virgilio F, Adinolfi E. Extracellular purines, purinergic receptors and tumor growth. Oncogene [Internet]. 2017; 36: 293–303. Available at: http://www.nature.com/articles/onc2016206
13. Volonté C, D'Ambrosi N. Membrane compartments and purinergic signalling: The purinome, a complex interplay among ligands, degrading enzymes, receptors and transporters. FEBS J [Internet]. 2009; 276: 318–29. Available at: http://doi.wiley.com/10.1111/j.1742-4658.2008.06793.x
14. Hanahan D, Weinberg RA. Hallmarks of cancer: The next generation. Cell [Internet]. 2011; 144: 646–74. Available at: https://linkinghub.elsevier.com/retrieve/pii/S0092867411001279
15. Campos-Contreras ADR, Díaz-Muñoz M, Vázquez-Cuevas FG. Purinergic Signaling in the Hallmarks of Cancer. Cells [Internet]. 2020; 9: 1612. Available at: https://www.mdpi.com/2073-4409/9/7/1612
16. Shah D, Romero F, Stafstrom W, Duong M, Summer R. Extracellular ATP mediates the

late phase of neutrophil recruitment to the lung in murine models of acute lung injury. Am J Physiol - Lung Cell Mol Physiol [Internet]. 2014; 306: L152–61. Available at: https://www.physiology.org/doi/10.1152/ajplung.00229.2013
17. Sperlágh B, Haskó G, Németh Z, Vizi ES. ATP released by LPS increases nitric oxide production in raw 264.7 macrophage cell line via P2Z/P2X7 receptors. Neurochem Int [Internet]. 1998; 33: 209–15. Available at: https://linkinghub.elsevier.com/retrieve/pii/S0197018698000254
18. Gusovsky F, Daly JW, Yasumoto T, Rojas E. Differential effects of maitotoxin on ATP secretion and on phosphoinositide breakdown in rat pheochromocytoma cells. FEBS Lett [Internet]. 1988; 233: 139–42. Available at: http://doi.wiley.com/10.1016/0014-5793%2888%2981371-1
19. Takai E, Tsukimoto M, Harada H, Sawada K, Moriyama Y, Kojima S. Autocrine regulation of TGF-β1-induced cell migration by exocytosis of ATP and activation of P2 receptors in human lung cancer cells. J Cell Sci [Internet]. 2012; 125: 5051–60. Available at: http://jcs.biologists.org/cgi/doi/10.1242/jcs.104976
20. Vázquez-Cuevas FG, Martínez-Ramírez AS, Robles-Martínez L, et al. Paracrine Stimulation of P2X7 Receptor by ATP Activates a Proliferative Pathway in Ovarian Carcinoma Cells. J Cell Biochem [Internet]. 2014; 115: 1955–66. Available at: http://doi.wiley.com/10.1002/jcb.24867
21. Liu H, Yuan M, Yao Y, Wu D, Dong S, Tong X. In vitro effect of Pannexin 1 channel on the invasion and migration of I-10 testicular cancer cells via ERK1/2 signaling pathway. Biomed Pharmacother [Internet]. 2019; 117: 109090. Available at: https://linkinghub.elsevier.com/retrieve/pii/S0753332219311862
22. Pedersen S, Pedersen SF, Nilius B, Lambert IH, Hoffmann EK. Mechanical stress induces release of ATP from Ehrlich ascites tumor cells. Biochim Biophys Acta - Biomembr [Internet]. 1999; 1416: 271–84. Available at: https://linkinghub.elsevier.com/retrieve/pii/S0005273698002284
23. Pellegatti P, Raffaghello L, Bianchi G, Piccardi F, Pistoia V, Di Virgilio F. Increased level of extracellular ATP at tumor sites: In vivo imaging with plasma membrane luciferase. El Khoury J, Ed. PLoS One [Internet]. 2008; 3: e2599. Available at: https://dx.plos.org/10.1371/journal.pone.0002599
24. Lecciso M, Ocadlikova D, Sangaletti S, et al. ATP release from chemotherapy-treated dying leukemia cells Elicits an immune suppressive effect by increasing regulatory T cells and Tolerogenic dendritic cells. Front Immunol [Internet]. 2017; 8. Available at: http://journal.frontiersin.org/article/10.3389/fimmu.2017.01918/full
25. Michaud M, Martins I, Sukkurwala AQ, et al. Autophagy-dependent anticancer immune responses induced by chemotherapeutic agents in mice. Science (80-) [Internet]. 2011; 334: 1573–7. Available at: https://www.sciencemag.org/lookup/doi/10.1126/science.1208347
26. Loo JM, Scherl A, Nguyen A, et al. Extracellular metabolic energetics can promote cancer progression. Cell [Internet]. 2015; 160: 393–406. Available at: https://linkinghub.elsevier.com/retrieve/pii/S0092867414015888
27. Allard B, Beavis PA, Darcy PK, Stagg J. Immunosuppressive activities of adenosine in cancer. Curr Opin Pharmacol [Internet]. 2016; 29: 7–16. Available at: https://linkinghub.elsevier.com/retrieve/pii/S1471489216300443
28. Poth JM, Brodsky K, Ehrentraut H, Grenz A, Eltzschig HK. Transcriptional control of adenosine signaling by hypoxia-inducible transcription factors during ischemic or

inflammatory disease. J Mol Med [Internet]. 2013; 91: 183–93. Available at: http://link.springer.com/10.1007/s00109-012-0988-7
29. Sitkovsky M V., Lukashev D, Apasov S, et al. Physiological control of immune response and inflammatory tissue damage by hypoxia-inducible factors and adenosine A2A receptors. Annu Rev Immunol [Internet]. 2004; 22: 657–82. Available at: http://www.annualreviews.org/doi/10.1146/annurev.immunol.22.012703.104731
30. Spychala J. Tumor-promoting functions of adenosine. Pharmacol Ther [Internet]. 2000; 87: 161–73. Available at: https://linkinghub.elsevier.com/retrieve/pii/S016372580000053X
31. Ohta A, Gorelik E, Prasad SJ, et al. A2A adenosine receptor protects tumors from antitumor T cells. Proc Natl Acad Sci U S A [Internet]. 2006; 103: 13132–7. Available at: http://www.pnas.org/cgi/doi/10.1073/pnas.0605251103
32. Synnestvedt K, Furuta GT, Comerford KM, et al. Ecto-5'-nucleotidase (CD73) regulation by hypoxia-inducible factor-1 mediates permeability changes in intestinal epithelia. J Clin Invest [Internet]. 2002; 110: 993–1002. Available at: http://www.jci.org/articles/view/15337
33. Burnstock G. Introduction to Purinergic Signalling in the Brain. Adv Exp Med Biol [Internet]. 2013; 986: 1–12. Available at: http://www.ncbi.nlm.nih.gov/pubmed/22879061
34. Ferrari D, McNamee EN, Idzko M, Gambari R, Eltzschig HK. Purinergic Signaling During Immune Cell Trafficking. Trends Immunol [Internet]. 2016; 37: 399–411. Available at: https://linkinghub.elsevier.com/retrieve/pii/S1471490616300072
35. Burnstock G. Purinergic nerves. Pharmacol Rev [Internet]. 1972; 24: 509–81. Available at: http://www.ncbi.nlm.nih.gov/pubmed/4404211
36. Lustig KD, Shiau AK, Brake AJ, Julius D. Expression cloning of an ATP receptor from mouse neuroblastoma cells. Proc Natl Acad Sci U S A [Internet]. 1993; 90: 5113–7. Available at: http://www.pnas.org/cgi/doi/10.1073/pnas.90.11.5113
37. Webb TE, Simon J, Krishek BJ, et al. Cloning and functional expression of a brain G-protein-coupled ATP receptor. FEBS Lett [Internet]. 1993; 324: 219–25. Available at: http://doi.wiley.com/10.1016/0014-5793%2893%2981397-I
38. Surprenant A, Rassendren F, Kawashima E, North RA, Buell G. The cytolytic P2Z receptor for extracellular ATP identified as a P2X receptor (P2X7). Science (80-) [Internet]. 1996; 272: 735–8. Available at: https://www.sciencemag.org/lookup/doi/10.1126/science.272.5262.735
39. Burnstock G. Purine and pyrimidine receptors. Cell Mol Life Sci [Internet]. 2007; 64: 1471–83. Available at: http://link.springer.com/10.1007/s00018-007-6497-0
40. Sitkovsky M V., Ohta A. The 'danger' sensors that STOP the immune response: The A2 adenosine receptors? Trends Immunol [Internet]. 2005; 26: 299–304. Available at: https://linkinghub.elsevier.com/retrieve/pii/S1471490605001031
41. Burnstock G. Purine and purinergic receptors. Brain Neurosci Adv [Internet]. 2018; 2: 239821281881749. Available at: http://journals.sagepub.com/doi/10.1177/2398212818817494
42. Sitkovsky M V. Use of the A 2A adenosine receptor as a physiological immunosuppressor and to engineer inflammation in vivo. Biochem Pharmacol [Internet]. 2003; 65: 493–501. Available at: https://linkinghub.elsevier.com/retrieve/pii/S0006295202015484
43. Inoue Y, Yoshimura K, Kurabe N, et al. Prognostic impact of CD73 and A2A adenosine

receptor expression in non-small-cell lung cancer. Oncotarget [Internet]. 2017; 8: 8738–51. Available at: https://www.oncotarget.com/lookup/doi/10.18632/oncotarget.14434
44. Puchałowicz K, Tarnowski M, Baranowska-Bosiacka I, Chlubek D, Dziedziejko V. P2X and P2Y receptors—role in the pathophysiology of the nervous system. Int J Mol Sci [Internet]. 2014; 15: 23672–704. Available at: http://www.ncbi.nlm.nih.gov/pubmed/25530618
45. Idzko M, Ferrari D, Eltzschig HK. Nucleotide signalling during inflammation. Nature [Internet]. 2014; 509: 310–7. Available at: http://www.nature.com/articles/nature13085
46. Kawate T, Michel JC, Birdsong WT, Gouaux E. Crystal structure of the ATP-gated P2X4 ion channel in the closed state. Nature [Internet]. 2009; 460: 592–8. Available at: http://www.nature.com/articles/nature08198
47. Karasawa A, Kawate T. Structural basis for subtype-specific inhibition of the P2X7 receptor. Elife [Internet]. 2016; 5. Available at: https://elifesciences.org/articles/22153
48. McCarthy AE, Yoshioka C, Mansoor SE. Full-Length P2X7 Structures Reveal How Palmitoylation Prevents Channel Desensitization. Cell [Internet]. 2019; 179: 659-670.e13. Available at: https://linkinghub.elsevier.com/retrieve/pii/S0092867419310682
49. Illes P, Müller CE, Jacobson KA, et al. Update of P2X receptor properties and their pharmacology: IUPHAR Review 30. Br J Pharmacol [Internet]. 2020; bph.15299. Available at: http://www.ncbi.nlm.nih.gov/pubmed/33125712
50. Scheuplein F, Schwarz N, Adriouch S, et al. NAD + and ATP Released from Injured Cells Induce P2X 7 -Dependent Shedding of CD62L and Externalization of Phosphatidylserine by Murine T Cells . J Immunol [Internet]. 2009; 182: 2898–908. Available at: http://www.jimmunol.org/lookup/doi/10.4049/jimmunol.0801711
51. Lecut C, Frederix K, Johnson DM, et al. P2X 1 Ion Channels Promote Neutrophil Chemotaxis through Rho Kinase Activation . J Immunol [Internet]. 2009; 183: 2801–9. Available at: http://www.jimmunol.org/lookup/doi/10.4049/jimmunol.0804007
52. Mulryan K, Gitterman DP, Lewis CJ, et al. Reduced vas deferens contraction and male infertility in mice lacking P2X1 receptors. Nature [Internet]. 2000; 403: 86–9. Available at: http://www.nature.com/articles/47495
53. Nurden AT. Does ATP act through P2X1 receptors to regulate platelet activation and thrombus formation? J Thromb Haemost [Internet]. 2007; 5: 907–9. Available at: http://doi.wiley.com/10.1111/j.1538-7836.2007.02456.x
54. Xu GY, Shenoy M, Winston JH, Mittal S, Pasricha PJ. P2X receptor-mediated visceral hyperalgesia in a rat model of chronic visceral hypersensitivity. Gut [Internet]. 2008; 57: 1230–7. Available at: https://gut.bmj.com/lookup/doi/10.1136/gut.2007.134221
55. Souslova V, Cesare P, Ding Y, et al. Warm-coding deficits and aberrant inflammatory pain in mice lacking P2X3 receptors. Nature [Internet]. 2000; 407: 1015–7. Available at: http://www.nature.com/articles/35039526
56. Jarvis MF, Burgard EC, McGaraughty S, et al. A-317491, a novel potent and selective non-nucleotide antagonist of P2X3 and P2X2/3 receptors, reduces chronic inflammatory and neuropathic pain in the rat. Proc Natl Acad Sci U S A [Internet]. 2002; 99: 17179–84. Available at: http://www.pnas.org/cgi/doi/10.1073/pnas.252537299
57. Cockayne DA, Hamilton SG, Zhu QM, et al. Urinary bladder hyporeflexia and reduced pain-related behaviour in P2X3-deficient mice. Nature [Internet]. 2000; 407: 1011–5.

Available at: http://www.nature.com/articles/35039519
58. Finger TE, Danilova V, Barrows J, et al. Neuroscience: ATP signalling is crucial for communication from taste buds to gustatory nerves. Science (80-) [Internet]. 2005; 310: 1495–9. Available at: https://www.sciencemag.org/lookup/doi/10.1126/science.1118435
59. Sim JA, Chaumont S, Jo J, et al. Altered hippocampal synaptic potentiation in P2X4 knock-out mice. J Neurosci [Internet]. 2006; 26: 9006–9. Available at: http://www.jneurosci.org/cgi/doi/10.1523/JNEUROSCI.2370-06.2006
60. Tsuda M, Shigemoto-Mogami Y, Koizumi S, et al. P2X4 receptors induced in spinal microglia gate tactile allodynia after nerve injury. Nature [Internet]. 2003; 424: 778–83. Available at: http://www.nature.com/articles/nature01786
61. Cockcroft S, Gomperts BD. The ATP4- receptor of rat mast cells. Biochem J [Internet]. 1980; 188: 789–98. Available at: https://portlandpress.com/biochemj/article/188/3/789/12154/The-ATP4-receptor-of-rat-mast-cells
62. Burnstock G, Knight GE. The potential of P2X7 receptors as a therapeutic target, including inflammation and tumour progression. Purinergic Signal [Internet]. 2018; 14: 1–18. Available at: http://link.springer.com/10.1007/s11302-017-9593-0
63. Benzaquen J, Heeke S, Janho dit Hreich S, et al. Alternative splicing of P2RX7 pre-messenger RNA in health and diseases: Myth or reality? Biomed J [Internet]. 2019; 42: 141–54. Available at: https://linkinghub.elsevier.com/retrieve/pii/S2319417019302513
64. Burnstock G. P2X ion channel receptors and inflammation. Purinergic Signal [Internet]. 2016; 12: 59–67. Available at: http://link.springer.com/10.1007/s11302-015-9493-0
65. Burnstock G. The therapeutic potential of purinergic signalling. Biochem Pharmacol [Internet]. 2018; 151: 157–65. Available at: https://linkinghub.elsevier.com/retrieve/pii/S000629521730504X
66. Buell G, Chessell IP, Michel AD, et al. Blockade of human P2X7 receptor function with a monoclonal antibody. Blood [Internet]. 1998; 92: 3521–8. Available at: http://www.ncbi.nlm.nih.gov/pubmed/9808543
67. He Y, Taylor N, Fourgeaud L, Bhattacharya A. The role of microglial P2X7: Modulation of cell death and cytokine release. J Neuroinflammation [Internet]. 2017; 14: 135. Available at: http://jneuroinflammation.biomedcentral.com/articles/10.1186/s12974-017-0904-8
68. Young CNJ, Chira N, Róg J, et al. Sustained activation of P2X7 induces MMP-2-evoked cleavage and functional purinoceptor inhibition. J Mol Cell Biol [Internet]. 2018; 10: 229–42. Available at: https://academic.oup.com/jmcb/article/10/3/229/4084680
69. Smart ML, Gu B, Panchal RG, et al. P2X7 receptor cell surface expression and cytolytic pore formation are regulated by a distal C-terminal region. J Biol Chem [Internet]. 2003; 278: 8853–60. Available at: http://www.jbc.org/lookup/doi/10.1074/jbc.M211094200
70. Feng YH, Li X, Zeng R, Gorodeski GI. Endogenously expressed truncated P2X7 receptor lacking the C-terminus is preferentially upregulated in epithelial cancer cells and fails to mediate ligand-induced pore formation and apoptosis. Nucleosides, Nucleotides and Nucleic Acids [Internet]. 2006; 25: 1271–6. Available at: http://www.tandfonline.com/doi/abs/10.1080/15257770600890921
71. Costa-Junior HM, Vieira FS, Coutinho-Silva R. C terminus of the P2X7 receptor: Treasure hunting. Purinergic Signal [Internet]. 2011; 7: 7–19. Available at:

http://link.springer.com/10.1007/s11302-011-9215-1
72. Mansoor SE, Lü W, Oosterheert W, Shekhar M, Tajkhorshid E, Gouaux E. X-ray structures define human P2X 3 receptor gating cycle and antagonist action. Nature [Internet]. 2016; 538: 66–71. Available at: http://www.nature.com/articles/nature19367
73. Hattori M, Gouaux E. Molecular mechanism of ATP binding and ion channel activation in P2X receptors. Nature [Internet]. 2012; 485: 207–12. Available at: http://www.nature.com/articles/nature11010
74. Kasuya G, Yamaura T, Ma XB, et al. Structural insights into the competitive inhibition of the ATP-gated P2X receptor channel. Nat Commun [Internet]. 2017; 8: 876. Available at: http://www.nature.com/articles/s41467-017-00887-9
75. Karasawa A, Michalski K, Mikhelzon P, Kawate T. The P2X7 receptor forms a dye-permeable pore independent of its intracellular domain but dependent on membrane lipid composition. Elife [Internet]. 2017; 6. Available at: https://elifesciences.org/articles/31186
76. Pellegatti P, Raffaghello L, Bianchi G, Piccardi F, Pistoia V, Di Virgilio F. Increased Level of Extracellular ATP at Tumor Sites: In Vivo Imaging with Plasma Membrane Luciferase. El Khoury J, Ed. PLoS One [Internet]. 2008; 3: e2599. Available at: https://dx.plos.org/10.1371/journal.pone.0002599
77. Riteau N, Gasse P, Fauconnier L, et al. Extracellular ATP is a danger signal activating P2X7 receptor in lung inflammation and fibrosis. Am J Respir Crit Care Med. 2010; 182: 774–83.
78. Seman M, Adriouch S, Scheuplein F, et al. NAD-induced T cell death: ADP-ribosylation of cell surface proteins by ART2 activates the cytolytic P2X7 purinoceptor. Immunity [Internet]. 2003; 19: 571–82. Available at: https://linkinghub.elsevier.com/retrieve/pii/S1074761303002668
79. Adriouch S, Bannas P, Schwarz N, et al. ADP-ribosylation at R125 gates the P2X7 ion channel by presenting a covalent ligand to its nucleotide binding site. FASEB J [Internet]. 2008; 22: 861–9. Available at: https://onlinelibrary.wiley.com/doi/abs/10.1096/fj.07-9294com
80. Adriouch S, Ohlrogge W, Haag F, Koch-Nolte F, Seman M. Rapid Induction of Naive T Cell Apoptosis by Ecto-Nicotinamide Adenine Dinucleotide: Requirement for Mono(ADP-Ribosyl)Transferase 2 and a Downstream Effector. J Immunol [Internet]. 2001; 167: 196–203. Available at: http://www.jimmunol.org/lookup/doi/10.4049/jimmunol.167.1.196
81. Di Virgilio F, Adinolfi E. Extracellular purines, purinergic receptors and tumor growth. Oncogene [Internet]. 2017; 36: 293–303. Available at: http://www.nature.com/articles/onc2016206
82. Sanz JM, Chiozzi P, Ferrari D, et al. Activation of Microglia by Amyloid β Requires P2X 7 Receptor Expression . J Immunol [Internet]. 2009; 182: 4378–85. Available at: http://www.jimmunol.org/lookup/doi/10.4049/jimmunol.0803612
83. Di Virgilio F, Giuliani AL, Vultaggio-Poma V, Falzoni S, Sarti AC. Non-nucleotide agonists triggering P2X7 receptor activation and pore formation. Front Pharmacol [Internet]. 2018; 9. Available at: http://journal.frontiersin.org/article/10.3389/fphar.2018.00039/full
84. Niemi K, Teirilä L, Lappalainen J, et al. Serum Amyloid A Activates the NLRP3 Inflammasome via P2X 7 Receptor and a Cathepsin B-Sensitive Pathway . J Immunol

[Internet]. 2011; 186: 6119–28. Available at: http://www.jimmunol.org/lookup/doi/10.4049/jimmunol.1002843
85. Frohm M, Agerberth B, Ahangari G, et al. The expression of the gene coding for the antibacterial peptide LL-37 is induced in human keratinocytes during inflammatory disorders. J Biol Chem [Internet]. 1997; 272: 15258–63. Available at: http://www.jbc.org/lookup/doi/10.1074/jbc.272.24.15258
86. Dorschner RA, Pestonjamasp VK, Tamakuwala S, et al. Cutaneous injury induces the release of cathelicidin anti-microbial peptides active against group A streptococcus. J Invest Dermatol [Internet]. 2001; 117: 91–7. Available at: https://linkinghub.elsevier.com/retrieve/pii/S0022202X15412928
87. Elssner A, Duncan M, Gavrilin M, Wewers MD. A Novel P2X 7 Receptor Activator, the Human Cathelicidin-Derived Peptide LL37, Induces IL-1β Processing and Release . J Immunol [Internet]. 2004; 172: 4987–94. Available at: http://www.jimmunol.org/lookup/doi/10.4049/jimmunol.172.8.4987
88. Tomasinsig L, Pizzirani C, Skerlavaj B, et al. The human cathelicidin LL-37 modulates the activities of the P2X 7 receptor in a structure-dependent manner. J Biol Chem [Internet]. 2008; 283: 30471–81. Available at: http://www.jbc.org/lookup/doi/10.1074/jbc.M802185200
89. Adinolfi E, Callegari MG, Ferrari D, et al. Basal activation of the P2X7 ATP receptor elevates mitochondrial calcium and potential, increases cellular ATP levels, and promotes serum-independent growth. Mol Biol Cell [Internet]. 2005; 16: 3260–72. Available at: https://www.molbiolcell.org/doi/10.1091/mbc.e04-11-1025
90. Ferrari D, Chiozzi P, Falzoni S, et al. Extracellular ATP triggers IL-1 beta release by activating the purinergic P2Z receptor of human macrophages. J Immunol [Internet]. 1997; 159: 1451–8. Available at: http://www.ncbi.nlm.nih.gov/pubmed/9233643
91. Yang D, He Y, Muñoz-Planillo R, Liu Q, Núñez G. Caspase-11 Requires the Pannexin-1 Channel and the Purinergic P2X7 Pore to Mediate Pyroptosis and Endotoxic Shock. Immunity [Internet]. 2015; 43: 923–32. Available at: https://linkinghub.elsevier.com/retrieve/pii/S1074761315004094
92. Bidula S, Dhuna K, Helliwell R, Stokes L. Positive allosteric modulation of P2X7 promotes apoptotic cell death over lytic cell death responses in macrophages. Cell Death Dis [Internet]. 2019; 10: 882. Available at: http://www.nature.com/articles/s41419-019-2110-3
93. Bernier LP, Ase AR, Chevallier S, et al. Phosphoinositides regulate P2X4 ATP-gated channels through direct interactions. J Neurosci [Internet]. 2008; 28: 12938–45. Available at: http://www.jneurosci.org/cgi/doi/10.1523/JNEUROSCI.3038-08.2008
94. Ferrari D, Pizzirani C, Adinolfi E, et al. The Antibiotic Polymyxin B Modulates P2X 7 Receptor Function . J Immunol [Internet]. 2004; 173: 4652–60. Available at: http://www.jimmunol.org/lookup/doi/10.4049/jimmunol.173.7.4652
95. Ferrari D, Pizzirani C, Gulinelli S, et al. Modulation of P2X 7 receptor functions by polymyxin B: Crucial role of the hydrophobic tail of the antibiotic molecule. Br J Pharmacol [Internet]. 2007; 150: 445–54. Available at: http://doi.wiley.com/10.1038/sj.bjp.0706994
96. Zemkova H, Khadra A, Rokic MB, Tvrdonova V, Sherman A, Stojilkovic SS. Allosteric regulation of the P2X4 receptor channel pore dilation. Pflugers Arch Eur J Physiol [Internet]. 2015; 467: 713–26. Available at: http://link.springer.com/10.1007/s00424-014-1546-7

97. Muller C. Medicinal Chemistry of P2X Receptors: Allosteric Modulators. Curr Med Chem [Internet]. 2015; 22: 929–41. Available at: http://www.eurekaselect.com/openurl/content.php?genre=article&issn=0929-8673&volume=22&issue=7&spage=929
98. Nörenberg W, Sobottka H, Hempel C, et al. Positive allosteric modulation by ivermectin of human but not murine P2X7 receptors. Br J Pharmacol [Internet]. 2012; 167: 48–66. Available at: http://doi.wiley.com/10.1111/j.1476-5381.2012.01987.x
99. Baqi Y, Hausmann R, Rosefort C, Rettinger J, Schmalzing G, Müller CE. Discovery of potent competitive antagonists and positive modulators of the P2X2 receptor. J Med Chem [Internet]. 2011; 54: 817–30. Available at: https://pubs.acs.org/doi/10.1021/jm1012193
100. Dhuna K, Felgate M, Bidula SM, et al. Ginsenosides act as positive modulators of P2X4 receptors. Mol Pharmacol [Internet]. 2019; 95: 210–21. Available at: http://molpharm.aspetjournals.org/lookup/doi/10.1124/mol.118.113696
101. Helliwell RM, Shioukhuey CO, Dhuna K, et al. Selected ginsenosides of the protopanaxdiol series are novel positive allosteric modulators of P2X7 receptors. Br J Pharmacol [Internet]. 2015; 172: 3326–40. Available at: http://doi.wiley.com/10.1111/bph.13123
102. Jiang LH, Rassendren F, Surprenant A, North RA. Identification of amino acid residues contributing to the ATP-binding site of a purinergic P2X receptor. J Biol Chem [Internet]. 2000; 275: 34190–6. Available at: http://www.jbc.org/lookup/doi/10.1074/jbc.M005481200
103. Di Virgilio F, Dal Ben D, Sarti AC, Giuliani AL, Falzoni S. The P2X7 Receptor in Infection and Inflammation. Immunity [Internet]. 2017; 47: 15–31. Available at: https://linkinghub.elsevier.com/retrieve/pii/S1074761317302807
104. Murgia M, Hanau S, Pizzo P, Rippa M, Di Virgilio F. Oxidized ATP. An irreversible inhibitor of the macrophage purinergic P(2Z) receptor. J Biol Chem [Internet]. 1993; 268: 8199–203. Available at: http://www.ncbi.nlm.nih.gov/pubmed/8463330
105. Adinolfi E, Cirillo M, Woltersdorf R, et al. Trophic activity of a naturally occurring truncated isoform of the P2X7 receptor. FASEB J [Internet]. 2010; 24: 3393–404. Available at: https://onlinelibrary.wiley.com/doi/abs/10.1096/fj.09-153601
106. Becker D, Woltersdorf R, Boldt W, et al. The P2X7 carboxyl tail is a regulatory module of P2X7 receptor channel activity. J Biol Chem [Internet]. 2008; 283: 25725–34. Available at: http://www.jbc.org/lookup/doi/10.1074/jbc.M803855200
107. Kopp R, Krautloher A, Ramírez-Fernández A, Nicke A. P2X7 Interactions and Signaling – Making Head or Tail of It. Front Mol Neurosci [Internet]. 2019; 12. Available at: https://www.frontiersin.org/article/10.3389/fnmol.2019.00183/full
108. Denlinger LC, Fisette PL, Sommer JA, et al. Cutting Edge: The Nucleotide Receptor P2X 7 Contains Multiple Protein- and Lipid-Interaction Motifs Including a Potential Binding Site for Bacterial Lipopolysaccharide . J Immunol [Internet]. 2001; 167: 1871–6. Available at: http://www.jimmunol.org/lookup/doi/10.4049/jimmunol.167.4.1871
109. Roger S, Pelegrin P, Surprenant A. Facilitation of P2X7 receptor currents and membrane blebbing via constitutive and dynamic calmodulin binding. J Neurosci [Internet]. 2008; 28: 6393–401. Available at: http://www.jneurosci.org/cgi/doi/10.1523/JNEUROSCI.0696-08.2008
110. Roger S, Mei ZZ, Baldwin JM, et al. Single nucleotide polymorphisms that were identified in affective mood disorders affect ATP-activated P2X7 receptor functions. J

Psychiatr Res [Internet]. 2010; 44: 347–55. Available at: https://linkinghub.elsevier.com/retrieve/pii/S0022395609002283
111. Watters JJ, Sommer JA, Fisette PL, et al. P2X7 nucleotide receptor: Modulation of LPS-induced macrophage signaling and mediator production. Drug Dev Res [Internet]. 2001; 53: 91–104. Available at: http://doi.wiley.com/10.1002/ddr.1176
112. Robinson LE, Shridar M, Smith P, Murrell-Lagnado RD. Plasma membrane cholesterol as a regulator of human and rodent P2X7 receptor activation and sensitization. J Biol Chem [Internet]. 2014; 289: 31983–94. Available at: http://www.jbc.org/lookup/doi/10.1074/jbc.M114.574699
113. Allsopp RC, Evans RJ. Contribution of the juxtatransmembrane intracellular regions to the time course and permeation of ATP-gated P2X7 Receptor Ion Channels. J Biol Chem [Internet]. 2015; 290: 14556–66. Available at: http://www.jbc.org/lookup/doi/10.1074/jbc.M115.642033
114. Sluyter R. The P2X7 Receptor. In 2017: 17–53. Available at: http://link.springer.com/10.1007/5584_2017_59
115. Amstrup J, Novak I. P2X7 receptor activates extracellular signal-regulated kinases ERK1 and ERK2 independently of Ca2+ influx. Biochem J [Internet]. 2003; 374: 51–61. Available at: https://portlandpress.com/biochemj/article/374/1/51/43691/P2X7-receptor-activates-extracellular
116. Yan Z, Li S, Liang Z, Tomić M, Stojilkovic SS. The P2X7 Receptor Channel Pore Dilates under Physiological Ion Conditions. J Gen Physiol [Internet]. 2008; 132: 563–73. Available at: https://rupress.org/jgp/article/132/5/563/43869/The-P2X7-Receptor-Channel-Pore-Dilates-under
117. Smart ML, Panchal RG, Bowser DN, Williams DA, Petrou S. Pore formation is not associated with macroscopic redistribution of P2X7 receptors. Am J Physiol Physiol [Internet]. 2002; 283: C77–84. Available at: https://www.physiology.org/doi/10.1152/ajpcell.00456.2001
118. Bannas P, Adriouch S, Kahl S, Braasch F, Haag F, Koch-Nolte F. Activity and specificity of toxin-related mouse T cell ecto-ADP- ribosyltransferase ART2.2 depends on its association with lipid rafts. Blood [Internet]. 2005; 105: 3663–70. Available at: https://ashpublications.org/blood/article/105/9/3663/21290/Activity-and-specificity-of-toxinrelated-mouse-T
119. Barth K, Weinhold K, Guenther A, Young MT, Schnittler H, Kasper M. Caveolin-1 influences P2X7 receptor expression and localization in mouse lung alveolar epithelial cells. FEBS J [Internet]. 2007; 274: 3021–33. Available at: http://doi.wiley.com/10.1111/j.1742-4658.2007.05830.x
120. Garcia-Marcos M, Pérez-Andrés E, Tandel S, et al. Coupling of two pools of P2X 7 receptors to distinct intracellular signaling pathways in rat submandibular gland. J Lipid Res [Internet]. 2006; 47: 705–14. Available at: http://www.jlr.org/lookup/doi/10.1194/jlr.M500408-JLR200
121. Zhao Q, Yang M, Ting AT, Logothetis DE. PIP2regulates the ionic current of P2X receptors and P2X 7 receptor-mediated cell death. Channels [Internet]. 2007; 1: 47–56. Available at: http://www.tandfonline.com/doi/abs/10.4161/chan.3914
122. Resh MD. Palmitoylation of ligands, receptors, and intracellular signaling molecules. Sci STKE [Internet]. 2006; 2006: re14–re14. Available at: https://stke.sciencemag.org/lookup/doi/10.1126/stke.3592006re14
123. Gonnord P, Delarasse C, Auger R, et al. Palmitoylation of the P2X7 receptor, an ATP-

gated channel, controls its expression and association with lipid rafts. FASEB J [Internet]. 2009; 23: 795–805. Available at: https://onlinelibrary.wiley.com/doi/abs/10.1096/fj.08-114637
124. Lenertz LY, Wang Z, Guadarrama A, Hill LM, Gavala ML, Bertics PJ. Mutation of putative N-linked glycosylation sites on the human nucleotide receptor P2X7 reveals a key residue important for receptor function. Biochemistry [Internet]. 2010; 49: 4611–9. Available at: https://pubs.acs.org/doi/10.1021/bi902083n
125. Browne LE, Compan V, Bragg L, North RA. P2X7 Receptor Channels Allow Direct Permeation of Nanometer-Sized Dyes. J Neurosci [Internet]. 2013; 33: 3557–66. Available at: http://www.jneurosci.org/cgi/doi/10.1523/JNEUROSCI.2235-12.2013
126. Macian F. NFAT proteins: key regulators of T-cell development and function. Nat Rev Immunol [Internet]. 2005; 5: 472–84. Available at: http://www.nature.com/articles/nri1632
127. Savio LEB, de Andrade Mello P, da Silva CG, Coutinho-Silva R. The P2X7 Receptor in Inflammatory Diseases: Angel or Demon? Front Pharmacol [Internet]. 2018; 9. Available at: http://journal.frontiersin.org/article/10.3389/fphar.2018.00052/full
128. Feske S. Calcium signalling in lymphocyte activation and disease. Nat Rev Immunol [Internet]. 2007; 7: 690–702. Available at: http://www.nature.com/articles/nri2152
129. Lee M, Park J. Regulation of NFAT activation: a potential therapeutic target for immunosuppression. Mol Cells [Internet]. 2006; 22: 1–7. Available at: http://www.ncbi.nlm.nih.gov/pubmed/16951543
130. Fracchia KM, Pai CY, Walsh CM. Modulation of T Cell Metabolism and Function through Calcium Signaling. Front Immunol [Internet]. 2013; 4. Available at: http://journal.frontiersin.org/article/10.3389/fimmu.2013.00324/abstract
131. Adinolfi E, Pizzirani C, Idzko M, et al. P2X7 receptor: Death or life? Purinergic Signal [Internet]. 2005; 1: 219–27. Available at: http://link.springer.com/10.1007/s11302-005-6322-x
132. Smart ML, Gu B, Panchal RG, et al. P2X7 receptor cell surface expression and cytolytic pore formation are regulated by a distal C-terminal region. J Biol Chem [Internet]. 2003; 278: 8853–60. Available at: http://www.jbc.org/lookup/doi/10.1074/jbc.M211094200
133. Young CNJ, Górecki DC. P2RX7 purinoceptor as a therapeutic target-The second coming? Front Chem [Internet]. 2018; 6. Available at: https://www.frontiersin.org/article/10.3389/fchem.2018.00248/full
134. Pelegrin P, Surprenant A. Pannexin-1 mediates large pore formation and interleukin-1β release by the ATP-gated P2X7 receptor. EMBO J [Internet]. 2006; 25: 5071–82. Available at: http://emboj.embopress.org/cgi/doi/10.1038/sj.emboj.7601378
135. Riedel T, Lozinsky I, Schmalzing G, Markwardt F. Kinetics of P2X7 receptor-operated single channels currents. Biophys J [Internet]. 2007; 92: 2377–91. Available at: https://linkinghub.elsevier.com/retrieve/pii/S0006349507710433
136. Browne LE, Compan V, Bragg L, North RA. P2X7 receptor channels allow direct permeation of nanometer-sized dyes. J Neurosci [Internet]. 2013; 33: 3557–66. Available at: http://www.jneurosci.org/cgi/doi/10.1523/JNEUROSCI.2235-12.2013
137. Harkat M, Peverini L, Cerdan AH, et al. On the permeation of large organic cations through the pore of ATP-gated P2X receptors. Proc Natl Acad Sci U S A [Internet]. 2017; 114: E3786–95. Available at: http://www.pnas.org/lookup/doi/10.1073/pnas.1701379114
138. Pippel A, Stolz M, Woltersdorf R, Kless A, Schmalzing G, Markwardt F. Localization of

the gate and selectivity filter of the full-length P2X7 receptor. Proc Natl Acad Sci U S A [Internet]. 2017; 114: E2156–65. Available at: http://www.pnas.org/lookup/doi/10.1073/pnas.1610414114
139. Takeuchi O, Akira S. Pattern Recognition Receptors and Inflammation. Cell [Internet]. 2010; 140: 805–20. Available at: https://linkinghub.elsevier.com/retrieve/pii/S0092867410000231
140. Franchi L, Warner N, Viani K, Nuñez G. Function of Nod-like receptors in microbial recognition and host defense. Immunol Rev [Internet]. 2009; 227: 106–28. Available at: http://doi.wiley.com/10.1111/j.1600-065X.2008.00734.x
141. Vajjhala PR, Mirams RE, Hill JM. Multiple binding sites on the pyrin domain of ASC protein allow self-association and interaction with NLRP3 protein. J Biol Chem [Internet]. 2012; 287: 41732–43. Available at: http://www.jbc.org/lookup/doi/10.1074/jbc.M112.381228
142. Duncan JA, Bergstralh DT, Wang Y, et al. Cryopyrin/NALP3 binds ATP/dATP, is an ATPase, and requires ATP binding to mediate inflammatory signaling. Proc Natl Acad Sci U S A [Internet]. 2007; 104: 8041–6. Available at: http://www.pnas.org/cgi/doi/10.1073/pnas.0611496104
143. Solle M, Labasi J, Perregaux DG, et al. Altered cytokine production in mice lacking P2X7 receptors. J Biol Chem. 2001; 276: 125–32.
144. Dinarello CA. The IL-1 family and inflammatory diseases. Clin Exp Rheumatol. 2002; 20.
145. Meylan E, Tschopp J, Karin M. Intracellular pattern recognition receptors in the host response. Nature [Internet]. 2006; 442: 39–44. Available at: http://www.nature.com/articles/nature04946
146. Ogura Y, Sutterwala FS, Flavell RA. The Inflammasome: First Line of the Immune Response to Cell Stress. Cell [Internet]. 2006; 126: 659–62. Available at: https://linkinghub.elsevier.com/retrieve/pii/S0092867406010129
147. Franchi L, Eigenbrod T, Muñoz-Planillo R, Nuñez G. The inflammasome: A caspase-1-activation platform that regulates immune responses and disease pathogenesis. Nat Immunol [Internet]. 2009; 10: 241–7. Available at: http://www.nature.com/articles/ni.1703
148. Di Virgilio F. Liaisons dangereuses: P2X7 and the inflammasome. Trends Pharmacol Sci [Internet]. 2007; 28: 465–72. Available at: https://linkinghub.elsevier.com/retrieve/pii/S0165614707001848
149. Martinon F, Pétrilli V, Mayor A, Tardivel A, Tschopp J. Gout-associated uric acid crystals activate the NALP3 inflammasome. Nature [Internet]. 2006; 440: 237–41. Available at: http://www.nature.com/articles/nature04516
150. Mariathasan S, Weiss DS, Newton K, et al. Cryopyrin activates the inflammasome in response to toxins and ATP. Nature [Internet]. 2006; 440: 228–32. Available at: http://www.nature.com/articles/nature04515
151. Kanneganti TD, Özören N, Body-Malapel M, et al. Bacterial RNA and small antiviral compounds activate caspase-1 through cryopyrin/Nalp3. Nature [Internet]. 2006; 440: 233–6. Available at: http://www.nature.com/articles/nature04517
152. Ghiringhelli F, Apetoh L, Tesniere A, et al. Activation of the NLRP3 inflammasome in dendritic cells induces IL-1B-dependent adaptive immunity against tumors. Nat Med [Internet]. 2009; 15: 1170–8. Available at: http://www.nature.com/articles/nm.2028
153. la Sala A, Ferrari D, Corinti S, Cavani A, Di Virgilio F, Girolomoni G. Extracellular ATP Induces a Distorted Maturation of Dendritic Cells and Inhibits Their Capacity to Initiate

Th1 Responses. J Immunol [Internet]. 2001; 166: 1611–7. Available at: http://www.jimmunol.org/lookup/doi/10.4049/jimmunol.166.3.1611
154. Wilkin F, Stordeur P, Goldman M, Boeynaems J-M, Robaye B. Extracellular adenine nucleotides modulate cytokine production by human monocyte-derived dendritic cells: dual effect on IL-12 and stimulation of IL-10. Eur J Immunol [Internet]. 2002; 32: 2409–17. Available at: https://onlinelibrary.wiley.com/doi/10.1002/1521-4141(200209)32:9%3C2409::AID-IMMU2409%3E3.0.CO;2-H
155. Bours MJL, Swennen ELR, Di Virgilio F, Cronstein BN, Dagnelie PC. Adenosine 5'-triphosphate and adenosine as endogenous signaling molecules in immunity and inflammation. Pharmacol Ther. 2006; 112: 358–404.
156. Park M, Kim J, Phuong NTT, et al. Involvement of the P2X7 receptor in the migration and metastasis of tamoxifen-resistant breast cancer: effects on small extracellular vesicles production. Sci Rep [Internet]. 2019; 9: 11587. Available at: http://www.nature.com/articles/s41598-019-47734-z
157. Solini A, Simeon V, Derosa L, et al. Genetic interaction of P2X7 receptor and VEGFR-2 polymorphisms identifies a favorable prognostic profile in prostate cancer patients. Oncotarget [Internet]. 2015; 6: 28743–54. Available at: https://www.oncotarget.com/lookup/doi/10.18632/oncotarget.4926
158. Zhang Y, Ding J, Wang L. The role of P2X7 receptor in prognosis and metastasis of colorectal cancer. Adv Med Sci [Internet]. 2019; 64: 388–94. Available at: https://linkinghub.elsevier.com/retrieve/pii/S1896112619300069
159. Kwon JH, Nam ES, Shin HS, Cho SJ, Park HR, Kwon MJ. P2X7 receptor expression in coexistence of papillary thyroid carcinoma with hashimoto's thyroiditis. Korean J Pathol [Internet]. 2014; 48: 30–5. Available at: http://www.jpatholtm.org/journal/view.php?doi=10.4132/KoreanJPathol.2014.48.1.30
160. Giannuzzo A, Saccomano M, Napp J, Ellegaard M, Alves F, Novak I. Targeting of the P2X7 receptor in pancreatic cancer and stellate cells. Int J Cancer [Internet]. 2016; 139: 2540–52. Available at: http://doi.wiley.com/10.1002/ijc.30380
161. De Marchi E, Orioli E, Pegoraro A, et al. The P2X7 receptor modulates immune cells infiltration, ectonucleotidases expression and extracellular ATP levels in the tumor microenvironment. Oncogene [Internet]. 2019; 38: 3636–50. Available at: http://www.nature.com/articles/s41388-019-0684-y
162. Zitvogel L, Kepp O, Galluzzi L, Kroemer G. Inflammasomes in carcinogenesis and anticancer immune responses. Nat Immunol [Internet]. 2012; 13: 343–51. Available at: http://www.nature.com/articles/ni.2224
163. Martins I, Tesniere A, Kepp O, et al. Chemotherapy induces ATP release from tumor cells. Cell Cycle [Internet]. 2009; 8: 3723–8. Available at: http://www.tandfonline.com/doi/abs/10.4161/cc.8.22.10026
164. Lertsuwan J, Ruchirawat M. Inhibitory effects of ATP and adenosine on cholangiocarcinoma cell proliferation and motility. Anticancer Res [Internet]. 2017; 37: 3553–61. Available at: http://ar.iiarjournals.org/content/37/7/3553.abstract
165. Jelassi B, Chantme A, Alcaraz-Pérez F, et al. P2X 7 receptor activation enhances SK3 channels- and cystein cathepsin-dependent cancer cells invasiveness. Oncogene [Internet]. 2011; 30: 2108–22. Available at: http://www.nature.com/articles/onc2010593
166. Qiu Y, Li WH, Zhang HQ, Liu Y, Tian XX, Fang WG. P2X7 mediates ATP-driven invasiveness

in prostate cancer cells. Kanellopoulos J, Ed. PLoS One [Internet]. 2014; 9: e114371. Available at: https://dx.plos.org/10.1371/journal.pone.0114371
167. Chadet S, Jelassi B, Wannous R, et al. The activation of P2Y2 receptors increases MCF-7 breast cancer cells migration through the MEK-ERK1/2 signalling pathway. Carcinogenesis [Internet]. 2014; 35: 1238–47. Available at: https://academic.oup.com/carcin/article-lookup/doi/10.1093/carcin/bgt493
168. de Andrade Mello P, Bian S, Savio LEB, et al. Hyperthermia and associated changes in membrane fluidity potentiate P2X7 activation to promote tumor cell death. Oncotarget [Internet]. 2017; 8: 67254–68. Available at: https://www.oncotarget.com/lookup/doi/10.18632/oncotarget.18595
169. Choi JH, Ji YG, Ko JJ, Cho HJ, Lee DH. Activating P2X7 Receptors Increases Proliferation of Human Pancreatic Cancer Cells via ERK1/2 and JNK. Pancreas [Internet]. 2018; 47: 643–51. Available at: http://journals.lww.com/00006676-201805000-00019
170. Nie J, Huang GL, Deng SZ, et al. The purine receptor P2X7R regulates the release of pro-inflammatory cytokines in human craniopharyngioma. Endocr Relat Cancer [Internet]. 2017; 24: 287–96. Available at: https://erc.bioscientifica.com/view/journals/erc/24/6/287.xml
171. Bae JY, Lee SW, Shin YH, Lee JH, Jahng JW, Park K. P2X7 receptor and NLRP3 inflammasome activation in head and neck cancer. Oncotarget [Internet]. 2017; 8: 48972–82. Available at: https://www.oncotarget.com/lookup/doi/10.18632/oncotarget.16903
172. Qian F, Xiao J, Hu B, Sun N, Yin W, Zhu J. High expression of P2X7R is an independent postoperative indicator of poor prognosis in colorectal cancer. Hum Pathol [Internet]. 2017; 64: 61–8. Available at: https://linkinghub.elsevier.com/retrieve/pii/S0046817717301041
173. Hofman P, Cherfils-Vicini J, Bazin M, et al. Genetic and pharmacological inactivation of the purinergic P2RX7 receptor dampens inflammation but increases tumor incidence in a mouse model of colitis-associated cancer. Cancer Res [Internet]. 2015; 75: 835–45. Available at: http://cancerres.aacrjournals.org/cgi/doi/10.1158/0008-5472.CAN-14-1778
174. Adinolfi E, Capece M, Franceschini A, et al. Accelerated tumor progression in mice lacking the ATP receptor P2X7. Cancer Res [Internet]. 2015; 75: 635–44. Available at: http://cancerres.aacrjournals.org/cgi/doi/10.1158/0008-5472.CAN-14-1259
175. Roger S, Jelassi B, Couillin I, Pelegrin P, Besson P, Jiang LH. Understanding the roles of the P2X7 receptor in solid tumour progression and therapeutic perspectives. Biochim Biophys Acta - Biomembr [Internet]. 2015; 1848: 2584–602. Available at: https://linkinghub.elsevier.com/retrieve/pii/S0005273614003642
176. Slater M, Danieletto S, Gidley-Baird A, Teh LC, Barden JA. Early prostate cancer detected using expression of non-functional cytolytic P2X7 receptors. Histopathology [Internet]. 2004; 44: 206–15. Available at: http://doi.wiley.com/10.1111/j.0309-0167.2004.01798.x
177. Barden JA, Baird AG. Therapeutic Targeting of the Cancer-Specific Cell Surface Biomarker nfP2X7. J Clin Cell Immunol [Internet]. 2016; 7. Available at: https://www.omicsonline.org/open-access/therapeutic-targeting-of-the-cancerspecific-cell-surface-biomarker-nfp2x7-2155-9899-1000432.php?aid=74849
178. Liu Z, Liu Y, Xu L, et al. P2X7 receptor predicts postoperative cancer-specific survival of patients with clear-cell renal cell carcinoma. Cancer Sci [Internet]. 2015; 106: 1224–31.

Available at: https://onlinelibrary.wiley.com/doi/10.1111/cas.12736
179. Li X, Qi X, Zhou L, et al. P2X7 receptor expression is decreased in epithelial cancer cells of ectodermal, uro-genital sinus, and distal paramesonephric duct origin. Purinergic Signal [Internet]. 2009; 5: 351–68. Available at: http://link.springer.com/10.1007/s11302-009-9161-3
180. Gilbert S, Oliphant C, Hassan S, et al. ATP in the tumour microenvironment drives expression of nfP2X 7 , a key mediator of cancer cell survival. Oncogene [Internet]. 2019; 38: 194–208. Available at: http://www.nature.com/articles/s41388-018-0426-6
181. Calik I, Calik M, Sarikaya B, et al. P2x7 receptor as an independent prognostic indicator in gastric cancer. Bosn J Basic Med Sci [Internet]. 2020; 20: 188–96. Available at: https://bjbms.org/ojs/index.php/bjbms/article/view/4620
182. Santos AA, Cappellari AR, de Marchi FO, et al. Potential role of P2X7R in esophageal squamous cell carcinoma proliferation. Purinergic Signal [Internet]. 2017; 13: 279–92. Available at: http://link.springer.com/10.1007/s11302-017-9559-2
183. Slater M, Danieletto S, Pooley M, Teh LC, Gidley-Baird A, Barden JA. Differentiation between cancerous and normal hyperplastic lobules in breast lesions. Breast Cancer Res Treat [Internet]. 2004; 83: 1–10. Available at: http://link.springer.com/10.1023/B:BREA.0000010670.85915.0f
184. Huang S, Chen Y, Wu W, et al. MiR-150 promotes human breast cancer growth and malignant behavior by targeting the pro-apoptotic purinergic P2X7 receptor. Navarro A, Ed. PLoS One [Internet]. 2013; 8: e80707. Available at: https://dx.plos.org/10.1371/journal.pone.0080707
185. Greig AVH, Linge C, Healy V, et al. Expression of purinergic receptors in non-melanoma skin cancers and their functional roles in A431 cells. J Invest Dermatol [Internet]. 2003; 121: 315–27. Available at: https://linkinghub.elsevier.com/retrieve/pii/S0022202X15303572
186. Slater M, Barden JA. Differentiating keratoacanthoma from squamous cell carcinoma by the use of apoptotic and cell adhesion markers. Histopathology [Internet]. 2005; 47: 170–8. Available at: http://doi.wiley.com/10.1111/j.1365-2559.2005.02155.x
187. White N, Butler PEM, Burnstock G. Human melanomas express functional P2X7 receptors. Cell Tissue Res [Internet]. 2005; 321: 411–8. Available at: http://link.springer.com/10.1007/s00441-005-1149-x
188. Raffaghello L, Chiozzi P, Falzoni S, Di Virgilio F, Pistoia V. The P2X7 receptor sustains the growth of human neuroblastoma cells through a substance P-dependent mechanism. Cancer Res [Internet]. 2006; 66: 907–14. Available at: http://cancerres.aacrjournals.org/lookup/doi/10.1158/0008-5472.CAN-05-3185
189. Amoroso F, Capece M, Rotondo A, et al. The P2X7 receptor is a key modulator of the PI3K/GSK3β/VEGF signaling network: Evidence in experimental neuroblastoma. Oncogene [Internet]. 2015; 34: 5240–51. Available at: http://www.nature.com/articles/onc2014444
190. A. Barden J. Non-Functional P2X7: A Novel and Ubiquitous Target in Human Cancer. J Clin Cell Immunol [Internet]. 2014; 05. Available at: https://www.omicsonline.org/open-access/nonfunctional-px-a-novel-and-ubiquitous-target-in-human-cancer-2155-9899.1000237.php?aid=28020
191. Solini A, Cuccato S, Ferrari D, et al. Increased P2X7 receptor expression and function in thyroid papillary cancer: A new potential marker of the disease? Endocrinology [Internet]. 2008; 149: 389–96. Available at:

https://academic.oup.com/endo/article/149/1/389/2455133
192. Künzli BM, Berberat PO, Giese T, et al. Upregulation of CD39/NTPDases and P2 receptors in human pancreatic disease. Am J Physiol - Gastrointest Liver Physiol [Internet]. 2007; 292: G223–30. Available at: https://www.physiology.org/doi/10.1152/ajpgi.00259.2006
193. Boldrini L, Giordano M, Alì G, et al. P2X7 protein expression and polymorphism in non-small cell lung cancer (NSCLC). J Negat Results Biomed [Internet]. 2014; 13: 16. Available at: https://jnrbm.biomedcentral.com/articles/10.1186/1477-5751-13-16
194. Schmid S, Kübler M, Korcan Ayata C, et al. Altered purinergic signaling in the tumor associated immunologic microenvironment in metastasized non-small-cell lung cancer. Lung Cancer [Internet]. 2015; 90: 516–21. Available at: https://linkinghub.elsevier.com/retrieve/pii/S016950021530074X
195. Buell GN, Talabot F, Gos A, et al. Gene structure and chromosomal localization of the human P2X7 receptor. Recept Channels [Internet]. 1998; 5: 347–54. Available at: http://www.ncbi.nlm.nih.gov/pubmed/9826911
196. Zhou L, Qi X, Potashkin JA, Abdul-Karim FW, Gorodeski GI. MicroRNAs miR-186 and miR-150 down-regulate expression of the pro-apoptotic purinergic P2X7 receptor by activation of instability sites at the 3'-untranslated region of the gene that decrease steady-state levels of the transcript. J Biol Chem [Internet]. 2008; 283: 28274–86. Available at: http://www.jbc.org/lookup/doi/10.1074/jbc.M802663200
197. Sluyter R, Stokes L. Significance of p2x7 receptor variants to human health and disease. Recent Patents DNA Gene Seq [Internet]. 2011; 5: 41–54. Available at: http://www.ncbi.nlm.nih.gov/pubmed/21303345
198. Xiao J, Sun L, Yan H, et al. Metaanalysis of P2X7 gene polymorphisms and tuberculosis susceptibility. FEMS Immunol Med Microbiol [Internet]. 2010; 60: 165–70. Available at: https://academic.oup.com/femspd/article-lookup/doi/10.1111/j.1574-695X.2010.00735.x
199. Al-Shukaili A, Al-Kaabi J, Hassan B. A comparative study of interleukin-1β production and P2x7 expression after Atp stimulation by peripheral blood mononuclear cells isolated from rheumatoid arthritis patients and normal healthy controls. Inflammation [Internet]. 2008; 31: 84–90. Available at: http://link.springer.com/10.1007/s10753-007-9052-0
200. Thunberg U, Tobin G, Johnson A, et al. Polymorphism in the P2X7 receptor gene and survival in chronic lymphocytic leukaemia. Lancet [Internet]. 2002; 360: 1935–9. Available at: https://linkinghub.elsevier.com/retrieve/pii/S0140673602119179
201. Baralle FE, Giudice J. Alternative splicing as a regulator of development and tissue identity. Nat Rev Mol Cell Biol [Internet]. 2017; 18: 437–51. Available at: http://www.nature.com/articles/nrm.2017.27
202. Wang ET, Sandberg R, Luo S, et al. Alternative isoform regulation in human tissue transcriptomes. Nature [Internet]. 2008; 456: 470–6. Available at: http://www.nature.com/articles/nature07509
203. Tazi J, Bakkour N, Stamm S. Alternative splicing and disease. Biochim Biophys Acta - Mol Basis Dis [Internet]. 2009; 1792: 14–26. Available at: https://linkinghub.elsevier.com/retrieve/pii/S0925443908001932
204. Pan Q, Shai O, Lee LJ, Frey BJ, Blencowe BJ. Deep surveying of alternative splicing complexity in the human transcriptome by high-throughput sequencing. Nat Genet [Internet]. 2008; 40: 1413–5. Available at: http://www.nature.com/articles/ng.259

205. Kim MS, Pinto SM, Getnet D, et al. A draft map of the human proteome. Nature [Internet]. 2014; 509: 575–81. Available at: http://www.nature.com/articles/nature13302
206. Kim HK, Pham MHC, Ko KS, Rhee BD, Han J. Alternative splicing isoforms in health and disease. Pflugers Arch Eur J Physiol [Internet]. 2018; 470: 995–1016. Available at: http://link.springer.com/10.1007/s00424-018-2136-x
207. Merkin J, Russell C, Chen P, Burge CB. Evolutionary dynamics of gene and isoform regulation in mammalian tissues. Science (80-) [Internet]. 2012; 338: 1593–9. Available at: https://www.sciencemag.org/lookup/doi/10.1126/science.1228186
208. Stamm S. Regulation of alternative splicing by reversible protein phosphorylation. J Biol Chem [Internet]. 2008; 283: 1223–7. Available at: http://www.jbc.org/lookup/doi/10.1074/jbc.R700034200
209. Lim KH, Ferraris L, Filloux ME, Raphael BJ, Fairbrother WG. Using positional distribution to identify splicing elements and predict pre-mRNA processing defects in human genes. Proc Natl Acad Sci U S A [Internet]. 2011; 108: 11093–8. Available at: http://www.pnas.org/cgi/doi/10.1073/pnas.1101135108
210. Montes M, Sanford BL, Comiskey DF, Chandler DS. RNA Splicing and Disease: Animal Models to Therapies. Trends Genet [Internet]. 2019; 35: 68–87. Available at: https://linkinghub.elsevier.com/retrieve/pii/S0168952518301720
211. Zhang W, Hu C, Zhu Z, Luo H. Effect of P2X7 receptor on tumorigenesis and its pharmacological properties. Biomed Pharmacother [Internet]. 2020; 125: 109844. Available at: https://linkinghub.elsevier.com/retrieve/pii/S0753332220300342
212. Hastings ML, Resta N, Traum D, Stella A, Guanti G, Krainer AR. An LKB1 AT-AC intron mutation causes Peutz-Jeghers syndrome via splicing at noncanonical cryptic splice sites. Nat Struct Mol Biol [Internet]. 2005; 12: 54–9. Available at: http://www.nature.com/articles/nsmb873
213. Chen LL, Trent JC, Wu EF, et al. A missense mutation in KIT kinase domain 1 correlates with imatinib resistance in gastrointestinal stromal tumors. Cancer Res [Internet]. 2004; 64: 5913–9. Available at: http://cancerres.aacrjournals.org/lookup/doi/10.1158/0008-5472.CAN-04-0085
214. Narla G, DiFeo A, Reeves HL, et al. A germline DNA polymorphism enhances alternative splicing of the KLF6 tumor suppressor gene and is associated with increased prostate cancer risk. Cancer Res [Internet]. 2005; 65: 1213–22. Available at: http://cancerres.aacrjournals.org/lookup/doi/10.1158/0008-5472.CAN-04-4249
215. Liu LX, Lee NP, Chan VW, et al. Targeting cadherin-17 inactivates Wnt signaling and inhibits tumor growth in liver carcinoma. Hepatology [Internet]. 2009; 50: 1453–63. Available at: http://doi.wiley.com/10.1002/hep.23143
216. Mazoyer S, Puget N, Perrin-Vidoz L, Lynch HT, Serova-Sinilnikova OM, Lenoir GM. A BRCA1 nonsense mutation causes exon skipping [1]. Am J Hum Genet [Internet]. 1998; 62: 713–5. Available at: https://linkinghub.elsevier.com/retrieve/pii/S0002929707638518
217. Cheewatrakoolpong B, Gilchrest H, Anthes JC, Greenfeder S. Identification and characterization of splice variants of the human P2X7 ATP channel. Biochem Biophys Res Commun [Internet]. 2005; 332: 17–27. Available at: https://linkinghub.elsevier.com/retrieve/pii/S0006291X05008685
218. Pan H, Ni H, Zhang LL, et al. P2RX7-V3 is a novel oncogene that promotes tumorigenesis in uveal melanoma. Tumor Biol [Internet]. 2016; 37: 13533–43. Available at:

http://link.springer.com/10.1007/s13277-016-5141-8
219. Skarratt KK, Gu BJ, Lovelace MD, et al. A P2RX7 single nucleotide polymorphism haplotype promotes exon 7 and 8 skipping and disrupts receptor function. FASEB J [Internet]. 2020; 34: 3884–901. Available at: https://onlinelibrary.wiley.com/doi/abs/10.1096/fj.201901198RR
220. Giuliani AL, Colognesi D, Ricco T, et al. Trophic activity of human P2X7 receptor isoforms A and B in osteosarcoma. Kanellopoulos J, Ed. PLoS One [Internet]. 2014; 9: e107224. Available at: https://dx.plos.org/10.1371/journal.pone.0107224